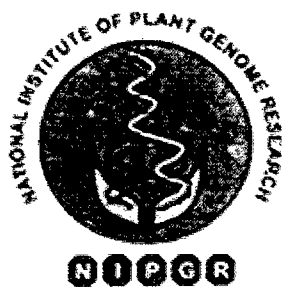


**Cloning and characterization of gene
encoding peroxidase from
*Catharanthus roseus***

Thesis submitted to
Jawaharlal Nehru University
New Delhi
For the award of the degree of

Doctor of Philosophy
by

Santosh Kumar



National Institute of Plant Genome Research
New Delhi-110067, INDIA

2009



NATIONAL INSTITUTE OF PLANT GENOME RESEARCH

(Formerly known as National Centre for Plant Genome Research)
(An Autonomous Institution of the Department of Biotechnology, Ministry of Science and Technology, Government of India)

Aruna Asaf Ali Marg, Post Box Number 10531, New Delhi-110067

CERTIFICATE

The research work embodied in this thesis entitled "**Cloning and characterization of gene encoding peroxidase from *Catharanthus roseus***" has been carried out at National Institute of Plant Genome Research, New Delhi, India. This work is original and has not been submitted so far in part or in full, for the award of any degree or diploma by any university.



Dr. Alok Krishna Sinha
(Supervisor), NIPGR



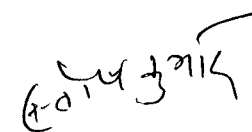
Dr. Sudip Chattopadhyay
(Director), NIPGR

Ph. : 26741612, 26741614, 26741617, Fax : 91-11-26741658
E-mail : nipgr@nipgr.res.in; Website : <http://www.nipgr.res.in>



DECLARATION

I hereby declare that the research work embodied in this thesis entitled “**Cloning and characterization of gene encoding peroxidase from *Catharanthus roseus***” has been carried out by me under the supervisions of late Dr. Jayanti Sen and Dr. Alok Krishna Sinha, at National Institute of Plant Genome Research, New Delhi, India.


Santosh Kumar
(Candidate)

February, 2009

Acknowledgements

The writing of a dissertation can be a lonely and isolating experience, yet it is obviously not possible without the personal and practical support of numerous people.

*First of all, I would like to express my gratitude to my former doctoral advisor late Dr. Jayanti Sen for introducing me to the wonderful world of *Catharanthus roseus* genomics. I wish to thank to my present supervisor Dr. Alok Krishna Sinha for his guidance, patience and the opportunity to carry out present work in lab.*

I thank Dr. Sudip Chattopadhyay, Officiating Director, NIPGR for his support and encouragement through out the course of this work.

I express my sincere gratitude towards Prof of eminence Dr. Asis Datta, former director, NIPGR, for his constant encouragement and allowing me to work in this prestigious institute.

It gives me pleasure to thank Prof Sushil Kumar for his valuable suggestions and constant encouragement.

I thank Dr. Naveen Chandra Bisht for allowing me to use his lab facilities for my experiments. Thanks are due to Drs. Debasis Chattopadhyay, Praveen Verma, Sabhyata Bhatia, Manoj Prasad, Niranjana Chakraborty, Shubhra Chakraborty, Geetanjali Yadav, Manoj Majee, Ashverya Laxmi and Mukesh Jain for their supportive attitude.

I also wish to thank research fellows Drs. Jyoti Batra, Ajaswata Dutta, Ravindra Kumar, Snehangshu Kundu, Manoj Rajput, Rakesh Shukla, Niroj Shethy, Vijaykumar S. Meli and Bhumika Shokeen for the countless times that I have sought opinion and advice over the past years, and for valuable suggestion and solution to the challenges of my research.

I owe a special note of gratitude to my fellow workers Dipul, Monika, Prabhakar, Dhammaprakash, Kundan, Susheel, Hema and Vani.

My appreciation also goes out to all members of the Lab 102 and the Lab 16(Old CPMB) who have helped me during the course of this research. In particular I thank the help of my batch mates Sreeramaiah, Archana, Vineeta, Mani Kant, Kamal, Aarti, Nasheeman, Shallu as both colleagues and good friends.

I would like to thank Sunilji, Arun, Shobharam, Ashok, Surendra and other technical staff for their help. I also thank Laukhi da and Rafik for their help.

Last, but in no way least, I am extremely grateful to my family. My parents have been a constant source of encouragement, unwavering faith

and support throughout the many days working on this thesis. I also want to thank my brother Sunil for his insights and support. Special thanks to Pawan, Sanchita, Jayeeta and Rehna my juniors, for there everlasting love that help in allowing me to find my path in life.

I take this opportunity to thank all those who have helped me knowingly or unknowingly all through my tenure.

I acknowledge CSIR and NIPGR for providing financial assistance.

Santosh Kumar

Dedicated to my Parents and Guides

Abbreviations

\$	Dollar
%	percentage
α	Alpha
β	Beta
λ	Lambda
μ l	Microlitre
μ m	Micrometer
μ M	Micromolar
$^{\circ}$ C	Degree celsius
2, 4-D	2, 4-Dichlorophenoxyacetic acid
3-D	Three dimensional
Å	Angstrom
ABA	Abscisic acid
aCrPrx1	Antisense CrPrx1
APS	Ammonium persulfate
APX	Ascorbate peroxidase
AVLB	A-3', 4' anhydrovinblastine
BAP	6-benzylamino purine
BLAST	Basic Local Alignment Search Tool
bp	Base pairs
C18	Carbon 18
ca	Approximately
CaMV	Cauliflower Mosaic Virus
CAT	Catalase
cDNA	Complementary Deoxy ribonucleic acid
cm	Centimeter
CrPrx	<i>Catharanthus roseus</i> Peroxidase
CSV	Comma Separated Values
CTAB	Cetyl Trimethyl Ammonium Bromide
CycD3	Cyclin D3
d	Day
DEPC	DiEthylPyroCarbonate
DMSO	Dimethyl sulfoxide
DNA	Deoxyribonucleic acid
DNase	Deoxy ribonuclease
DOPA	3,4-dihydroxy-L-phenylalanine
DOS	Disk Operating System
DTT	Dithiotretiol
DW	Dry weight
EC number	Enzyme Commission number
EDTA	Ethylene diamine tetra acetic acid
EtBr	Ethidium bromide
GBF	G-box binding factor
Glu	Glutamic acid
GUS	β -glucuronidase
h	Hour
His	Histidine
IgG	Immune globulin G

IPTG	Isopropyl- β -D-thiogalactopyranosid
ITB	Inoue transfer buffer
J	Joule
JA	Jasmonic Acid
kb	Kilo base pair
kDa	Kilodalton
kg	Kilogram
LB	Luria Bertani
lb	Pound
LD-PCR	Long Distance-Polymerase Chain Reaction
liq N ₂	Liquid Nitrogen
m	Meter
mA	Milli ampere
MEGA	Molecular Evolutionary Genetics Analysis
mg	Miligram
mGFP	Modified Green Fluorescent Protein
MIA	Monoterpenoid Indole Alkaloid
min	Minute
ml	Mililitre
mm	Milimeter
mM	Millimolar
Mn ²⁺	Manganese ions
MOPS	3-(N-morpholino)propanesulfonic acid
MS	Murashige-Skoog
MSH	MS reducing media
MV	Methyl viologen
MY	Million Years
N/D	Not detected
NAA	Naphthalene Acetic Acid
NADPH	Reduced Nicotinamide Adenine Dinucleotide Phosphate
NCBI	National Center for Biotechnology Information
nm	Nano meter
NO	Nitric Oxide
NOS	Nopaline Synthase
nt	Nucleotide
NUP	Nested Universal Primer
OD	Optical density
ORCA3	Octadecanoid-responsive Caratharanthus APETALA2-domain protein3
ORF	Open reading frame
PAGE	Polyacrylamide gel electrophoresis
PAL	Phenylalanine Ammonia-Lyase
PCR	Polymerase Chain Reaction
PEG	Polyethylene Glycol
pH	Potential hydrogen, a measure of acidity or alkalinity
Phe	Phenylalanine
pI	Isoelectric point
PIPES	Piperazine-1,4-bis(2-ethanesulfonic acid)
PMSF	Phenylmethanesulphonylfluoride
psi	Pound per square inch

PVP	Polyvinylpyrrolidone
PVPP	Polyvinylpolypyrrolidone
qRT-PCR	Quantitative Real Time Polymerase Chain Reaction
RACE	Rapid Amplification of cDNA Ends
RNA	Ribonucleic Acid
RNaseA	Ribonuclease A
ROS	Reactive Oxygen Species
rpm	Revolutions per minute
RPS9	Ribosomal protein S9
RT	Room temperature
RT-PCR	Reverse Transcriptase PCR
sCrPrx1	Sense CrPrx1
SD	Standard Deviation
SDS	Sodium Dodecyl sulphate
SM Buffer	Sodium Magnesium Buffer
SMART	Switching Mechanism At 5' end of RNA Transcript
SSC	Sodium saline citrate
Syn.	Synonyms
TAE	Tris-acetate-EDTA
TEM	Transmission electron microscopy
TEMED	N,N,N',N'-Tetramethylethylenediamine
Tm	Melting Temperature
TMV	Tobacco Mosaic Virus
TRM	Tobacco Root induction Medium
TSM	Tobacco Shoot induction Medium
U	Unit
UPM	Universal Primer Mix
USA	United States of America
UTR	Upstream region
UV	Ultra Violet
V	Volt
v/v	Volume by volume
vol.	Volume
w/v	Weight by volume
wt	Weight
X-gal	5-bromo-4-chloro-3-indolyl-beta-Dgalactopyranoside
YEB	Yeast Extract Broth

Contents

Certificate
Declaration
Dedication
Acknowledgements
Abbreviations

Chapter 1:	General Introduction	1-6
Chapter 2:	Review of Literature	7-33
2.1	<i>Catharanthus roseus</i> and its importance as alkaloid producing plant	7
2.2	Monoterpenoid Indole Alkaloid pathway and its localization in plant system	11
2.2.1	Tissue specific localization of MIA pathway	15
2.2.2	Sub-cellular localization of MIA pathway enzymes	18
2.3	Involvement of peroxidase in MIA pathway	20
2.4	Peroxidases and their presence in plant kingdom	23
2.5	Structure of Class III plant peroxidase	24
2.6	Multiplicity of Peroxidase genes	25
2.7	Regulation of peroxidases in plants	26
2.8	Molecular technique used in study of peroxidases	30
2.9	A brief with Peroxiredoxin	33
Chapter 3:	Materials and Methods	34-80
3.1.1	Plant material	34
3.1.2	Bacterial strains	34
3.1.3	Plasmid vectors	34
3.1.4	Chemicals and stocks	35
3.1.5	List of oligonucleotides/primers	37
3.1.6	Specialized primers for the cloning in expression vectors	39
3.1.7	Specialized primers used for the Real time PCR	41
3.1.8	Composition of growth mediums	42
3.1.8.1	Luria Broth (LB)	42
3.1.8.2	YEB	42
3.1.8.3	SOB	43
3.1.8.4	NZY	43
3.1.8.5	Gamborg's B5 medium	43
3.1.8.6	Murashige and Skoog medium	44
3.1.8.7	Tobacco shoot induction media (TSM)	46
3.1.8.8	Tobacco root induction media (TRM)	46
3.1.8.9	MSH (Murashige and Skoog medium without sucrose and organic ingredients)	47

3.2	Methods	47
3.2.1	General sterilization procedures	47
3.2.2	Plant growth conditions and maintenance	47
3.2.3	Primer designing	47
3.2.3.1	Design of degenerate plant peroxidase primers	47
3.2.3.2	Designing of full length gene specific primers and primers with restriction sites	48
3.2.3.3	Design of Gene specific primers for 5' and 3' RACE	48
3.2.3.4	Design of Real time PCR primers	49
3.2.4	Recombinant DNA techniques	49
3.2.4.1	Polymerase Chain Reaction	49
3.2.4.1.2	Degenerate PCR amplification	49
3.2.4.1.3	PCR amplification of peroxidase genes	49
3.2.4.1.4	PCR amplification for cloning of genes in pBI121 and pCAMBIA vector using phusion Taq DNA polymerase	50
3.2.4.2	Cloning of DNA fragments	50
3.2.4.2.1	Electrophoretic separation of DNA samples	50
3.2.4.2.2	Elution of DNA from agarose gel	50
3.2.4.2.3	Ligation	51
3.2.4.2.3.1	Ligation in pGEM-T Easy vector	51
3.2.4.2.3.2	Ligation in pBI121 and pCAMBIA vectors	51
3.2.4.2.4	Preparation of competent cells	51
3.2.4.2.4.1	Preparation of <i>E. coli</i> (DH5 α) ultra competent cells	51
3.2.4.2.4.2	Preparation of <i>Agrobacterium</i> competent cells	52
3.2.4.2.5	Bacterial transformation	52
3.2.4.2.5.1	Transformation of <i>E. coli</i>	52
3.2.4.2.5.2	Transformation of <i>Agrobacterium</i>	52
3.2.4.2.5.3	Confirmation for the presence of inserts	53
3.2.4.2.5.4	Colony PCR	53
3.2.4.2.5.5	Restriction digestion	53
3.2.4.2.6	Nucleic acid preparations	53
3.2.4.2.6.1	Plasmid DNA extraction	53
3.2.4.2.6.2	Purification of the plasmid DNA by PEG precipitation method	54
3.2.4.2.6.3	Sequencing and analysis	54
3.2.5	Genomic DNA extraction	55
3.2.5.1	Small scale genomic DNA extraction for the PCR	55
3.2.5.2	Medium scale genomic DNA extraction	55
3.2.6	Southern blot analysis	56
3.2.6.1	Restriction digestion and gel electrophoresis	56
3.2.6.2	Transfer of DNA to nylon membranes	56
3.2.6.3	Southern hybridization	56
3.2.6.4	Preparation and ³² P labelling of DNA probes	56
3.2.6.5	Hybridization and autoradiography	57
3.2.6.6	Image analysis	57
3.2.7	RNA extraction	58

3.2.7.1	Total RNA extraction using TRIzol reagent	58
3.2.7.2	Total RNA extraction using LiCl precipitation method	58
3.2.7.3	Total RNA extraction extraction for performing 5' and 3' RACE	58
3.2.7.4	RNA quantification	59
3.2.7.5	Denaturing formaldehyde gel preparation for electrophoresis	59
3.2.8	Northern blot analysis	59
3.2.8.1	Transfer and fixation of denatured RNA to nylon membranes	59
3.2.8.2	Radioactive probe preparation and purification	60
3.2.8.3	Hybridization, washing and autoradiography	60
3.2.8.4	Image analysis	60
3.2.8.5	Removal of radioactive probe from membranes	60
3.2.9	Real time PCR	60
3.2.10	Cloning of full length gene using 5' and 3' RACE	61
3.2.10.1	First Strand cDNA synthesis	61
3.2.10.2	cDNA amplification by LD-PCR	62
3.2.10.3	Amplification of DNA for 5' RACE and 3' RACE	62
3.2.10.4	3' RACE amplifications	62
3.2.10.5	5' RACE amplifications	63
3.2.11	Preparation of Yeast elicited <i>C. roseus</i> suspension cell culture cDNA library	63
3.2.11.1	Preparation of <i>C. roseus</i> suspension cell culture	63
3.2.11.2	Elicitor treatment of cell suspension	64
3.2.11.3	Total RNA and mRNA extraction	64
3.2.11.4	Synthesis of cDNA	64
3.2.11.5	Preparation of cDNA library in phage	65
3.2.12	Screening of <i>C. roseus</i> cDNA library	65
3.2.12.1	Preparation of host bacteria	65
3.2.12.2	Plating out the library for screening	66
3.2.12.3	Preparation of nylon membranes for the plaque lifting	66
3.2.12.4	Plaque lifting on Hybond-N nylon membrane	66
3.2.12.5	Hybridization, washing and autoradiography	66
3.2.12.6	Purification of plaque clones of interest and PCR confirmatory test	67
3.2.12.7	<i>In vivo</i> excision of the pBLUESCRIPT phagemid vector containing insert from the λ -ZAP vector	67
3.2.13	<i>In silico</i> analysis	69
3.2.14	<i>In vitro</i> techniques	70
3.2.14.1	Sterilization of seeds	70
3.2.14.2	Germination of seeds	70
3.2.14.3	Generation of transgenic calli: Transformation of <i>C. roseus</i> with recombinant <i>A. tumefaciens</i>	71

3.2.14.3.1	Explant Preparation for transformation	71
3.2.14.3.2	Preparation of recombinant <i>A. tumefaciens</i> culture	71
3.2.14.3.3	Transformation and co-cultivation	71
3.2.14.3.4	Generation of transgenic calli on antibiotic media	71
3.2.14.3.5	Determination of transgenic calli	72
3.2.14.3.6	Transformation efficiency	72
3.2.14.4	Generation of transgenic tobacco	72
3.2.14.4.1	Explant Preparation for transformation	72
3.2.14.4.2	Preparation of recombinant <i>A. tumefaciens</i> culture	72
3.2.14.4.3	Transformation and co-cultivation	72
3.2.14.4.4	Generation of transgenic shoots on antibiotic media	73
3.2.14.4.5	Transfer of transgenic tobacco plants to pot	73
3.2.14.4.6	Growth Index study	73
3.2.14.4.7	Growth rate measurement for transgenic tobacco plants	73
3.2.14.5	Evaluation of T1 generation of transgenic tobacco plants	73
3.2.14.5.1	Seeds sterilization	73
3.2.14.5.2	Seeds plating on stress media	74
3.2.14.5.3	Cold stress treatments	74
3.2.14.6	Histochemical GUS staining and Fluorescence microscopy	74
3.2.14.7	Confocal Imaging	75
3.2.15	Stress treatments	75
3.2.16	Leaf chlorophyll determination	76
3.2.17	Measurement of chlorophyll fluorescence to measure photosynthesis	76
3.2.18	Protein extraction, immunoblot preparation and enzyme assay	76
3.2.18.1	Total soluble protein extraction from <i>C. roseus</i> tissue for immunoblot preparation	76
3.2.18.2	Determination of total protein content of supernatant	77
3.2.18.3	Western blotting	77
3.2.18.4	Total soluble protein extraction from <i>C. roseus</i> tissue and peroxidase enzyme assay	78
3.2.18.5	Total soluble protein extraction from transgenic tobacco and <i>C. roseus</i> leaf calli and peroxidase enzyme assay	78
3.2.19	Biochemical analysis	79
3.2.19.1	Total alkaloid extraction	79
3.2.19.2	HPLC analysis	80

Chapter 4:	Results and Discussion	81-171
4.1:	Cloning, characterization and localization of a novel basic peroxidase gene <i>CrPrx</i> from <i>Catharanthus roseus</i>	81-103
4.1.1	Introduction	81
4.1.2	Results	82
4.1.2.1	Cloning of <i>CrPrx</i> gene	82
4.1.2.2	Use of degenerate primer pairs to amplify peroxidase fragment	82
4.1.2.3	Screening of <i>C. roseus</i> yeast elicited cDNA library for cloning of <i>CrInt1</i> full-length	85
4.1.2.3.1	Construction of yeast elicited cDNA library	85
4.1.2.3.2	Screening of <i>C. roseus</i> yeast elicited cDNA library	85
4.1.2.4	Purification of clones with insert and characterization of the library of inserts	86
4.1.2.5	In vivo excision, plasmid isolation and size estimation of the selected clones	87
4.1.2.6	Sequence analysis of the full-length <i>C. roseus</i> peroxidases cDNAs	87
4.1.2.7	Introns and exons in <i>CrPrx</i> genomic clone	90
4.1.2.8	Phylogenetic analysis	91
4.1.2.9	Gene copy number of <i>CrPrx</i>	94
4.1.2.10	Expression pattern of <i>CrPrx</i> in <i>C. roseus</i>	95
4.1.2.10.1	Tissue specific expression of the <i>CrPrx</i> gene	95
4.1.2.10.2	Tissue specific protein profile of <i>CrPrx</i>	95
4.1.2.10.3	Stress regulation of <i>CrPrx</i> gene	96
4.1.2.11	Total peroxidase activity profile in <i>C. roseus</i>	98
4.1.2.12	Subcellular localization of <i>CrPrx</i> using GUS-GFP- <i>CrPrx</i> fused protein	100
4.1.3	Discussion	102
4.1.4	Conclusion	103
4.2:	Cloning of two novel peroxidase <i>Prx3</i> and <i>Prx4</i> genes from <i>Catharanthus roseus</i>	104-125
4.2.1	Introduction	104
4.2.2	Results	104
4.2.2.1	Cloning of partial peroxidase genes using degenerate PCR	104
4.2.2.2	Cloning of full length <i>Prx3</i> and <i>Prx4</i> genes	105
4.2.2.3	Bioinformatics analysis of <i>Prx3</i> and <i>Prx4</i>	107
4.2.2.4	Gene copy number of <i>Prx3</i> and <i>Prx4</i>	108
4.2.2.5	Phylogenetic analysis of <i>Prx3</i> and <i>Prx4</i> with the selected peroxidase sequences from peroxidase database	109
4.2.2.5.1	Phylogenetic relationship based on the cellular localization	109
4.2.2.5.2	Phylogenetic relationship with the class III peroxidase sequences categorized on the basis	111

	of stress regulation	
4.2.2.5.3	Phylogenetic analysis based on tissue specific expression	115
4.2.2.6	The <i>Prx3</i> and <i>Prx4</i> expressed differentially in different tissues	120
4.2.2.7	Localization studies with <i>Prx3</i> -GFP fusion protein in <i>Nicotiana tabacum</i>	121
4.2.3	Discussion	121
4.2.4	Conclusion	125
4.3:	Ectopic expression of two differentially localized <i>Catharanthus roseus</i> peroxidases <i>CrPrx</i> and <i>CrPrx1</i> genes in <i>Nicotiana tabacum</i>	126-143
4.3.1	Introduction	126
4.3.2	Results	127
4.3.2.1	Construction of binary vector for overexpression of <i>CrPrx</i> and <i>CrPrx1</i> in tobacco	127
4.3.2.2	Preparation of transgenic tobacco plants	128
4.3.2.3	Southern blot analysis of selected transgenic lines	129
4.3.2.4	Growth rate of the selected transgenic tobacco lines grown in green house under controlled condition	130
4.3.2.5	Expression analysis of <i>CrPrx</i> and <i>CrPrx1</i> in transgenic tobacco	131
4.3.2.6	Estimation of oxidative stress tolerance of the transformed plants overexpressing peroxidase	132
4.3.2.7	Assay of peroxidase activity in transgenic tobacco	133
4.3.2.8	Effect of peroxidase overexpression on photosynthesis of tobacco plants	134
4.3.2.8.1	Measurement of quantum efficiency (Fv/Fm) of photosystem II	134
4.3.2.8.2	Measurement of effective quantum yield ($\Delta F/F_m'$) of photosystem II	135
4.3.2.9	Evaluation of T1 generation transgenic tobacco	135
4.3.2.9.1	Effect of Salt stress on germination	135
4.3.2.9.2	Effect of dehydration stress on seedling germination	137
4.3.2.9.3	Cold stress and its effect on transgenic seedlings	137
4.3.3	Discussion	140
4.3.4	Conclusion	143

4.4	Overexpression and down regulation of two differentially localized peroxidase <i>CrPrx</i> and <i>CrPrx1</i> genes in <i>Catharanthus roseus</i> leaf induced calli lines	144-170
4.4.1	Introduction	144
4.4.2	Results	147
4.4.2.1	Overexpression and Suppression of <i>CrPrx</i> and <i>CrPrx1</i>	147
4.4.2.1.1	Construction of Chimeric <i>CrPrx</i> and <i>CrPrx1</i> sense gene in pBI121 vector	147
4.4.2.1.2	Antisense T-DNA construction	147
4.4.2.2	Transformation of <i>C. roseus</i> leaf disk and generation of leaf calli	150
4.4.2.3	Screening of transgenic <i>C. roseus</i> leaf calli	150
4.4.2.4	Morphological features of the transgenic lines	152
4.4.2.5	Expression and down regulation of <i>CrPrx</i> and <i>CrPrx1</i> in <i>C. roseus</i> calli lines	154
4.4.2.6	Study of growth index in selected transgenic calli lines	155
4.4.2.7	Guaiacol peroxidase activity assays with transgenic calli	156
4.4.2.8	Estimation of total alkaloid and targeted MIAs in transgenic calli	158
4.4.2.9	Alkaloid profiles in transgenic calli lines with <i>CrPrx</i> sense and antisense construct	158
4.4.2.10	Alkaloid profiles in transgenic calli lines with <i>CrPrx1</i> sense and antisense construct	160
4.4.2.11	Expression profile of MIA biosynthetic pathway genes in selected transgenics calli	162
4.4.3	Discussion	166
4.4.4	Conclusion	170
Chapter 5:	Summary	171-173
Chapter 6:	References	174-192
Appendix	Published paper	

CHAPTER 1



General Introduction

“*Jagatyevam anoushadham na kinchit vidyate dravyam vashaannarthayagayoh*”, this verse from ancient Indian literature rightly says that there is nothing in this universe, which is non-medicinal, which cannot be made use of for many purposes by different modes. *Catharanthus roseus* is also one of such very important medicinal plants. Periwinkle (*Catharanthus roseus* (L.) G. Don, synonym *Vinca rosea* L., *Lochnera rosea* Reich.) is a tropical perennial plant, native to Madagascar and it belongs to Apocynaceae family. Presently, it is mainly grown in tropical and subtropical regions. The name of the plant was given by George Don and its taxonomy was defined in 1956 (Gupta, 1977; Kohlmüzer, 1968). *C. roseus* produces a wide range of secondary metabolites, some of which present high therapeutic values such as antitumoral monoterpene indole alkaloids (MIAs), vinblastine and vincristine, and the hypotensive MIA, ajmalicine. Samira et al. (2006) has shown that a complex multicellular organization of the MIA biosynthetic pathway occurred in *C. roseus* aerial organs. Biosynthesis of vinblastine is very complicated and rather difficult. In *C. roseus*, biosynthesis of vinblastine begins with the amino acid tryptophan and monoterpene geraniol. It requires the involvement of at least 35 intermediates, 30 enzymes, 30 biosynthetic and at least 2 regulatory genes, and 7 intra and intercellular compartments (van der Heijden et al., 2004) (Fig. 1.1). The precursors for monoterpene indole alkaloid (MIA) pathway are obtained from shikimate and mevalonate pathways of primary metabolic pool which provide tryptophan and secologanin respectively (Facchini, 2001). Secologanin constitutes the terpene moiety of the MIAs and is a highly oxygenated multifunctional iridoid glucoside. Its biosynthesis starts with geranyl diphosphate (GPP), which is built from two isoprene units via terpene biosynthesis. GPP is subsequently hydrolyzed and oxidized to 10-hydroxy-geraniol. Finally secologanin is obtained via several partly unknown intermediates. Tryptamine which provides indole moiety of the pathway formed by decarboxylation of tryptophan and comes from shikimate pathway. Tryptamine and secologanin is then condensed in a reaction catalyzed by the enzyme strictosidine synthase (STR) (Kutchan, 1993). The product, gluco-alkaloid strictosidine, is the building block for 3000 different alkaloids. This large number is made possible by the reactive aglycone, which arises after hydrolysis of strictosidine by enzyme strictosidine glucosidase (SGD). The resulting unstable strictosidine-aglycone is biochemically converted by mostly uncharacterized enzyme reactions leading to cathenamine. Cathenamine is the branching point for several MIA sub pathways including ajmalicine-serpentine, and catharanthine and vindoline, the two monomeric precursors of the final dimeric MIAs vinblastine and vincristine (Fig. 1.1).

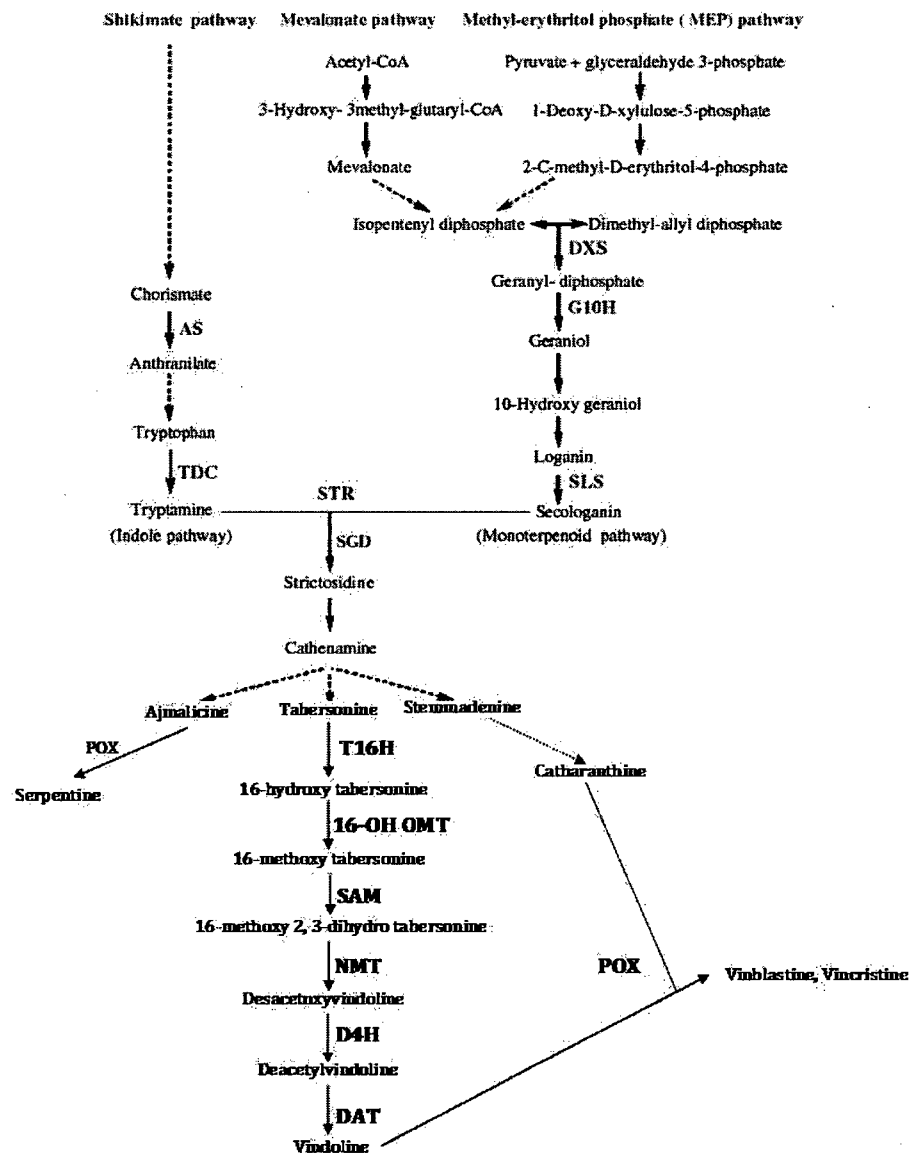


Fig. 1.1: Monoterpenoid indole alkaloid Pathway (MIA). Schematic diagram of MIA pathway. DXS 1-deoxy-D-xylulose-5-phosphate, G10H geraniol 10-hydroxylase, SLS secologanin synthase, AS anthranilate synthase α -subunit, TDC tryptophan decarboxylase, STR strictosidine synthase, SGD strictosidine β -glucosidase, SAM (S-adenosyl-L-methionine), POX Peroxidase, T16H tabersonine 16-hydroxylase, D4H desacetoxyvindoline-4-hydroxylase, DAT deacetylvindoline 4-O-acetyltransferase; 16-hydroxytabersonine O-methyltransferase (OMT). 2, 3-dihydro-3-hydroxytabersonine- N-methyl transferase (NMT), deacetylvindoline 4-O-acetyltransferase. (D4H) desacetoxyvindoline 4-hydroxylase, (DAT) deacetylvindoline 4-O-acetyltransferase.

Furthermore the NADPH-dependent cathenamine reductase leads to conversion of catharanthine to ajmalicine which is subsequently oxidized by peroxidase to form serpentine. The bisindoles are derived from the coupling of catharanthine and vindoline. Catharanthine is thought to be formed from strictosidine via 4, 21- dehydrogeissoschizine, stemmadenine and dehydrosecodine but it remains

still unclear (van der Heijden et al., 2004). The transformation of tabersonine to vindoline involves six strictly ordered reactions (De Luca et al., 1998) involving enzymes T16H (tabersonine 16-hydroxylase), SAM (S-adenosyl-L-methionine), 16-hydroxytabersonine O-methyltransferase (OMT), 2, 3-dihydro-3-hydroxytabersonine-N-methyl transferase (NMT), (D4H) desacetoxyvindoline 4-hydroxylase and (DAT) deacetylvindoline 4-O-acetyltransferase. The enzyme anhydrovinblastine synthase couples catharanthine and vindoline to yield AVLB. AVLB synthase had been purified and characterized from *C. roseus* leaves. This heme protein has a molecular weight of 45 kDa and shows peroxidase activity (Sottomayor et al., 1998). Later on gene responsible for coding of peroxidase was reported to be *CrPrx1* (Costa et al., 2008).

Peroxidases are divided into three classes: I, II and III. Among these class III plant peroxidases are present in all land plants. They are members of a large multigenic family. In their regular catalytic cycle, class III plant peroxidases catalyze the reduction of H₂O₂ by taking electrons to various donor molecules such as phenolic compounds, lignin precursors, auxin or secondary metabolites (Hiraga et al., 2001). Their encoding genes form large multigenic families (Tognolli et al., 2002; Duroux and Welinder, 2003; Passardi et al., 2004a) that are present in all green plants except unicellular green algae (Passardi et al., 2004a). Apart from secondary metabolism, peroxidases are also involved in the early stage of germination to final step of senescence, through control of cell elongation, defence mechanisms, and several other roles (Passardi, 2005).

Peroxidases are known in the evolutionary history for their action as protection from free radicals so that land colonization of earlier plants can be feasible. Due to their versatile nature, a number of isoforms reported from various plants e.g. *Arabidopsis* contains 73 class III peroxidases and rice contain 138 peroxidases in nature (Welinder et al., 2002 and Passardi et al., 2004). At least 12 isoforms of peroxidase had also been reported in database from tobacco. Recently a vacuolar class III peroxidase gene had been reported from *C. roseus* (Costa et al., 2008). In all these class III plant peroxidase reported the extension of amino acid stretch at C-terminal decides their vacuolar nature with an exception of barley peroxidase (BP1) where N-terminal is equally important.

Due to the presence of large number of isoforms in peroxidase, it is very difficult to assign a particular function for any one of them. The function of peroxidase is predicted on the basis of their subcellular localization. The peroxidases which are secreted outside the cell function in cell wall synthesis or suberization, similarly vacuolar targeted peroxidase has function in degradation of secondary metabolites. The peroxidase function is also correlated with expression pattern whether spatial or temporal in nature. Various techniques were utilized to study the structure and function of peroxidases. Schuller et al. (1996) reported the first complete structure of a class III peroxidase as peanut peroxidase at 2.7 Å resolution, which served as a model for other class III enzymes including the much studied horseradish peroxidase. Based on amino acid composition the peroxidase can be structurally defined as a single polypeptide chain containing 300 residues in length with a single non-covalently bound heme. They are also known as monomeric glycoproteins with four conserved disulfide bridges and two calcium ions. Structurally in all plant peroxidases 10 helices are commonly present with the additional three helices only present in class III peroxidases e.g. in horseradish peroxidase C1 subunit (HRPC) and peanut peroxidase (PNP). Out of three unique helices which is the insertion between helices F and G participate in interaction along the heme access channel (Fig. 1.2). This helices is variable between HRPC and PNP.

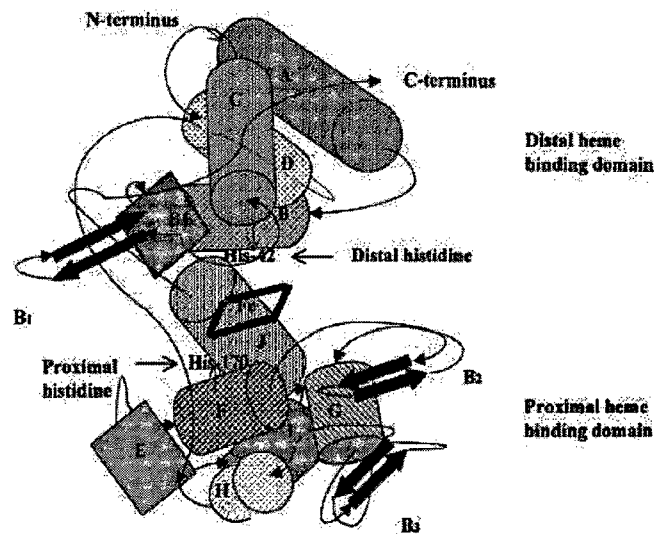


Fig. 1.2: A diagrammatic representation of the structure of plant peroxidase. Ten helices (A-J) and β -sheets (β_1 , β_2 , and β_3) are represented by cylinders and parallel arrows, respectively. Reverse turns and coils that connect the helices and β -sheets are shown as connecting lines. The proximal and distal heme-binding domains and the proximal and distal histidine residues (HRP-C numbering) are indicated. The rectangular box present between the proximal and distal heme-binding regions indicates the position of the central heme prosthetic group. (Adapted from Welinder, 1985).

Heterologous expression is a powerful tool to characterize structure and function of any gene. *E. coli* system is well studied system for heterologous expression of many genes. Crystallization studies for structural characterization were performed with *E. coli* expressed recombinant peroxidase genes (Østergaard et al., 2000; Henriksen et al., 2001). Bacterial expression system has also been utilized to know the substrate specificity of the peroxidases. Hushpalian et al. (2007) examined the role of the conserved glutamic acid residue in anionic plant peroxidases with regard to substrate specificity and stability. They showed that glutamic acid-141 is a heme ‘bodyguard’ in anionic tobacco peroxidase. Apart from bacterial expression several other system were also utilized for large scale protein production and baculovirus-insect cell system is one of them. Carpin et al. (2001) identified a Ca²⁺-pectate binding site on an apoplastic peroxidase by mutating four clustered arginine residues and expressing in baculovirus-insect cell system.

Peroxidases have been difficult to study through classical genetics and biochemistry. In plants functional characterization of gene can be elucidated by antisense, over expression or ectopic expression studies (Sherf et al., 1993; Lagrimini et al., 1990; Kawaoka et al., 2003). Sherf et al. (1993) reported that the constitutive, high level expression of antisense tomato anionic peroxidase genes (*tap1/tap2*) transcript in transgenic tomato plants prevented the wound, ABA and pathogen-induced accumulation of tap transcripts and hence, synthesis of the highly anionic peroxidase protein. They also found that abolishing of the highly inducible tap activity did not significantly inhibit suberization of the wound periderm of the tomato fruit. The over expression of anionic peroxidase by 10-fold in transgenic tobacco plants resulted in wilting (Lagrimini et al., 1990). In hybrid aspen, ectopic expression of a horseradish peroxidase enhanced growth rate and increases oxidative stress resistance (Kawaoka et al., 2003). These enzymes have also been found to get induced as defensive responses to wounding and against pathogen or insect attack. Although recent studies have provided some information regarding stress inducible responses of this enzyme, further studies are necessary to reveal regulatory mechanisms at the molecular level. Moreover the secondary metabolite biosynthetic pathways have also been reported to be induced under several biotic as well as abiotic stress conditions. With this background, the study of cloning and characterizing the gene encoding the peroxidase enzyme for the last dimerization step of MIA biosynthesis would be of

special significance to understand the regulation of the MIA pathway for finally engineering the production of dimeric alkaloids.

In view of the above, the different objectives that were proposed are defined below:

1. Isolation of full length peroxidase cDNA clones and their functional characterization.
2. Expression of *C. roseus* peroxidase cDNA in heterologous system
3. Over expression of peroxidase and study of accumulation of dimeric alkaloids in leaf specific cell lines.

CHAPTER 2



Review of Literature

The most fascinating property of plants is that in spite of being immobile; they are capable of facing and surviving challenges of biotic and abiotic adversities on their stride. This capability of elegantly defending and responding precisely in plants is relatable to their ability to synthesize an array of phytochemicals as secondary metabolites.

Plants synthesize a vast range of organic compounds that are traditionally classified as primary and secondary metabolites, although the precise boundaries between the two groups can in some instances be somewhat blurred. Primary metabolites are compounds that have essential roles associated with photosynthesis, respiration, growth and development. These include phytosterols, acyllipids, nucleotides, amino acids and organic acids. Other phytochemicals, many of which accumulate in surprisingly higher concentrations in some species are referred to as secondary metabolites. Secondary metabolites are structurally diverse and many are generated by a limited number of species within the plant kingdom. Although ignored for long, their function in plants is now attracting attention as some appear to play a key role in protecting plants from herbivores and microbial infection, as attractants for pollinators and seed dispersing animals, as allelopathic agents, UV protectants and signal molecules in the formation of nitrogen fixing root nodules in legumes. Secondary metabolites are also of interest because of their use as dyes, fibres, glues, oils, waxes, flavouring agents, drugs and perfumes, and they are viewed as potential sources for natural drugs, antibiotics, insecticides and herbicides (Croteau et al., 2000; Dewick, 2002).

2.1 *Catharanthus roseus* and its importance as alkaloid producing plant

The red or Madagascar periwinkle *Catharanthus roseus* (L.) G. Don - syn. *Lochnera rosea* (L.) Reichb. f. or *Vinca rosea* (L.), representative of the family Apocynaceae, originates in the tropical forests of Madagascar and is now found pan-tropically. It is currently cultivated in China, India, Madagascar, Israel, United States and in all countries of central and southern Europe. The name of the plant was given by George Don and its taxonomy was defined in 1956 (Gupta, 1977; Kohlmüzer, 1968). In the tropical and subtropical zones, these plants reach a height of 30–120 cm. The phytochemistry, biology and methods of the culture of *Catharanthus roseus* have been intensely investigated from 1950s (Moreno et al., 1995). *C. roseus* is a small

shrub with single or slightly branched stems; flowers are produced in the upper (Buchwald et al., 2007). The main root of the periwinkle is white, 20-40 cm long, and scarcely branched. Stem is erect, cylindrical, green or reddish in colour, woody and branched near the base. It grows to a height of about 1 m (in Europe 40-80 cm), and spreads out over an area of about 0.6-0.7 m along with main diameter. It tends to recline for a short way up in its early stages of growth before becoming erect. Opposite leaves, have a short petiole, are ovate-elliptical or lanceolate with an acute or sub-acute apex. The upper surface of the leaves is oil-green, shiny, glossy and glabrous while lower one is paler and opaque. Flowers of *C. roseus* are pedicellate, growing singly or two-by-two on short peduncles at the apex or from the leaf axils (Buchwald et al., 2007). Calyx is funnel-like while corolla is tubular, which ranges from pure white to deep pink, with obovate lobes. The fruit is follicle in nature which splits early. Seeds are 3 mm long, 1 mm wide, black, and characteristically grooved on the surface, with a mass 2-2.4 g of 100 seeds. In temperate zones, alkaloid content of the leaves is the highest at the end of summer (middle of September). Periwinkle (as an annual herb) has a long vegetation period. The first ripe fruits appear within 180-200 days of sowing. The plants develop slowly after sprouting. In India, flowering takes place continuously from the middle of March to the first frosts (Mishra et al., 2001). Periwinkle requires lot of warmth with an optimum temperature for germination of 20-22⁰C and an average temperature of 18⁰C and more required in the later stages of growth. Development of plant ceases at 10⁰C, and the plant freezes at 0⁰C. The general temperature requirements are 10-34⁰C, with an optimum temperature requirement of 20-30⁰C. It requires lots of water with a minimum requirement of 800-1000 mm of precipitation during the vegetation period. Annual rainfall requirements are 800-1400 mm, with an optimum between 100-1200 mm. *C. roseus* grows adequately on those soils which are somewhat loose, have good structure, are easily warmed and have good water-exploitation ability. Soils should be rich in nutrients and pH requirements are 5.5-7.5, with an optimum of 6-7. The Madagascar periwinkle is a tender species, growing outdoors in warmer regions of the World and requires a greenhouse in cooler areas in order for maintenance of optimum control of both temperature and moisture.



Fig. 2.1: Diagrammatic representation of *C. roseus* plant with seeds and fruits.

C. roseus has been historically used to treat a wide assortment of diseases. European herbalists used the plant for conditions as varied as headache to a folk remedy for diabetes. It has more than 130 known alkaloids, some of which are approved as antineoplastic agents to treat leukemia, Hodgkin's disease, malignant lymphomas, neuroblastoma, rhabdomyosarcoma, Wilms' tumor and other cancers. Extracts from the dried or wet leaves of plants are applied as a paste on wounds in some rural communities. In various countries the use of this plant in folk medicine in different preparations are described in detail in table 2.1.

Table 2.1: Important traditional medicinal uses of *C. roseus.**

Country	Part of plant used	Disease cured	Method of use
India	Whole plant	Cancer, Hodgkin's, menorrhagia and diabetes	Hot water extracts of dried entire plants
	Nodes	Cuts and wounds	Pulp of nodes mixed with cow dung and used externally
Australia	Leaves	Menorrhagia, diabetes	Hot water extract of dried part
	Root bark	Febrifuge	Hot water extract of dried part
Brazil	Root	Fever and malaria	Decoction of dried root
China	Aerial parts	Menstrual regulator	Hot water extract of dried part
France	Leaves	Antigalactagogue	Hot water extract of dried part
Kenya	Root	Stomach problem	Decoction of dried root

Pakistan	Ovule	Diabetes	Hot water extract of dried part
Peru	Entire plants	Heart disease, leishmaniasis, cancer	Hot water extract of dried part
Phillippines	Root	Emmenagogue	Hot water extract of dried part
	Leaves	Diabetes, amenorrhea and menorrhagia	Hot water extract of dried part
	Root	Abortion, emmenagogue, dysmenorrheal	Hot water extract of dried part
USA	Leaves	Euphoriant	Dried leaves smoked
Venda	Root	Venereal disease	Water extract of dried root

*Source: Medicinal Plants of the world: An illustrated scientific guide to important medicinal plants and their uses (Wink, 2004).

The main reason for the interest in *C. roseus* is its ability to synthesize a wide range of Monoterpenoid Indole Alkaloids (MIAs) which are valued due to their wide spectrum of pharmaceutical effects. The types of medicinal effects that are of particular importance to us are: diuretic (vindoline, catharanthine), antihypertensive (ajmalicine, serpentine), and anticancer (vinblastine and vincristine) (Kohlmüzer 1968). The plant possesses a large number of (MIAs), with over 130 compounds isolated and identified (Verpoorte et al., 1997; Samuelsson, 1999). Total alkaloid concentration in root amounts to 2–3% or reaches up to 9% in fibrous roots, whereas leaves contain ca 1% of alkaloids. A very small amount of these compounds is found in the flowers as well. The anticarcinogenic indoles, vinblastine (VLB) and vincristine (VCR)—used in leukemias and lymphomas are present in leaves while ajmalicine, used as antihypertensive (for the circulatory disorders, high blood pressure and related maladies) or sedative agents, is contained in roots. VLB and VCR occur in very low concentrations of 20 mg to 1 gram per ton in plant material, respectively (Tyler, 1988), but they are still considered as the most interesting chemotherapeutic compounds currently accessible for clinical use (Pezzuto, 1997). Vincristine and vinblastine are derived from the condensation of the monoterpenoids, catharanthine and vindoline. Other compounds synthesized by *C. roseus*, such as vindoline and

catharanthine, possessing diuretic properties, are present in leaves and roots, respectively (Parrek et al., 1981). The total amount of *C. roseus* material in trade is not known; however, figures from Madagascar indicate an annual export of about 1000 tonnes. The price paid for vincristine is reported to reach US\$ 200,000/kg. In another estimate, the worldwide trade in vincristine is worth about US\$ 50 million per year. The concentration of both vinblastine and vincristine in the plant material (leaves, roots) is very low, 0.0005 percent on a dry weight basis. Therefore, huge quantities have to be harvested, in order to obtain a substantial amount of alkaloids. For the production of 3 kg of Vinca alkaloids, which is the annual need worldwide around 300 tonnes of plant material has to be extracted (Verpoorte et al., 1993).

2.2 Monoterpenoid Indole Alkaloid pathway and its localization in plant system

As stated before, the importance of *C. roseus* is due to the presence of MIA pathway which leads to the production of more than 130 alkaloids among which the most important compounds are vincristine and vinblastine known for their antitumoral properties. The overall pathway presents a multiblock construction involving several sub-pathways, i.e. the indole pathway, the methylerythritol phosphate (MEP) pathway, the monoterpene-secoiridoid pathway and the MIA pathway itself (Fig. 2.2). The indole pathway is derived from the shikimate pathway, with chorismate being the branching point between the indole pathway leading to the biosynthesis of the indolic precursor of MIAs (tryptamine), and diverse metabolic routes such as the phenylpropanoid pathway (lignins, lignans, flavonoids). For the indole pathway which provides the indole moiety, two *C. roseus* cDNAs have been cloned and functionally characterized to encode enzymes involved in the first and last steps of the pathway, respectively: the anthranilate synthase α -subunit (ASA; Bongaerts, 1998) and tryptophan decarboxylase (TDC; De Luca et al., 1989) (Fig. 2.2, Table 2.2).

Table 2.2: MIA-related enzymes for which cloning and/or enzymatic activity have been reported in *C. roseus*.

Pathway / branch Genes and/or enzymes	Abbreviations	GenBank accession number	Reference
Indoles			
Anthranilate synthase α - subunit	ASA	AJ250008	Bongaerts, (1998)
Tryptophan decarboxylase	TDC	X67662	De Luca et al. (1989)
Methyl erythritol phosphate			
1-Deoxy-D-xylulose 5- phosphate synthase	DXS	AJ011840	Chahed et al. (2000)
1-Deoxy-D-xylulose 5- phosphate reductoisomerase	DXR	AF250235	Veau et al. (2000)
2C-Methyl-D-erythritol 2,4- cyclodiphosphate synthase	MECS	AF250236	Veau et al. (2000)
(E)-4-hydroxy-3-methylbut-2- enyl diphosphate synthase	HDS	AY184810	Unpublished
Monoterpene-secoiridoids			
Geraniol 10-hydroxylase (CYP76B6)	G10H	AJ251269	Collu et al. (2001)
Cytochrome P450-reductase	CPR	X69791	Meijer et al. (1993b)
10-Hydroxygeraniol oxidoreductase	10HGO	AY352047	Unpublished
7-Deoxyloganin 7- hydroxylase	DL7H		
Secologanin synthase (CYP72A1)	SLS	L10081	Irmmler et al. (2000)
Monoterpene indole alkaloids			
Strictosidine synthase	STR	X53602	McKnight et al. (1990)
Strictosidine b-glucosidase	SGD	AF112888	Geerlings et al. (2000)

Minovincinine 19-hydroxy- Oacetyltransferase	MAT	AF253415	Laflamme et al. (2001)
Tabersonine 16-hydroxylase (CYP71D12)	T16H	AJ238612	Schroder et al. (1999)
16-Hydroxytabersonine O- methyltransferase	16-OMT	EF444544	Levac et al. (2008)
2,3-Dihydro-3- hydroxytabersonine-N-methyl transferase	NMT		Dethier and De Luca, (1993)
Desacetoxyvindoline-4- hydroxylase	D4H	AF008597	Vazquez-Flota et al. (1997)
Deacetylvindoline 4-O- acetyltransferase	DAT	AF053307	St-Pierre et al. (1998)
Peroxidase	CrPrx1	AM236087	Costa et al. (2008)

The MEP pathway is a novel plastidic pathway involved in the production of isopentenyl diphosphate (IPP), previously thought to be solely synthesised via the cytosolic mevalonate pathway (Lichtenthaler et al., 1997; Lichtenthaler, 1999; Rodríguez-Concepción and Boronat, 2002). The pool of IPP synthesised through the MEP pathway is further used to fuel different primary metabolic syntheses, such as chlorophylls (phytol moiety), carotenoids, gibberellins and abscisic acid (Kasahara et al., 2002; Lichtenthaler et al., 1997; Lichtenthaler, 1999). In *C. roseus*, IPP derived from the MEP pathway is also incorporated in MIAs (Contin et al., 1998; Chahed et al., 2000; Veau et al., 2000; Oudin et al., 2007a). To date, four *C. roseus* cDNA sequences involved in MEP pathway have been cloned namely, 1-deoxy- D-xylulose 5-phosphate synthase (DXS; Chahed et al., 2000), 1-deoxy- D-xylulose 5-phosphate reductoisomerase (DXR; Veau et al., 2000), 2-C-methyl-D-erythritol 2,4-cyclodiphosphate synthase (MECS; Veau et al., 2000) and (E)-4-hydroxy-3-methylbut-2-enyl diphosphate preparation HDS or GCPE; Oudin et al., 2007b (Fig. 2.2, Table, 2.2).

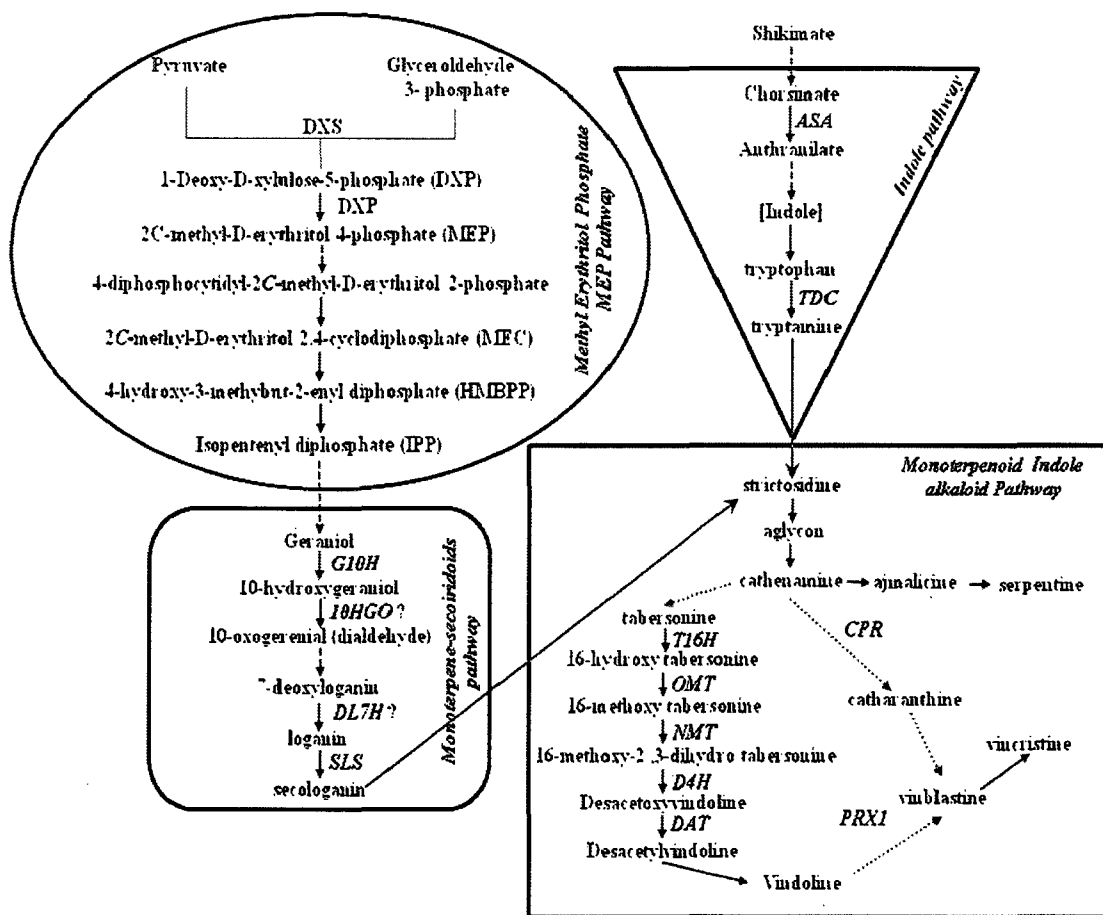


Fig. 2.2: Biosynthetic pathway of monoterpene indole alkaloids featuring cell-specific gene expression patterns in *C. roseus* aerial organs and roots. DXS, 1-deoxy-D-xylulose- 5-phosphate (DXP) synthase; DXR, DXP reductoisomerase; MECS, 2C-methyl-D-erythritol-2, 4-cyclodiphosphate (MEC) synthase; HDS (or GCPE), (E)-4-hydroxy-3-methylbut- 2-enyl diphosphate synthase; G10H (CYP76B6), geraniol 10-hydroxylase; CPR, cytochrome P450-reductase; 10HGO, 10-hydroxygeraniol oxidoreductase; DL7H, 7-deoxyloganin 7-hydroxylase; SLS (CYP72A1), secologanin synthase; ASA, anthranilate synthase α -subunit; TDC, tryptophan decarboxylase; STR, strictosidine synthase; SGD, strictosidine β -glucosidase; MAT, minovincinine 19-hydroxy-O-acetyltransferase; OMT, 16-hydroxytabersonine O-methyltransferase; NMT, 2,3-dihydro-3-hydroxytabersonine-N-methyl transferase; T16H (CYP71D12), tabersonine 16-hydroxylase; D4H, desacetoxyvindoline 4-hydroxylase; DAT, deacetylvindoline 4-O-acetyltransferase; PRX1, peroxidase. The localisation of the expression of the different genes primarily came from the following references: TDC, STR, D4H and DAT, St-Pierre et al., (1999); SLS, Irmeler et al. (2000); MAT, Laflamme et al. (2001); DXS, DXR, MECS and G10H, Burlat et al. (2004). Solid lines indicate a single (enzymatic) step, whereas dashed lines indicate a poorly known pathway.

A soluble vacuolar strictosidine synthase (STR) catalyses the stereospecific condensation reaction of tryptamine and secologanin into 3- α -(S)-strictosidine, a central precursor of several MIAs (reviewed by De Luca, 1993). The structural diversity of MIAs comes first from the deglycosylation of strictosidine by

strictosidine β -glucosidase (SGD). The resulting unstable strictosidine-aglycone is biochemically converted by mostly uncharacterized enzyme reactions leading to cathenamine. Cathenamine is the branching point for several MIA subpathways including Corynanthe, Iboga and Aspidosperma classes of alkaloids such as ajmalicine, catharanthine and tabersonine, respectively (Fig. 2.2). Some scientific reports support the occurrence and existence of a NADPH-dependent enzymatic activity of cathenamine reductase and peroxidase involved in the conversion of cathenamine to ajmalicine and ajmalicine to serpentine, respectively (Hemscheidt and Zenk, 1985; El-Sayed and Verpoorte, 2005). The steps involved in the catharanthine pathway still remain unclear (van der Heijden et al., 2004). However, the enzymatic reactions leading to synthesis of vindoline have been focus of extensive research and thus are well understood and known.

The vindoline branch of the pathway involves hydroxylation of tabersonine by cytochrome P450-dependent mono-oxygenase, tabersonine 16-hydroxylase (T16H) (Schröder et al., 1999; St-Pierre and De Luca, 1995), O-methylation via 16-hydroxytabersonine- 16-O-methyltransferase (16-OH OMT), followed by an uncharacterized conversion to 2,3-dihydro-16-methoxytabersonine, and by a chloroplast thylakoid-associated 2,3-dihydro-16-methoxytabersonine N-methyltransferase (NMT) reaction to yield desacetoxyvindoline. Desacetoxyvindoline 4-hydroxylase (D4H) (Vazquez-Flota et al., 1997) and deacetylvindoline 4-O-acetyltransferase (DAT) (St-Pierre et al., 1998) catalyse the last two steps in vindoline biosynthesis. While several of these genes have been characterized, the three reaction steps between 16-hydroxytabersonine and desacetoxyvindoline have yet to be characterized in detail (van der Heijden et al., 2004).

2.2.1 Tissue specific localization of MIA pathway

All of the 36 chemically characterized *C. roseus* bisindole alkaloid (dimeric MIAs) have been extracted from aerial organs, mostly from leaves, and to a lesser extent from shoots and flowers (van der Heijden et al., 2004). One of the two precursors of dimeric MIAs, vindoline, has also been extracted from aerial organs and not from roots. Among the MIAs presented in figure 2.2, only strictosidine, ajmalicine and serpentine have been extracted from both roots and aerial organs. Some reports had shown to have extracted strictosidine, ajmalicine, serpentine, tabersonine,

minovincinine, and catharanthine using cell culture, callus culture and hairy root culture, but no reproducible production of vindoline or dimeric MIAs have been reported. Thus, looking at the metabolites themselves, it appears that a major part of the MIA pathway, including the final steps involved in the production of the dimeric MIAs, occur within aerial organs, and that a small subset of the central part of the simplified pathway presented in figure 2.2 (i.e. from strictosidine to serpentine) is also present in roots. In agreement with these results, Northern blot analysis of the expression of genes involved in the pathway within plant organs revealed that 10 of the 11 genes studied are expressed in aerial organs, mostly in young parts of the plant, such as young developing leaves and flower buds (Fig. 2.2, Table 2.2). Only MAT showed no specific expression in such organs, as this particular gene was involved in a lateral root specific pathway from tabersonine to minovincinine (Fig. 2.2, Table 2.3; Laflamme et al., 2001). The absence of dimeric MIAs and one of their precursors (vindoline) within sub-aerial organs was further confirmed by the absence of root- and hairy root-specific expression of D4H and DAT, the genes involved in the last two last steps of vindoline biosynthesis (Table 2.3, Fig. 2.2). On the other hand, all the other genes involved in the earlier steps in the pathway showed both aerial organ-specific expression and root- or hairy root-specific expression (Table 2.3, Fig. 2.2). Even if partial analysis of proteins and the corresponding enzyme activity distribution within plant organs confirm that the end of the vindoline pathway is restricted to aerial organs, earlier enzymatic steps in the pathway show that vindoline pathway could also be found both in aerial organs and roots (Table 2.3, Fig. 2.2).

Table 2.3: Tissue-specific distribution of MIA-related mRNAs corresponding to enzymes and their corresponding enzymatic activities.

Pathway branch Gene/enzyme name abbreviations	Tissues mRNA distribution (Northern blot)																	
	C: Cotyledons, CC: cell culture, EC: Etiolated cotyledons, EH: Etiolated hypocotyls, Era: Etiolated radicles, ESd: Etiolated seedlings, F: Flowers, FB: Flower buds, Fr: Fruits, H: Hypocotyls, HRT: Hairy root tips, L: Leaves, P: Petals, R: Roots, Ra: Radicles, S: Stems, Sd: Seedlings, YL: Young leaves																	
	C	C	E	E	Er	ES	F	FB	F	H	HR	L	P	R	Ra	S	S	Y
	C	C	C	H	a	d			r		T						d	L
<i>Indoles</i>	De Luca et al., 1989; Pasquali et al., 1992; Collu et al., 2001																	
ASA																		
TDC		◇				◆							#		•			☼
<i>MEP</i>	Burlat et al., 2004; Courdavault et al., 2005; Chahed et al., 2000; Veau et al., 2000;																	
DXS		◇						■							•		§	☼
DXR		◇						■							•		§	☼
MECS		◇						■							•		§	☼
HDS																		
<i>Secoiridoids</i>	Collu et al., 2001; Burlat et al., 2004; Meijer et al., 1993b;																	
G10H		◇						■							•		§	☼
CPR		◇					♣					#		•		§		
10HGO																		
DL7H																		
SLS																		
<i>MIAs</i>	Pasquali et al., 1992; Collu et al., 2001; Geerlings et al., 2000; Laflamme et al., 2001; Schroder et al., 1999; Vazquez-Flota et al., 1997; Laflamme et al., 2001																	
STR		◇					♣					#		•				☼
SGD		◇					♣					#		•		§		
MAT						◆				▮	—			•				

T16H		◇															
OMT																	
NMT																	
D4H	◻		▲	■	♠			‡	▮		#			\$	§	♪	
DAT						♣					#	▶			§	♪	☀
CRPRX1						♣	▨	‡			#				§		☀

Cotyledons (◻), Cell culture (◇), Etiolated cotyledons (▲), Etiolated hypocotyls (■), Etiolated radicles (♠), Etiolated seedlings (◆), F Flowers (♣), Flower buds (▨), Fruits (‡), Hypocotyls (▮), Hairy root tips (—), Leaves (#), Petals (▶), Roots (●), Radicles (\$), Stems (§), Seedlings (♪), Young leaves (☀).

2.2.2 Sub-cellular localization of MIA pathway enzymes

Three main approaches have been used to study subcellular localization density gradient centrifugation, cytochemistry with chromogenic substrates, and immunocytochemistry. In some cases these approaches have showed contradicting results, e.g. STR has been found to localize both to cytoplasm as well as to the vacuole (De Luca and Cutler, 1987; McKnight et al., 1991; Stevens et al., 1993). Many sub-cellular compartments have been implicated in the MIA pathway. Although not all the studies mentioned have been performed in *C. roseus*, there have been reports of similar procedure in other plants e.g. the MEP pathway is well known to be localized to plastids (Lichtenthaler, 1999; Oudin et al., 2007a). Among Indoles, studies with density gradient centrifugation have shown that TDC is cytosolic. The secoiridoids like SLS, which is P450 enzyme has not been clearly localized, but sequence analysis has shown that the putative C-terminal ER membrane anchoring signal is absent in the SLS sequence (Irmiler et al., 2000). Generally the cytochrome P450 enzymes are localized to endoplasmic reticulum (ER) membrane, but some may be localized to other endo membranes such as plastid inner or outer envelopes (Froehlich et al., 2001; Watson et al., 2001) or mitochondria (Okuda, 1994). One study reported that both SLS substrate (loganin) and product (secologanin) are localized to the vacuole, surprisingly arguing for a tonoplast localization of SLS (Contin et al., 1999).

Table 2.4: Sub-cellular localization of MIA-related enzymes in *C. roseus* cells.

Pathway branch Gene/enzyme abbreviations	Sub-cellular localization	Technique used for localization	Reference
Indoles			
ASA TDC	Cytosol	Density gradient	De Luca and Cutler, (1987); Stevens et al. (1993)
MEP			
DXS	Plastids		
DXR	Plastids		
MECS	Plastids		
HDS	Plastids (not demonstrated in <i>C. roseus</i>)		
Secoiridoids			
G10H, CPR 10HGO, DL7H			
SLS	Substrate and product localized to the vacuole	No C-term Pro-rich motif (ER membrane anchoring signal?)	Irmeler et al. (2000); Contin et al. (1999)
MIAs			
STR	Cytosol Vacuole Vacuole	Density gradient Immunocytochemistry Density gradient	De Luca and Cutler, (1987) McKnight et al. (1991) Stevens et al. (1993)
SGD	Endoplasmic reticulum	Density gradient Cytochemistry	Gerlings et al. 2000
MAT			
T16H	Endoplasmic reticulum	Density gradient	St-Pierre et al. (1995)
OMT			
NMT	Cytoplasmic membrane	Density gradient	De Luca and Cutler, (1987)
D4H			
DAT	Cytosol	Density gradient	De Luca and Cutler, (1987)
CrPrX1	Vacuole	Cytochemistry	Costa et al. (2008)

It has been proposed that SGD and T16H (another P450 enzyme) localized to the ER and ER membranes, respectively (Geerlings et al., 2000; St-Pierre and De Luca, 1995). NMT has been proposed to be plastidic, while DAT has been co-eluted with cytoplasmic markers (De Luca and Cutler, 1987). An original approach using vindoline-specific antibodies in immunocytochemical localisation studies at the TEM level reported vindoline accumulation within the vacuole, small vesicles, and periphery of the cytoplasm (Brisson et al., 1992). Finally, cytochemical studies have suggested a vacuolar localization for CrPrx1 (Costa et al., 2008). On the basis of these results, some models have been proposed for the sub-cellular compartmentalization of the MIA pathway (van der Heijden et al., 2004). Only one of these models has been studied using immunocytochemistry (McKnight et al., 1991), and none has confirmed the enzyme localization in plant cells producing alkaloids by microscopy. There are several ways through which the localization of the pathway enzymes can be studied like immunogold labeling experiments in TEM which requires production of pure antibodies. An alternative or complementary method could be *Agrobacterium tumefaciens* mediated transient expression in *C. roseus* leaves or petals in fusion with a reporter protein like green fluorescence protein (GFP) under the control of a constitutive or a cell specific promoter. Such a method allows accurate visualization of the green fluorescence by confocal microscopy, as well as the sub-cellular localization of several fusion proteins with the same GFP specific antibody in TEM.

2.3 Involvement of peroxidase in MIA pathway

The importance of the TIA pathway is due to its final product viz. anticancer drugs vincristine and vinblastine. The structural elucidation of vinblastine and vincristine showed that they were dimeric MIAs, of which one moiety corresponds to the unaltered structure of vindoline and the other moiety closely resembles catharanthine (Fig. 1.1). In face of these structural similarities and their natural abundance, vindoline and catharanthine were immediately considered as monomeric precursors of the dimeric alkaloids, later confirmed by feeding experiments (Gröger, 1985; Schütte, 1986; Meijer et al., 1993a). Semi synthetic process for the synthesis of dimerics with natural configuration was reported successfully for the first time by Potier et al. (1975) through a modified Polonovski reaction. In this reaction, catharanthine N-oxide was treated with trifluoroacetic anhydride in the presence of vindoline, leading

C5-C18 skeletal fragmentation of catharanthine (Fig. 2.3), followed by nucleophilic attack of the C18 position by vindoline, and formation of coupling bond (Potier et al., 1975; Langlois et al., 1976). The modified Polonovski reaction later called the Potier-Polonovski reaction, resulted in the formation of an unstable iminium dimer which after reduction with NaBH₄, yielded α -3', 4'-anhydrovinblastine (Fig. 2.3).

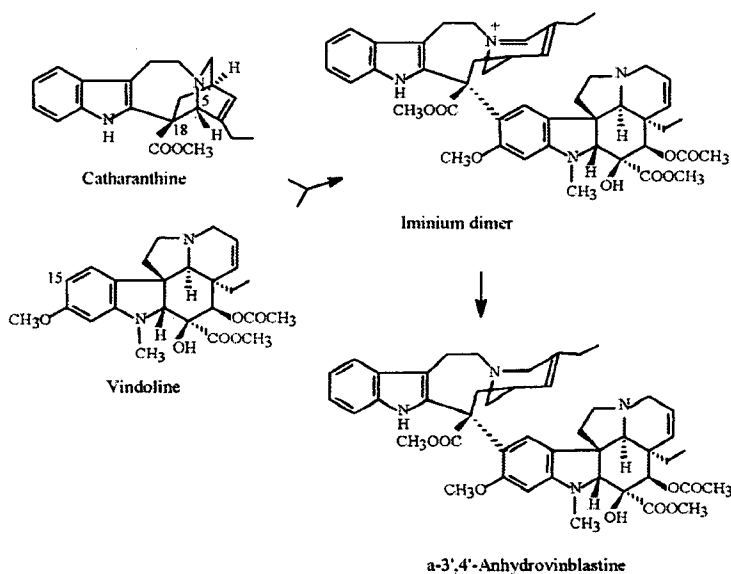


Fig. 2.3: Biosynthesis of α -3', 4'-anhydrovinblastine from the monomeric precursors catharanthine and vindoline. The coupling of catharanthine and vindoline originates an unstable iminium cation that is reduced to yield α -3', 4'-anhydrovinblastine (Sottomayor et al., 2004).

The chemical coupling of catharanthine and vindoline to yield anhydrovinblastine led to the obvious hypothesis that this compound might also be the first product of dimerization in the plant, and the dimeric precursor of vinblastine and vincristine. Scott et al. (1978), isolated anhydrovinblastine with incorporation of radiolabeled catharanthine and vindoline from *C. roseus* plants, thus proving that anhydrovinblastine is converted into vinblastine and other dimeric alkaloids, confirming its role as a precursor of the anticancer alkaloids (Stuart et al., 1978; Baxter et al., 1979, 1982). The exact biosynthetic pathway from the monomeric precursor to vinblastine and other dimeric alkaloids confirming its role as precursors to vinblastine and vincristine has not been completely determined. However, it is hypothesized that both anhydrovinblastine and iminium ion are interconvertible i.e. both can be incorporated into vinblastine and vincristine.



TH-16448

615.32
K9605
cl

The search for the enzyme responsible for the dimerization reaction resulted in the finding that peroxidase-like activities extracted from cell suspension cultures were capable of performing the coupling of catharanthine and vindoline into dimmeric iminium ion easily reduced to anhydrovinblastine (Endo et al., 1988; Misawa et al., 1988; Smith et al., 1988). Horseradish peroxidase, a commercial plant peroxidase was also capable of performing the coupling reaction (Goodbody et al., 1988).

Finally anhydrovinblastine had been proved actually to be a major alkaloid present in *C. roseus* leaves, representing together with catharanthine and vindoline, the three major alkaloids of the plant (Balsevich and Bishop, 1989; Naaranlahti et al., 1991; Sottomayor et al., 1998). This indicated the presence of high *in vivo* dimerization activity in leaves.

A single purification step of chromatography on phenyl-sepharose CL-4B, leads to a pool of fractions in which dimerizing as well as peroxidase activity was shown and the activity strictly depended on the presence of H₂O₂. This further indicated the nature of the peroxidase as coupling enzyme (Sottomayor et al., 1996). Further purification of fraction showed dimerizing activity leading to the isolation of CrPrx1 protein with an estimated molecular weight of 45,400 by SDS-PAGE (Sottomayor and Ros Barceló, 2003).

The CrPrx1 showed an optimal pH of 6.5 for dimerization activity, but it also showed significant activity at 4-5 pH range, the pH range commonly found in plant vacuoles. Together with its dimerization activity, CrPrx1 also showed peroxidative activity towards several phenolics and alkaloid substrates (Sottomayor and Ros Barceló, 2003). The peroxidase activity was also observed towards vacuolar substrates like DOPA and ascorbate (Takahama, 1992). Later, *CrPrx1* was cloned and characterized for dimerizing as well as peroxidase activity (Costa et al., 2008). Tissue specific expression pattern of the *CrPrx1* revealed its absence in root tissue.

Peroxidases have also been implicated in oxidation of ajmalicine to serpentine. The striking conformity was shown between the time course of serpentine content and the activity of peroxidase in cultured cell (Blom et al., 1991). It was also found that ajmalicine can be converted efficiently into serpentine by peroxidase extracted from vacuoles and by intact isolated vacuoles (Blom et al., 1991). Misra et

al. (2006) established *in vitro* conversion of ^3H -ajmalicine into ^3H -serpentine by *C. roseus* root extracts.

2.4 Peroxidases and their presence in plant kingdom

Peroxidases are heme-containing enzymes ubiquitous in the plant kingdom. The term “peroxidase” means an enzyme catalyzing oxidoreduction between hydrogen peroxide and reductants ($\text{H}_2\text{O}_2 + \text{AH}_2 \rightarrow 2\text{H}_2\text{O} + \text{A}$). Peroxidases belong to a super family which comprises Class I enzymes from mitochondria, chloroplasts, and bacteria; Class II from fungi; and Class III from higher plants based on their structural and catalytic properties (Welinder, 1991; Chart 2.1).

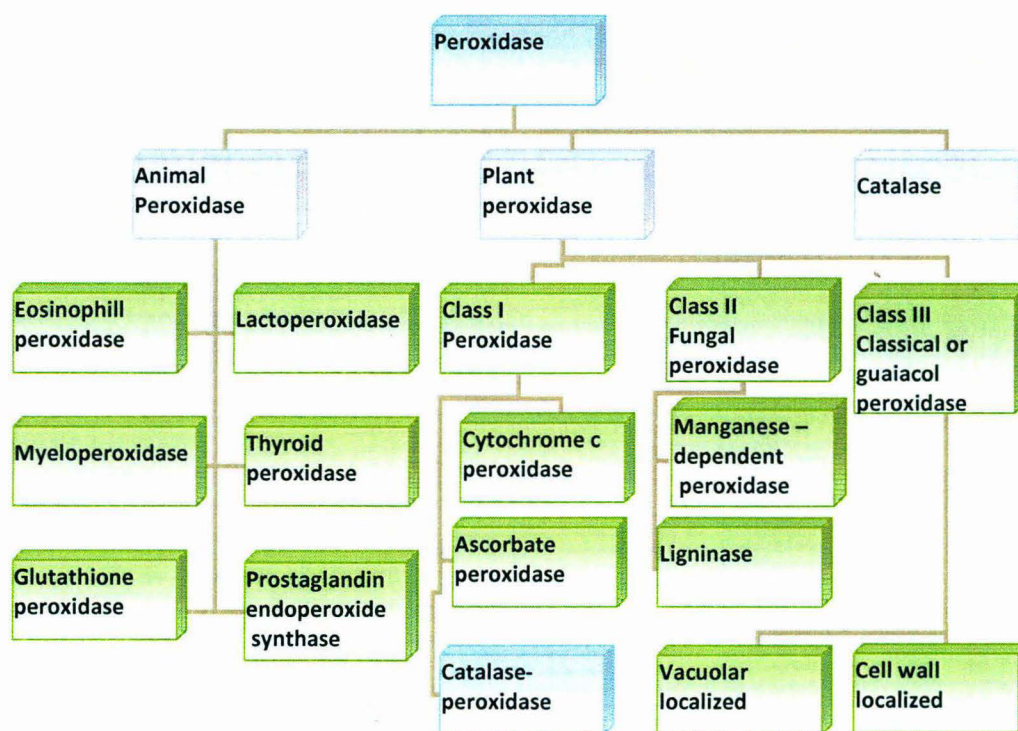


Chart 2.1: Classification of Peroxidases.

The first peroxidase superfamily consists of enzymes in animals such as glutathione peroxidase (EC 1.11.1.9), myeloperoxidase (EC 1.11.1.7), thyroid peroxidase (EC 1.11.1.7), eosinophil peroxidase (EC 1.11.1.7), lactoperoxidase (EC 1.11.1.7) and a partial region of prostaglandin endoperoxide synthase (EC 1.14.99.1). Although the glutathione peroxidase is categorized into animal peroxidase superfamily, its activity has also been detected in plants, and several cDNAs encoding its homologs have actually been isolated from plants (Churin et al., 1999).

The second peroxidase superfamily consists of catalases (EC 1.11.1.6) in animals, plants, bacteria and yeast. Although the active sites of myeloperoxidase and cytochrome c peroxidase (a member of the animal and plant peroxidase superfamilies respectively) have similar architectures, the overall primary sequences and 3-dimensional structures of these peroxidases are quite different, implying that these superfamily genes evolved from distinct ancestral genes (Taurog, 1999).

The amino acid sequences were found to be highly variable among the members of the plant peroxidase superfamily, with less than 20% identity in most divergent cases. Based on the differences in primary structure, the plant peroxidase superfamily can be divided further into three classes (Welinder 1992, classes I, II and III in Chart 1). Class I plant peroxidases include the intercellular enzymes in plants, bacteria and yeast, e.g. microbial cytochrome c peroxidase (EC 1.11.1.5), bacterial catalase-peroxidase (EC 1.11.1.6) and ascorbate peroxidase (EC 1.11.1.11). Ascorbate peroxidase was purified from bovine eye, and its N-terminal sequence was found to be homologous to that of plant enzymes, implying that ascorbate peroxidase is not plant-specific (Wada et al., 1998). Class II plant peroxidases are extracellular peroxidases from fungi, including lignin peroxidase (EC 1.11.1.14) and Mn²⁺-dependent peroxidase (EC 1.11.1.13). Class III plant peroxidase (EC 1.11.1.7), which were originally described as peroxidases, are plant enzymes that are secreted outside the cells or transported into vacuoles, peroxidase includes horseradish peroxidase, which is commercially available enzyme that is frequently conjugated to an antibody for chromogenic detection.

2.5 Structure of Class III plant peroxidase

Structurally class III peroxidase or guaiacol peroxidase have three highly conserved domains, the distal heme-binding domain, the central conserved domain of unknown function, and the proximal heme-binding domain (I, II and III in Fig. 2.4). Distal histidine is necessary for the catalytic activity; these histidine residues are present in all known heme-containing peroxidase sequences. Both the position and the arrangement of these domains are strictly conserved among peroxidases (Riechmann and Meyerowitz, 1998; Eulgem et al., 2000). The substrate and the resulting products are specific to the functioning of each peroxidase enzyme.



Fig. 2.4: Structural features of class III peroxidase. The features of a representative peroxidase, horseradish peroxidase isoenzyme C, are schematically presented according to the reported amino acid sequence (Welinder, 1976) and 3-dimensional structure (Gajhede et al., 1997). N-terminal signal peptide (SP) and C-terminal extension (CE) are indicated by gray boxes. Only vacuolar peroxidases contain CE. Filled boxes represent a conserved catalytic and distal heme-binding domain (I), a proximal heme-binding domain (III), and a central conserved domain (II) of unknown function (Buffard et al., 1990). The hatched box present a region presumed to be important for determining the specific function. Invariable distal histidine (Hd), proximal histidine (Hp) and eight cysteine residues (C1 to C8), which form a disulfide bond network as indicated, are shown above and below the boxes respectively.

Chittoor et al. (1999) showed a correlation between primary structure and the expression profile of pathogen. They compared a peptide region spanning from proximal heme-binding site to vicinity of the 7th invariable cysteine residue indicated by hatched box in (Fig. 2.4). This region is fundamentally divergent in length and sequence among peroxidases, and it forms a part of the substrate access channel in peanut and horseradish peroxidases (Schuller et al., 1996, Gajhede et al., 1997). Thus authors suggested that 40 to 50 C-terminal amino acids region from the proximal heme-binding site reflected the biological function of each peroxidase, namely the reactivity to the reductants.

2.6 Multiplicity of Peroxidase genes

Class III peroxidases are heme containing proteins generally encoded by large number of paralogous genes (Welinder, 1992). These large multigenic families are present in all land plants, but have not been detected in unicellular green algae (Passardi et al., 2004). From the appearance of the first class III peroxidase, probably around the emergence of the terrestrial plants 450 MY ago, to the most recently evolved plants, the number of gene copies have largely increased. *Arabidopsis* genome, known to harbor a high number of multigenic families and it contains 73 peroxidase genes (Tognalli et al., 2002; Welinder et al., 2002). In rice, 138 peroxidase genes were distributed among the 12 chromosomes (Passardi et al., 2004). This increase in number of peroxidase genes seems to be correlated with the evolution of the plant

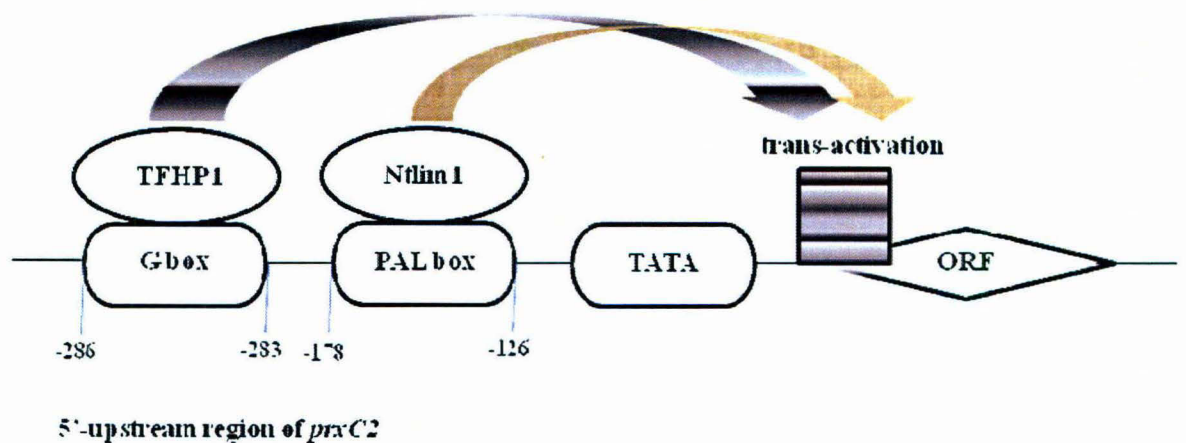
architecture and complexity, as well as with the diversity of the biotopes and the pathogens.

Multigenic families originate from gene duplications resulting from different mechanisms (Zhang, 2003): un-equal crossing-over, various transposition events, duplication of large chromosome segments or polyploidization. One of the transposition events, the retrotransposition of cDNA, is characterized by the loss of introns and the random insertion of regulatory sequences within the genome. In this case, duplicated genes are usually not transcribed and rapidly degenerate into pseudogenes (Casacuberta and Santiago, 2003). On the other hand, direct transposition sequences (without RNA intermediate) create new genes with higher chances to retain their functionality. Miniature inverted-repeat transposable elements (MITE) belong to this category. Their replication is probably mediated by a trans-acting transposase that recognise specific sequences present on every MITE called terminal inverted repeats (Casacuberta and Santiago, 2003). MITEs are extremely frequent in rice genome and are generally found in gene-rich regions (Mao et al., 2000). Finally segmental, chromosomal or whole genome duplications are relatively frequent in plants and are not a source of tandem repeats (Skrabanek and Wolfe, 1998; Zhang, 2003).

2.7 Regulation of peroxidases in plants

Expressions of plant peroxidase genes are complicated since they are regulated at different time and places by various kinds of biotic and abiotic stresses. The expression profiles of the peroxidase genes indicate possible roles of peroxidase in multiple physiological processes. A large number of studies, however have been conducted describing the temporal and spatial control of the expression of specific peroxidase genes: physical wounding induces the expression of rice *poxA* and *poxN* (Ito et al., 2000), tobacco *tpoxN1* (Hiraga et al., 2000), sweet potato *swpa1*, *swpa2*, *swpa3*, and *swpn1* (Huh et al., 1997; Kim et al., 1999), horseradish *prxC2* (Kawaoka et al., 1994b), and tomato *tap1/tap2* (Mohan et al., 1993b); phytohormone ABA induces the expression of pine *PpPrx75* (Charvet-Candela et al., 2002), duckweed basis peroxidase (Chaloupkova and Smart, 1994) and tomato and potato anionic peroxidase (Roberts and Kolattukudy, 1989); and cooling at 4⁰C induces the expression of sweet potato *swpa1*, *swpa2* and *swpa3*, but reduces the expression of

sweet potato *swpn1* (Huh et al., 1997; Kim et al., 1999). Information about the timing and tissue specificity of peroxidase gene expression is important, as it may reveal the real function of a specific peroxidase isozyme encoded by that gene. For example the expression profile of a *Sesbania rostrata* peroxidase (*SrPrx*) upregulated during nodulation implied that gene encodes a peroxidase isozyme that functions in nodulation process (Herder et al., 2007). Profiles of tissue-specific expression for a number of plant peroxidase genes were also compared to those of lignified tissues, since some specific plant peroxidases are thought to be important in the biosynthesis of lignin (Klotz et al., 1998). Some of these studies supported the role of plant peroxidases in lignin biosynthesis (Østergaard et al., 2000) while others suggested a role for plant peroxidase in defense, growth, and development (Klotz et al., 1998).



Source Yoshida et al. 2003

Fig. 2.5: Molecular mechanism of the regulation of horseradish *prxC2* promoter activity. Cis and trans acting factors of the wound-inducible *prxC2* promoter. The first cis element contains a *G-box* consensus, a common element found in promoter regions of several stress responsive genes; the second cis element was found to contain a sequence similar to *PAL-box* element, an elicitor-responsive cis element in the promoter of the parsley phenylalanine ammonia-lyase gene (Lois et al., 1989). A trans factor (*TFHP-1*) containing bZip and helix-loop-helix motifs that binds to G-box region, and a trans factor (*Ntlm1*) binds to the PAL-box region have been isolated.

There is however, only limited information is available regarding the mechanisms by which plants regulate specific expression of peroxidase genes. Promoter analysis in a heterologous host confirmed wound and fungus responsive activity of the legume *Shpx6b* promoter, which contains a motif similar to the methyl jasmonate (MeJA) responsive element (Curtis et al., 1997). Analysis of the rice *poxA* promoter in transgenic tobacco plant has revealed UV and wound-responsive *cis*

elements within 144 bp of the *poxA* translation start site (Ito et al., 2000). In the expression of the HRP (*prxC2*) gene, two cis elements and two cognate trans factors have been reported (Fig. 2.5) (Kawaoka et al., 1994; Kaothien et al., 2000). These two sets of cis elements and trans factors are important in both basal and wound-inducible activity of the *prxC2* promoter in transgenic tobacco plants (Kaothien et al., 2002). Different peroxidases regulated as a result of induction by different environmental factors are listed in table 4.5.

Table 4.5: List of principal plant peroxidase genes.

Plant	Gene	Expression and/or functional analysis	Reference
<i>Picea abies</i>	<i>SPI2</i>	Pathogen inducible	Fossdal et al. (2001)
<i>Gossypium hirsutum</i> (cotton)	n.d.a	Bacterial inducible	Assigbetse et al. (1999)
<i>Cucumis sativas</i> (cucumber)	<i>Cuper2</i>	Ethylene inducible	Morgens et al. (1990)
<i>Cucurbita pepo</i> (zucchini)	<i>APRX</i>	Cell-wall-bound	Carpin et al., 2001
<i>Populus</i>	<i>prxA3a</i> , <i>prxA4a</i> <i>PXP1</i> , <i>PXP11</i> , <i>PXP22</i> , <i>PXP3-4</i>	Xylem of stem and root	Christensen et al. (2001)
<i>Arabidopsis thaliana</i>	<i>prxCa</i> , <i>prxEa</i> , <i>prxCb</i> , <i>Nine prxr</i> genes, <i>ATP1a</i> , <i>ATP2a</i> , <i>ATP15a</i> , <i>ATP24a</i> , <i>ATPA2</i>	Promoter All organs All organs Wound inducible (ATP2a also) Promoter	Intapruk et al. (1994) Capelli et al. (1996) Kjaersgard et al. (1997) Cheong et al. (2002) Østergaard et al. (2000)
<i>Armoracia rusticana</i> (horseradish)	<i>prxC1</i> <i>prxC2</i>	Promoter, transgenic analysis	Fujiyama et al. (1988)

		Wound inducible, promoter	Fujiyama et al. (1990)
<i>Glycine max</i> (soybean)	<i>SPOD4.1, Prx2, Ep</i>	Seed coat	Huangpu et al. (1996)
<i>Stylosanthes humilis</i>	<i>Shpx6a, Shpx6b</i>	Pathogen and JA inducible, promoter	Curtis et al. (1997)
<i>Arachis hypogaea</i> (peanut)	<i>prxPNC1, prxPNC2</i>	Wound inducible	Breda et al. (1993)
<i>Medicago sativa</i> (alfalfa)	<i>Msprx1A, Msprx1b, Msprx1C</i>	Pathogene inducible	el-Turk et al. (1996)
<i>Nicotiana tabacum</i> (tobacco)	<i>tpoxC1, tpoxN1, NtpoxAN</i>	TMV inducible TMV, wound, and ethylene inducible Promoter, transgenic analysis	Hiraga et al. (1999) Hiraga et al. (2000) Klotz et al. (1998)
<i>Lycopersicon esculentum</i> (tomato)	<i>TPX1, TPX2, TAP1, TAP2</i>	Salt and wound inducible Transgenic analysis Promoter (wound), antisense analysis Wound inducible, antisense analysis	Botella et al. (1993) Amaya et al. (1999) Mohan et al. (1993a) Sherf et al. (1993)
<i>Solanum tuberosum</i> (potato)	<i>Stprx2</i>	Wound inducible	Collinge and Boller, (2001)
<i>Ipomoea batatas</i> (sweet potato)	<i>Swpa2, Swpa3</i>	Promoter, transgenic analysis	Huh et al. (1997)
<i>Oryza sativa</i> (rice)	<i>POX22.3, POX8.1, POX5.1, prxRPA, prxRPN</i>	pathogen inducible wound and ethylene inducible	Chittoor et al. (1997) Ito et al. (1994) Ito et al. (2000)
<i>Triticum aestivum</i> (wheat)	<i>pox1, pox2, pox3, pox4</i>	powdery mildew induced (pox2)	Baga et al. (1995)

<i>Catharanthus roseus</i> (Madagascar periwinkle)	<i>CrPrx</i> <i>CrPrx1</i>	Methyl jasmonate inducible Stress regulation studies not performed	Kumar et al. (2007) Costa et al. (2008)
--	-----------------------------------	---	--

2.8 Molecular characterization of peroxidases

One of the most important aspects in characterization of a gene is to know its function. There are various ways by which the function of gene is deciphered e.g.

1. Tissue specific as well as sub cellular localization
2. *In vitro* enzymatic activity
3. Characterization of over expressed lines
4. Abolition of the gene transcript or insertional inactivation of gene

The expression profiles of the peroxidase genes indicate possible roles of peroxidases in multiple physiological processes. Lagrimini and Rothstein, (1987) reported differences in the organ specificity and stress response of 12 different tobacco peroxidases. *In situ* hybridization analysis on expression of three peroxidases in Norway spruce seedlings showed that mRNA coding for PX1 and PX2 accumulated in the cytoplasm of young, developing tracheids within the current growth ring where lignifications is occurring (Marjamaa et al., 2006). Expression profiles of *SSP* (Stigma-Specific Peroxidase) in flower bud using *in situ* hybridization revealed its function in pollen-stigma interaction and in the protection of stigmas from pathogen attack (McInnis et al., 2005). *In situ* hybridization showed *Srprx1* transcripts are co localized along with a root nodule extensin (SrRNE1) around bacterial infection pockets and infection threads suggests a function in nodulation process (Den Herder et al., 2007). Based on the N or C-terminal extension the peroxidases were destined to secretory, apoplastic or vacuolar targeted in nature. The chimeric gene-fusion construct using GFP, GUS or both are utilized in study of peroxidase function based on their final destination. Marjamaa et al. (2006) using chimeric fusions with EGFP (enhanced green fluorescent protein) and expressing in tobacco protoplasts showed that spruce PX1 peroxidase is processed via the endoplasmic reticulum (ER) most likely for secretion to the cell wall. So the PX1 plays a role in maturation of the

spruce tracheid secondary cell wall. Vacuolar localization of GFP-CrPrx1 fusion protein reinforces possible involvement of *CrPrx1* in MIA metabolism (Costa et al., 2008).

In vitro enzymatic study using heterologously expressed proteins were utilized to observed the important structural elements present in peroxidase. Carpin et al. (2001) demonstrated that APRX from *Arabidopsis thaliana* bears a Ca^{2+} pectate binding site formed by four cluster arginines using an *in vitro* binding test with the heterologusly expressed site directed mutated APRX. Glu141 plays a role in the stabilization of tobacco anionic peroxidase by preventing the heme dissociation from the active centre when studied using the Glu141Phe substitution expressed in *E. coli* (Hushpulian et al., 2007).

Recombinant DNA technology has been used to investigate the precise physiological functions of plant genes. Some plant peroxidase genes have been expressed transgenically and the phenotypes of these transgenic plants yield information about their functions. The NtpoxAN gene, which encodes an anionic peroxidase in tobacco (*Nicotiana tabacum*), was placed under the control of the CaMV 35S promoter and introduced back into tobacco (Lagrimini et al., 1990, 1997). The transgenic tobacco plants exhibited peroxidase activity 2 to 10-fold higher than that of the wild-type plants and displayed chronic severe wilting through loss of turgor in leaves, initiated at the time of flowering. Although alteration of indoleacetic acid (IAA) metabolism by overexpression of anionic peroxidase was examined, no significant difference in IAA levels was observed. In transgenic plants expressing higher peroxidase activity, however, root elongation was insensitive to exogenously applied IAA. Lagrimini et al. (1997) proposed that the overexpression of the tobacco anionic peroxidase results in diminished root mass from fewer root branches, which contributes to wilting.

tpx2 cDNA, which encodes a cell-wall-associated peroxidase involved in modifying of cell wall architecture in tomato (*Lycopersicon esculentum*), was placed under the control of the CaMV 35S promoter and introduced into tobacco plants (Amaya et al., 1999). By investigating ten independent transgenic plants, authors found that overexpression of the *tpx2* gene had no effect on wild-type development under normal growth conditions; however, the germination rate of the transgenic plants were increased greatly under conditions of high salt (250 mM NaCl) or osmotic

stress (470 mM Mannitol). Thermoporometry calculations indicated a lower mean pore size in the walls of transgenic seeds. Therefore, they speculated that the salt-tolerant phenotype seen in the transgenic tobacco is due to a higher water-retaining capacity in transgenic seeds.

The genes *tap1* and *tap2* encode anionic peroxidases from tomato and potato that are inducible by wounding, fungus, elicitors and ABA (Sherf, 1993). Transgenic tomato plants producing a chimeric antisense transcript corresponding to the 5' region of both *tap1* and *tap2* were generated. The resulting defect in *tap1* or *tap2* activity did not appear to significantly inhibit the suberization of the wound periderm of the tomato fruit.

Anionic (*swpa1*) and neutral (*swpn1*) peroxidases from sweet potato (*Ipomoea batatas*) were overproduced in transgenic tobacco plants under the control of the CaMV 35S promoter. Leaves of transgenic plants with either the *swpa1* or *swpn1* gene showed higher peroxidase activity than those of nontransgenic control plants. When tobacco leaf disks were treated with 10 μ M methyl viologen (MV; paraquat), *swpa1* transgenic plants showed a reduction in membrane damage of about 25% relative to *swpn1* transgenic or untransformed control plants. Leaves of the *swpn1* transgenic and the control plants were also bleached more than those of the *swpa1* transgenic by 1 μ M MV treatment. These results indicate that the increased H₂O₂ scavenging capacity provided by overproduction of *swpa1* peroxidase (a guaiacol-type peroxidase) confers increased oxidative-stress tolerance to the transgenic plants (Yun et al., 2000).

Antisense of cytosolic ascorbate peroxidase in tobacco displayed a significant increase in ozone injury following high-level ozone exposure (Orver and Ellis, 1997). Lower level ozone exposure reveals even more drastic differences between the antisense and control plants. Double antisense of cytosolic ascorbate peroxidase (APX) or catalase (CAT) appeared to be less sensitive to oxidative stress than single antisense plants lacking APX or CAT (Rizhsky et al., 2002).

So it can be said that in plant cells, class III peroxidases are present in soluble, ionically- and covalently cell wall bound forms. They are involved in many functions viz. ROS generation and regulation, H₂O₂ level regulation, and oxidation of various substrates (which leads to the catabolism or the polymerization of substrates). The high number of isoform allows a fine balance between antagonistic peroxidase function such as cell wall cross linking and loosening. The variation of the number of

isoforms between species could explain the numerous discrepancies reported on the regulation of the different peroxidases related to different physiological processes.

2.9 A brief with Peroxiredoxin

Peroxiredoxins (Prxs) are abundant low-efficiency peroxidases located in distinct cell compartments including the chloroplast and mitochondrion. They are grouped into four classes based on their structural and biochemical properties. The catalytic center contains a cysteinyl residue that reduces diverse peroxides and is regenerated via intramolecular or intermolecular thiol-disulfide-reactions and finally by electron donors such as thioredoxins and glutaredoxins. Peroxiredoxins constitute the most recently identified group of H₂O₂-decomposing antioxidant enzymes. In addition to the reduction of H₂O₂, Prx proteins also detoxify alkyl hydroperoxides and peroxinitrite, despite the fact that significant differences exist in substrate specificity and kinetic properties. Through this activity Prx is likely to modulate oxolipid-dependent and NO related signalling (Baier and Dietz, 1999, 2005; Rhee et al., 2005). Experimental evidence exists for a triple Prx function in plant cell biology as (i) antioxidant, (ii) modulator of cell signalling pathways, and (iii) redox sensor. Based on sequence similarities and catalytic mechanisms, four types of Prx proteins are distinguished viz. 1-Cys Prx, 2-Cys Prx, PrxQ, and type-II Prx (Rouhier and Jacquot, 2002; Dietz, 2003). Interestingly there is no report to date of peroxiredoxin action in alkaloid metabolism.

CHAPTER 3



Materials and Methods

Methods were carried out according to standard procedures (Sambrook et al., 1989) or using manufacturer's specifications (except where cited in text). Materials and methods used routinely, and for the purpose of generating general resources for use throughout this study are described below.

3.1.1 Plant material

Seeds of *C. roseus* var. Pink were obtained from Rajdhani nursery, New Delhi and grown in the experimental nursery of National Institute of Plant Genome Research, New Delhi,

3.1.2 Bacterial strains

Strains	Genotype
<i>E. coli</i> DH5 α	<i>SupE44</i> Δ <i>lacU169</i> (\emptyset 80 <i>lacZ</i> Δ M15) <i>hsdR17</i> <i>recA1 endA1 gyrA96 thi-1 relA1</i>)
<i>E. coli</i> BL21-CodonPlus $\text{\textcircled{R}}$ -RP	B F- <i>ompT hsdS</i> (r _B - m _B -) <i>dcm</i> ⁺ Tet ^r <i>gal l</i> (DE3) <i>endA Hte [argU proL Cam^r] [argU ileY</i> <i>leuW Strep/Spec^r]</i>
<i>E. coli</i> XL-1 Blue	(<i>mcrA</i>)183 .(<i>mcrCB-hsdSMR-mrr</i>)173 <i>endA1</i> <i>supE44 thi-1 recA1 gyrA96 relA1 lac [F'roAB</i> <i>lacIqZ.M15 Tn10 (Tetr)]</i>
<i>E. coli</i> BL21 DE-3	B F- <i>dcm ompT hsdS</i> (r _B - m _B -) <i>gal</i> (DE3)
<i>Agrobacterium tumefaciens</i> GV3101	Chromosomal marker gene -rifamicin
<i>A. tumefaciens</i> LBA4404	Chromosomal marker gene -rifamicin and Ti- plasmid marker gene-spectinomycin and Streptomycin

3.1.3 Plasmid vectors

Vector	Source	Purpose
pGEM-T Easy	Promega	Cloning vector
pBI121	Generous gift	Binary vector
pCAMBIA 1303	Cambia	Binary vector
pCAMBIA 1302	Cambia	Binary vector
pGEX 4T-2	Amersham	Expression vector

3.1.4 Chemicals and stocks

Type	Materials	Source
Molecular weight and concentration markers	1 kb ladder, 500 bp ladder, supermix DNA ladder, λ DNA	Bangalore-Genei, India Amersham, USA
X-ray films and cassettes	Hyperfilm and hypercassettes	Kodak, India Amersham, USA
Nylon membrane	Hybond N Hybond C-Extra	Amersham, USA
Antibiotic	Ampicillin (100 mg/ml) Cefotaxime Kanamycin	Amersham, USA Nicholas Piramal India Limited Sigma, USA
Radioisotope	α ^{32}P -dCTP	Amersham, USA BARC, India Perkin Elmer, USA
Disposable filters	Polypropylene (0.2 and 0.45 μm)	Sigma, USA, Sartorius, USA
Enzymes	Commonly used restriction enzymes Taq DNA polymerase Powerscript reverse transcriptase Superscript III reverse transcriptase T4 DNA ligase RNaseA RNase free Dnase Pfu DNA polymerase Titanium taq polymerase	NEB, UK Bangalore-Genei, India Clontech, USA Fermentas, USA Invitrogen, USA Promega, NEB Fermentas, USA Bangalore-Genei, India Qiagen, USA Promega, USA Clontech, USA

	Phusion taq DNA polymerase	Finnzymes, Finland
	Type VI Horseradish peroxidase	Sigma, USA
Hormones	2,4-D, NAA, BAP	Sigma, USA
Culture media	Luria broth, tryptone, yeast extract, peptone, beef extract, bacto-agar, MgSO ₄ , NaCl, sucrose, phytigel, myo-inositol	Difco, USA Qualigens, India Sigma, USA Amersham, USA
Fine chemicals	TRIZol, DEPC, SDS, PEG-8000, LiCl, EDTA, EtBr, β-mercaptoethanol, sephadex G-50, Methylene blue, MOPS, agarose, CTAB, bromo phenol blue, phenol, tris base, DMSO, PIPES, IPTG, glucose, CaCl ₂ , Skim milk powder, Methyl jasmonate, Polyvinylpyrrolidone, polyvinylpyrrolidone, <i>o</i> -phenylenediamene, Bradford reagent, Guaiacol, Ascorbate, Methyl viologen, PMSF, Protease inhibitor Cocktail	Sigma, Aldrich, USA Amersham, USA Invitrogen, USA Calbiochem, USA Titan biotech, India
Plasticwares	Microcentrifuge tubes, micro tips, PCR tubes, reagent bottles, 96 well PCR plates, sterilization unit, oak-ridge and falcon tubes	Tarsons, India Polylab, India Axygen, India
Glasswares	Reagent bottles, flasks, measuring cylinders, trays, beakers, culture tubes	Borosil, India Schott Duran, India

Kits	NEBlot kit	NEB, USA
	SMART cDNA library construction kit	Clontech, USA
	p-GEMT easy vector system	Promega, USA
	MinElute gel extraction kit	Qiagen, USA
	QIAquick PCR purification kit	Qiagen, USA
	mRNA isolation kit	Roche, Germany
	RNeasy Mini Kit	Qiagen, USA
	HiYield™ Gel/PCR DNA Extraction Kit, Microspin HR columns	RBC Bioscience Corporation, Taiwan Amersham, USA
Oligonucleotides/primers	Gene and vector specific	Microsynth, Switzerland Sigma-Genosys, USA
CrPrx Polyclonal Antibodies	Anti rabbit IgG	Bangalore genie, India
HRP conjugated goat anti-rabbit IgG	Goat anti-rabbit IgG	Pierce, USA
SuperSignal® West Pico Chemiluminescent	Chemiluminescent substrate	Pierce, USA
Miscellaneous Chemicals	H ₂ SO ₄ , Ethylacetate, Acetone, HCl	Qualigens fine chemicals, USA

3.1.5 List of oligonucleotides/primers

Genes/ vector/cDNA (Code)	Primer Code	Primer Sequence
Degenerate plant peroxidase primers	PF1	5' AGRCTTCAYTTYCATGAYTGC 3'
	PR1	5' GTGNSCMCCDRRSARRGCDAC 3'
	PF2	5' AGRCTTCAYTTYCATGAYTGT 3'
	PR2	5' CATYTCDGHYCAHGABAC 3'

	DCPF1 DCPR1	5' CTICAT/C TTT/CCAT/CGAG/ATGC 3' 5' GTG/ATGIG/CCICCG/A/T/CGATAGG GCG/A/T/CAC 3'
<i>Catharanthus roseus</i> peroxidase (<i>CrPrx</i>) full length primers	PFLF1 PFLR1	5' CACGAGCTGACCTTCACTGTC 3' 5' GCTCACCACCATTACATTGC 3'
Gene specific primer <i>CrPrx</i> (GSP2) and (GSP4)	RACE2 RACE4	5' GAAGCCCTTGAAAGGGAGTGTCTGGAG 3' 5' GAGGCTCTCATTGTGGTCTGGGAGATG 3'
<i>C. roseus</i> peroxidase (<i>CrPrx1</i>) full length primers	CPNF CPNR	5' GGAACCATGGCTTTTTCTTC 3' 5' GCAGAACTCATGAATACGCA 3'
<i>C. roseus</i> peroxidase (<i>Prx3</i>) full length primers	CRPRX3F2 CRPRX3R	5' AGCTAATAAAGTCTCTCGATCAAAGG 3' 5' TCAGAGCAACTTTATTGAACTTGGTG 3'
Gene specific primer <i>Prx3</i>	GSP3 GSP4 NGSP3 NGSP4	5' GGCCCTCCCAAAGCGACCACTGA 3' 5' TGATATTCTTGCCATTGCTGCCCGT 3' 5' ACGGGCAGCAATGGCAAGAATATCA 3' 5' TCAGTGGTCGCTTTGGGAGGGCC 3'
<i>C. roseus</i> peroxidase (<i>Prx4</i>) full length primers	CRPRX4F CRPRX4R	5' CTCTTCAGCTCAGCTTTCCACT 3' 5' CATGAACTTTGACATTGGGATATAAA 3'
Gene specific primer <i>Prx4</i>	GSP5 GSP6 NGSP5 NGSP6	5' TCACATTCCAGCTAGGCCACCCA 3' 5' ACATCCTCGCCATTGCAGCTCGGG 3' 5' CCCGAGCTGCAATGGCGAGGATGT 3' 5' TGGGTGGGCCTAGCTGGAATGTGA 3'
Kanamycin gene specific primer	KanF KanR	5' GATTGAACAAGATGGATTGCACG 3' 5' CAGAAGAAGCTCGTCAAGAAGGCG 3'
Vector specific (pGEM-T Easy)	M13F	5' CCCAGTCACGACGTTGTAAAACG 3'

primers	M13R	5' AGCGGATAACAATTTACACACAGG 3'
Vector specific (pBI121) sequencing primers	PBI121SF	5' GGATTGATGTGATATCTCCA 3'
	PBI121SR	5' GATCAATTCCACAGTTTTTCG 3'
Vector specific (pGEX 4T-2) sequencing primers	PGXSF	5' CTGGCAAGCCACGTTTGGTG 3'
	PGXSR	5' GGAGCTGCATGTGTCAGAGG 3'
Vector specific (pCAMBIA) sequencing primers	PACMBSF	5' GTTGTGTGGAATTGTGAGCG 3'
	PACMBSR	5' GTTTTCCCAGTCACGACGTT 3'
RPS9 gene full length primer	RPS9F	5' CATTTTGTATCGGCTCTTAG 3'
	RPS9R	5' CATCCAAAACCTCCTACATG 3'
Primers used for cDNA synthesis	SMART IV (RNA oligos)	5' AAGCAGTGGTATCAACGCAGAGTGGCCAT ACGGCCGGG 3'
	CDS-III A	5' ATTCTAGAGGCCGAGGCGGCCGACAT Gd(T) ₃₀ N ₁ N 3' (N=A,G,C or T) (N ₁ =A,G / (C)
	CDS V	5'-(T) ₂₅ V N-3' (N = A, C, G, or T; V = A, G, or C)
	NUP	5' AAGCAGTGGTATCAACGCAGAGT 3'
	LUPM	5' CTAATACGACTCACTATAGGGCAAGCAGT GGTATCAACGCAGAGT 3'
	SUPM	5' CTAATACGACTCACTATAGGGC 3'

3.1.6 Specialized primers for the cloning in expression vectors

Purpose and name of construct	Primer Code	Restriction Enzyme site	Primer Sequence
<i>C. roseus</i> peroxidase	PBIPF-1	<i>Xba</i> I	5' TCTAGAGCCATGGCTTCCAA

(<i>CrPrx</i>) overexpression primers sCrPrx (pBI121-CrPrx)	PBIPR-1	<i>Sma</i> I	AACTC 3' 5' CCCCAGGGCCAAAAGCAA CTAC 3'
<i>C. roseus</i> peroxidase (<i>CrPrx</i>) antisense primers aCrPrx (3'-anti CrPrx-pBI121)	CRPBIASF1 CRPBIASR1	<i>Sma</i> I <i>Xba</i> I	5' CCCCAGGGCCATGGCTTCCA AAACTCTC 3' 5' CTCTAGAGTATTCCATCCA TCCCCTCTG 3'
<i>C. roseus</i> peroxidase (<i>CrPrx</i>) GST fusion protein primers (PPGX) pGEX4T-2-CrPrx	GSTPF2 GSTPR1	<i>Eco</i> R I <i>Sal</i> I	5' GGAATTCCTCATGGCTTCCA AAAC 3' 5' GGTCGACCTCACCACCATT ACA 3'
<i>C. roseus</i> peroxidase (<i>CrPrx</i>) GUS-GFP fusion protein primer (PGFP)	PGFPR1	<i>Spe</i> I	5' GGACTAGTATGTAACCTTATT AGCTACATAT 3'
<i>C. roseus</i> peroxidase (<i>CrPrx1</i>) overexpression primers sCrPrx1 (pBI121-CrPrx1)	CPNRF CPNRR	<i>Xba</i> I <i>Bam</i> HI	5' GCTCTAGAGGAAGGAAC CATGGCTTTT 3' 5' CGGGATCCTTGGAGCAG AACTCATGAAT 3'
<i>C. roseus</i> peroxidase (<i>CrPrx 1</i>) antisense primers aCrPrx1 (3'-anti CrPrx-pBI121)	CPNAF CPNAR	<i>Bam</i> H I <i>Xba</i> I	5' CGGGATCCGAAGGAACC ATGGCTTTTT 3' 5' GCTCTAGAGCAGAACTC ATGAATACGCA 3'
<i>C. roseus</i> peroxidase (<i>Prx3</i>) GUS-GFP fusion protein primer	PGFPF1	<i>Nco</i> I	5' GCCATGGCTAGCTAATAAA GTCTCTC 3'

(PGFP3) pCAMBIA1303-CrPrx	PGFPR2	<i>Spe</i> I	5' GGACTAGTATTAACCCTCC TACAATTTTTC 3'
------------------------------	--------	--------------	--

3.1.7 Specialized primers used for the Real time PCR

Name of Gene	Primer Code	Primer Sequence
<i>CrPrx1</i>	RTCRP1F1	5' CCTTTTGATTTCTGCCCACTTT 3'
	RTCRP1R1	5' ACTGTTGGTGGCCGAGTTG 3'
<i>CrPrx</i>	RTCRPF1	5' CTTCTTCCTTGTCATTCTCTCCTTCT 3'
	RTCRPR1	5' TGCCTCGGCTTCATTTTCAG 3'
<i>Prx3</i>	RTCRP3F1	5' CTCGATCAAAGGCAAAAATGG 3'
	RTCRP3R1	5' CCCAGAACAGCTTCTCATCATTATT 3'
<i>Prx4</i>	RTCRP4F1	5' TTTGAAAGAAGCCCGAATGG 3'
	RTCRP4R1	5' ACAAAGCAATCATGGAAGAACAAG 3'
<i>Dat</i>	RTDATF1	5' AATCCCTCAGCCGCTATAACC 3'
	RTDATR1	5' ACGGATACGCACGTTTGGTAT 3'
<i>D4h</i>	RTD4HF1	5' GACTTGAACTTTCATGCTGCTACAC 3'
	RTD4HR1	5' TCTCATCAAAAGCCTTCAATTCC 3'
<i>G10H</i>	RTG10HF1	5' CAGGACCATCGCCATTGC 3'
	RTG10HR1	5' TTGTGTGGTTGGTCGCCTAA 3'
<i>SGD</i>	RTSGDF1	5' CATTGCCTACCCAGTATCC 3'
	RTSGDR1	5' CGATGAACGATGGGCTTGTT 3'
<i>SLS</i>	RTSLSF1	5' GAAAGGCAATTGCTGCCACTA 3'
	RTSLSR1	5' GCCCAATCCAACACTCTCCAT 3'

<i>STR</i>	RTSTRF1	5' TGCTTCACTCCCATCATTTACAGT 3'
	RTSTRR1	5' CTGCCATCATGGATTTAGATTCAG 3'
<i>ZCT1</i>	RTZCT1F1	5' CATGGGCGTGAAGAGATTCA 3'
	RTZCT1R1	5' CCGACTTTAGAAAGAAGCATCAAAC 3'
<i>ZCT2</i>	RTZCT2F1	5' CCGATGAAGCGTACGAGAGAA 3'
	RTZCT2R1	5' TCAAGCAATTCGCCATAGTTGT 3'
<i>ZCT3</i>	RTZCT3F1	5' CACCTACACCTGTTTTTCAATACGA 3'
	RTZCT3R1	5' GCCCATGGCTGATCTAGATAGC 3'
<i>ORCA3</i>	RTORCA3F1	5' TCAATTATTATGTAAATGTGGTGGCTAGT 3'
	RTORCA3R1	5' AAAAAGTTGGCATTGATGAATACTGA 3'
<i>CRACTIN</i>	RTCRACTINF1	5' CTATGTTCCCAGGTATTGCAGATAGA 3'
	RTCRACTINR1	5' GCTGCTTGGAGCCAAAGC 3'
<i>RPS9</i>	RTRPS9F1	5' GGGCGGCAGCTGAGAA 3'
	RTRPS9R1	5' TGAAGGTCTTACCATAGTTGCGATAA 3'

3.1.8 Composition of growth mediums

3.1.8.1 Luria Broth (LB)

Components	(g/l)
Yeast Extract	5.0
Bacto Tryptone	10.0
NaCl	10.0

pH was adjusted to 7.0 and autoclaved, for solid media 17 g/l agar was added and autoclaved

3.1.8.2 YEB

Components	(g/l)
Yeast Extract	1.0

Beef Extract	5.0
Bacto Peptone	5.0
Sucrose	5.0
MgSO ₄ . 7H ₂ O	0.492

The pH was adjusted to 7.0 and autoclaved, for solid media 17 g/l agar was added and autoclaved

3.1.8.3 SOB

Components	(g/l)
Yeast Extract	5.0
Tryptone	20.0
NaCl	0.5
KCL	0.186

The pH 7.0 was adjusted with 2N NaOH and autoclaved, for solid media 17 g/l agar was added before autoclaving

3.1.8.4 NZY

Components	(g/l)
NaCl	5.0
MgSO ₄ .7H ₂ O	2.0
Yeast extract	5.0
NZamine (Casein Hydrolysate)	10.0

The pH was adjusted to 7.5 with 2N NaOH and autoclaved, for top agar 7 g/l agarose, while for lower agar 15 g/l agar was added before autoclaving

3.1.8.5 Gamborg's B5 medium

Compounds	(mg/l)
Macronutrients	
KNO ₃	3,000
(NH ₄) ₂ SO ₄	134
CaCl ₂ .2H ₂ O	150

MgSO ₄ . 7H ₂ O	500
NaH ₂ PO ₄	150
Micronutrients	
H ₃ BO ₃	3.0
CoCl ₂ .6H ₂ O	0.025
CuSO ₄ .5H ₂ O	0.025
Na ₂ MoO ₄ .2H ₂ O	0.25
ZnSO ₄ .7H ₂ O	2
MnSO ₄ .2H ₂ O	10.0
KI	0.75
Vitamins	
Nicotinic acid	1
Pyridoxine HCl	1
Thiamine HCl	10
Other organics	
Myo-inositol	100
Carbon source	
Sucrose	30,000
Gelling agent	
Phytigel	2,800

The pH of the medium was adjusted to 5.7-5.8 before addition of phytigel

3.1.8.6 Murashige and Skoog medium

Preparation of stock solutions

Compounds	(g/l)
Macronutrients (20X)	
KNO ₃	38
NH ₄ NO ₃	33
CaCl ₂ .2H ₂ O	8.8

MgSO ₄ . 7H ₂ O	7.4
KH ₂ PO ₄	3.4

Each component is mixed separately in 150 ml of water and finally mixed with each other to make 1 litre as final volume.

Micronutrients (1000X)

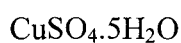
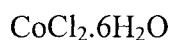
Compounds	(mg/200 ml)
H ₃ BO ₃	1260
Na ₂ MoO ₄ .2H ₂ O	50
ZnSO ₄ .7H ₂ O	1720
MnSO ₄ .2H ₂ O	4460
KI	166

Fe-EDTA (1000X)

Compounds	(g/100 ml)
C ₁₀ H ₁₃ N ₂ O ₈ Na ₂	3.73
FeSO ₄ .7H ₂ O	2.734

pH of the solution is set at 3.0 to 4.0

Following components are weighing separately as 500 mg per 10 ml and added 10 µl to this stock.



MS Organics (1000X)

Compounds	(mg/200 ml)
Nicotinic acid	1000
Pyridoxine HCl	2000
Thiamine HCl	20
Glycine	400

3.1.8.7 Tobacco shoot induction media (TSM)

Components	Amount per litre
MS major	50 ml
MS minor	1 ml
B5 Vitamins	1 ml
Fe-EDTA	1 ml
NAA	0.1 mg
BAP	1 mg
Sucrose	30

Gelling agent

Phytigel	2.8 g
----------	-------

The pH of the medium was adjusted to 5.7-5.8 before addition of phytigel

3.1.8.8 Tobacco root induction media (TRM)

Components	Amount per litre
MS major	50 ml
MS minor	1 ml
B5 Vitamins	1 ml
Fe-EDTA	1 ml
NAA	0.1 mg
Sucrose	30

Gelling agent

Phytigel	2.8 g
----------	-------

The pH of the medium was adjusted to 5.7-5.8 before addition of phytigel

3.1.8.9 MSH (Murashige and Skoog medium without sucrose and organic ingredients)

Components	Amount per litre
MS major	25 ml
MS minor	0.5 ml
Fe-EDTA	1 ml
Gelling agent	
Phytigel	2.8 g

The pH of the medium was adjusted to 5.7-5.8 before addition of phytigel

3.2 Methods

3.2.1 General sterilization procedures

The glasswares, tissue culture tools and culture media were sterilized by autoclaving at a temperature of 120⁰C under 15 lb psi pressures for 20 min. The antibiotics and other heat labile components were filter sterilized with a sterile 0.2 µm cellulose nitrate filter.

3.2.2 Plant growth conditions and maintenance

The seeds were soaked overnight in tap water and sown in soil (eight to ten seeds/pot) and allowed to germinate in growth chamber maintained at 26-28⁰C and 60-70% humidity. Six to eight weeks old plantlets were transferred to the field and maintained throughout the year. Simultaneously, plantlets were also maintained in growth chamber under controlled conditions. *C. roseus* plantlets of different varieties grown under aseptic conditions were maintained in culture room at 25±1⁰C under 2000 lux light (Philips cool white fluorescent light) for 16/8 h light and dark photoperiod.

3.2.3 Primer designing

Different softwares were used for designing of different primers.

3.2.3.1 Design of degenerate plant peroxidase primers

Degenerate plant peroxidase primers were designed on the basis of highly conserved amino acid sequences of proteins encoded by peroxidase gene family, namely,

RLHFHDC for forward degenerate primers, VALLGAHSV G and VSCSDI for reverse degenerate primers (Fig. 3.1).

```

gi|1389835|gb|AA02926.1|          MSFTFYKSSCPKLESITTKELKEVFKEDIGQALGLLRLEFHDCFWEGCDG 84
gi|46451429|gb|AA597959.1|       LSWFTFYKSSCPKVESIIQKELKELFKKIVQALGLLRLEFHDCFWLGCDDG 81
gi|5002238|gb|AA097376.1|AF145  LSYSFTSRTCPKLESIVRKELEKVFKDMGQAPALLRIFFHDCFWQGCDDG 84
gi|23621325|gb|BAB97197.2|      LDQNYFYGTCFQFTEILVWQGLVASTFTDPTGPAALVPLVFHDCGQNGCDDG 82
gi|7453855|gb|AAF63027.1|AF244  LYFQFYDESCFQAQIVRSVVAQVNSRDRMAASLLRLEFHDCFWNGCDA 88
gi|7453853|gb|AAF63026.1|AF244  LHFQFYDESCPOLHQIIFSVVAQVNSRDRMAASLLRLEFHDCFWKCCDA 99
gi|7653147|dbj|BAJ94962.1|      LTFQFYDESCFRAQIVRQVVEKAVARDREMLASLLRLEFHDCFWKCCDA 77
gi|34903044|ref|NP_912869.1|     LFPQFYDESCPKAKEIVQSEVVAQVARETRMAASLVLEFHDCFWEGCDA 92
gi|37536450|ref|NP_922527.1|     LRVGFTDNSCPAAELIVQQEVSEANSANPGLAAGLVLEFHDCFWKCCDA 94
gi|6204761|gb|AAD11482.1|       LGLGFTANSCPKAEQIVLRFVHDEHMAFSLAALIRNEFHDCFWKCCDA 99
gi|15236620|ref|NP_193504.1|     ----YYQATCPDFNRIIVRETVTPKQQQOFTTAAAGTLRLEFHDCFWKCCDA 75
gi|4927284|gb|AA033072.1|AF149  LVEDFYKDSCPQAEETIREQWELLTKRHKNTAFSRLNIFHDCFWESCD 76
gi|10597182|gb|BAB16317.1|     LAENFTYKDSCPQAEETIREQWELLTKRHKNTAFSRLNIFHDCFWESCD 81
gi|10241560|emb|CAB71128.2|     LLNFTYKESCPQAEETIREQWELLTKRHKNTAFSRLNIFHDCATQCCDA 81
      *  **  .  ::  :      .  .  *  ***  :  **.
      <----->
  
```

Fig. 3.1: Amino acid sequence used for design of degenerate primer. A representative of conserved region present in class III peroxidase sequences used for design of forward degenerate primer.

3.2.3.2 Designing of full length gene specific primers and primers with restriction sites

Full length gene specific primers and primers with restriction sites were designed on the basis of submitted sequences in the NCBI database representing the complete gene using a DOS based program, ‘PRIMER’. For designing of forward and reverse primer pair, the GC content was maintained between 35-50% and the range of Tm was chosen between 50-65°C. For primer pair of each target gene, the difference of 2-5°C in the Tm values was maintained. However, a run of more than three similar nucleotides at a time and presence of secondary structure were avoided.

3.2.3.3 Design of Gene specific primers for 5' and 3' RACE

Gene specific primers for 5' and 3' RACE were designed using Primer3, an online available software tool for designing primers. The parameters for designing of the primers were:

Primer length: 23-28 nt, optimum 25 nt

- % GC concentration: 50-70, optimum 54
- Tm: 65-72°C, optimum 70°C

Other parameter remains default.

3.2.3.4 Design of Real time PCR primers

Real time PCR primers were designed from the gene specific sequences of few MIA pathway genes and their regulators, downloaded directly from NCBI database. Primer Express version 3.0 (Applied biosystems, Foster city, USA) was used for designing the real time PCR primers. The parameters for designing of primers were kept as default with amplicon length as 50 to 150 bases, primer length 20 bases, T_m 58 to 60⁰C, %GC concentration varies from 30 to 80% and there should be less than two G+C with in 5 nucleotide at 3' end.

3.2.4 Recombinant DNA techniques

3.2.4.1 Polymerase Chain Reaction

3.2.4.1.2 Degenerate PCR amplification

PCR amplifications were performed with degenerate oligonucleotide primers using the cDNA as template. A 25 µl reaction mixture contained 25-50 ng DNA template, 1µl of 10 µM of each primer, 1 µl of 2.5 mM dNTPs, 2.5 µl of 10X Taq buffer containing 15 mM MgCl₂ and 2 U of Taq DNA polymerase. Reaction conditions were as follows, initial denaturation at 94⁰C for 2 min followed by 10 cycles of denaturation at 94⁰C for 45 sec, annealing at 48⁰C for 30 sec extension at 72⁰C for 1 min and again 28 cycles of denaturation at 94⁰C for 45 sec annealing at 58⁰C for 30 sec and extension at 72⁰C for 1 min; with final extension at 72⁰C for 10 min after which reaction was terminated at 4⁰C.

3.2.4.1.3 PCR amplification of peroxidase genes

PCR amplifications were performed with full length gene specific primers using the cDNA as template. A 50 µl reaction mixture contained 25-50 ng DNA template, 1µl of 10 µM of each primer, 1 µl of 10 mM dNTPs, 5 µl of 10X Taq buffer containing 15 mM MgCl₂ and 1U of Pfu Taq DNA polymerase. Reaction conditions were as follows, initial denaturation at 94⁰C for 2 min, followed by 29 cycles of denaturation at 94⁰C for 45 sec, annealing at 60⁰C for 45 sec and extension at 72⁰C for 1 min; with final extension at 72⁰C for 10 min.

3.2.4.1.4 PCR amplification for cloning of genes in pBI121 and pCAMBIA vector using Phusion Taq DNA polymerase

PCR amplifications were performed with specialized primers using the eluted fulllength gene as template. A 50 µl reaction mixture contained 25-50 ng DNA templates, 2.5 µl of 10 µM of each primer, 1 µl of 10 mM dNTPs, 5 µl of 10X Phusion Taq buffer and 1 U of Phusion Taq DNA polymerase. Reaction conditions were as follows: initial denaturation at 98°C for 30 sec, followed by 35 cycles of denaturation at 98°C for 10 sec, annealing at 55°C for 30 sec and extension at 72°C for 90 sec; with final extension at 72°C for 10 min.

3.2.4.2 Cloning of DNA fragments

3.2.4.2.1 Electrophoretic separation of DNA samples

Electrophoresis was carried out using standard procedures. 0.8 % to 2.5 % (w/v) agarose gels were cast in 1x TAE buffer (0.04 M Tris-acetate, 1.0 mM Na₂EDTA, pH 8.0). DNA samples were mixed with 0.2 volumes of 6X Ficoll loading buffer (15 % (w/v) Ficoll 400, 0.25 % (w/v) bromophenol blue, 0.25 % (w/v) xylene cyanol). Gels were electrophoresed in 1X TAE buffer at 40 to 100 V for 30 min to 16 h. DNA was visualized by ethidium bromide staining (5 µg/µl) and photographed under UV light at either 302 nm (preparative gels) or 260 nm (gels for Southern analysis).

3.2.4.2.2 Elution of DNA from agarose gel

The PCR product of each target gene was separated on 1% agarose/EtBr gel while separation of RACE amplified product was performed on 2% agarose/EtBr gel. A single band was observed for each target gene and the size of each amplified product was determined by comparing with the size marker (500 bp ladder). The DNA bands were excised out in 1.5 ml microcentrifuge tubes and DNA was eluted out using Qiagen MinElute Gel Extraction Kit according to manufacturer's instructions. The excised gel was incubated at 50°C for 10 min in 3 vol. of QG buffer with occasional vortexing to solubilize agarose. One gel volume isopropanol was added to the solubilized DNA and mixed properly by inversion. To bind DNA, the solution was transferred to MinElute column and centrifuged for 1 min at 13000 rpm. The flow through was discarded and 500 µl of QG buffer was added to MinElute column and centrifuged again for 1 min at 13000 rpm. After discarding the flow through, 750 µl of PE buffer was added and centrifuged for 1 min at 13000 rpm. The MinElute

column was further centrifuged for 1 min at 13000 rpm and 10 µl EB buffer (10 mM Tris-Cl, pH 8.5) was added for DNA elution and allowed to stand for 5 min before centrifugation. The eluted DNA was run on 1% agarose/EtBr gel alongwith the concentration and size markers for checking.

3.2.4.2.3 Ligation

3.2.4.2.3.1 Ligation in pGEM-T Easy vector

The different gel purified DNA fragments used in this study were ligated to the pGEM-T Easy vector using T4 DNA ligase and incubated overnight at 4⁰C. The ligation reaction was carried out in 10 µl reaction volume containing 2X ligation buffer, 50 ng vector DNA, PCR product and 1 µl T4 DNA ligase (3 weiss units/µl).

3.2.4.2.3.2 Ligation in pBI121 and pCAMBIA vectors

The *CrPrx* and *CrPrx1* from *C. roseus* were cloned in pBI121 prior to GUS gene under CaMV 35S promoter while for pCAMBIA the *CrPrx*, *Prx3* genes were fused to GUS-GFP or GFP gene under CaMV 35S promoter. The genes were amplified by PCR amplification using specific pair of primers with restriction sites present in cloning vector pBI121 at the 5' end of the primers. The desired fragment and the vector were digested with same pair of enzymes, purified from the agarose gel and ligation reaction was set up with both digested fragment and vector. The reaction was carried out overnight in 10 µl reaction volume at 16⁰C or 22⁰C (as per company's recommendation for ligase enzyme).

3.2.4.2.4 Preparation of competent cells

3.2.4.2.4.1 Preparation of *E. coli* (DH5α) ultra competent cells

Ultra competent cells preparation was carried out based on Inoue method (Inoue et al., 1990) with minor modifications. A single bacterial colony (2-3 mm in diameter) was inoculated in 5 ml SOB medium (20 g/l tryptone, 5 g/l YE and 0.5 g/l NaCl) and incubated overnight at 18⁰C. One ml of overnight grown culture was reinoculated in 50 ml of SOB media and grown at 18⁰C with gentle shaking till the OD₆₀₀ of 0.5-0.6 was attained. The cells were harvested after centrifugation at 5000 rpm for 10 min. The media was discarded and the pellet containing the bacterial cells were resuspended in 15 ml ice cold ITB solution (MnCl₂.4H₂O, CaCl₂.2H₂O, KCl, PIPES) by vortexing and cells were pelleted down at 5000 rpm for 10 min at 4⁰C. The cells

were again resuspended in 5 ml ITB, to which 500 µl sterile DMSO was added, mixed well and incubated on ice for 10 min. The cell suspension was dispensed into 1.5 ml eppendorf tubes, snap frozen in liquid nitrogen and stored at -80°C.

3.2.4.2.4.2 Preparation of *Agrobacterium* competent cells

Agrobacterium competent cells were prepared by CaCl₂ method. *A.tumefaciens* strain LBA 4404 and GV 3101 was grown in 50 ml of YEB medium at 28°C with vigorous shaking until its OD₆₀₀ reached 0.5-0.8. The culture was chilled on ice and centrifuged at 3,000x g for 5 min at 4°C to pellet down the cells. The pellet was resuspended in 1 ml of 20 mM CaCl₂ and 0.1 ml of resuspended competent cells were aliquot in pre-chilled eppendorf tubes and stored at -80°C for further use.

3.2.4.2.5 Bacterial transformation

3.2.4.2.5.1 Transformation of *E. coli*

The steps of transformation were carried out in laminar hood under sterile conditions. The competent DH5α strain was used for the transformation of ligated DNA fragments. The ligation mixture was added to the competent cells and mixed by gently tapping and incubated on ice for 20 min. The cells were subjected to heat shock at 42°C for 50 sec and immediately chilled on ice for 5 min. This was followed by addition of 0.9 ml of LB media and incubated at 37°C for 45-60 min with gentle shaking (120-150 rpm). The bacterial cells were pelleted down at 4,000 rpm for 5 min and the LB media was decanted off. The bacterial cells were resuspended in 200 µl fresh LB media and added onto solid LB plate containing appropriate antibiotic (ampicillin, 100 mg/l for pGEM-T Easy and kanamycin, 50 mg/l for pBI121), 7 µl of 20% IPTG and 40 µl of 2% X-gal to perform blue white selection of the recombinant colonies. The plates were then incubated at 37°C overnight. Colonies were confirmed for transformation by PCR or restriction digestion.

3.2.4.2.5.2 Transformation of *Agrobacterium*

Agrobacterium transformation is done by freeze thaw method. During *Agrobacterium* transformation, 1-3 µg of plasmid DNA was added onto frozen competent cells of *Agrobacterium* and then the cells were thawed at 37°C water bath for 5 min. Thereafter, 1 ml YEB medium was added and the tube was incubated at 28°C for 2-4 hrs with gentle shaking. Transformed cells were plated with proper antibiotics and

kept at 28°C incubator for 2-3 days for colonies to grow. The transformed colonies were checked by PCR or restriction digestion.

3.2.4.2.5.3 Confirmation for the presence of inserts

Colony PCR and/or restriction digestion of isolated colonies were used to confirm the transformed cells, containing recombinant plasmid.

3.2.4.2.5.4 Colony PCR

The colony PCR was performed by carrying out the lysis of randomly selected white bacterial colonies at 95°C for 10 min. For performing plasmid PCR, 50 ng of plasmid DNA was taken for performing PCR reaction. The reaction for both colony and plasmid PCR were similar and the PCR reactions were carried out using vector specific primers, or gene specific primers alongwith 10X PCR buffer, dNTPs and Taq DNA polymerase. The amplification was carried out for 30 cycles involving denaturation at 94°C for 45 sec, annealing at 58°C for 30 sec and extension at 72°C for 1 min. Final extension was carried at 72°C for 7 min. The amplified product was loaded onto 1% agarose/EtBr gel alongwith 1 kb ladder to confirm the presence and size of the inserts.

3.2.4.2.5.5 Restriction digestion

The presence of the inserts were further confirmed by restriction digestion of the plasmid DNA using specific restriction enzymes based on multiple cloning sites present in vector. Plasmid DNA (2-3 µg) was digested using 1 U of enzyme and 10X buffer in 20 µl reaction volume. The reaction mix was incubated for 3 h at 37°C and the presence of inserts was checked by loading onto 1% agarose/EtBr gel alongwith DNA ladder. The identities of the colonies showing presence of inserts by plasmid/colony PCR and restriction digestion were confirmed by sequencing.

3.2.4.2.6 Nucleic acid preparations

3.2.4.2.6.1 Plasmid DNA extraction

The alkaline lysis method of Sambrook et al. (1989) was used for the mini-scale preparation of plasmid DNA. A sterile culture tube containing 5 ml LB medium with 100 µg/ml ampicillin for vectors having β-lactamase gene or 50 µg/ml of kanamycin for the vectors having neomycin phosphotransferase gene was inoculated with a single transformed bacterial colony and grown overnight on an orbital shaker at 37°C.

Cells were pelleted by centrifugation at 13000 rpm for 1 min in a benchtop centrifuge and the supernatant discarded. Cells were resuspended in 200 μ l plasmid I solution (50 mM glucose, 25 mM Tris-HCl pH 8.0, 10 mM Na₂EDTA) and placed on ice for approximately 10 min. Lysis of bacterial cells was done by the addition of 300 μ l freshly made plasmid II solution (0.2 N NaOH, 1 % SDS), followed by placement on ice for further 10 min. Chromosomal DNA and cell debris were precipitated by the addition of 300 μ l 3 M NaAc pH 4.8, followed by gentle inversion of the tube, and placement on ice for 5 minutes. This mixture was then centrifuged at 13,000 rpm for 10 min at 4°C and the supernatant was transferred to a fresh microcentrifuge tube for RNaseA (20 μ g/ml) treatment at 45°C for 1 h. The DNA was extracted twice with chloroform followed by separation of upper aqueous phase containing the plasmid DNA in a fresh microcentrifuge tube. Equal volume of isopropanol was added for DNA precipitation by centrifugation at 10,000 rpm for 10 min at room temperature, which was followed by washing the pellet with 70% ethanol. Finally the DNA was vacuum dried and dissolved in 32 μ l of cold sterile water.

3.2.4.2.6.2 Purification of the plasmid DNA by PEG precipitation method

The plasmid DNA was precipitated by adding 40 μ l PEG8000 (13%) and 8 μ l NaCl (4M) to the dissolved DNA, mixed well by tapping and incubated on ice for 30 min. The DNA was precipitated by spinning at 13,000 rpm for 20 min. Finally the pellet was washed two times with 70% ethanol, vacuum dried, dissolved in 20 μ l of cold sterile water and stored at -20°C.

3.2.4.2.6.3 Sequencing and analysis

The identities of putative cDNA clones were confirmed by sequencing using dideoxynucleotide chain termination method (Sanger et al., 1977). Sequencing was performed using Big Dye Terminator kit version 3.0 (Applied biosystems, Foster city, USA) and analyzed with the 3700 ABI Prism 96 capillary sequence analyzer. Nucleotide sequences for both the strands were determined using vector specific (M13 forward and reverse) primer pairs and a sequence homology analysis was performed using blastn and blastx program in NCBI database (Altschul et al., 1997).

3.2.5 Genomic DNA extraction

3.2.5.1 Small scale genomic DNA extraction for the PCR

The method used for the small-scale extraction of DNA from leaves was modified from Stewart and Laura (1993) and Edwards et al. (1991). Fresh leaves or callus lyophilized tissue (50 mg) was placed in a 2 ml eppendorf tube after which 600 µl DNA extraction buffer (2% CTAB, 1.42 M NaCl, 20 mM EDTA, 100 µM Tris Cl pH 8.0, 2% PVP (w/v), 5 mM Ascorbic acid) containing 3 µl β-mercaptoethanol was added and crushed with a small pestle. The homogenized tissue was kept at 70°C. Extraction was performed by adding 600 µl of chloroform/iso-amyl alcohol (24:1) followed by mixing on an orbital rotor for 10 min at 500 rpm. The sample was centrifuged for 10 min at 1000x g at 22°C and the supernatant transferred to a fresh tube. After the supernatant was collected, 0.7 vol. of isopropanol were added followed by gentle mixing at RT to allow the DNA to precipitate. The DNA was then pelleted by centrifugation for 20 min at 14000x g in a benchtop centrifuge, and the supernatant discarded. After washing the pellet with 1 ml 70 % ethanol, the DNA was air-dried and resuspended overnight at 4°C in 50 µl sterile nanopure water.

3.2.5.2 Medium scale genomic DNA extraction

The leaves [5 g, fresh weight (FW)] of *C. roseus* or *Nicotiana tabacum* were crushed in liq N₂. The powdered tissue was transferred to 50 ml oak-ridge tubes containing 30 ml prewarmed extraction buffer [Tris-Cl, pH 8.0 (100 mM), EDTA (25 mM), NaCl (1.5 M), 2.5% CTAB, 2% β-mercaptoethanol and 1% PVP] and incubated for 1 h at 60°C. The phase separation was carried out twice with 15 ml chloroform: iso-amyl alcohol (24:1, v/v), mixed well by inversion and incubated for 10 min at room temperature. The tubes were centrifuged at 10000 rpm for 10 min at room temperature. The aqueous phase was collected with cut tips to fresh oak-ridge tube and 0.6 volume of isopropanol was added to it. This was incubated at room temperature for 1 h. DNA was precipitated by centrifuging at 10000 rpm for 20 min and the pellet was washed with 70% ethanol. The pellet was air dried and dissolved in 500 µl TE [Tris-Cl, pH 8.0 (10 mM) and 1 mM EDTA] buffer. RNaseA (50 µg/ml) treatment was carried out at 37°C for 2 h. The DNA was extracted with equal volume of chloroform: iso-amyl alcohol (24:1, v/v). The DNA was precipitated by adding 2.5 vol. of absolute ethanol and the pellet was washed with 70% ethanol. The pellet was

air-dried and DNA was dissolved in 100 μ l sterile water. The genomic DNA was quantified spectrophotometrically and concentration was calculated against the standard value of 1 OD₂₆₀ = 50 μ g/ml.

3.2.6 Southern blot analysis

3.2.6.1 Restriction digestion and gel electrophoresis

Genomic DNA (10 μ g) was digested using 40-50 U of appropriate restriction enzyme in 100 μ l reaction volume overnight (16-20 h) at 37°C. Complete digestion was desirable for the preparation of Southern blots; hence 5 μ l of the reaction was fractionated on a 1% mini-gel after the 16 h digestion period to observe the extent of digestion. If genomic DNA was partially digested after this time, a further 10 U of enzyme was added and reaction was further incubated at 37°C for 1 h to 2 h. The digested DNA was separated on 1% agarose gel in 1X TAE electrophoresis buffer (40 mM Tris-acetate, 1 mM EDTA) alongwith with size marker (supermix DNA ladder).

3.2.6.2 Transfer of DNA to nylon membranes

After fractionation of DNA by gel electrophoresis on 0.7% agarose, the gel was soaked in depurination solution (0.2 N HCl) for 20 min followed by soaking the gel in denaturation buffer (1.5 M NaCl, 0.5 M NaOH) for 45 min with constant gentle agitation. After denaturation, the gel was treated with neutralization buffer (0.5 M Tris pH 7.4, 1.5 M NaCl) for 45 min. The gel was rinsed with deionized water in between each treatment. The gel was finally soaked in neutral transfer buffer (10X SSC) for 20 min prior to transfer to the membrane. The transfer of DNA to membrane was carried out overnight at room temperature using 10X SSC as transfer buffer by upward capillary action similar to the protocol followed for northern blotting. The DNA was fixed to the membrane using UV crosslinker.

3.2.6.3 Southern hybridization

Southern hybridization experiments involving the use of radiolabelled probes were carried out in radioactive room taking adequate precautions.

3.2.6.4 Preparation and ³²P labelling of DNA probes

The template DNA was labeled by random priming reaction using NEBlot kit in 50 μ l reaction. Template DNA (25-50 ng) was dissolved in nuclease free water (36-38 μ l) and denatured in boiling water bath for 5 min. To the denatured DNA, 5 μ l 10X

klenow buffer, 2 μ l dATP, dTTP, dGTP (0.5 mM each), 2 μ l α^{32} P dCTP (3,000 ci/mmol, 50 μ Ci) and 1 μ l DNA Polymerase I (Klenow fragment) were added and incubated at 37°C for 1 h. The reaction was terminated by either adding 5 μ l of 0.2 M EDTA (pH 8.0) or immediately transferring to ice for 5 min. The synthesized probe was separated from unincorporated nucleotides by gel filtration on Amersham S-200 spin column by initially packing of column by centrifugation at 13000 rpm for 1 min. The packed column was used for purification from unincorporated nucleotide by centrifugation at 13000 rpm for 2 min.

3.2.6.5 Hybridization and autoradiography

The membranes were incubated for 2-3 h at 60°C in prehybridization buffer containing 0.5 M sodium phosphate (pH 7.2), 7% (w/v) SDS and 1 mM EDTA (pH 8.0). The radiolabeled probe was denatured by heating at 100°C for 5 min. The reaction was stopped by rapidly placing it on ice followed by its direct addition to the prehybridization solution. Hybridization was carried out for 14-16 h at 60°C. For washing, the hybridization solution was discarded and the membranes were washed two times with 2X SSC and 0.1 % SDS (w/v) at room temperature for 5 min. The wash buffer was discarded and the membranes were further washed in prewarmed 0.2X SSC and 0.1% (w/v) SDS twice at 60°C for 15 min. During the washing procedures, care was taken to prevent drying of the labeled membranes.

For autoradiography, the semi-dried membranes were exposed to X-ray films using hypercassettes and the cassettes were stored at -80°C for 1-4 d (depending on the counts). The exposed X-ray film was developed in dark room by incubating the X-ray films in developer solution (hydroquinone and potassium hydroxide) for 2-10 min depending on the appearance of signal. The film was rinsed with water briefly and transferred to fixer for 2-10 min till the film appears transparent.

3.2.6.6 Image analysis

Radioactive images were scanned with a high-resolution scanner (Fluro-S Multimager, BIO-RAD, USA) and the gel images were scanned with AlphaImager™ 2200. The band intensities were quantified with AlphaImager software (Alpha Innotech Corporation, San Leandro, CA, USA).

3.2.7 RNA extraction

Prior to RNA extractions, the glasswares, mortars, pestles and spatulas were baked at 200°C for 5-6 h and all the plasticwares, gel trays and combs were treated with 3% H₂O₂ to avoid RNase contamination.

3.2.7.1 Total RNA extraction using TRIzol reagent

The tissue samples (100-250 mg) were pulverized with liq N₂ and homogenized properly with 1 ml TRIzol reagent (phenol-guanidine isothiocyanate). For separation of aqueous and organic phases, 200 µl chloroform was added, mixed well and incubated at room temperature for 15 min. The mixture was centrifuged at 12,000x g for 15 min at 2 to 8°C. The aqueous phase containing RNA was collected in fresh microcentrifuge tube and was precipitated with isopropanol at 12,000x g for 10 min at 2 to 8°C. The RNA pellet was further washed with 70% ethanol at 7,500x g for 5 min at 2 to 8°C followed by air drying the pellet. Finally the pellet was dissolved in 20 µl of DEPC treated sterile water. Store RNA at -15 to -20°C.

3.2.7.2 Total RNA extraction using LiCl precipitation method

The tissue samples were crushed with liq N₂ and the powdered tissue was transferred to fresh microcentrifuge tubes containing equal volume of extraction buffer (3 M sodium acetate pH 5.2, 10% SDS and 0.5 M EDTA pH 8.0) and water saturated phenol (pH 4.0-5.0). The suspension was mixed well by vortexing and centrifuged at 13000 rpm for 10 min at room temperature. The supernatant was collected in a fresh microcentrifuge tube and equal volume of chloroform and water saturated phenol was added to it. This was vortexed briefly to ensure proper mixing followed by centrifugation at 13000 rpm for 5 min at 4°C. The RNA was precipitated by adding 1/3rd volume of 10 M LiCl and incubated on ice for 1 h. After spinning at 10000 rpm for 10 min, the RNA pellet was initially washed with 2.5 M LiCl for 10 min at 10000 rpm followed by 70% ethanol wash for 5 min at 8000 rpm. The pellet was air dried and dissolved in 20 µl of DEPC treated sterile water.

3.2.7.3 Total RNA extraction extraction for performing 5' and 3' RACE

For preparation of RACE ready cDNA total RNA isolation was performed with the RNAsasy Plant Mini Kit (Qiagen, USA) from 100 mg of frozen material

following manufacturer's protocol. The isolated RNA was treated with RNase free DNase (Qiagen, USA) to remove any contaminating DNA.

3.2.7.4 RNA quantification

The quality and quantity of RNA were determined by measuring the absorbance at 260 and 280 nm respectively. The concentration of RNA was calculated by comparing with the standard value, i.e., $1 \text{ OD}_{260} = 40 \mu\text{g/ml}$. The purity of RNA was determined by calculating the ratio A_{260}/A_{280} for each sample. The RNA samples with A_{260}/A_{280} ratio of 1.8-2.0 were considered pure.

3.2.7.5 Denaturing formaldehyde gel preparation for electrophoresis

Total RNA was run on 1.5% denaturing formaldehyde gel, for which 100 ml of denaturing gel was prepared by boiling 1.5 g agarose in 72 ml DEPC treated water. The solution was allowed to cool to 55°C and 10 ml of 10X MOPS and 18 ml of deionized formaldehyde (2.2 M) were added to it. Finally the solution was mixed well and poured on to gel tray and allowed to solidify. Denaturation reaction was prepared by incubating 20 μg of total RNA with 10X MOPS electrophoresis buffer (2 μl), formaldehyde (4 μl), formamide (10 μl) and 1 mg/ml EtBr (2 μl) at 80°C for 10 min. 6X RNA gel loading buffer (2 μl) was added, mixed well and the reaction mixture was loaded on to 1.5% denaturing gel. The gel was run on 1X MOPS electrophoresis buffer at 5-6 V/cm for 4-5 h. The RNA was visualized by placing the gel on a piece of saran wrap on a UV transilluminator.

3.2.8 Northern blot analysis

3.2.8.1 Transfer and fixation of denatured RNA to nylon membranes

The gel after electrophoresis was rinsed with DEPC treated water for 5 min followed by equilibration of the gel in 20X SSC for 20 min. The RNA was transferred to nylon membrane by upward capillary transfer method. The transfer system was assembled by sequentially placing a prewet whatman (3 mm) paper on a glass tray followed by the gel in reverse orientation, prewet nylon membrane, three prewet whatman papers (3 mm), paper towels, glass plates and weight at the top of the set up. The transfer of RNA from gel to the membrane was carried using 20X SSC as transfer buffer for 14-16 h. Care was taken to remove bubbles in between gel and the nylon membrane to

ensure proper transfer. The assembly was dismantled and the membrane was rinsed with 6X SSC for 5 min. The RNA was cross linked to the membrane by UV irradiation. After cross linking, the membrane was stained with methylene blue (0.03% in 0.5 M sodium acetate, pH 5.2) solution for 3-5 min to visualize the RNA. Excess stain was removed using sterile water.

3.2.8.2 Radioactive probe preparation and purification

Radioactive probe preparation and purification was same as prepared in case of southern hybridization.

3.2.8.3 Hybridization, washing and autoradiography

Prehybridization and hybridization experiments were performed as mentioned before in the section of southern analysis. The temperature for prehybridization and hybridization experiments was maintained at 60⁰C. For washing, the membrane was initially rinsed with wash buffer containing 2X SSC and 0.1% SDS at room temperature for 10 min followed by washing the membrane two times with 0.2X SSC and 0.1% SDS wash buffer for 15 min at 65⁰C. Autoradiography was performed as mentioned before.

3.2.8.4 Image analysis

Radioactive images were scanned with a high-resolution scanner (Fluro-S Multimager, BIO-RAD, USA) and the gel images were scanned with AlphaImagerTM 2200. The band intensities were quantified with AlphaImager software (Alpha Innotech Corporation, San Lecandro, CA, USA).

3.2.8.5 Removal of radioactive probe from membranes

Bound probe was removed from membranes by incubating them in 500 ml of boiling stripping solution (0.1 % SDS, 2 mM Na₂EDTA, pH 8.0) for 30 min, or until solution had reached RT. Membranes were washed with 2X SSC before proceeding to next step. To ensure efficient removal of probe membranes were sealed in plastic bags and re-exposed to X-ray film for 2 days. Membranes were stored in the dark at 4⁰C.

3.2.9 Real time PCR

SYBR green q-RT PCR was performed on an Applied Biosystem Step OneTM Real-Time PCR system. In each run, 2 µl of diluted cDNA was used as template for amplification per reaction. The samples was added to 18 µl of reaction mixture

containing 6.2 µl of sterile MQ-water, 10 µl of Power SYBR green PCR master mix (Applied Biosystems) 0.9 µl of each forward and reverse 20 pico moles (pm) primers (Table 3.1.7). Real time PCR amplification was carried out for 50 cycles of 94⁰C 10 sec, 76⁰C for 15 sec and 72⁰C for 55 sec. The temperature range for the analysis of melting curve was 60⁰C to 90⁰C over 30 sec. All reactions were performed in triplicate. Following formulas were used to calculate the relative quantification between internal control and expression of gene to be studied.

$RQ = 2^{-\Delta\Delta CT}$ where $\Delta\Delta CT = \Delta C_T(\text{test sample}) - \Delta C_T(\text{calibrator sample})$

Calibrator sample is the control sample on which relative expression is measured.

$\Delta C_T = C_T(\text{experimental gene}) - C_T(\text{Actin or others house keeping gene})$

C_T = The crossing threshold cycle, it is the cycle at which there is a significant increase in fluorescence with a manual threshold set above the background fluorescence or a specified threshold. C_T is inversely proportional to the logarithm of the initial number of template molecules.

3.2.10 Cloning of full length gene using 5' and 3' RACE

For 3' RACE 5 µg of total RNA isolated from flower tissue of *C. roseus* was reverse transcribed using CDS-III A primer and RevertAidTM H Minus M-MuLV RT-reverse transcriptase (Fermentas Life Sciences, USA) following clontech BD SMART 3' RACE protocol. After incubation at 42⁰C for 1.5 h in a hot lid thermal cycler, the reaction was stopped by heating at 70⁰C. This makes the 3' RACE ready cDNA which was used for further amplification and cloning of 3' ends of gene using the protocol discussed later.

For Amplification of 5' end strategy LD-PCR method was followed.

3.2.10.1 First Strand cDNA synthesis

Total RNA (5 µg) isolated from flower tissue was combined with 1 µl SMART IV (RNA) oligonucleotide, 1 µl CDS-III A PCR primer and deionized water to make the reaction volume upto 5 µl. The contents were mixed and incubated at 72⁰C for 2 min. 5X first strand buffer (2 µl), 1 µl DTT (20 mM), 1 µl dNTP mix (10 mM each) and 1 µl RevertAidTM H Minus M-MuLV RT-reverse transcriptase (Fermentas Life Sciences, USA) were added and the components were mixed well. The contents were

incubated at 42⁰C for 1 h in a hot lead thermal cycler and subsequently placed on ice to terminate the reaction.

3.2.10.2 cDNA amplification by LD-PCR

For cDNA amplification, 2 µl first strand cDNA, 80 µl deionized water, 10 µl, 10X PCR buffer, 2 µl 10 µM dNTP mix, 2 µl SMART IV as 5' PCR primer, 2 µl CDS-IIIA as 3' PCR primer and 5 µl 10X PCR buffer mix were added and the contents were mixed well by gently flicking the tube. The thermal cycling was initiated using the following cycling conditions: initial denaturation at 95⁰C for 1 min followed by 20 cycles of denaturation at 95⁰C for 15 sec and annealing and extension at 68⁰C for 6 min. After completion of cDNA amplification, 5 µl of the double stranded (ds) cDNA was loaded onto 1.2% agarose/EtBr gel to check the concentration and quality of cDNA synthesized. The ds cDNA was diluted 50 times by adding sterile water and used for the amplicfication of 5' end of gene as discussed below.

3.2.10.3 Amplification of DNA for 5' RACE and 3' RACE

PCR amplifications were performed with 5' and 3' RACE primers (gene specific primers) and 10X UPM followed by secondary amplification with nested and gene specific primers using the RACE ready cDNA as template for the 3' and LD PCR product for 5' RACE. A 50 µl reaction mixture contained 25-50 ng DNA template, 1 µl of 10 µM of each primer, 1 µl of 10 mM dNTPs, 5 µl of 10X Taq buffer containing 15 mM MgCl₂ and 1 U of Taq DNA polymerase. The PCR cycling parameters were as follows

3.2.10.4 3' RACE amplifications

When primer annealing temperature is >70⁰C

Intial two step protocol of 5 cycles 94⁰C for 30 sec and 72⁰C for 3 min followed by 3 step protocol of 5 cycles of denaturation of 94⁰C for 30 sec, annealing at 70⁰C for 30 sec and extension at 72⁰C for 3 min, followed by final 25 cycles of denaturation at 94⁰C for 30 sec, annealing at 68⁰C for 30 sec and extension at 72⁰C for 3 min.

When primer annealing temperature is 60-70⁰C

A 3 step protocol of 25 cycles of denaturation at 94⁰C for 30 sec, annealing at 68⁰C for 30 sec and extension at 72⁰C for 3 min used. The amplified product was resolved

on 2% TAE agarose/EtBr gel alongwith markers for checking and expected size band was eluted as discussed in cloning of DNA fragments.

3.2.10.5 5' RACE amplifications

The PCR cycling parameters used were of two step “touchdown” PCR as double stranded cDNA was used as template. Amplification involved 39 cycles of PCR reaction and the cycling conditions were: of 25 sec denaturation at 94⁰C and 3 min extension at 72⁰C for 7 cycles followed by 32 cycles of 25 sec denaturation at 94⁰C and 3 min extension at 67⁰C. Final extension of 7 min at 67⁰C was carried out after which the reaction was terminated at 4⁰C. Secondary PCR was performed using nested primers which involved 25 cycles of PCR reaction and the cycling conditions were: 25 sec denaturation at 94⁰C and 3 min extension at 72⁰C for 5 cycles followed 25 sec denaturation at 94⁰C and 3 min extension at 67⁰C for 20 cycles and final extension for 7 min at 67⁰C followed by termination of reaction at 4⁰C. The amplified product was resolved on 2% TAE agarose/EtBr gel alongwith markers for checking and expected size band was eluted as discussed in cloning of DNA fragments.

3.2.11 Preparation of Yeast elicited *C. roseus* suspension cell culture cDNA library

Yeast extract elicited *C. roseus* leaf suspension cell culture was used for cDNA library preparation. Cell suspension culture preparation was performed using the method as described by Dutta (2006).

3.2.11.1 Preparation of *C. roseus* suspension cell culture

C. roseus compact callus cluster (CCC) cultures were grown from leaf tissue of 6-8 weeks old seedlings in Gamborg's basal media supplemented with 1 mg/l 2,4-D and 0.1 mg/l BAP (BD3) (Sigma Chemicals). Culture was maintained by transferring approximately 1 g (fresh weight) of compact callus in 50 ml of fresh solid medium regularly at every 21 days (which constituted a single passage) for a period of twenty subcultures. Cell suspension culture was initiated by transferring 1 g CCC cultures (fresh weight) from third passage of its growth to 50 ml liquid Gamborg's basal media supplemented with 0.5 mg/l 2,4-D and 0.1 mg/l BAP (BD11) in 250 ml Erlenmeyer flask and kept on a gyratory shaker (100 rpm). Suspension culture was maintained by transferring approximately 10 ml suspension. in 50 ml of fresh liquid medium regularly at every 7 days interval (which constituted a single passage) for a period of ten subcultures (Fig. 3.2).

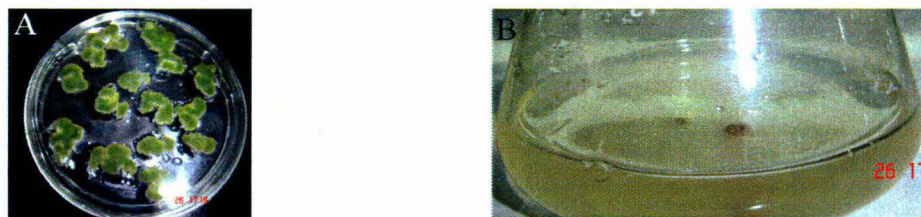


Fig. 3.2: Leaf induced callus (A) and cell suspension (B) cultures.

3.2.11.2 Elicitor treatment of cell suspension

C. roseus suspension culture (4 days old) was treated with purified Yeast Extract (YE) (Difco, Germany) to a final concentration of 400 µg/ml. The treated culture was maintained in 250 ml Erlenmeyer flask containing 50 ml of BD11 media and kept on a gyratory shaker (100 rpm). The treated cells were pelleted down after 30 min of treatment at 2000 rpm for 10 min. The cells were harvested in liquid nitrogen and stored at -80°C.

CLONTECH SMART™ cDNA library construction kit was used cDNA library preparation with following procedure.

3.2.11.3 Total RNA and mRNA extraction

Total RNA was extracted from 1 g of cell suspension (fresh weight) by Lithium Chloride method as discussed previously (Menke et al., 1996). Two microgram mRNA isolated from 250 µg total RNA using mRNA isolation kit (Roche, Mannheim, Germany) was used for cDNA synthesis according to the manufacturer's instructions. Total RNA and mRNA were quantified using GeneQuant Pro (Amersham Pharmacia Biotech, Uppsala) and checked on 1.5% denaturing agarose gel before proceeding for cDNA synthesis.

3.2.11.4 Synthesis of cDNA

First strand synthesis was performed as per manufacturer (CLONTECH) recommendations using SMART IV™ oligonucleotide and CDS-IIIA/3' PCR Primer. Reverse transcription reaction was performed using PowerScript™ reverse transcriptase by incubating at 42°C for 1 hr. Second strand synthesis was performed using LD PCR reaction with 5' PCR primer and CDS-IIIA/3' PCR primer. Proteinase K digestion was done to inactivate DNA polymerase activity. The cDNA was digested using *EcoR* I restriction enzyme and allowed to pass through CHROMO

SPIN-400 column for size fractionation. The cDNA was packaged in phagemid vector λ ZAP II to generate λ ZAP II library.

3.2.11.5 Preparation of cDNA library in phage

The cDNA library was constructed in λ ZAP II using the *EcoR* I cloning site. Three different ligation reactions were set up to optimize the ligation of cDNA with vector. Overnight ligation at 16°C with T₄ DNA ligase was performed. Ligated DNA was packaged in phage using pakagene extract (stratagene, USA) as per manufacturer protocol.

Titre of library was checked using the XL-1 Blue as host strain. Overnight culture of XL-1 Blue grown in 10 ml of LB media without antibiotic at 37°C, 180 rpm was used as starter culture for 50 ml LB with supplements of 10 mM MgSO₄ and 0.4% Maltose. The bacterial culture (OD₆₀₀ of 0.5) was centrifuged and the pellet was dissolved in 100 μ l SM buffer. The library was diluted (10^{-4} - 10^{-7}) in SM buffer and 2 μ l of each dilution was combined with 100 μ l of XL1-Blue MRF' cells (OD₆₀₀ of 0.5). The phage library was incubated with the XL1-Blue MRF' cells for 15 minutes at 37°C to allow the phage to attach to the cells. These phage attached bacteria were plated on agar plate after mixing with NZY top agar, melted and cooled to ~48°C, and plated immediately onto dry, pre-warmed NZY agar plates. The plates were allowed to set for 10 minutes and incubated at 37°C upside down until phages appear. Plaque titre was determined [in plaque-forming units per milliliter (pfu/ml)], using the following formula:

$$\frac{\text{Number of plaques} \times \text{dilution factor} \times 1000}{\text{Volume plated } (\mu\text{l})}$$

3.2.12 Screening of *C. roseus* cDNA library

3.2.12.1 Preparation of host bacteria

XL1-Blue MRF' glycerol stock was streaked onto LB-tetracycline agar plates and incubated at 37°C overnight. In the morning, a 50 ml LB broth, supplemented with 10 mM MgSO₄ and 0.2% (w/v) maltose, was inoculated with a single colony and grown at either 37°C with shaking for 4-6 h (OD₆₀₀ 1.0), or overnight at 30°C with shaking at 200 rpm. Cells were collected by centrifuging at 1000x g for 10 min, and the supernatant discarded. The cells were then gently resuspended in half the original

volume with sterile 10 mM MgSO₄, and aliquots diluted to an OD₆₀₀ of 0.5 with sterile 10 mM MgSO₄.

3.2.12.2 Plating out the library for screening

In a sterile 15 ml tube, 300 µl of OD₆₀₀ 0.5 diluted plating cells was mixed with 3000 pfu phage and incubated at 37⁰C for 15 min to allow the bacteria to adsorb phage. 4 ml NZY top agar which had been melted and cooled to 45⁰C, was added to the phage/bacteria mixture, then poured immediately onto a pre-warmed (37⁰C) 140 mm LB plate and rocked until the surface of the plate was covered. The plates were kept for 10 min at room temperature to harden and then placed inverted in a 37⁰C incubator. After about 5-8 h, plaques would begin to form. When plaques reached up to 1-2 mm in diameter then the plates were kept at 4⁰C till further use.

3.2.12.3 Preparation of nylon membranes for the plaque lifting

The nylon membrane (0.2 micron, Hybond-N amersham) was cut of 130 mm diameter and soaked in double distilled water. The membrane was wrapped in the filter paper and autoclaved in a sealed bag.

3.2.12.4 Plaque lifting on Hybond-N nylon membrane

Sterile nylon membranes were used for the lifting of plaques from cool plates in a laminar hood. The nylon membrane was kept on the plates for 5 min and pierced at three different positions to mark the orientation with the plates. The membrane was removed carefully with forceps. The membrane was kept on filter paper soaked with denaturation buffer (1.5 M NaCl, 0.5 M NaOH) for 5 min in a upside down position so that plaque doesn't come directly in touch with the buffer. After denaturation nylon membrane was kept on filter paper soaked in neutralization buffer (0.5 M Tris pH 7.4, 1.5 M NaCl) in same position for 5 min. The membrane was later on washed with 2X SSC and cross linked in UV cross linker as in case of southern and northern. The dried membrane was wrapped in saran wrap and kept in freeze till further use.

3.2.12.5 Hybridization, washing and autoradiography

Prehybridization and hybridization experiments with membranes were performed as mentioned earlier in the section of southern analysis. The temperature for prehybridization and hybridization experiments was maintained at 65⁰C. For washing, the membrane was initially rinsed with wash buffer containing 2X SSC and 0.1% SDS at room temperature for 10 min followed by washing the membrane two times

with 0.2X SSC and 0.1% SDS wash buffer for 30 min at 65°C. Autoradiography was performed as mentioned before with slight modification that the membranes were completely dried and X-Ray film were marked as orientation of the membranes. Comparison of the developed X-Ray with the original plate revealed the locations of positive plaques.

3.2.12.6 Purification of plaque clones of interest and PCR confirmatory test

Plaques identified as positive by primary screening were removed from the gel as a plug, using a cut-off end of a 1000 µl pipette tip. The plug was then placed into 500 µl SM buffer (20 mM Tris HCl pH 7.5, 100 mM NaCl, 10 mM MgSO₄) with 20 µl of chloroform. Phage was allowed to diffuse into SM buffer overnight and then the supernatant was transferred to a new tube. The titre of the phage was determined, and secondary and tertiary screenings were carried out as previously described. In order to minimize inclusion of inserts in the cDNA library and to avoid the false positive screening results, individual plaques were selected randomly after tertiary screening and purification and used as a template for PCR. Each PCR was performed in a 25 µl final volume containing 0.4 µM of each primer (M13F-M13R, table 3.1.5), 0.2 mM each dNTPs, 1X PCR buffer, 1 U of Taq DNA polymerase and seeded with 1 µl phage. PCR parameters were as follows: an initial denaturation at 94°C for 3 min, followed by 35 cycles of 30 sec at 94°C, 45 sec at 58°C and 30 sec at 72°C. Final extension was carried out at 72°C for 10 min. Amplifications were performed in a Biorad Thermal cycler (Biorad, USA). Amplified products were visualised on 1% agarose/EtBr gels and compared against DNA size marker.

3.2.12.7 *In vivo* excision of the pBLUESCRIPT phagemid vector containing insert from the λ-ZAP vector

After cDNA clones of interest were identified in the intact Lambda ZAP vector by radio labeled probe, a representative clone was selected for further processing as a process of *in vivo* biological excision of the insert and sub-cloning into a plasmid vector using the single clone excision protocol as per the Stratagene instruction manual. A timeline of the procedure follows:

Day 1

1. The plaque of interest was cored from agar plate and transferred to a sterile microcentrifuge tube containing 500 µl SM buffer and 20 µl chloroform,

vortexed, and incubated at 4⁰C overnight to release the phage particle into SM buffer.

2. A culture of XL1-Blue MRF` cells supplemented with 0.2% maltose and 10 mM

MgSO₄ was grown overnight at 30⁰C.

Day 2

3. The XL1-Blue MRF` cells were spun down (1000x g) and resuspended at OD₆₀₀ of 1.0 in 10 mM MgSO₄.
4. In a 50 ml Falcon tube the following were combined:
 - a. 200 µl of XL1-Blue MRF` cells at an OD₆₀₀ of 1.0
 - b. 250 µl of phage stock (containing >1x10⁵ phage particles)
 - c. 1 µl of ExAssist helper phage (>1 x 10⁶ pfu/µl)
5. The Falcon tube was incubated at 37⁰C for 15 min.
6. 3 ml of NZY broth was added to the Falcon tube and incubated at 37⁰C with shaking, overnight.
7. SOLR culture in NZY broth, without supplement, was grown overnight at 30⁰C with shaking.

Day 3

8. The SOLR cells were spun down (1000x g) and resuspended at OD₆₀₀ of 1.0 in 10 mM MgSO₄.
9. The Falcon tube was heated at 65-70⁰C for 20 min, and then spun at 1000x g for 15 min.
10. The supernatant, containing the excised pBLUESCRIPT phagemid vector packaged as filamentous phage particles, was decanted into a sterile Falcon tube.
11. 200 µl of freshly grown, diluted to OD₆₀₀ of 1.0, SOLR cells were added to two Falcon tubes - one tube then received 100 µl of the phage supernatant from step 10 the other tube received 10 µl.
12. Both tubes were incubated at 37⁰C for 15 min.

13. 300 µl of NZY broth was added to each tube and incubated at 37°C for 45 min.
14. 1 µl and 200 µl of the cell mixture from each tube was plated on LB-kanamycin agar plates (50 µg/ml) and incubated at 37°C overnight.
15. Positive colonies were screened on the basis of colony PCR and further processed.

3.2.13 *In silico* analysis

Initial designing of degenerate primers was done using WISE2 (Birney et al., 2004) and clustalW 1.82 alignment software. Similarity searches were performed using BLAST analysis methods (Altschul et al., 1997). Predictions based on translated amino acid sequences were generated by software programs available at the ExPASy proteomics server of the Swiss Institute of Bioinformatics. The nucleotide alignment of peroxidases for making phylogenetic tree was done using MAFFT version 5.667 programme (Kato et al., 2005). The phylogenetic tree was constructed following maximum parsimony method using MEGA2 and MEGA4 programme (Kumar et al., 2001 and Tamura et al., 2007). A parameter of close-neighbor interchanges (CNI) having a search level 3 and 100 bootstrap replicates were considered for this purpose.

Table 3.1.8: Softwares used for *in silico* analysis are listed below.

Function	Program used	Web Site
General alignment	ClustalW	http://www.ebi.ac.uk/clustalw
Pair wise alignment	Align	http://blast.ncbi.nlm.nih.gov/bl2seq/wblast2.cgi
Amino acid to nucleotide alignment	WISE2	www.ebi.ac.uk/Wise2/
Alignment for submission to Phylogenetic tree preparation	MAFFT v6.240	http://align.genome.jp/mafft
Homology search	blastn; blastx	http://www.ncbi.nlm.nih.gov/BLAST
Restriction mapping	TACG V3	http://athena.bioc.uvic.ca/tacg3/form.html

	NEBcutter V2.0	http://tools.neb.com/NEBcutter2/index.php
Reverse complementation	Reverse Complement	http://bioinformatics.org/sms/rev_comp.html
Phylogenetic tree	MEGA 2.0	http://www.megasoftware.net/
Open Reading Frame Finder	ORF Finder	http://www.ncbi.nlm.nih.gov/projects/gorf/ http://ca.expasy.org/tools/dna.html
Translation of nucleotide to amino acid	Translate	
Computation of pI/MW value of protein	Compute pI/Mw tool	http://ca.expasy.org/tools/pi_tool.html
Protein Pattern and profile searches	ScanProsite	http://ca.expasy.org/tools/scanprosite/
Reverse complementary	Reverse Complement	http://bioinformatics.org/sms/rev_comp.html

3.2.14 *In vitro* techniques

3.2.14.1 Sterilization of seeds

Seeds of *C. roseus* were soaked in tap water. Next day, seeds were washed with 7% teepol for 10 min followed by washing the seeds in running tap water to remove excess detergent. Under laminar hood, the seeds were first sterilized by 4% Sodium hypochlorite for 5 min. followed by washing in sterile water for 5 min, thrice. The seeds were also treated with 100% ethanol for 10 sec and washed with sterile water as in the previous step.

3.2.14.2 Germination of seeds

Sterile seeds were blot dried and allowed to germinate initially in dark on half strength of Gamborg's B5 basal media (Gamborg et al., 1968) for 4-5 d in dark. Seeds showing germination were then transferred to light and were maintained at 25±2⁰C,

70% relative humidity and 2000 lux light (Philips cool white fluorescent light) for 16/8 h light and dark photoperiod.

3.2.14.3 Generation of transgenic calli: Transformation of *C. roseus* with recombinant *A. tumefaciens*

3.2.14.3.1 Explant Preparation for transformation

The explants were taken from 2 months old seedlings grown under aseptic conditions and subcultured every six weeks. The leaf (1x1 cm²) explants were cut from seedling and preincubated on tobacco shoot induction media (TSM) for 24 h in dark. Approximately 50-100 explants were used for each experiment.

3.2.14.3.2 Preparation of recombinant *A. tumefaciens* culture

Single colony of *Agrobacterium* was inoculated in 50 ml of YEB medium and grown overnight at 28°C with continuous shaking at 200 rpm until OD₆₀₀ reached 0.5-0.6. This culture was directly used for transformation.

3.2.14.3.3 Transformation and co-cultivation

Agrobacterium culture of OD₆₀₀ 0.5-0.6 was used for transformation of overnight incubated explants. The agrobacterium culture was pelleted at 5000 rpm for 10 min and resuspended in MS-basal media in 1/10th dilution of initial bacterial culture. The explants were incubated for 20 min in the agrobacterium solution. Finally after 20 min, explants were washed with sterile water for three times and blot dried on sterile blotting paper for few seconds. The explants were then cocultivated on TSM medium at 25±2°C for 2 d in dark.

3.2.14.3.4 Generation of transgenic calli on antibiotic media

To remove excess of *Agrobacterium* from explant after 2 d of cocultivation, the explants were transferred to TSM medium containing Kanamycin (300 mg/l) and cefotaxime (250 mg/l) and incubated in light and were maintained at 25±2°C, 70% relative humidity and 2000 lux light (Philips cool white fluorescent light) for 16/8 h light and dark photoperiod. The explants were subcultured every week on new TSM medium containing antibiotics. The transgenic calli were excised from explants and maintained at 25±2°C, 16/8 h light and dark photoperiod and transferred to fresh medium every week till harvesting for analysis.

3.2.14.3.5 Determination of transgenic calli

Transgenic calli were evaluated on the basis of PCR amplification. About 100 mg of tissue were excised from calli and lyophilized in a lyophilizer. The genomic DNA isolated from this lyophilized tissue were used for performing PCR amplification using vector specific as well as kanamycin gene specific primers.

3.2.14.3.6 Transformation efficiency

Transformation efficiency was calculated with the following formula:

$$\text{Transformation efficiency} = \frac{\text{No. of transgenic calli} \times 100}{\text{No. of explants infected}}$$

3.2.14.4 Generation of transgenic tobacco

Standard leaf disk transformation procedure is used for the generation of transgenic tobacco.

3.2.14.4.1 Explant Preparation for transformation

The explants were taken from 2 months old seedlings grown under aseptic conditions and subcultured every six weeks. The leaf (1x1 cm²) disks were cut from seedling and preincubated on tobacco shoot induction media (TSM) for 24 h in dark. Approximately 20-30 explants were used for each experiment.

3.2.14.4.2 Preparation of recombinant *A. tumefaciens* culture

Single colony of *Agrobacterium* was inoculated in 50 ml of YEB medium and grown overnight at 28°C with continuous shaking at 200 rpm until OD₆₀₀ reached 0.5-0.6. This culture was directly used for transformation.

3.2.14.4.3 Transformation and co-cultivation

Agrobacterium culture of OD₆₀₀ 0.5-0.6 was used for transformation of overnight incubated explants. The agrobacterium culture was pelleted at 5000 rpm for 10 min and resuspended in MS-basal media in 1/10th dilution of initial bacterial culture. The explants were incubated for 20 min in the agrobacterium solution. Finally after 20 min explants were washed with sterile water for three times and blot dried on sterile blotting paper for few seconds. The explants were then cocultivated on TSM medium at 25±2°C for 2 d in dark.

3.2.14.4.4 Generation of transgenic shoots on antibiotic media

The explants were transferred after two days of co-cultivation to TSM medium containing Kanamycin (300 mg/l) and cefotaxime (250 mg/l) and incubated in light and were maintained at $25\pm 2^{\circ}\text{C}$, 70% relative humidity and 2000 lux light (Philips cool white fluorescent light) for 16/8 h light and dark photoperiod. The explants were subcultured after every week on new TSM medium containing antibiotics. The newly developed shoots were excised from explants and transferred to the TSM medium lacking NAA hormone.

3.2.14.4.5 Transfer of transgenic tobacco plants to pot

After development of well established root and shoot system in the tissue culture the tobacco plants were transferred to the pots containing sterile compost. The pots were initially kept under cover of polythene bags to conserve the moisture. These potted plants were transferred to soil after 15 days and kept in a green house under daylight conditions at $25\pm 2^{\circ}\text{C}$ for further studies.

3.2.14.4.6 Growth Index study

The active growing phase for different transgenic calli was determined by calculating the growth index at I, II, III and IV week. After each interval, tissue was subcultured to a new media. The increase in (fresh wt) was calculated for each tissue type by subtracting wt of media with tissue to the already weighed media without tissue. The growth index was calculated with the following formula:

$$\text{G. I.} = \frac{\text{Increase in dry weight} \times 100}{\text{Initial dry weight (DW)}}$$

3.2.14.4.7 Growth rate measurement for transgenic tobacco plants

Stem length was used to estimate the growth rate of plants. Stem length was measured from the top of the shoot apex to the base of the stem.

3.2.14.5 Evaluation of T1 generation of transgenic tobacco plants

3.2.14.5.1 Seeds sterilization

Wild type and T1 seeds of transgenic tobacco were surface sterilized with 70% ethanol in a microcentrifuge tube for 1 min with constant agitation under a laminar flow hood. After the treatment, ethanol was removed using a pipette. The seeds were immersed in 2% (v/v) sodium hypochlorite solution containing a drop of Tween 20

for 15 min, agitated occasionally by tapping the microcentrifuge tube and subsequently washed at least six times with autoclaved Milli-Q water.

3.2.14.5.2 Seeds plating on stress media

For salt stress, the seeds were germinated on two different salt containing media as 0.25 M NaCl and 0.25 M KCl. Seeds were considered to be germinated after radical and green cotyledons emergence occurred. Seed germination after 3 days on MS medium was used as control and compared to seed germination on high salt medium which were evaluated after 13 days. The observation was recorded over a period of 8 days. The seedlings weight was evaluated after 21 days.

3.2.14.5.3 Cold stress treatments

For cold stress the seeds were grown in medium containing half-strength Murashige and Skoog medium without sucrose and organic ingredients (MSH) for 21 days in a culture room maintained at $25\pm 2^{\circ}\text{C}$ under a 16 h light/8 h dark cycle and each rack was illuminated with light ($50\text{-}100\ \mu\text{mol}\cdot\text{m}^{-2}$ per s) provided by four white fluorescent tubes Phillips Champion 40W/54). The 21-day-old seedlings were transferred to a cold chamber maintained at $8\pm 1^{\circ}\text{C}$ for 15 days. The plates then were transferred back to culture-room conditions for recovery of seedlings. Observations were recorded after 15 days of recovery.

3.2.14.6 Histochemical GUS staining and Fluorescence microscopy

Histochemical localization of GUS activity was analyzed after incubating the samples in X-Gluc buffer (50 mM Sodium Phosphate buffer, pH 7.0, 10 mM EDTA, 0.1% Triton X-100, 5 mM Potassium Ferrocyanide and 3.8 mM 5-bromo-4-chloro-3-indolyl glucuronide) at 37°C for 12 h. For sectioning, leaf discs stained with GUS were mounted in Jung tissue freezing medium (Leica Instruments, Germany). Frozen sections of 30 micron were layered on glass slides with a Cryomicrotome (CM 1510S; Leica Instruments, Germany) adjusted to -16°C for microscopy. Sections (30 micron) were put under a cover slip and viewed by Diascopic microscopy (Nikon Eclipse 80i, Japan) for histochemical GUS staining. GFP localization was viewed by Epifluorescence microscopy (Nikon Eclipse 80i) using cubes of dichroic mirror with excitation filter and barrier filter combination sets for detection of FITC. Images were captured with a digital camera (model DXM 1200C Nikon Japan) and saved using

image capturing software ACT-1C (Nikon, Japan) and further processed using Image-Pro Express image analysis software (Media Cybernetics, USA).

3.2.14.7 Confocal Imaging

Green Fluorescent Protein (GFP) was observed under Leica TCS SP2 AOBS Laser Confocal Scanning Microscopy (Leica, Microsystems, Exton, PA). For imaging GFP the 488 nm line of the Argon Laser was used for excitation and emission was detected at 520 nm. Differential Interference contrast (DIC) images were captured using the transmission light detector of the confocal microscope. Images were assembled using photoshop 5.0 (Adobe Systems)

3.2.15 Stress treatments

Six-eight month old potted mature plants of *C. roseus* var. Pink were subjected to different stress conditions in the following manner:

Wounding stress was performed by puncturing the young leaves attached to plants several times across the apical lamina with surgical blade, which effectively wounded ~40% of the leaf area.

For cold stress, whole plants were kept at 4⁰C while controlled plants were maintained in the green house at 25⁰C.

Methyl jasmonate treatment was applied on leaves detached from plants and kept on paper soaked in 1/10 MS basal media by painting on the adaxial surface of the leaves and the tray containing the leaves was sealed with saran wrap. In controlled experiment, similar leaves were painted with double distilled water containing the same amount of ethanol required for dissolving methyl jasmonate.

For UV treatment, young leaves were detached from the plants and kept on 1/10 MS media. A short term exposure (2 min) of leaves under UV lamp (λ_{\max} 312 nm; 28 J m⁻²s⁻¹) was done which was followed by incubation on 1/10th MS medium for various time periods before harvesting. For each treatment young leaves, first to third from the shoot apex, were used. The leaves were harvested at different time points by snap freezing in liquid nitrogen and stored in -80⁰C for further analyses

For oxidative stress treatments, fully expanded leaves (approximately 1.0 cm²) cut from plants grown in the greenhouse were floated on either H₂O₂, Methyl Viologen (MV) or distilled water at 25⁰C in strong light conditions of 2000 μ mol m⁻²s⁻¹.The

chlorophyll a and b contents of the leaf tissues were determined by spectrophotometry as follows.

3.2.16 Leaf chlorophyll determination

Total chlorophyll estimation from tobacco leaves was performed using DMF method (Kanneganti and Gupta, 2008). About 20 mg of leaf tissue was added to the eppendorf tube containing 800 μ l DMF (N-N dimethyl formamide) and incubated in dark for 2 h at room temperature. After completion of 2 h, the OD of the solvent was taken at 663.8 and 646.8 nm wavelengths. The total chlorophyll content was calculated using the following formula: $[\text{chl a +b}] = 17.67 \times A_{646.8} + 7.12 \times A_{663.8}$.

3.2.17 Measurement of chlorophyll fluorescence to measure photosynthesis

Chlorophyll fluorescence was measured by using imaging PAM chlorophyll fluorometer (Walz, Effeltrich, Germany). PAM stands for the pulse-amplitude-modulation in which fluorescence is excited by very brief but strong light pulses from light emitting diodes. The leaf of plant for which measurement has to be made was kept on the stage of instrument and initiated by default parameter the instrument. Effective quantum yield of PSII (YII) was calculated as: $YII = \Delta F/F_m' = (F_m'F_t)/F_m'$, where F_t was the fluorescence yield at any time (steady state) and F_m' was the maximum yield reached in a pulse of saturating light during illumination. All the measurements were done in a closed chamber under controlled growth conditions. For each plant at least four leaves were used and within each leaf three different positions were selected for data recording.

3.2.18 Protein extraction, immunoblot preparation and enzyme assay

3.2.18.1 Total soluble protein extraction from *C. roseus* tissue for immunoblot preparation

Plant tissue was pulverized with a mortar and pestle in the presence of liquid nitrogen and the powder was treated with 4 ml of extraction buffer (100 mM sodium phosphate (pH 7.5), 2 mM DTT and 5% w/v polyvinylpyrrolidone) per gram fresh weight of tissue (Di Fiore et al., 2002). The homogenous mixture was centrifuged at 17,500x g for 30 min at 4⁰C to separate the protein fraction from cell debris. The supernatant containing the total soluble protein was analyzed by means of western blot analysis.

3.2.18.2 Determination of total protein content of supernatant

Total soluble protein content was determined using the Bradford assay procedure as follows.

Standard curve was prepared using four dilutions from a 1 mg/ml protein stock solution of BSA. This is accomplished by adding '0' (blank), 10, 20, 40, 80 and 100 μ l of protein stock solution to individual tubes and adjust the volume to 100 μ l with water. These samples were prepared in five replicates. To these samples 900 μ l of Bradford reagent (Sigma) was added and mixed thoroughly. The mixture was incubated for five minutes at room temperature and spectrophotometer was used for calculation of Optical Density (OD) at 595 nm. Linear curve was prepared using the spectrophotometer reading from which the unknown concentration of protein was determined.

3.2.18.3 Western blotting

Samples (20 μ g of each) were boiled for 10 min in an equal volume of 2X SDS-PAGE sample buffer with 0.2 M DTT, undissolved material was removed by centrifugation at 10,000 g. Prestained protein molecular weight marker (Fermentas, USA) were used in gels to visualize the size of protein and efficiency of transfer onto the nylon membrane (Hybond C-extra, Amersham). The proteins were electroblotted for overnight at 90 mA in a Bio-Rad mini trans-blot system. The blotting buffer was 192 mM Glycine, 25 mM Tris, pH 8.3, containing 10% (v/v) methanol. For immunodetection, blotted nylon membrane was blocked with blocking buffer, i.e. 5% decream milk in TBS (10 mM Tris pH 7.6 and 0.15 M NaCl) for 1 h. The blocked nylon membrane was incubated in CrPrx antibodies with 1:1000 dilution in buffer containing 1% decream milk in TBST (10 mM Tris pH 7.6, 150 mM NaCl and 0.05% w/v Tween-20) for 1 h. Unbound primary antibodies were removed by washing in TBST buffer and the membrane was then incubated for 1 h at room temperature in TBS buffer containing HRP conjugated goat anti-rabbit IgG (diluted to 1:100,000). Following the removal of unbound secondary antibody, peroxidase activity of HRP was revealed using SuperSignal® West Pico Chemiluminescent Substrate (Pierce, USA).

3.2.18.4 Total soluble protein extraction from *C. roseus* tissue and peroxidase enzyme assay

Frozen tissues (2 g fresh wt) were crushed to fine powder in chilled mortar and pestle, while half of the sample was used for protein extraction and the other half was used for RNA extraction. Total protein was extracted for enzyme assay following the methods described by Misawa et al. (1988) and El-Sayed et al. (2005) with certain modifications. The powdered sample was homogenized with 2 vol. of Tris HCl buffer (100 mM, pH 6.8) after addition of 50 mg of polyvinylpyrrolidone (Sigma Aldrich, USA). The homogenous mixture was centrifuged at 14,000x g for 30 min. at 4⁰C. The supernatant was used for determination of peroxidase activity. Protein concentration was determined following the method as described by Bradford (1976), using bovine serum albumin as standard as discussed above. All the steps of protein extraction were performed at 4⁰C.

Peroxidase activity was assayed colorimetrically using *o*-phenylenediamine (OPD) (Sigma-Aldrich, USA) as oxidizable substrate. The assay condition for OPD oxidation was same as described by Endo et al. (1988) with slight modifications. Crude extracts (2-4 μ l) from different parts of plant were added separately to buffer containing 100 mM Tris HCl, pH 6.8 and 3.7 mM OPD. Sample volume was adjusted to 1 ml with 100 mM Tris HCl pH 6.8. The reaction was started with the addition of 8.8 mM H₂O₂ followed by incubation at room temperature in the dark condition. Reaction was stopped after 10 min by adding 5 N H₂SO₄ (100 μ l). Absorbance was measured at 492 nm and the enzyme activity was calculated in units using the extinction coefficient, 1.578 mM⁻¹cm⁻¹ (Romano et al., 2000). One OPD unit is defined as the amount of enzyme that oxidizes 0.01 μ mol OPD per min. The experiments for activity assay were carried out in triplicate manner and were repeated for three times.

3.2.18.5 Total soluble protein extraction from transgenic tobacco and *C. roseus* leaf calli and peroxidase enzyme assay

Leaf tissue (1 g) from greenhouse-grown control and transformed tobacco plants with peroxidase gene *CrPrx* and *CrPrx1* was homogenized and extracted in a 4 ml buffer containing 1 mM ascorbate, 1 mM EDTA, and 50 mM potassium phosphate (pH 7.0). The homogenate was centrifuged at 14,000x g for 20 min. at 4⁰C. The supernatant was collected and again centrifuged in ultracentrifuge at 35000 rpm for 30 min. at

4°C. The supernatant was collected and protein concentration was determined by Bradford assay (1976) as discussed above. Peroxidase activity with guaiacol or ascorbate as the reducing substrate was determined in a 1 ml reaction mixture containing 50 mM potassium phosphate (pH 7.0), 1 mM guaiacol or ascorbate, and 0.5 mM H₂O₂. The oxidation of guaiacol was followed by a change in A₄₇₀ (€ 26.6 mM⁻¹ cm⁻¹) while for ascorbate the change was A₂₉₀ (€ 2.8 mM⁻¹ cm⁻¹). Total protein from transgenic *C. roseus* leaf calli was extracted using 250 mg of tissue with the methodology discussed for transgenic tobacco protein extraction.

3.2.19 Biochemical analysis

3.2.19.1 Total alkaloid extraction

For extraction of total alkaloid from *C. roseus* leaf, root and *in vitro* tissues, the protocol of Singh et al., 2000 was followed. Tissues were harvested at various time periods and dried at 37°C. The dried tissue was crushed to powder and the dry weight was measured. Total alkaloid was extracted from 1 g of powdered tissue (DW) three times with methanol (10-15 ml). The extract was reduced to 1/3rd volume after air drying and 3% HCl was added to it and mixed properly. To the acidified solution equal volume of ethyl acetate was added and phase separation was allowed to take place for 30 min. The lower layer was collected and the phase separation was again carried out with ethyl acetate for three times. The pH of the extract was set at 8.5 with liquor ammonia. The lower layer was discarded and equal volume of chloroform was added to the upper layer. The extraction was carried out for three times and extract was allowed to dry at room temperature. Finally the extract was dissolved in 1 ml methanol and stored at -20°C.

For the callus tissue, lyophilization drying was performed followed by crushing it to fine powder and the dry weight was measured. Extraction of total alkaloid was performed in methanol as 10 ml per gram of powdered tissue thrice. The upper phase was collected after centrifugation in oakridge tube in sorvall rotor at 14000x g for 15 minutes at room temperature and dried to 1/3rd volume in 50 ml falcon tube. After drying the sample 7 ml of 3% HCl was added to it and mixed properly. To this solution equal volume of ethyl acetate was added and phase separation was allowed to take place for 30 min. The lower layer was collected in new falcon tube and the phase separation was again carried out two more times. The pH of the extract was set at 8.5

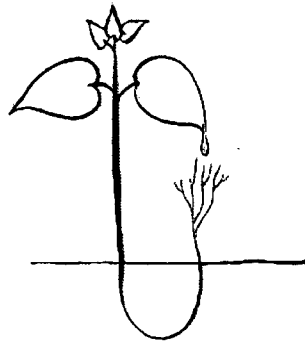
with liquor ammonia. To this collected lower layer equal volume of chloroform (i.e. 7 ml) was added, mixed well and the lower layer was collected in new falcon tube. The procedure of chloroform extraction was performed two times more and the collected sample was air dried at room temperature up to 2 ml volume. This 2 ml sample was transferred to 2 ml eppendorf of known weight and whole extract was dried in this eppendorf only. Finally the extract was dissolved in 500 μ l of methanol and stored at -20⁰C until analysis was performed using HPLC. Amount of total alkaloid was measured as follows.

Amount of total alkaloid= wt of vacant eppendorf-wt of eppendorf after drying the sample

3.2.19.2 HPLC analysis

The HPLC analysis of specific MIAs was performed according to Singh et al. (2000) with minor modifications. Chromatographic separation of major indole alkaloids of *C. roseus* was carried out on a reversed-phase C18 column with binary gradient mobile phase profile. The identification of the compounds was based on the retention time and comparison of the UV spectra with those of the authentic standards. Solutions of different authentic samples (tryptophan, tryptamine, catharanthine, vindoline, vinblastine, vincristine, ajmalicine and serpentine) were prepared in methanol (1 mg/ml) and used in different concentrations for the preparation of calibration graphs, linear in the range of “0.25 to 100 μ g”. Quantification analysis based on area of the peak and it was repeated during the same time as mentioned above for each tissue with three replicates and the mean as well as standard deviations were calculated.

CHAPTER 4



Results and Discussion

4.1: Cloning, characterization and localization of a novel basic peroxidase gene CrPrx from Catharanthus roseus

4.1.1 Introduction

Catharanthus roseus (L.) G. Don (Apocynaceae) is the commercial source of a large number of monoterpenoid indole alkaloids (MIAs), with over 130 compounds isolated and identified (Verpoorte et al., 1997; Samuelsson, 1999). It is one of the most extensively investigated medicinal plants, chiefly due to the presence of two of the most important anti-tumor agents employed in medicine, the bisindole alkaloids vinblastine and vincristine, which get accumulated in leaves along with the other important TIAs used in pretreatment of circulatory ailments (anti-hypertensives) such as ajmalicine and serpentine, accumulating in roots (Creasey, 1994).

It is known that biosynthesis of vinblastine in *C. roseus* plants begins with the amino acid tryptophan and a monoterpenoid geraniol. The whole pathway requires the involvement of at least 35 intermediates, 30 enzymes, 30 biosynthetic and at least 2 regulatory genes. All the terpenoid indole alkaloids are derived from the common precursor strictosidine, which results from the fusion of tryptamine which is the decarboxylation product of tryptophan, with the monoterpenoid secologanin. After the deglycosilation of strictosidine, the terpenoid indole alkaloid biosynthetic pathway splits into two long branches leading to vindoline and catharanthine, the monomeric precursors of vinblastine and vincristine (Fig. 2.1). The coupling of vindoline and catharanthine leads to α -3', 4'-anhydrovinblastine, a common precursor for all dimeric monoterpenoid indole alkaloid (MIAs). Several lines of evidence indicate that vacuolar class III plant peroxidases may be responsible for oxidation of ajmalicine to serpentine. Also a vacuolar class III peroxidase has been reported to be involved in coupling of vindoline and catharanthine to α -3', 4'-anhydrovinblastine.

Peroxidases are ubiquitous class of enzymes that oxidize a vast array of organic and inorganic reducing compounds in the presence of hydrogen peroxide. Class III peroxidases are heme containing glycoproteins having various conserved domains which distinct them from class I ascorbate peroxidase (also found in plants) and class II fungal peroxidase (Welinder, 1992; Penel, 2000; Welinder et al., 2002). Higher plants possess large number of class III peroxidases. The *Arabidopsis* genome, for instance contains 73 annotated class III peroxidase genes, 65 of which are expressed in various tissues and therefore likely to encode functional enzymes (Valério et al., 2004). The rice genome however, contains over twice as many

peroxidase genes (138) as the *Arabidopsis* genome, largely as a consequence of gene duplication events (Passardi et al., 2004). A high level of redundancy is therefore expected among class III plant peroxidases in their various functions: oxidation of toxic reductants, lignifications, suberization, cross linking of cell wall proteins, salt tolerance, oxygen stress, auxin catabolism and defence responses to wounding and pathogen attack (Yoshida et al., 2003). The expressed proteins of class III peroxidase are targeted to secretory pathway by N-terminal signal and therefore are extraprotoplasmic in nature. These proteins are localized either in the cell wall or in the vacuole.

In this chapter cloning and characterization of a novel peroxidase gene (*CrPrx*) had been reported. The *CrPrx*-GFP fusion protein studies show that at subcellular level the *CrPrx* protein is localized to cell wall. The observed expression patterns suggest its potential role during stress conditions and elicitor treatment in *C. roseus*. The two intron class *CrPrx* expression studies shows its ubiquitous presence.

4.1.2 Results

4.1.2.1 Cloning of *CrPrx* gene

Cloning of *CrPrx* gene was performed using degenerate primers. The degenerate primers were designed from the conserved region present in class III peroxidases. These conserved regions were basically the active site of peroxidase. (for details, please refer to materials and methods section).

4.1.2.2 Use of degenerate primer pairs to amplify peroxidase fragment

Two sets of degenerate primer pairs namely PF-1 & PR-1 and PF2 & PR2 designed from the conserved region of Class III peroxidases were used for RT-PCR amplification. The template used was the cDNA prepared from total RNA isolated from different tissues of *C. roseus* var. pink. Degenerate PCR amplification with different primers shows different size of fragments (Fig. 4.1.1). The band seen in lanes 3, 5, 7, 9, 11, 13 and 15 shows desired size of fragments i.e. ~500 bp. The strongest amplification observed in lane 3, 5, 7, 9, 11, 13 and 15 were eluted and cloned in pGEM-T-Easy vector and subsequently used for the transformation of *Escherichia coli* DH5 α strain. PF2-PR2 primer pair amplification represented in lane 2, 4, 6, 8, 10, 12, 14, and 16 did not result in expected size. The white colonies obtained

from *E. coli* transformation were used for further confirmation of insert using colony PCR.



Fig. 4.1.1: RT-PCR amplification using cDNA prepared from tissue specific RNA using degenerate primers. Odd numbers lanes show amplification with PF1-PR1 primers while the even numbers show amplification with PF2-PR2 primers. The cDNA used as template was prepared from the total RNA of different tissues. M 500 bp ladder, 1-2 young leaves, 3-4 mature leaves, 5-6 old leaves, 7-8 flower bud, 9-10 flower, 11-12 fruit, 13-14 root, 15-16 internodal tissue.

Colony PCR was performed using vector specific primer M13F and M13R for confirming the presence of insert in the clones. Out of 15 (randomly selected) clones screened, all clones showed presence of the expected insert (Fig. 4.1.2).

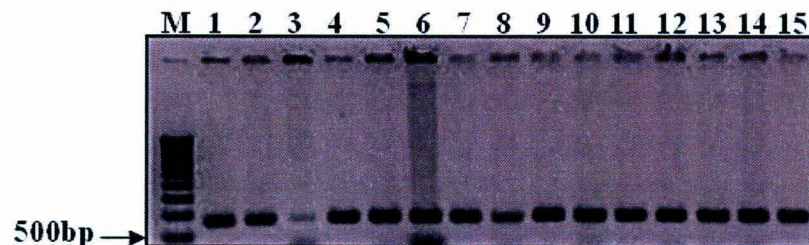


Fig. 4.1.2: Colony PCR of 15 randomly selected white bacterial colonies using M13F and M13R primers. M-500 bp ladder, 1-15 indicates the clone number.

Plasmid DNA isolated from randomly selected positive clones were further analyzed by restriction digestion by *EcoR* I enzyme. The restriction digestion of different clones with *EcoR* I when analyzed on the agarose gel electrophoresis showed

difference in insert sizes. Clones 2, 5, 6, 9 and 10 showed insert around 500 bp. These clones were sequenced using M13F and M13R primers.



Fig. 4.1.3: Restriction enzyme analysis for the selected plasmid DNA clones. One microgram of plasmid DNA was digested with 1 Unit of *EcoR* I for 1 h at 37°C. M stands for 500 bp ladder. 1-10 different plasmid clones.

Sequence analysis showed the size of the partial clone as 394 bp. This sequence was further compared with gene sequence information present in NCBI database using blastx analysis method. The blastx analysis method utilizes comparison of amino acid sequences of gene database to translated sequences of clones. The sequence of partial clone showed highest similarity with secretory peroxidase of *Avicennia marina* (95%) followed by *Nicotiana tabacum* secretory peroxidase (Fig. 4.1.4). Partial clone, named as *CrInt1* was submitted to Genbank database at NCBI and was assigned an accession number AY769111.

gi 10697182 dbj BAB16317.1	secretory peroxidase [Avicennia...	233	1e-60
gi 4927284 gb AAD33072.1	secretory peroxidase [Nicotiana t...	231	6e-60
gi 3982596 gb AAC83463.1	cationic peroxidase 2 [Glycine ma...	221	6e-57
gi 5002234 gb AAD37374.1	peroxidase [Glycine max]	221	6e-57
gi 1673671 gb AAA99868.1	peroxidase >gi 7433087 pir IT10790...	216	1e-55
gi 22135771 gb AAW91042.1	AT4g21960/T805_170 [Arabidopsis ...	210	8e-54
gi 1403136 emb CAA66862.1	peroxidase ATP1a [Arabidopsis th...	210	8e-54
gi 7269041 emb CAB79151.1	peroxidase prxr1 [Arabidopsis th...	210	8e-54
gi 10241560 emb CAB71128.2	cationic peroxidase [Cicer arie...	207	9e-53
gi 39867031 gb AAC84140.1	peroxidase [Cichorium intybus]	204	8e-52
gi 24417430 gb AAW60325.1	unknown [Arabidopsis thaliana]	168	5e-41

Fig. 4.1.4: Homology search for partial peroxidase clones. The blastx search analysis of a partial peroxidase clone obtained from amplification with degenerate primers.

4.1.2.3 Screening of *C. roseus* yeast elicited cDNA library for cloning of *CrInt1* full-length

4.1.2.3.1 Construction of yeast elicited cDNA library

The total RNA isolated from yeast elicited cell suspension culture were used for preparation of two microgram of poly (A) mRNA. This was converted into double-stranded cDNA and following ligation of an adapter and the release of an *Xho* I restriction site, was ligated to the *EcoR* I/*Xho* I cut phosphatase-treated ZAP II vector. The resulting DNA was packaged *in vitro* using Gigapack III gold extract and introduced into *E. coli* XL1-blue-MRF' strain. The titre of the primary library was 0.5×10^6 and its quality estimated by performing a blue/white color selection using IPTG (Isopropyl- β -D-thiogalactopyranosid) and X-gal (5-bromo-4-chloro-3-indolyl-beta-Dgalactopyranoside). 97% of the library (4.85×10^5) produced recombinant white plaques.

4.1.2.3.2 Screening of *C. roseus* yeast elicited cDNA library

The yeast elicited cDNA library was further screened with a 394 bp partial *CrInt1* as a probe at very high stringency conditions of hybridization at a temperature of 60°C and final washing with 0.1X SSC and 0.1% SDS. Primary screening of library revealed few positive plaques, which were screened out of 100,000 screened plaques (Fig. 4.1.5).

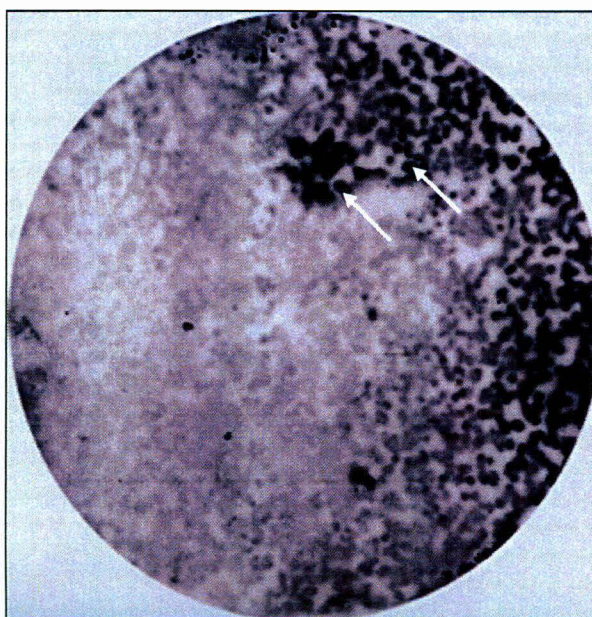


Fig. 4.1.5: X-ray film image showing primary screening using *CrInt1* probe. Positive plaques visible as black spots on the film (indicated by arrow).

For secondary screening, these positive phage plugs were picked and diluted in SM buffer before being plated at very low titre of 20-50 particles/plate. This allowed single plaques to be isolated. Each positive clone was screened at least three times to avoid false positive results and contamination with negative results. Positive plaques obtained from secondary screening (Fig. 4.1.6) were picked for further characterization.

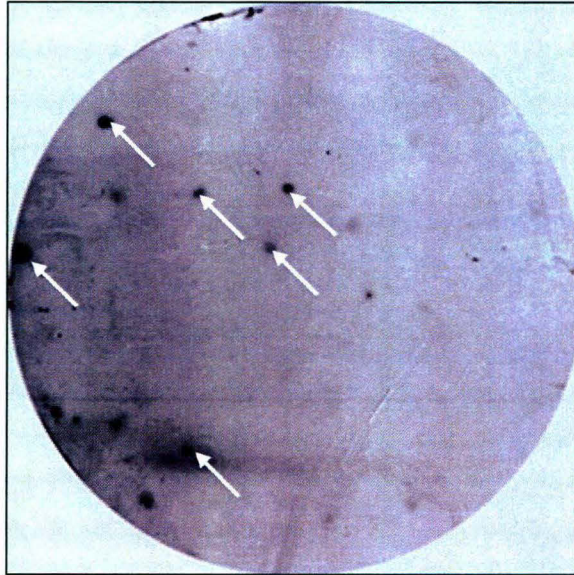


Fig. 4.1.6: Secondary screening of primary positive plaques. The arrows indicate positive plaque.

4.1.2.4 Purification of clones with insert and characterization of the library of inserts

More than 100 positive plaques detected after primary screening with *CrInt1* probe were utilized for secondary screening which resulted into 10 positive plaques. A subset of these plaques were subsequently tested with PCR to confirm the presence of the insert using the M13F and M13R primers which flank the multiple cloning site of the vector. The PCR amplification revealed 8 positive clones out of 10 with the size of ~2.5 kb which included both insert and flanking regions (Fig. 4.1.7).

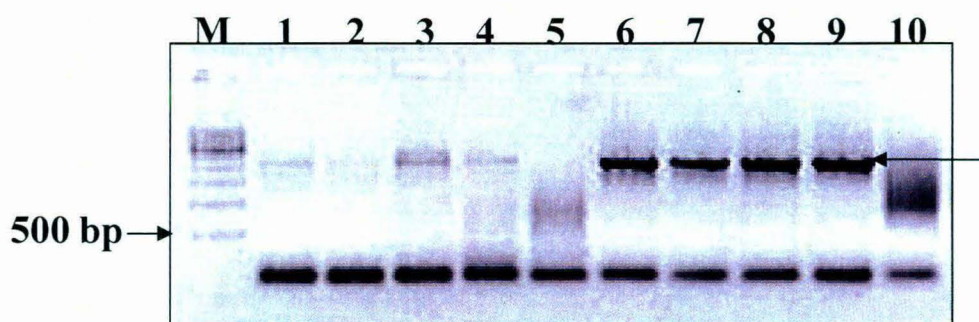


Fig. 4.1.7: Plaque PCR using the positive plaques after secondary screening. M size marker with 500 bp ladder, 1-10 plaque PCR with M13F-M13R primers, arrow indicates the positive amplification.

4.1.2.5 *In vivo* excision, plasmid isolation and size estimation of the selected clones

After screening the cDNA library, 4 clones (6-9, Fig. 4.1.7) were selected and analyzed further. The cloned inserts were excised and subcloned into a plasmid vector using ExAssist helper phage with SOLR strain, which efficiently excised the pBluescript SK (+) from the lambda ZAP vector. Colonies containing the pBLUESCRIPT vector with the cloned DNA insert were grown and selected to perform colony PCR. The colony PCR resulted in screening of positive clones with the insert size as ~1 kb (Fig. 4.1.8). These positive clones were utilized for plasmids DNA isolation and further sequence analysis using M13F-M13R primers.

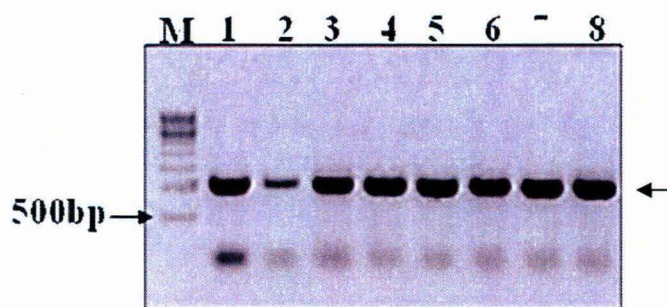


Fig. 4.1.8: Colony PCR of *in vivo* excised plasmid. To check the size of positive inserts with *in vivo* excised plasmid colony PCR using M13F-M13R primer was performed. M 500 bp ladder. Correct insert size is indicated by arrow.

4.1.2.6 Sequence analysis of the full-length *C. roseus* peroxidases cDNAs

The complete sequence of the CrPrx cDNA clone was found to be 1357 bp long (Fig. 4.1.9). A nucleotide blastn search demonstrated a high percent similarity of the sequence with Class III secretory peroxidase. Computational analysis of the *CrPrx* nucleotide sequence showed that it encodes a 330 amino acid polypeptide (Fig. 4.1.9). The molecular mass of this deduced protein was calculated to be 34.3 kDa, and it had

a theoretical pI of 9.02 excluding propeptide. The analysis of CrPrx protein using SIGNAL P v3.0 software (Bendtsen et al., 2004) identified a putative 21 amino acid signal peptide that was cleaved between Ala21 and Glu22. CrPrx protein showed an N-terminal extension of eight amino acids (Glu-Asn-Glu-Ala-Glu-Ala-Asp-Pro) before the start of the mature protein as an NX-propeptide (Fig. 4.1.9). The N-glycosylation site predicted by NetNGlyc 1.0 Servers predicts a single N-glycosylation site as NESL (Fig. 4.1.9).

```

1  ggcacgagctgaccttcactgtctacttcggacacgtaatcc
43  ATGGCTTCCAAAACCTCTCTTCTTCTTGTTCATTCTCTCTCTCTCT
1   M A S K T L E F L V I L S F S
88  GCTCTCTCAACTTTTGCTGAAAATGAAGCCGAGGCAGCCCTGGT
16  A L S T F A E N E A E A D P G
133 CTTGTAATGAAGTATTACAAGGATTCATGTCTCAAGCTGAAGAT
31  L V M N Y Y K D S C P Q A E D
178 ATCATCAGGGAACAAGTCAAACCTCTTTACAAACATCACAAAGAAC
46  I I R E Q V K L L Y K H H K N
223 ACCGCTTCTCTTGCTAAGGAACATTTCCATGATTGCTTTGTC
61  T A F S W L R N I F H D C F V
268 GAATCTTGTGATGCTTCATTGTTGCTGGACTCAACTAAAAAAGTC
76  E S C D A S L L L D S T K K V
313 CTGTCTGAGAAGGAAACAGATAGGAGTTTTGGAATGAGGAATTC
91  L S E K E T D R S F G M R N F
358 AGATACCTGAAGACATCAAAGAAGCCCTTGAAAGGGAGTGTCT
106 R Y L E D I K E A L E R E C P
403 GGAGTTGTTTCTTGTGCTGATATTCTTGTTTTGTCTGCAAGAAAT
121 G V V S C A D I L V L S A R N
448 GGCATTGTTTCGTTAGGAGGGCCATTTATCCCTCTTAAAACCGGA
136 G I V S L G G P F I P L K T G
493 AGAAGAGATGGCAGGAGAAGCAGAGCAGAGATACTGGAGCAACAT
151 R R D G R R S R A E I L E Q H
538 CTCCCAGACCACAATGAGAGCCTCACTGTTGTTCTTGAGAGGTTT
166 L P D H N E S L T V V L E R F
583 GGATCTATGGCATCAATACCCCTGGCTTGGTTGCCTTGCTAGGT
171 G S I G I N T P G L V A L L G
628 GCTCATAGTGTGGGAGAACCCTGTTGTAAGCTGGTTTCTATGCT
186 A H S V G R T H C V K L V H R
673 TTATATCCAGAGGTGGATCCTGCATTTCCAGAGAGCCATGTTTCAG
201 L Y P E V D P A F P E S H V Q
718 CACATGTTAAAGAAGTGCCCTGATCCAATTCCTGATCCAAGGCA
216 H M L K K C P D P I P D P K A
763 GTACAATATGTAAGAAATGACAGAGGAACACCTATGAAATAGAC
231 V Q Y V R N D R G T P M K L D
808 AACAATTATTACAGAAACATCTTGGACAACAAGGGCTTGTGCTA
246 N N Y Y R N I L D N K G L L L
853 GTCGATACCAATTAGCCACAGACAAAAGAACAAAACCAATTTGTC
261 V D H Q L A T D K R T K P F V
898 AAGAAAATGGCAAAAAGCCAAGATTACTTCTTTAAGGAATTTGCA
276 K K M A K S Q D Y F F K E F A
943 AGAGCCATTACTATTCTGTCTGAAAATAACCCTCTTACTGGTACT
293 R A I T I L S E N N P L T G T
988 AAAGGTGAGATTAGAAAGCAGTGTAAATGTAGCTAATAAGTTACAT
318 K G E I R K Q C N V A N K L H
1033 TAGaagattagattatgaaatccccttcttttctttcatgattgt
333 *
1077 aatcaattgtaatcatgaggaagaagaaccagaggggatggatggaataagttt:ttttaa
1141 aaggcctccaaaatgatgttagttgctttggcataggcaa:tgtaatgttggtgacatttc
1207 tttgttactttgcaactatcatgtattgtactaggtggcttcttcatgttcccttcatgttatggg
1278 gggcctgatggccatggatggtccttgacttgaatattggatgaatgcactgtaatacaagttg
1345 tttt taaaaaaaaaaaaaaaaaaaaa

```

Fig. 4.1.9: Complete CrPrx cDNA sequence and its translation product. The 5'-UTR and 3'-UTR are represented in lower case; the stop codon is indicated by *. The putative signal peptide is boxed in gray. A predicted NX-propeptide is boxed. A predicted N-Glycosylation site (NESL) is underlined. Nucleotide sequences in red represent predicted polyA signal sequences.

BLAST searches revealed significant sequence identity between CrPrx and a number of other class III plant peroxidases (EC 1.11.1.7), particularly with secretory peroxidases from *Avicennia marina* (accession number AB049589) and *Nicotiana tabacum* (accession number AF149252) (Fig. 4.1.10). The amino acid sequences of seven mature peroxidases, including CrPrx, were all close to 300 residues (Fig. 4.1.10). They showed 33-86% amino acid identity and shared 67 conserved residues. When compared with horseradish peroxidase (HRP)-C (Welinder, 1976), the translated polypeptide shown to contain all the eight conserved cysteines for disulfide bonds, and all the indispensable amino acid required for heme binding, peroxidase function, and coordination of two Ca²⁺ ions (Fig. 4.1.10).

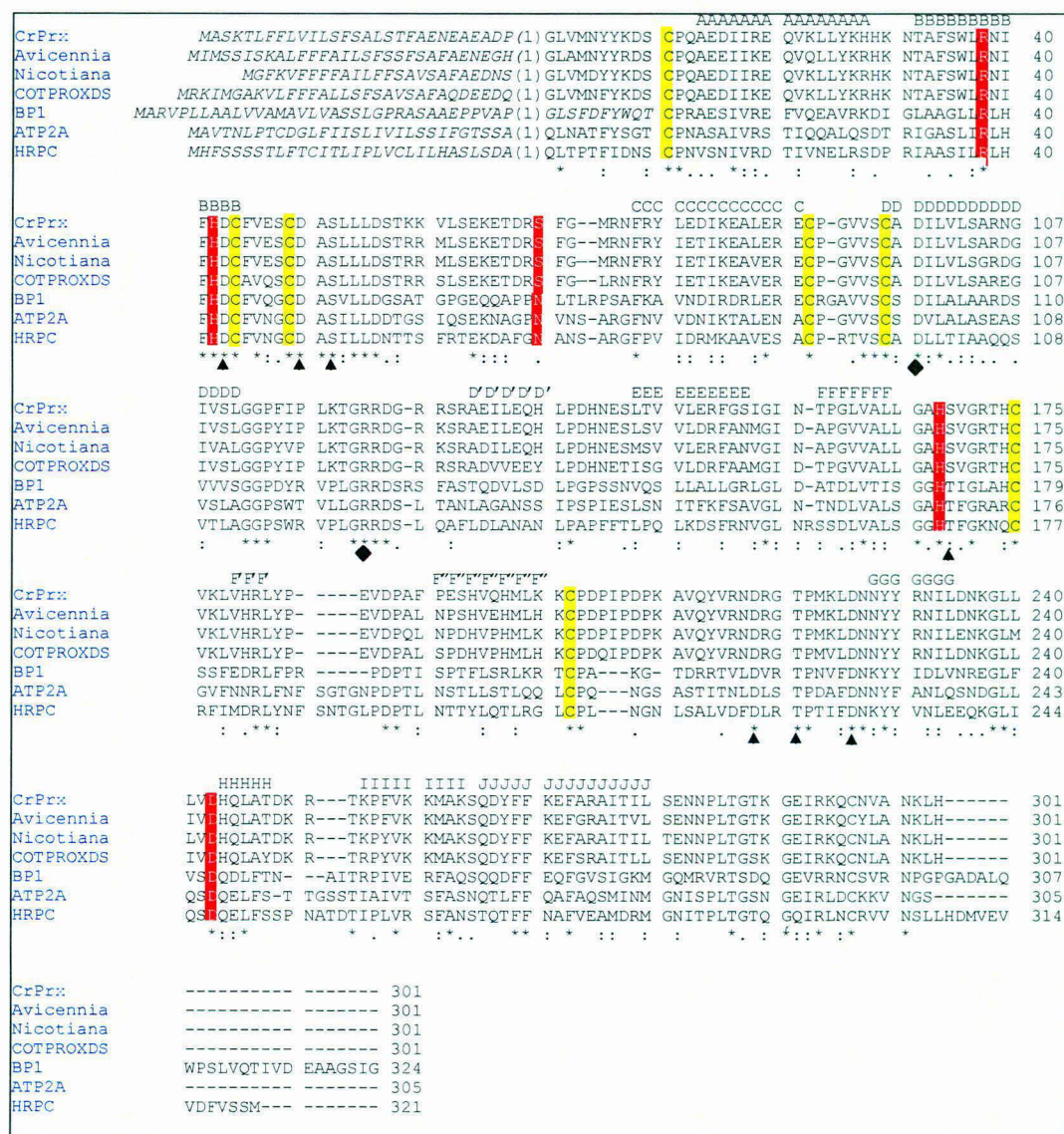


Fig. 4.1.10: CLUSTALW 1.82 multiple alignment of translated amino acid sequence of CrPrx with closest peroxidases. The peroxidase sequences retrieved from the NCBI database, i.e. *Avicennia* (BAB16317), *Nicotiana* (AAD33072), cotton (COTPROXDS) (AAA99868), barley grain peroxidase (Bp1) (AAA32973), ATP2A (Q42578) and HRP-C (AAA33377). Residue numbers start at the putative mature proteins in analogy with HRPC.

Pre-protein sequences are shown in italics, conserved residues are indicated by * and amino acids forming buried salt bridge are indicated by ♦. The amino acid side chains involved in Ca²⁺ ion binding is marked by ▲; S-S bridge formed by cysteines is in yellow color and heme binding sites are highlighted in reverse print. The location of α-helices, A-J, as observed in horseradish peroxidase (HRPC) (Welinder et al. 1999) is indicated above the aligned sequences.

4.1.2.7 Introns and exons in *CrPrx* genomic clone

To obtain an insight into the complete sequence of *CrPrx*, PCR was performed using primer pair PFLF1 and PFLR1, designed to anneal to 5'-UTR and 3'-UTR (accession number DQ415956), with genomic DNA of *C. roseus* as template. The amplified product upon cloning and sequencing was found to be 1793 bp long (accession number DQ484051). *CrPrx* consisted of four exons (268 bp, 189 bp, 172 bp, 405 bp, stop at UAG) and three introns which were more or less similar in size. The second intron in *CrPrx* was found to be largest and was even larger in size than the exons. This *CrPrx* structure supported the concept of origin of peroxidases from a common ancestral gene of peroxidase with three introns and four exons (Fig. 4.1.11A-B).

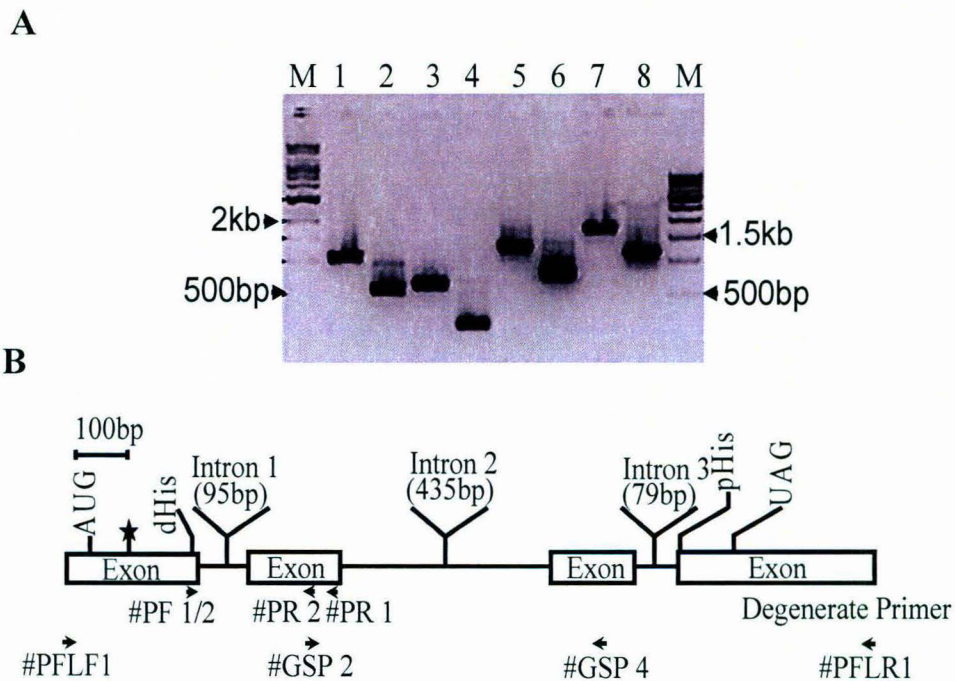


Fig 4.1.11: Intron mapping of *CrPrx* gene. (A) Lane M show size markers in base pairs, Lanes 2, 4, 6 and 8 show PCR reactions run on plasmid DNA harboring *CrPrx* cDNA, and lanes 1, 3, 5 and 7 show the same using genomic DNA of *C. roseus*. Primer pairs were: #GSP-4 and #PFLF-1 (lanes 1 and 2); #GSP-2 and #GSP-4 (lanes 3 and 4); #GSP-2 and #PFLR-1 (lanes 5 and 6); and #PFLF-1 and #PFLR-1 (lanes 7 and 8). (B) Schematic organization of the *CrPrx* gene the asterisk indicates the position of the codon encoding the first amino acid of the mature protein, and regions of the distal and proximal histidines are indicated by dHis and pHis.

4.1.2.8 Phylogenetic analysis

The relationship between *CrPrx* cDNA and other cDNAs encoding class III peroxidases was investigated using a parsimonious phylogenetic analysis. BLAST searches were used to identify other full-length peroxidase cDNA sequences showing close similarity to *CrPrx*. The varying degrees of expression patterns of peroxidase cDNAs in different tissues in different plant systems under stress was taken into consideration during this study (Table 4.1.1). Phylogenetic analysis was performed on the aligned nucleotide sequences corresponding to the cDNA open reading frames (Fig. 4.1.12). The tree was rooted with *Spinacea prx14* which may be distantly related to *CrPrx* sequence. Most of these cDNAs, with a few exceptions, are expressed both in vegetative and reproductive tissues, and are stress induced. *CrPrx* expression was also noted in all the tissues tested and found to be stress inducible. After its origin from *Spinacea prx14*, the tree showed a divergence from a liverwort peroxidase, indicating a distant relation of ancestral *Marchantia* peroxidase with this angiosperm *CrPrx* sequence.

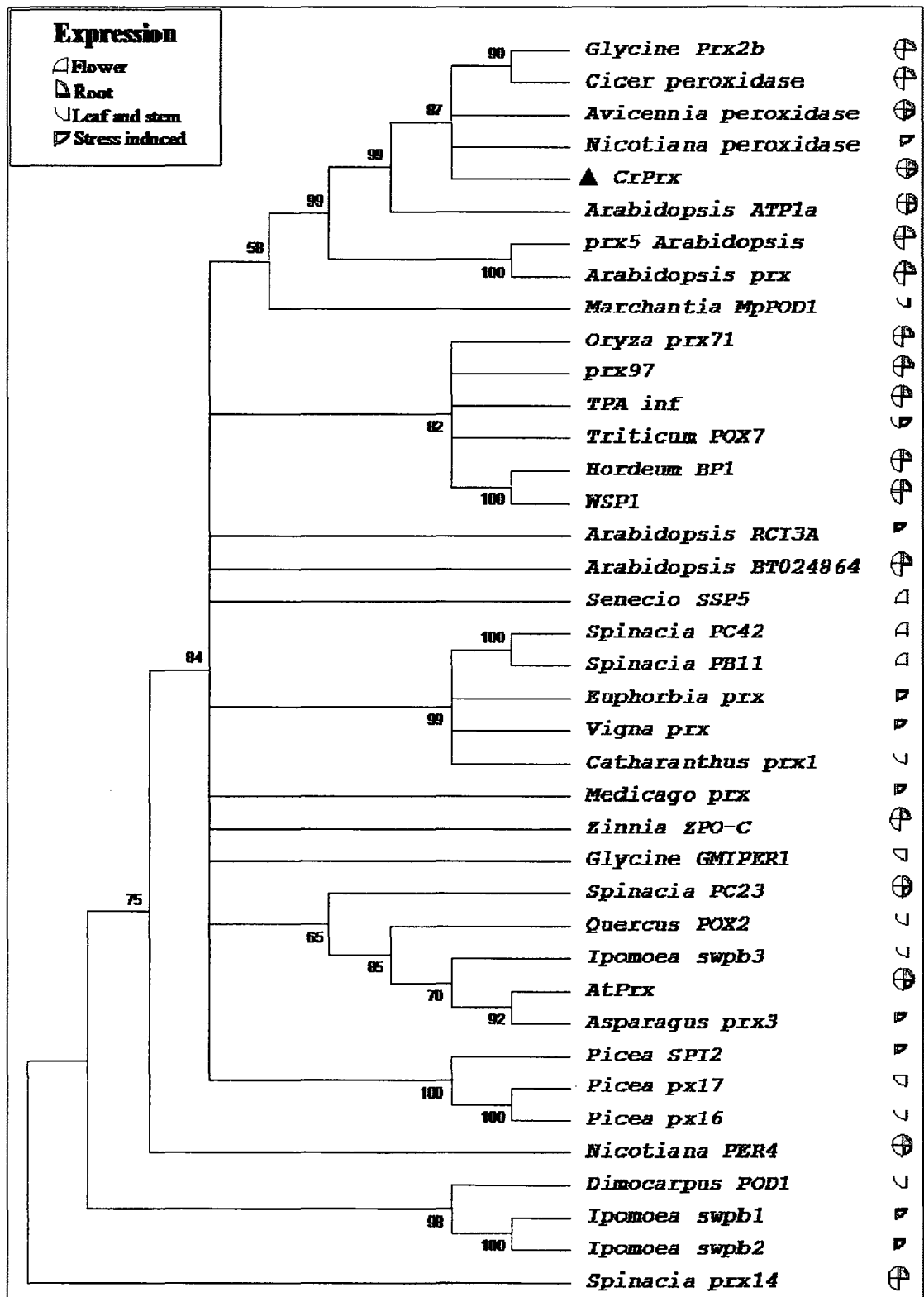


Fig. 4.1.12: Phylogenetic relationships between peroxidase cDNA, *CrPrx* and other related class III peroxidases. Alignment consists of the nucleotide sequences of coding regions. Bootstrap value mark the percentage frequency at which sequences group in 100 resampling replicates. The expression pattern is represented by semi-color circles indicating: floral, vegetative and stress inducible (abiotic and biotic) expression. Information on expression is referenced in Table 4.1.1, gathered from published and unpublished sources and from NCBI databases.

Table 4.1.1: List of the references used for sequence and expression data presented in figure 4.1.12 for phylogenetic analysis.

Label	Accession	MIPS	Reference
Glycine Prx2b	AF145348	NA	Unpublished
Cicer peroxidase	AJ271660	NA	Unpublished
Avicennia peroxidase	AJ271660	NA	Tanaka et al. (2002)
Nicotiana peroxidase	AF149251	NA	Blee et al. (2003)
CrPrx	AY924306	NA	Present study
Arabidopsis ATP1a	X98189	NA	Kjærsgård et al. (1997)
prx5 Arabidopsis	X98317	NA	Kjærsgård et al. (1997)
Arabidopsis prx	AY087458	NA	Haas et al. (2002)
Marchantia MpPOD1	AB086023	NA	Unpublished
Oryza prx71	BN000600	NA	Passardi et al. (2004)
prx97	BN000626	NA	Passardi et al. (2004)
TPA inf	BN000568	NA	Passardi et al. (2004)
Triticum POX7	AY857761	NA	Liu et al. (2005)
Hordeum BP1	M73234	NA	Johansson et al. (1992)
WSP1	AF525425	NA	Unpublished
Arabidopsis RCI3A	U97684	NA	Llorente et al. (2002)
Arabidopsis BT024864	BT024864	At5g40150	Unpublished
Senecio SSP5	AJ810536	NA	McInnis et al. (2005)
Spinacia PC42	Y10464	NA	Simon (1993)
Spinacia PB11	Y10462	NA	Simon (1993)
Euphorbia prx	AY586601	NA	Mura et al. (2005)
Vigna prx	D11337	NA	Ishige et al. (1993)
Catharanthus prx1	AM236087	NA	Unpublished
Medicago prx	X90693	NA	el-Turk et al. (1996)
Zinnia ZPO-C	AB023959	NA	Sato et al. (2006)
Glycine GMIPER1	AF007211	NA	Yi and Hwang (1998)
Spinacia PC23	Y10467	NA	Simon (1993)
Quercus POX2	AY443340	NA	Coelho (2003)
Ipomoea swpb3	AY206414	NA	Park et al. (2003)
AtPrx	AY065270	At5g05340	Unpublished

Asparagus prx3	AJ544516	NA	Holm et al. (2003)
Picea SPI2	AJ250121	NA	Fossdal et al. (2001)
Picea px17	AM293547	NA	Unpublished
Picea px16	AM293546	NA	Unpublished
Nicotiana PER4	AY032675	NA	Unpublished
Dimocarpus POD1	DQ650638	NA	Unpublished
Ipomoea swpb1	AY206412	NA	Park et al. (2003)
Ipomoea swpb2	AY206413	NA	Park et al. (2003)
Spinacia prx14	AF244923	NA	Unpublished

4.1.2.9 Gene copy number of *CrPrx*

Gene copy number is an essential step in characterization of any gene in the species because expression of a gene depends on the copy number. Southern blot analysis was performed using *C. roseus* genomic DNA to determine the copy number of *CrPrx* gene. The genomic DNA was digested using *Bgl* II, *EcoR* V and *Hind* III. The digested genomic DNA was transferred to a nylon membrane, and probed with ³²P-labeled *CrPrx* cDNA. In the genomic blot probed with *CrPrx* cDNA a single band was observed with *Bgl* II and *Hind* III enzyme while detection of two hybridizing bands was consistent with the fact that an internal *EcoR* V site existed within the coding region of gene (Fig. 4.1.13). The result suggested that the peroxidase gene was present as single copy in *C. roseus* genome.

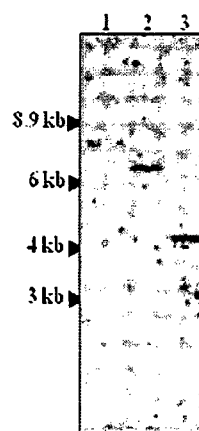


Fig. 4.1.13: DNA gel blot of *C. roseus* probed with full length *CrPrx* cDNA. Lanes 1, 2 and 3 shows the genomic DNA digested with *Bgl* II, *EcoR* V and *Hind* III restriction enzymes, respectively.

4.1.2.10 Expression pattern of *CrPrx* in *C. roseus*

4.1.2.10.1 Tissue specific expression of the *CrPrx* gene

Northern blot analysis revealed expression of *CrPrx* in different organs of *C. roseus* i.e. leaves (young, mature and old), flower buds, open flowers, fruits, roots and intermodal stem tissue (Fig. 4.1.14). Among vegetative tissues, the transcript was maximal in internodal stem tissues followed by roots, young leaves and mature leaves. Among reproductive tissues, the transcript was most abundant in fruits, followed by young buds. *CrPrx* expression was not detected in old leaves and flowers.

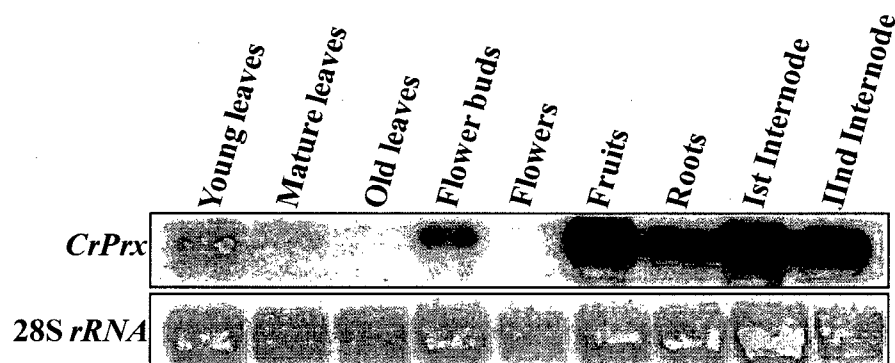


Fig. 4.1.14: Northern Blot of total RNA isolated from *C. roseus* leaves (young, mature and old), flower bud, flower, fruit, root and stem (Ist internode and IInd internode). Blot was prepared using 20 µg of total RNA which was loaded in each lane. The blot was probed with *CrPrx* cDNA as shown in upper panel while lower panel shows 28S rRNA stained with methylene blue staining.

4.1.2.10.2 Tissue specific protein profile of CrPrx

In order to purify CrPrx protein for preparation of antibody, a GST-CrPrx fusion protein was constructed in pGEX 4T-2 vector with CrPrx ORF (PPGX) and expressed in heterologous system. Since the protein was repeatedly found in inclusion body different concentrations of glutathione, sarcosyl and Triton X-100 were tested to achieve purification of the fusion protein (Fig. 4.1.15). The fusion of glutathione S-transferase (GST) leads to increase in size of GST-CrPrx fusion protein to the calculated molecular weight of 63 kDa. The purified protein was used for preparation of polyclonal antibodies against CrPrx in rabbit.

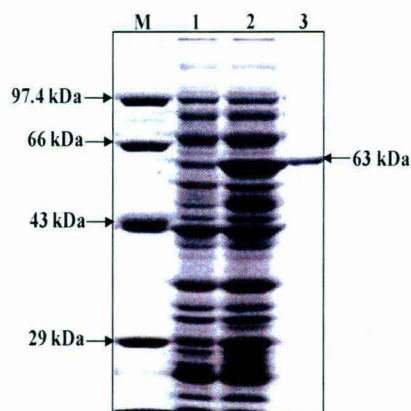


Fig. 4.1.15: Large-scale purification of GST fusion CrPrx protein; the mobility of the fusion protein matches its predicted molecular weight. Lanes M, 1, 2 and 3 show molecular weight markers, total protein from uninduced bacterial culture, induced bacterial lysate, and purified eluted CrPrx fusion protein, respectively.

Immunoblot analysis was performed using different organs of *C. roseus* revealed differential accumulation of CrPrx. The maximum level of CrPrx accumulation was present in the internodes followed by mature leaves (Fig. 4.1.16). In other parts of plant the CrPrx protein was not accumulated in enough amounts to be detected by western blot analysis.

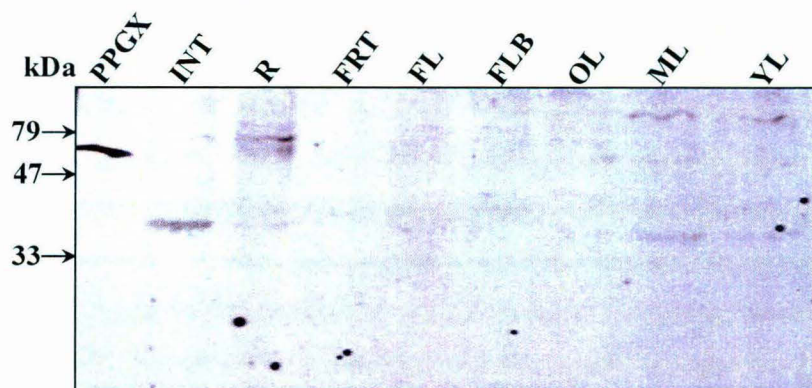


Fig. 4.1.16: Immunoblot analysis of CrPrx expression in various tissue types. Denaturing SDS/PAGE of total protein extracted from various organs, followed by immunoblotting using the antibodies to CrPrx. The blot was imaged on X-ray film using chemiluminescent substrate. PPGX is CrPrx cloned in pGEX 4T-2 expression vector as a GST fusion protein, INT, internode; R, root; FRT, fruit; FL, Flower; FLB, flower bud; OL, old leaves; ML, mature leaves; YL, young leaves.

4.1.2.10.3 Stress regulation of *CrPrx* gene

Class III peroxidase genes are reported to be induced in vegetative tissues by stress, particularly wounding (Mohan et al., 1993a and 1993b). To investigate whether *CrPrx* expression is also stress induced, leaves of *C. roseus* were subjected to different stress

conditions as well as methyl jasmonate (MJ) treatment and analyzed for *CrPrx* transcript regulation over a time course of 24 h. An increase in the level of *CrPrx* expression was noted with increasing time when leaves were either wounded or exposed to UV and cold treatments (Fig. 4.1.17A-B). The expression level reached its peak after 6 h of wound treatment, following an initial decline during the first hour. In the case of UV and cold exposure, the maximum transcript level was observed at 12 and 24 h respectively. On the other hand a gradual steady state increase in expression level of *CrPrx* was noted with increasing time in response to application of 100 μ M MJ on leaves. This was later confirmed by immunoblot analysis, which revealed accumulation of CrPrx in *C. roseus* leaves after 6 h of wound stress and 6-12 h treatment with 100 μ M MJ (Fig. 4.1.17C).

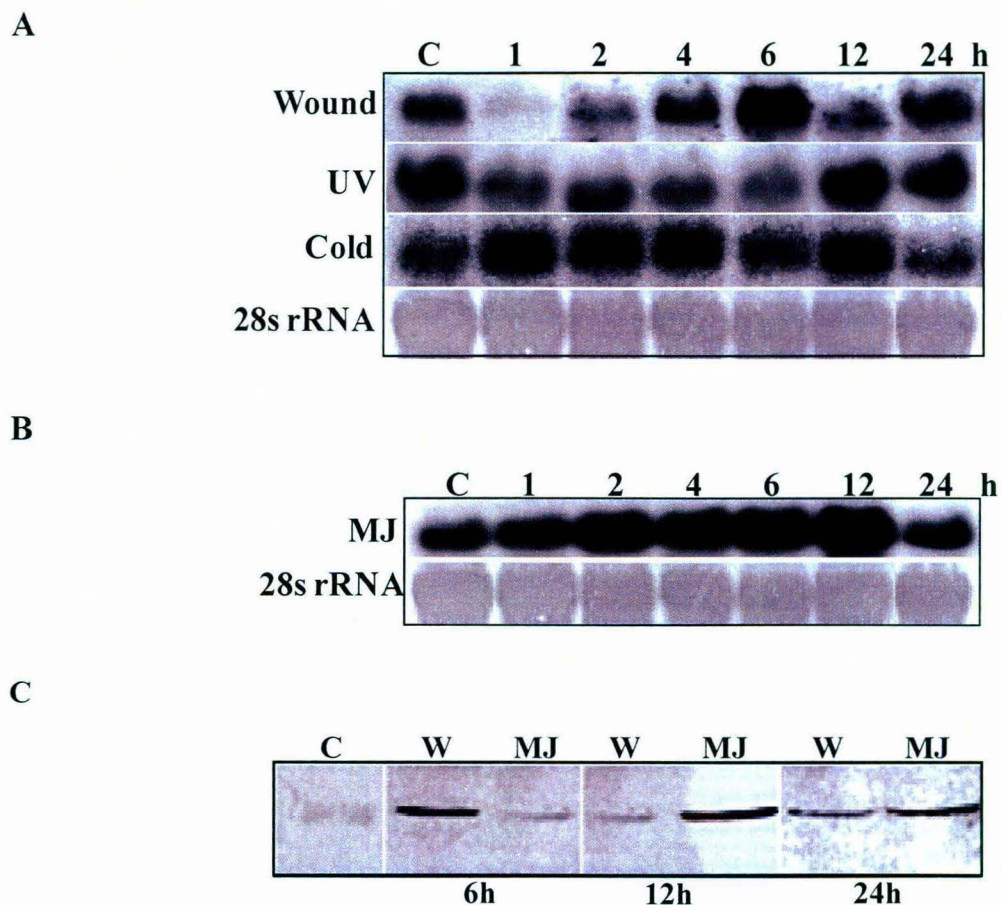


Fig. 4.1.17: Expression analysis of CrPrx transcript and protein under stress conditions. A, B) Transcript regulation of *CrPrx* under different abiotic stress conditions viz. wounding, Ultraviolet radiations, cold acclimation and 100 μ M methyl jasmonate treatment MJ; the lower panel shows methylene blue-stained 28S RNA as loading control. C) Immunoblot analysis of CrPrx after wounding and 100 μ M MJ treatment with antibodies to CrPrx. Blots were imaged on X-ray film using chemiluminescent substrate. C, untreated control; W, wounding; MJ, methyl jasmonate.

4.1.2.11 Total peroxidase activity profile in *C. roseus*

Total peroxidase activity was measured using ortho-phenyl diamine (OPD) as substrate. Total soluble protein extracted from 1 g of *C. roseus* tissues were used as peroxidase source for oxidation of OPD. The total peroxidase activity measured in Units was maximum in root tissue followed by more or less similar in other tissue (Fig. 4.1.18). It was also found that in the intermodal tissue where maximum accumulation of CrPrx protein was present did not show higher peroxidase activity.

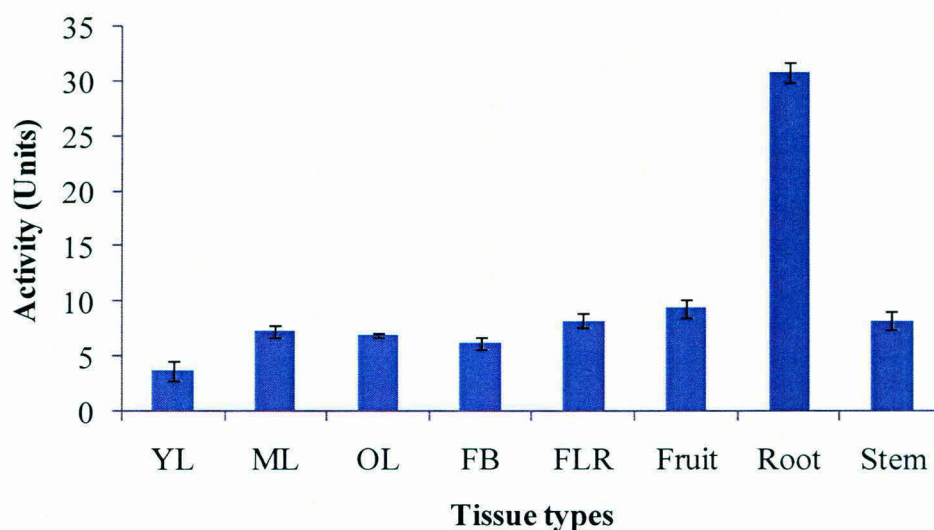
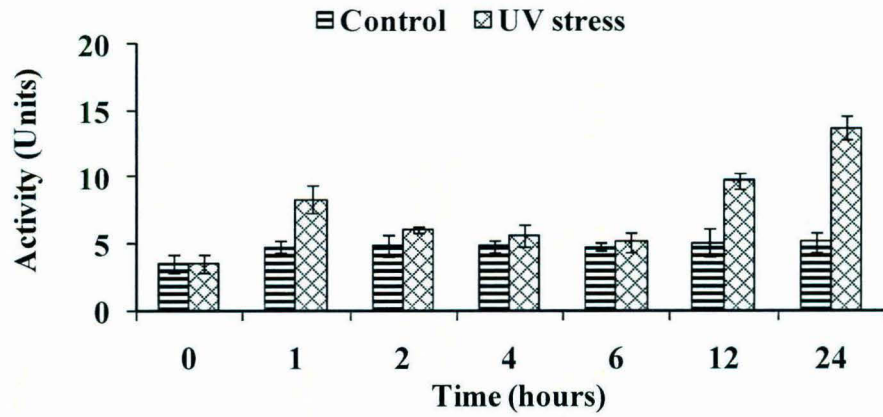


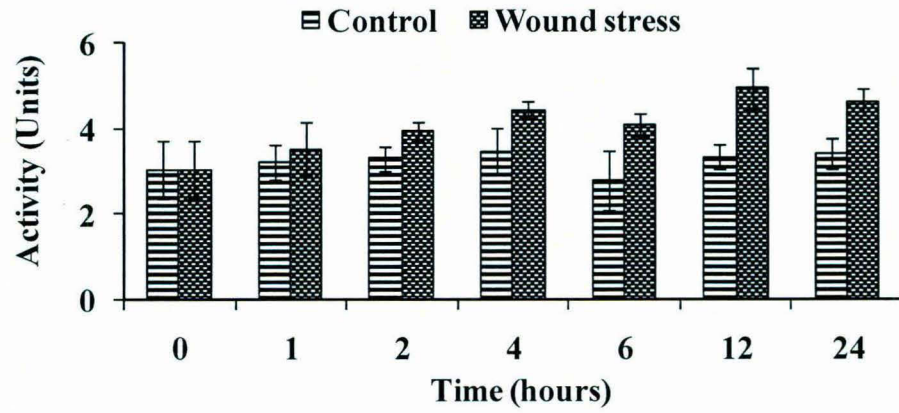
Fig. 4.1.18: Total basic peroxidase activity (Units) in different tissues of *C. roseus*. The total peroxidase activity was measured using OPD as substrate (n=3). Abbreviations YL, young leaves; ML, mature leaves; OL, old leaves, FB flower bud; FLR, flower. One OPD unit is defined as the amount of enzyme that oxidizes 0.01 μmol OPD per min.

Total peroxidase activity was found to be stress regulated as it was visible with the increase in OPD oxidation at certain time intervals after treatments with different abiotic stresses. Among abiotic stresses the maximum activity was observed when the seedlings were exposed under UV (Ultra Violet rays λ_{max} 312 nm; $28 \text{ J m}^{-2}\text{s}^{-1}$) treatment for two minutes (Fig. 4.1.19A).

A



B



C

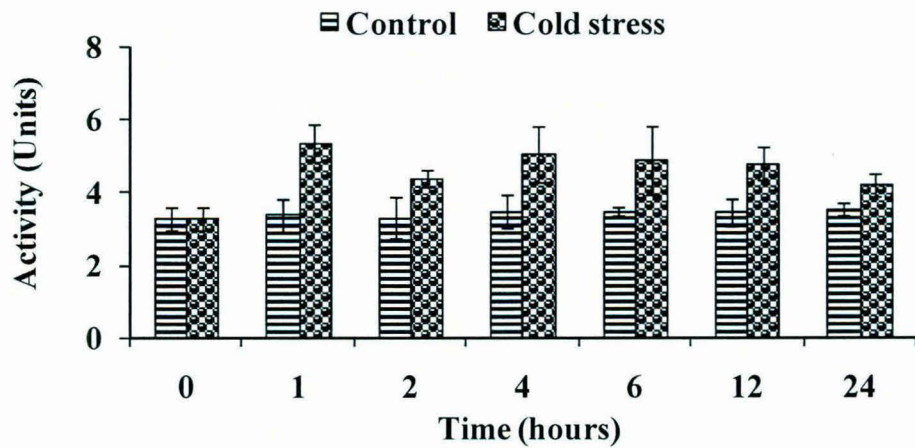


Fig. 4.1.19: Peroxidase activity (Units) in *C. roseus* young leaves under different stress treatments. A) UV stress treatment, B) Wounding stress treatment, C) Cold stress treatment (n=3).

During all the abiotic stresses there seems to be an initial bursts in the peroxidase activity just after an hour of treatment. The activity was found to be higher during wound stress and the maximum peroxidase activity was seen after 12 h of treatment (Fig. 4.1.19B). Cold stress also resulted in increase in the peroxidase activity (Fig. 4.1.19C).

Methyl jasmonate is one of the signaling compounds. A number of MIA pathway genes had shown to be controlled by jasmonate-responsive AP2 domain transcription factor (ORCAs). Application of 100 and 300 μM of the methyl jasmonate resulted in gradual increase and maximum peroxidase activity was observed after 24 h, though the activity was higher with 300 μM of the methyl jasmonate than with 100 μM (Fig 4.1.20).

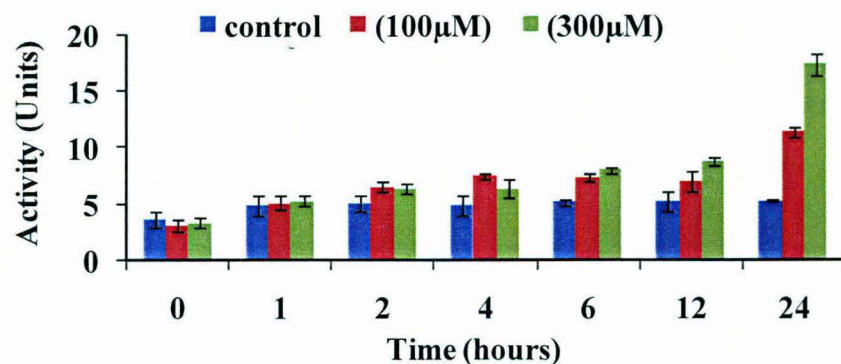


Fig. 4.1.20: Peroxidase activity (Units) in *C. roseus* young leaves under two different concentrations of methyl jasmonate. Methyl jasmonate was dissolved in ethanol and diluted in water before application on leaves (n=3).

4.1.2.12 Subcellular localization of CrPrx using GUS-GFP-CrPrx fused protein

To examine the subcellular localization of CrPrx, the *CrPrx* coding region was fused in-frame to the coding region for the N-terminal side of GUS and GFP under the control of the 35S promoter of cauliflower mosaic virus (CaMV) and transiently transformed in the leaves of *N. tabacum* and *C. roseus*. When the construct CrPrx–GUS–GFP was expressed in transformed tobacco and in *C. roseus*, GUS staining and green fluorescence were observed in the epidermal parenchymatous cell, CrPrx–GUS–GFP was found to be accumulated mostly in the cell walls, outer cell membranes and associated structures (Fig. 4.1.21A-B and 4.1.22A-B). On detailed examination, CrPrx-GFP fluorescent dots were visible in the part of epidermal cell wall abutting a mature guard cell in tobacco leaf tissue (Fig. 4.1.21B). In xylem

tissue, CrPrx-GFP fluorescence was observed specifically in the secondary wall thickenings both in tobacco and in *C. roseus* (Fig. 4.1.21F and 4.1.22D-E).

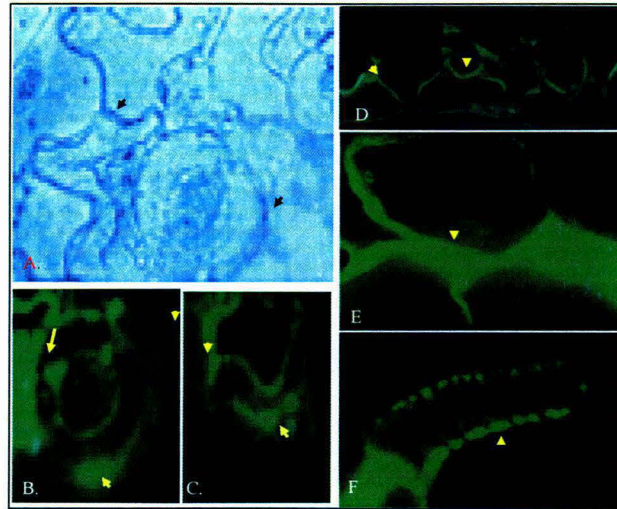


Fig. 4.1.21: GUS and GFP fluorescence patterns of CrPrx expression in *N. tabacum* leaf. A) GUS staining and B) GFP fluorescence patterns of the same. C–E) GFP fluorescence patterns of stomatal guard cells, leaf epidermal cells and F) xylem cells of transiently transformed *N. tabacum* with CrPrx–GUS–GFP. In epidermal and stomatal guard cells, CrPrx–GFP is restricted to the cell wall and associated structures, the membranes of the central vacuole, and the wall thickening of xylem cells (→).

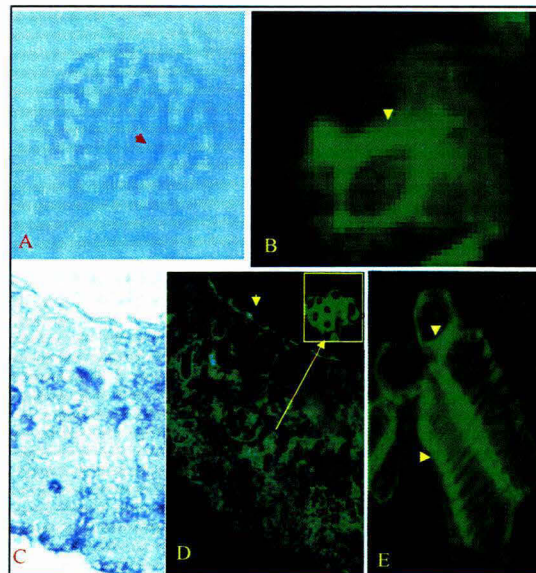


Fig. 4.1.22: GUS and GFP fluorescence patterns of CrPrx expression in *C. roseus* leaf. A) GUS staining and B) GFP fluorescence patterns of stomatal guard cells of *C. roseus*. C) GUS staining and D) GFP fluorescence patterns of leaf sections of *C. roseus*. B, D, E) CrPrx–GFP is restricted to the leaf epidermal cells B), guard cell walls D) and the wall thickening of xylem tissues E) of transiently transformed *C. roseus* with CrPrx–GFP.

The CrPrx-GUS-GFP fusion protein when used for transient transformation of *C. roseus* leaves it shows same position of localization to cell wall as predicted in tobacco (Fig. 4.1.22). Stomatal guard cells localization of CrPrx fusion protein was visible with the GUS staining (Fig. 4.1.22A) of leaves cross section confirmed with GFP localization (Fig. 4.1.22B). Fluorescent signal were observed in secondary cell wall thickening around epidermal layers of leaves cross section (Fig. 4.1.22E). These results confirmed the role for CrPrx in the cell wall related process as it was localized to cell wall in both *N. tabacum* and *C. roseus*.

4.1.3 Discussion

Cloning, characterization and localization of a novel *C. roseus* peroxidase, *CrPrx*, has been reported for the first time. This particular full-length *CrPrx* cDNA (1359 bp) and its functional product were noted to be localized and expressed in different tissues of the plant tested. Computational analysis revealed that the translated polypeptide sequence of *CrPrx* contains eight conserved cysteine residues forming disulfide bridges, two Ca²⁺ binding ligands, (Welinder, 1976; Welinder et al., 1992 and Smith et al., 1998). The inclusion of Ser96 and Asp99 in a salt bridge motif at the beginning of helix D and its connection to the following long loop by a tight hydrogen bonding network with Gly121-Arg122 was also an important feature in *CrPrx* (Welinder et al., 2002). The presence of a signal peptide and the lack of a carboxyl extension identifies CrPrx as a secretory (class III) plant peroxidase, rather than a vacuolar plant peroxidase. Unlike other class III peroxidases, the mature CrPrx polypeptide starts with a glycine (G) residue and not with glutamine (Q) residue. This feature will possibly make the CrPrx polypeptide unable to generate a pyrrolidone carboxyl residue (Z) (Gabaldon et al., 2005). The full-length *CrPrx* gene, like most of the plant peroxidase genes, contains three introns, which differ in their sizes (Tognolli et al., 2002). Phylogenetic analysis grouped CrPrx cDNA with the ancestral Marchantia peroxidase cDNA. The two peroxidase cDNAs that were found to be structurally most closely related to CrPrx are *A. marina* (Tanaka et al., 2002) and *N. tabacum* (Blee et al., 2003) peroxidase cDNAs. The CrPrx transcript and its translated product were found to be differentially expressed in different vegetative as well as reproductive tissues of *C. roseus* under normal conditions and upon exposure to stress as well as MJ treatment, confirming that it is organ specific, developmentally regulated, and stress-inducible as well as elicitor-inducible. The sub cellular localization study using

CrPrx–GUS–GFP is indicative of a correlation between the accumulation of CrPrx fusion protein and the parenchymatous as well as xylem cell wall thickening, both in tobacco and in *C. roseus*. The classical plant peroxidases (class III) are ascribed a variety of functional roles in plant systems, which include lignification, suberization, auxin catabolism, defense, stress, and developmentally related processes (Hiraga et al., 2001; Welinder et al., 2002; Veitch and Smith, 2001; Do et al., 2003). The stress-inducible nature of *CrPrx* cDNA and the localization of its functional product in cell walls in the present study suggest its apoplastic nature and its involvement in the stress-related as well as developmental processes in *C. roseus*. Jasmonic acid and its volatile derivative, MJ, collectively called jasmonates, are plant stress hormones that act as regulators of defense responses (Reymond and Farmer, 1998). The induction of secondary metabolite accumulation is an important stress response that depends on jasmonate as a regulatory signal (Memelink et al., 2001). In the present study, *CrPrx* was found to be expressed upon elicitation by MJ. A number of MIA biosynthetic pathway genes have also been shown to be regulated by jasmonate-responsive AP2 domain transcription factor (ORCAs) (van der Fits and Memelink, 2000; Aerts et al., 1994; El-Sayed and Verpoorte, 2005). These findings demonstrate that, like other MIA biosynthetic pathway genes, expression of *CrPrx* falls under an MJ-responsive control mechanism that operates in *C. roseus* under stress conditions. However, it is difficult to ascertain from the present investigation whether *CrPrx* has a similar function to that of AVLB synthase in *C. roseus*, because *CrPrx* was found to lack a vacuolar targeting signal and to be apoplastic in nature. The total peroxidase activity was also shown to increase 3 times when treated with 100 μ M Methyl jasmonate. Methyl jasmonate was also reported to enhance accumulation of ajmalicine and catharanthine in hairy roots, where the total alkaloid production increased about twofold (Flota-Vázquez et al., 1994).

4.1.4 Conclusion

The accumulated evidences suggest that *CrPrx* belongs to class III secretory peroxidase gene family and has three introns. It may be inferred that *CrPrx* gene encodes a functional protein and is localized in cell wall of epidermal as well as vascular cells in leaves. The expression of *CrPrx* is organ-specific and stress as well as MJ-inducible. Accordingly, we assume its involvement in stress regulation and developmental processes in *C. roseus*.

*4.2: Cloning of two novel peroxidase Prx3 and Prx4
genes from Catharanthus roseus*

4.2.1 Introduction

Peroxidases are ubiquitous class of enzymes that oxidize a vast array of organic and inorganic reducing compounds in the presence of hydrogen peroxide. Class III peroxidases have been mostly implicated in key process determining the architecture and defense properties of the plant cell wall, like lignin and suberin biosynthesis and cross linking reactions (Barceló et al., 2004; Bernards et al., 2004; Fry, 2004; Ralph et al., 2004; Gabaldón et al., 2005). In *C. roseus* root, a vacuolar peroxidase enzyme has been shown to convert ajmalicine to serpentine biochemically (Misra et al., 2006). However, information about the gene responsible for the conversion is still meager. In leguminous plant, the RIP1 (Rhizobium-induced) peroxidase is involved in cell wall alteration during early nodule development stage at the sites of infection thread formation (Salzwedel and Dazzo, 1993). Peroxidases also helps in root colonization as observed in mycorrhiza plant interaction (Münzenberger et al., 1997). The *CrPrx* gene which we cloned and sequenced, unfortunately did not show its localization to vacuole, the site for conversion of ajmalicine to serpentine. In order to clone the peroxidase targeted to vacuole another set of degenerate primers were designed from the conserved region and used for cloning of other peroxidase genes from *C. roseus*.

4.2.2 Results

4.2.2.1 Cloning of partial peroxidase genes using degenerate PCR

Total RNA isolated from leaf tissue of *C. roseus* was subjected to reverse transcription for synthesis of cDNA. Reverse transcription PCR using degenerate primers (DCPF1 and DCPR1) corresponding to conserved, heme-binding distal and proximal regions of peroxidases, yielded a two amplified fragment vary in sizes (Fig. 4.2.1). The expected size amplicon (~500 bp) was cloned in pGEM-T Easy vector and transformed in to *E. coli*, DH5 α strain. The clones were sequenced and analyzed by blastx tools from NCBI website. The sequence analysis revealed 4 different peroxidases out of which one matches with *CrInt2* (accession number AY837788) reported earlier from *C. roseus* table 4.2.1, while three new peroxidases identified from *C. roseus* namely *CrPrx2*, *Prx3* and *PrxFII*. The details of these partial peroxidases are mentioned in table 4.2.1. Full length genes were subsequently cloned from partial fragments of *Prx3* and *CrInt2*. Full length gene of *CrInt2* was named as *Prx4*.

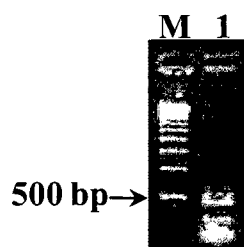


Fig. 4.2.1: Isolation of new peroxidase genes. RT-PCR amplification using degenerate primers DCPF1 and DCPR1 on *C. roseus* leaf cDNA as template (1), M) 500 bp ladders.

Table 4.2.1: Similarity search of peroxidases cloned using DCPF1 and DCPR1 primers with cDNA prepared from leaf tissue.

Name of clone	Size of fragment (in base pairs)	Homology (maximum) with the known peroxidase	Percent identity (closest peroxidase)	Score in bits
<i>CrInt2</i> (Accession number AY837788)	397	<i>Gossypium hirsutum</i> peroxidase (AAP76387)	85	211
<i>CrPrx2</i> (Accession number ABV24961)	405	Peanut Peroxidase, Cationic peroxidase 1 (PNPC1) (AAB06183)	74	205
<i>Prx3</i> (Accession number assigned for full length only)	405	<i>Nicotiana tabacum</i> peroxidase (BAA82306)	71	212
<i>PrxF11</i> (Accession number EU888475)	389	<i>Arabidopsis thaliana</i> ATP17a like protein peroxidase (BAD44575)	79	215

4.2.2.2 Cloning of full length *Prx3* and *Prx4* genes

For obtaining full length clone of *Prx3* and *Prx4* genes both 5' and 3' Rapid amplification of cDNA ends (RACE) was performed. Cloning of 5' end of *Prx3* was performed using CRPRX3F, GSP3 and NGSP3 while for *Prx4* the CRPRX5R and GSP7 were used on the double stranded cDNA prepared by LD-PCR method. Primary amplification showed the presence of smear but secondary PCR showed the presence of expected band of ~500 bp (Fig. 4.2.2). The expected band was eluted, cloned and sequenced. The BLAST alignment was performed after sequencing to find the overlapping sequences which were tiled to have 5' region of partial peroxidases.

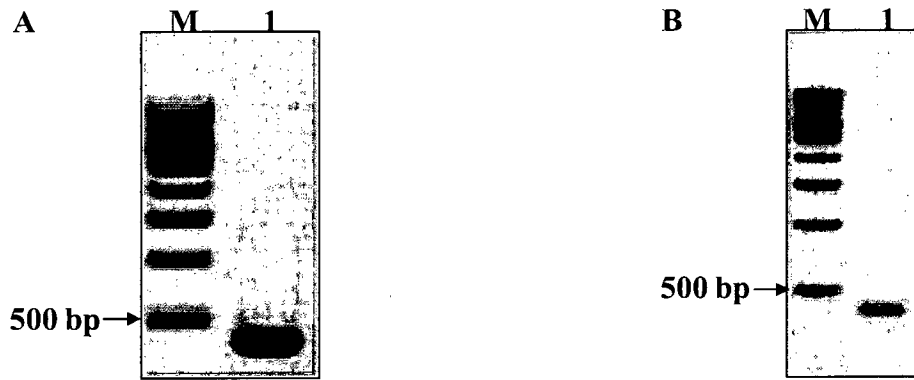


Fig. 4.2.2: Gel picture showing 5' RACE amplification products. A) amplification of 5' *Prx3*; M 500 bp ladder, 1 amplification with NUP and NGSP3; B) 5' *Prx4*; M 500 bp ladder, 1 amplification with NUP and GSP7

The 3' RACE was conducted, using CDS III primer for first-strand synthesis followed by PCR amplifications using primers GSP4 and NGSP4 for *Prx3* while CRPRX5F and GSP8 were used for *Prx4*, which resulted in ~900 bp and ~700 bp fragments for *Prx3* and *Prx4* respectively (Fig. 4.2.2A-B). These fragments, were excised from the gel, purified, cloned in the pGEM-T Easy vector and transformed in to competent cells. Plasmid DNA was isolated from the resulting white colonies and sequenced.



Fig. 4.2.3: Gel picture showing 3' RACE amplification products. A) 3' *Prx3*; M 100 bp ladder, 1 is amplification with UPM and GSP4, 2 is amplification with NUP and NGSP4; B) 3' *Prx4*; M 500 bp ladder, 1 is amplification with NUP and GSP8.

Finally full length gene primers were utilized for the RT-PCR amplification using following primer pairs CRPRX3F2-CRPRX3R for *Prx3* and CRPRX4F2-CRPRX4R for *Prx4* gene (Fig. 4.2.3). The full-length cDNA was cloned in pGEM-T Easy vector system and sequenced after plasmid isolation. The nucleotide sequences were submitted to GenBank database at NCBI with the accession number as EF 661875 for *Prx3* and AY837788 for *Prx4*. ORF sequences predicted for two ranged from 991 to 999 nucleotides in length (Table 4.2.2).

4.2.2.3 Bioinformatics analysis of Prx3 and Prx4

The complete sequence of *Prx3* cDNA was 1233 bp long and its ORF codes for 330 amino acid polypeptide (Table 4.2.2). There is a predicted 34 amino acid N-terminal signal peptide with SSA-QL cleavage site (Fig. 4.2.4), suggesting the final length of amino acids for the mature protein to be 309. Deduced Prx3 was cationic in nature with estimated *pI* value over 8. All the conserved cysteines, and the amino acids required for heme peroxidase function, were found in primary structure of Prx3 with a single glycosylation site (Fig. 4.2.4). In BLAST search, Prx3 showed the highest identity (73%) with *Nicotiana* peroxidase (BAA82306). The major difference between Prx4 and Prx3 was the presence of N-glycosylation site in signal peptide of Prx4 (Fig. 4.4.4).

Table 4.2.2: Properties of the predicted peroxidases present in the *C. roseus*.

Gene	ORF length, nt:s	Protein	Amino acids	N-terminal propeptide, aa:s	Molecular mass, mature protein kDa	<i>pI</i> , mature protein	C-terminal propeptide, aa:s	Potential glycosylation sites	Amino acid sequence identity (%) Prx3	Amino acid sequence identity (%) Prx4	Potential localization
<i>Prx3</i>	993	Prx3	330	34	31.8	9.07	None	1	100	71	Secreted
<i>Prx4</i>	957	Prx4	318	21	31.98	9.2	None	2	71	100	Secreted

The complete sequence of *Prx4* was 1055 bp long and its ORF encoded a polypeptide of 318 amino acids with a 21 amino acid predicted N-terminal signal peptide cleaved at SSA-QL (Fig. 4.2.4). The mature protein Prx4 was calculated to be basic in nature as like Prx3 (Table 4.2.2). The predicted Prx3 and Prx4 shared 71% amino acid sequence identity. The translated polypeptide contained all the eight conserved cysteines for disulfide bonds, all the indispensable amino acids required for heme binding, peroxidase function, coordination of two Ca²⁺-ions, and up to three potential N-glycosylation sites (Fig. 4.2.4). In BLAST search, Prx4 showed high level of amino acid sequence identity (80%) with *Nicotiana* peroxidase (BAA82306).

```

Prx3      MASSSSSSSSFSNFCIVIMVIVLSIIMRSCSQLSSEFTYSKIIPQVYNTVRKQVESAV
Prx4      MWPYINLGLCIPLLFLIGSSSAQLSTIDYYSKSCENVFNIVKSKQVHSAI
Nicotiana_prx  MASLKINAIVLFLVSLIGSSSAQLSTCFYYSKSCPKLYGIVKSAVQSAI
Quercus_prx  MAARSTSHSASSFLIVSLAVLWVIFSCNSSARLSTINFYYSKSCPKVFSIVQSVVHSAI
Ipomea_anionic_ MAVSVKALTAVLLCVLVLVCGCSAQLSPGFYYSKSCPKLFGIVNSVVRSAI
Peanut_Prx  -----XLSSNFYATKCFNALSTIKSAVNSAV
          ** : * ..** : .. : .. ** :

Prx3      SKEKRMGASLLRLRFHHCQFVQCCNGSILLDDTSSLRGEKTAGPNVGSVVRGFDVVDNIKSD
Prx4      LKEARMGASLLRLRFHHCQFVNGCCNGSILLDDTSSFTGEKRAAPNFNSARGFEVVDNIKSA
Nicotiana_prx  NKETRMGASLLRLRFHHCQFVNGCCNGSILLDDTSSFTGEKRAAPNVNSARGFEVIDNIKSA
Quercus_prx  SKQPRQGASLLRLRFHHCQFVNGCCNGSVLLDDTPTFTGEKTAGPNKGSIRGFEFVDEIKSK
Ipomea_anionic_ QKEARMGASLLRLRFHHCQFVNGCCNGSILLDDTSSFTGEKRAAPNFQARGFEVIDQIKSA
Peanut_Prx  AKEARMGASLLRLRFHHCQFVQCCNASVLLDDTSNFTGEKTAGPNANSIRGFEVIDIKSQ
          * : * ***** : ***** : ** : ***** : ** * ** * ***** : * **

Prx3      VEKVCQGVVSCADILAI AARDSVVALGGPSWKVKVGRDRSRTASLSGANSR-IPPTSNL
Prx4      VENVCQGVVSCADILAI AARDSVQILGGPSWNVKLGRRDATTASQAAAHNS-IPPTSNL
Nicotiana_prx  VEKVCQGVVSCADILAVTARDSVVALGGPNWVKLGRDRSRTASQSAANSR-IPPTSNL
Quercus_prx  VEKECQGVVSCADILAI AARDSVKILGGPKWDVKLGRDRSRTASLKAANSR-IPPTSNL
Ipomea_anionic_ VEKVCQGVVSCADILAIASRDSVTLGGPSWNVKLGRRDARTASQAAANS-IPPTSNL
Peanut_Prx  VESLCPGVVSCADILAVAARDSVVALGGASWNVLLGRDRSRTASLSANSR-LPAPFFNL
          ** : ***** : ***** : ** : ***** : ** * ** : ** : **

Prx3      RNLISSFQAVGLSAKDMVVLSGSHFIGQARCTVFRARIYNES-NIETSFARTRQGNCPPLP
Prx4      NALVSRFNALGLSTNDLVALSGSHFIGQARCTNFRARIYNENLNDAALAQTRRSNCPRP
Nicotiana_prx  NRLISSFSAVGLSTKDMVALSGAHTFIGQARCTNFRARIYNENLNDAFARTRQSNCPRS
Quercus_prx  SNLINRFKAKGLSTKDMVALSGAHTFIGQARCTVFRDRIYKDK-NIDSSFAKTRQNTCPKT
Ipomea_anionic_ NRLISSFSAVGLSTNDMVVLSGSHFIGQARCTNFRARIYNES-NIDSSFAQSRKGNCPRA
Peanut_Prx  SGLISAFSNKGFTRKELVTLSGAHTFIGQAQCTAFRTIYNES-NIDPTYAKSLQANCP--
          * : * : ***** : ***** : ** * ** : ** : ** : **

Prx3      TCG-NGDNLAPLQLQSPNGFQINYYKNLINKKGLLHSDQQLFNGGSTNSLVEAYSKDTKA
Prx4      SC-SRDNNLAPLQLQTPRAFQNNYYKNLVNRRQLLHSDQQLFNGGSTDSIVRSYSGNPPAS
Nicotiana_prx  SC-SGDNNLAPLQLQTPNKFENNYYFKNLVDDKGLLHSDQQLFNGGSADSIVTSYSNPPSS
Quercus_prx  TGLPGDNKIAPLQLQTPRAFQNNYYKNLIKQKGLLHSDQQLFNGGSTDSLVKKYSQDTKS
Ipomea_anionic_ SC-SGDNNLAPLQLQTPRIKENNYYVNLVNNKGLLHSDQQLFNGVSTDSIVRGYSTNPSK
Peanut_Prx  SV-CGDTNLSPELVTTNKFENNYYINLRNKKGLLHSDQQLFNGVSTDSQVTAYSNAAT
          : * : ***** : ** * ** : ** : ***** : ***** : ** * ** :

Prx3      FYSDFAAAMIKMGDISPLTGSNGEVRKNGRRVN-
Prx4      FASDFAAAMIKMGDISPLTGSNGQIRKNGRRIN-
Nicotiana_prx  FSSDFVTAMIKMGDIRPLTGSNGEIRKNGRRLN-
Quercus_prx  FYSDFVNAMIKMGDIQPLTGSNGEIRKNGRKNVH-
Ipomea_anionic_ FKSDFAAAMIKMGDIKPLTGNNGEIRKNGRRRN-
Peanut_Prx  FNTDFGNAMIKMGNLSPLTGTSGQIRKNGRTN-
          * : ** ***** : ***** : ** : ***** : **

```

Fig. 4.2.4: Clustal W (1.82) multiple amino acid sequence alignment of *Catharanthus roseus* Prx3 and 4 (Prx3 and Prx4) with Prx retrieved from NCBI database according to accession numbers: *Nicotiana_prx* (*Nicotiana tabacum*; BAA82306.1), *Quercus_prx* (*Quercus suber*; AAR31106), *Ipomea_anionic_* (*Ipomoea batatas*; AAP42508) and *Peanut_Prx* (*Arachis hypogaea*; pdb|1SCH|A). Predicted N-terminal-SSs are italicised, the heme-binding sites are marked in red, the calcium-binding sites in blue, S-S-bridge forming cysteines in reverse red and the putative N-glycosylation sites are in green color.

4.2.2.4 Gene copy number of *Prx3* and *Prx4*

Gene copy number analysis for *Prx3* and *Prx4* was performed using Southern blot hybridization. Ten microgram of genomic DNA was digested using *Hind* III, *Xba* I for both *Prx3* and *Prx4*. Digested genomic DNA was transferred to a nylon membrane and probed with ³²P-labeled *Prx3* and *Prx4* cDNA. On the analysis of gel blots with *Prx3* and *Prx4* cDNA, a single band was observed in both the cases of *Hind* III, *Xba* I

digested genomic DNA (Fig. 4.2.5A-B). These results suggested that the *Prx3* and *Prx4* genes are present in single copy in *C. roseus* genome.

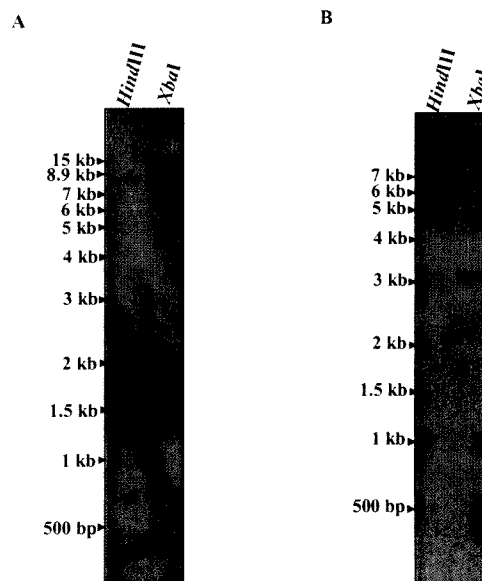


Fig. 4.2.5: Southern gel blot analysis for *Prx3* and *Prx4*. Ten microgram of *C. roseus* genomic DNA was subject to digestion with different restriction enzymes and resolved on 0.7% agarose gel. The gels were blotted to Hybond N membrane followed by hybridization with ^{32}P -labeled A) *Prx3*, B) *Prx4* cDNAs. The position of supermix ladder molecular weight is shown on right side.

4.2.2.5 Phylogentic analysis of *Prx3* and *Prx4* with the selected peroxidase sequences from peroxidase database

The peroxidase database Passardi et al. (2007) was utilized for the selection of class III complete peroxidase sequences which were grouped in different categories. These sequences were again found to be subdivided in different subgroups with each subgroup containing many sequences. The amino acid sequences of these peroxidases were first aligned individually with *Prx3*, *Prx4*, *CrPrx*, *CrPrx1*, *CrPrx2a* and *CrPrx2b* (All *C. roseus* class III peroxidase sequences reported in the database) and the most related sequences were utilized for preparation of phylogenetic tree.

4.2.2.5.1 Phylogenetic relationship based on the cellular localization

The Class III complete peroxidase sequences which were categorized based on cellular localization in peroxidase database and the *Arabidopsis* vacuolar peroxidase sequences reported by Welinder et al. (2002) were utilized for making a parsimonious tree utilizing MEGA 4.0 software (Tamura et al., 2007). The unrooted phylogenetic tree showed the features that *Prx3* and *Prx4* both are present as separate cluster but

close to the 6126 | *Triticum aestivum* peroxidase which is reported to be secretory in nature (Fig. 4.2.6). *C. roseus* peroxidases, *CrPrx* and *CrPrx1* characterized earlier were found in separate cluster with cell wall targeted and vacuolar targeted peroxidase respectively. Amino acid sequences of class III peroxidase selected for preparing phylogenetic analysis are listed in table 4.2.3.

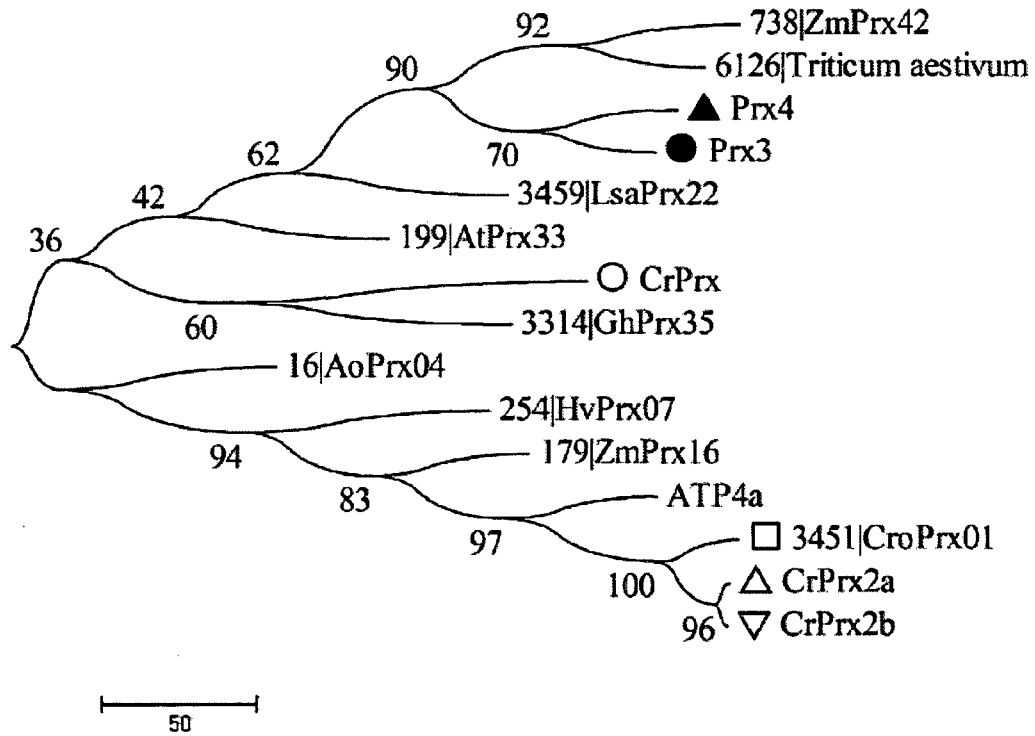


Fig. 4.2.6: Phylogenetic relationships of *Prx3* and *Prx4* with other Class III peroxidases sequences selected on basis of their cellular localization. The relationship was inferred using the Maximum Parsimony method (Eck and Dayhoff, 1966). The bootstrap consensus tree inferred from 1000 replicates is taken to represent the evolutionary history of the taxa analyzed (Felsenstein, 1985). Branches corresponding to partitions reproduced in less than 50% bootstrap replicates are collapsed. The percentage of replicate trees in which the associated taxa clustered together in the bootstrap test (1000 replicates) are shown next to the branches (Felsenstein, 1985). The MP tree was obtained using the Close-Neighbor-Interchange algorithm Nei and Kumar (2000) with search level 7 in which the initial trees were obtained with the random addition of sequences (10 replicates). The tree is drawn to scale; with branch lengths calculated using the average pathway method Nei and Kumar (2000) and are in the units of the number of changes over the whole sequence. All positions containing gaps and missing data were eliminated from the dataset (Complete Deletion option). There were a total of 238 positions in the final dataset, out of which 111 were parsimony informative. Phylogenetic analyses were conducted in MEGA4 (Tamura et al., 2007). The *Prx3* and *Prx4* were marked with ● and ▲ respectively other peroxidase reported from *C. roseus* were marked as *CrPrx* ○, *CrPrx1* (*CrPrx01*) □, *CrPrx2a* △ and *CrPrx2b* ▽.

Table 4.2.3: Selected Class III peroxidase sequences based on cellular localization used for the phylogenetic analysis of *Prx3* and *Prx4* (Fig.4.2.6).

Symbol	Accession No.	Localization
Prx3	ABV24960	Present study
Prx4	AY837788	Present study
3459 LsaPrx22	Lsa.10055*	Apoplastic
16 AoPrx04	BAA94962	Cell wall
738 ZmPrx42	AC211735 [†]	Plasma membrane bound
6126 (<i>Triticum aestivum</i>)	EU542600	Secreted
>254 HvPrx07	CAA05897	Vacuolar
3451 CroPrx01	AM236087	Vacuolar
199 AtPrx33	NP_190480	Cell wall
3314 GhPrx35	CAE54309	Apoplastic
179 ZmPrx16	AC211202	Cell wall
ATP4a	CAA67309	Vacuolar
CrPrx2a	CAP72489	Vacuolar
CrPrx2b	CAP72490	Vacuolar

*Accession number as found in UniGene database.

[†] Accession from chromosomal sequences from *Zea mays* sequencing project.

4.2.2.5.2 Phylogenetic relationship with the class III peroxidase sequences categorized on the basis of stress regulation

Stress regulated peroxidase sequences as reported in peroxidase database, were utilized for the preparation of phylogenetic tree. These sequences which were categorized under different stresses were selected on homology basis. The most similar sequences from each categories of stress induced/repressed peroxidase related with Prx3, Prx4, CrPrx, CrPrx1, CrPrx2a and CrPrx2b were utilized as an initial input for preparation of parsimonious tree (Fig. 4.2.7). Sequences used in preparation of phylogenetic tree are listed in table 4.2.4. Phylogenetic analysis shows that Prx4 clustered with that of AoPrx01 (*Asparagus* peroxidase) which is induced upon lignification. Prx3 was clustered near to *Colletotrichum* induced *Medicago* peroxidase. The other peroxidase from *C. roseus* viz CrPrx, CrPrx1, CrPrx2a and

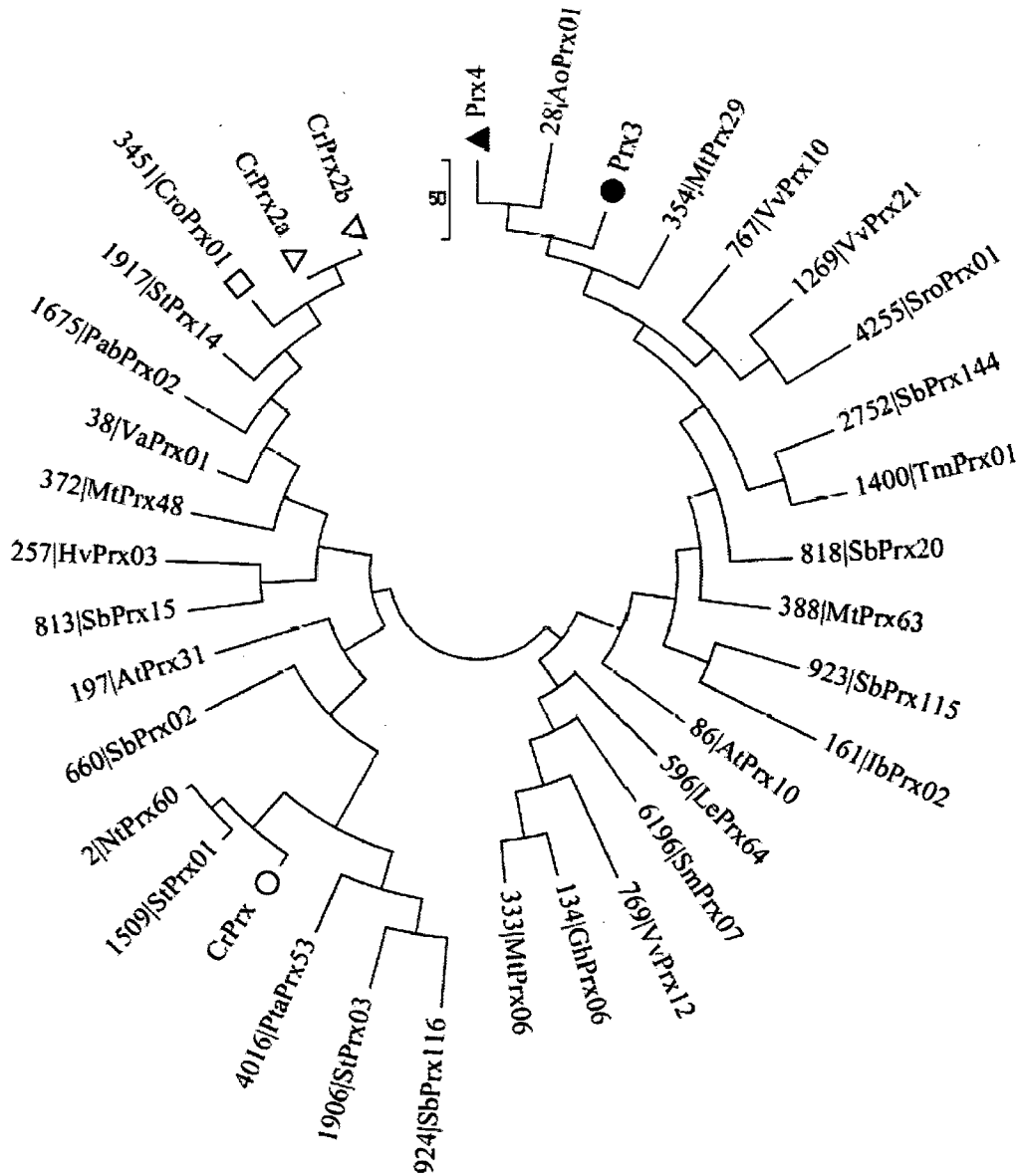


Fig. 4.2.7: Phylogenetic relationships of Prx3 and Prx4 with other Class III peroxidase sequences (38) selected on the basis of stress regulation. The relationship was inferred using the Maximum Parsimony method Eck and Dayhoff (1966). The bootstrap consensus tree inferred from 1000 replicates is taken to represent the evolutionary history of the taxa analyzed (Felsenstein, 1985). Branches corresponding to partitions reproduced in less than 50% bootstrap replicates are collapsed. The percentage of replicate trees in which the associated taxa clustered together in the bootstrap test (1000 replicates) is shown next to the branches Felsenstein (1985). The MP tree was obtained using the Close-Neighbor-Interchange algorithm Nei and Kumar (2000) with search level 7 in which the initial trees were obtained with the random addition of sequences (10 replicates). The tree is drawn to scale; with branch lengths calculated using the average pathway method Nei and Kumar (2000) and are in the units of the number of changes over the whole sequence. All positions containing gaps and missing data were eliminated from the dataset (Complete Deletion option). There were a total of 238 positions in the final dataset, out of which 111 were parsimony informative. Phylogenetic analyses were conducted in MEGA4 (Tamura et al., 2007). The Prx3 and Prx4 were marked with ● and ▲ respectively other peroxidase reported from *C. roseus* were marked as CrPrx ○, CrPrx1 (CrPrx01) □, CrPrx2a △ and CrPrx2b ▽

CrPrx2b, showed their closeness with peroxidases which were induced upon cold, drought, salt and pathogen stress. The result is found to be confined with the experimental evidence of CrPrx which was induced upon Ultraviolet Rays (UV) and methyl jasmonate (MJ) stress (Kumar et al., 2007).

Table 4.2.4: Genbank accessions numbers of the peroxidase genes regulated by different stress used for phylogentic tree preparation (Fig. 4.2.7).

Symbol	Accession No.	Inducer/Repressor*
Prx3	ABV24960	Present study
Prx4	AY837788	Present study
28 AoPrx01	CAD67477	Lignification
354 MtPrx29	CR932959 [†]	<i>Colletotrichum</i> inoculation
923 SbPrx115	BE359080*	Dark growth
161 IbPrx02	AF109124	Growth, Ozone ^Δ
388 MtPrx63	AC199762 [†]	Germination
767 VvPrx10	AM453059 [‡]	Abiotic stress
1269 VvPrx21	AM429435 [‡]	Abiotic stress
2752 SbPrx144	CX614188 [#]	Anaerobic stress, Brassinolide treatment, Gibberellic acid treatment
134 GhPrx06	AAL93154	bacterial-induced
333 MtPrx06	AC187465 [†]	Elicitor treatment (glucan, oligosaccharides, yeast extract, <i>Phytophthora</i> crude extract)
596 LePrx64	DU880423 [§]	Copper excess
6196 SmPrx07	FE427388, FE460737 [#]	Carbon starvation, Cold stress
1400 TmPrx01	AAW52715	Constitutively induced, Ethepon treatment, Methyl jasmonate treatment, Pathogen interaction, Powdery mildew attack, Salt stress
4016 PtaPrx53	CO160524 [#]	Flooded treatment, Sulfur deficiency
4255 SroPrx01	ABK59095	Hydrogen peroxide, Nod factor treatment, Nodulation
161 IbPrx02	AAF00093	Cold stress, Growth, Ozone treatment, Senescence, Temperature stress, Wounding

CrPrx	AAY26520	UV irradiation
3451 CroPrx01	CAJ84723	N/D
CrPrx2a	CAP72491	N/D
CrPrx2b	CAP72491	N/D
769 VvPrx12	AM476901 [‡]	Abiotic stress
818 SbPrx20	TC102062 [#]	Abscissic acid treatment, <i>Colletotrichum</i> inoculation, Dark growth, Ethylene treatment, Heat shock stress, Light growth, Oxidative stress, Pathogen interaction, Phosphate starvation, Salt stress, Wounding
813 SbPrx15	TC103101 [#]	Abscissic acid treatment, Acid treatment, Alkaline treatment Ethylene treatment, Heat shock, stress, Light growth, Oxidative stress
924 SbPrx116	TC105691 [#]	Acid treatment, Alkaline treatment, Oxidative stress
257 HvPrx03	TC161498 [#] , TC194050 [#]	<i>Blumeria</i> infection (Powdery mildew attack)
1509 StPrx01	TC169516 [#] , TC163866 [#] , TC175824 [#] , TC111720 [#]	Cold stress, Drought, Pathogen interaction, <i>Phytophthora</i> infection, Salt stress
372 MtPrx48	TC127667 [#] , TC131218 [#] , TC139998 [#]	<i>Aphanomyces euteiches</i> infection Drought, Elicitor treatment (glucan, oligosaccharides, yeast extract, <i>Phytophthora</i> crude extract), <i>Glomus versiforme</i> infection, Nitrogen starvation
38 VaPrx01	BAA01950	Nod factor treatment, Nodulation, Pathogen interaction, Phosphate starvation, <i>Phytophthora</i> infection <i>Rhizobium</i> inoculation
660 SbPrx02	TC114379 [#] , TC104358 [#]	Ethylene treatment, Wounding Acid treatment, Alkaline treatment, Ethylene treatment
1906 StPrx03	TC169248 [#] , TC88052 [#] , TC97573 [#] , TC122629 [#] , TC138834 [#]	Cold stress, Drought, Heat shock stress, Salt stress
1917 StPrx14	TC192708 [#] , TC163642 [#] , TC118916 [#]	Cold stress, Drought, Heat shock stress, Pathogen interaction, <i>Phytophthora</i> ,

		infection, Salt stress
86 AtPrx10	NP_175380	Hormon treatment, Stress treatment
197 AtPrx31	NP_189460	Dark growth, Hormon treatment, Stress treatment
2 NtPrx60	Q9XFL2 [¶]	Lignification
1675 PabPrx02	Q5W5I4 [¶]	Lignification

Δ Repressor of peroxidase

† Accession from chromosomal sequences from *Medicago truncatula*.

‡ Whole genome shotgun sequence

EST database

\$ genomic survey sequence

N/D Not Determined

¶ UniProt database

4.2.2.5.3 Phylogenetic analysis based on tissue specific expression

The amino acid sequences of peroxidase expressed in different types of tissue regions of plants were utilized for the construction of phylogenetic tree. The parsimonious tree shows that the *Prx3* and *Prx4* were present as separate cluster (Fig. 4.2.8). *Prx3* was found to be clustered along with citrus peroxidase *CsPrx07* which has maximum expression in shoot meristem, fruit and whole seedlings. The *Prx4* was also present as separate cluster and close to *AtPrx52* the *Arabidopsis* peroxidase which was expressed in siliques and *GmPrx30* a *Glycine max* peroxidase expressed in etiolated hypocotyls. Sequences utilized for the preparation of phylogenetic tree are listed in table 4.2.5.

which was shown to be expressed maximum in floral parts, clustered separately but close to *Brassica* peroxidase *BnPrx12* expressed maximum in anthers and seeds. Phylogentic tree prepared in this way is informative but the result needs to be confirmed with expression studies.

Table 4.2.5: Tissue types and accessions for the sequence data presented in figure 4.2.8 used for phylogenetic analysis.

Symbol	Accession No.	Tissue type
Prx3	ABV24960	Present study
Prx4	AY837788	Present study
1297 BnPrx12	EE447077 [#] , EV098600 [#]	Anthers, Seeds
1968 InPrx06	CJ754662 [#] , CJ766890 [#]	Buds, Flowers
1140 OsPrx130	CAH69372	Callus, Leaves, Roots
1121 OsPrx111	CAH69353	Callus, Coleoptiles, Flowers, Leaves, Radicles, Roots, Stems
144 GhPrx03	AAL93151	Cotyledons
1530 HvPrx17	TC167245 [#] , TC163933 [#] , TC164419 [#] , TC163127 [#]	Endosperm, Shoots, Spikes
322 PsPrx29	BAD97439	Epicotyls
254 HvPrx07	CAA05897	Coleoptiles, Embryosac, Epidermis, Leaves, Roots
3004 BoPrx32	AM060523 [#]	Etiolated seedlings
1696 PbPrx09	CV282462 [#] , DT517809 [#]	Flowers
1374 CsPrx06	Csi.5407 ^Σ	Fruits, Shoot meristems, Whole plant
>245 PpaPrx01	Ppa.921 ^Σ	Gamete, Protonema
735 ZmPrx39	ACF86224	Glumes, Ovaries, Silks
215 AtPrx49	NP_195361	Callus, Green siliques, Mixed tissues,

		Roots
359 MtPrx34	TC118924 [#] , TC136024 [#]	Cell culture, Immature pods, Leaves, Roots, Roots hairs, Roots nodules, Stems
770 VvPrx13	AM449831 [‡]	Berries, Flowers, Inflorescences, Mixed tissues
1405 TmPrx06	AAW52720	Leaf epidermis, Leaves
3119 PtPrx41	DT478196 [#]	Female inflorescence, Flowers, Leaves, Stems
525 GmPrx35	Gma.30052 ^Σ	Floral meristems, Hypocotyls, Leaves (fully expanded), Roots, Seed coats, Somatic embryos
2145 EgPrx01	EL688960, EL691410	Female inflorescence, Leaves, Male inflorescences
>1128 OsPrx118	CAH69360	Panicles, Roots
>763 VvPrx06	AM426597 [‡]	Berries, Fruits, Inflorescences, Mixed tissues, Pedicel
5107 VvPrx24	EC932103 [#]	Flowers, Leaves, Pericarps, Roots
4056 PalPrx04	BAF33315	Barks, Leaves, Petioles, Shoots, Xylem
162 HvPrx06	Q42853 ^Π	Pistils, Seeds
651 LePrx52	AP009266 [†]	Pollens
60 NsPrx01	AAA34050	Protoplasts
3997 CloPrx06	DY392397 [#]	Rhizomes
59 MtPrx01	Q40372 ^Π	Root tips, Roots, Roots hairs
96 AtPrx15	NP_179407	Mixed tissues, Roots, Rosettes
329 FcPrx01	Q8S3U4 ^Π	Latex, Rubber particles
354 MtPrx29	TC121615 [#] , TC127837 [#] ,	Flowers, Germinating seeds, Leaves,

	TC106851 [#]	Mycorrhizal roots, Seedling roots, Seedlings, Shoots
198 AtPrx32	NP_850652	Etiolated hypocotyls, Flowers, Mixed tissues, Roots, Rosettes, Seedling shoots
518 GmPrx30	Gma.31729 ^Σ	Etiolated hypocotyls, Immature flowers, Leaves, Roots, Seedlings
80 AtPrx04	NP_172906	Leaves, Roots, Senescing leaves
218 AtPrx52	NP_196153	Flowers, Mixed tissues, Siliques
252 CrPrx03	BE643121 [#]	Spores
6196 SmPrx07	FE427388 [#] , FE460737 [#]	Strobili (cone), Whole plant
52 NtPrx10	CAH17984	Leaves, Vascular tissue
>122 AtPrx29	NP_566565	Vegetative tissues
>1376 CsPrx07	CF835865 [#]	Shoot meristems, Whole seedlings
1716 PtrePrx01	BU888470 [#] , BU893600 [#] , BU867151	Barks, Cambium, Leaves, Petioles, Roots, Seeds, Wood
2073 PtaPrx28	Pta.17212, Pta.3054	Roots, Stems, Xylem
>1215 CruPrx1	EX920611, EX918877	Ovule, Young leaves
CrPrx	AAV26520	All tissues
3451 CroPrx01	CAJ84723	N/D
CrPrx2a	CAP72491	N/D
CrPrx2b	CAP72491	N/D

[#] EST database

^Σ Unigene cluster

[‡] Whole genome shotgun sequence

^Π UniProt database

[†] Accession from chromosomal sequences

4.2.2.6 *Prx3* and *Prx4* are expressed differentially in different tissues

To elucidate the functions of *Prx3* and *Prx4* gene in *C. roseus* and further validation of phylogenetic results, the transcript accumulation was surveyed in different organs through quantitative real time PCR (qRT-PCR). Relative quantitative PCR was performed to check the expression patterns of *Prx3* and *Prx4* gene in different parts of plant. The expression of both *Prx3* and *Prx4* was highest in stem followed by flower tissue which was somewhat relevant to their phylogenetic relationship with peroxidase expressed in floral parts. *Prx4* was found to be present in root and flower in almost equal quantity. The expression pattern for *Prx3* was followed as Stem>Flower>Fruit> Bud>Root>Young leaves>Mature leaves>Old leaves, while *Prx4* was present as Stem>Root>Flower>Fruit >Young leaves>Mature leaves>Old leaves>Bud (Fig. 4.2.9). Both *Prx3* and *Prx4* the expression was found least in older leaves, which indicating that the two genes are not associated with senescence activity. Results obtained through quantitative real time PCR were repeated by multiple independent experiments.

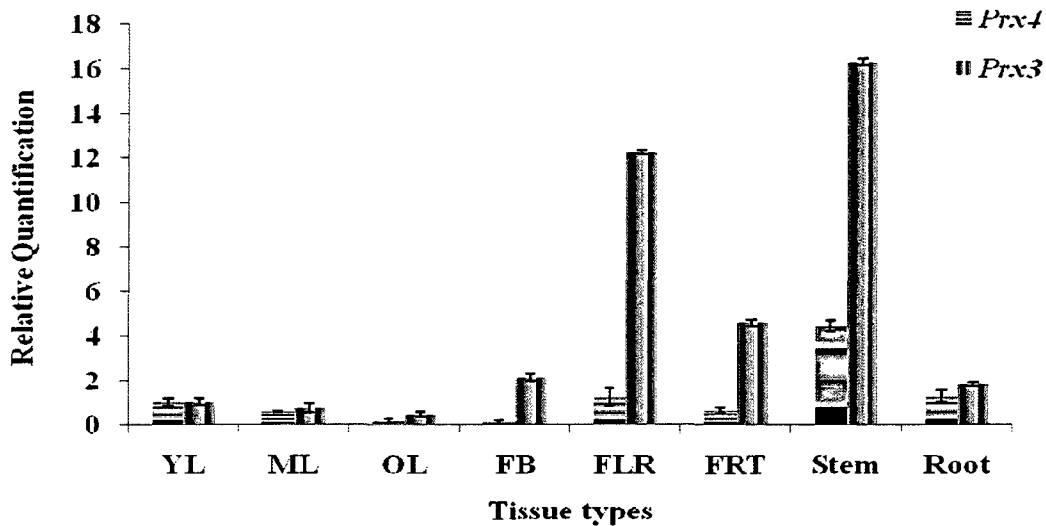


Fig. 4.2.9: Quantitative real time PCR analysis of *Prx3* and *Prx4* expression in different organs. Five microgram of total RNA from each tissue sample was reverse-transcribed and subject to real-time PCR analysis. The relative expression value of each gene was normalized to an endogenous control *CrActin* and calculated using $\Delta\Delta CT$ method (Applied Biosystems). Values are the results of triplicate analysis of two biological replicates. Error bars indicate the standard deviation of five independent experiments. Abbreviations YL, young leaves; ML, mature leaves; OL, old leaves; FB, flower bud; FLR, flower; FRT, fruit (n=3).

4.2.2.7 Localization of *Prx3* using Prx3-GFP fusion protein in *Nicotiana tabacum*

Subcellular localization of the *Prx3* was studied by expressing chimeric fusions of mGFP (pCAMBIA 1302) to *Prx3* ORF in tobacco leaf disc (Fig. 4.2.10A). Seven days after the transformation GFP fluorescence could be observed. Confocal microscope images of the transiently transformed leaves were visible as green fluorescence (Fig. 4.2.10C). For visualization of exact location the bright field images (Fig. 4.2.10B) were superimposed on the fluorescence images (Fig. 4.2.10D). The superimposed image reveals that the green fluorescence of the GFP marker is clearly localized in the apoplastic region of the cell. These finding suggested that the *Prx3* is secretory in nature and targeted outside of the cell to apoplast region.

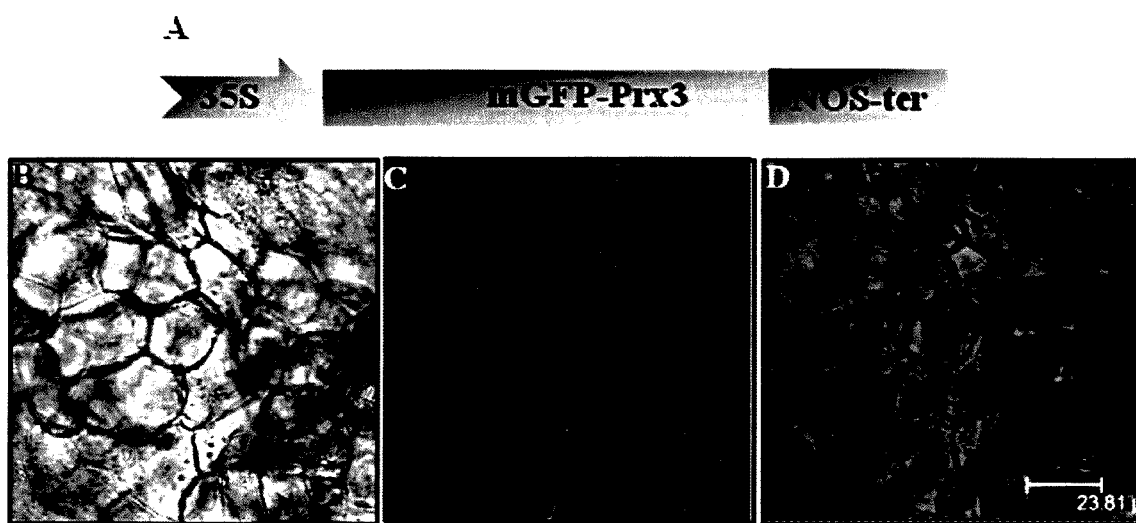


Fig. 4.2.10: Cell wall localization of the Prx3-GFP Fusion Protein in *Nicotiana tabacum*, viewed by Confocal Laser Scanning Microscopy. Cells were visualized after 7 days of *Agrobacterium* infection. A) Construct used for the GFP-Prx3 localization study, three images from the same tissue was shown B) Bright field image, C) GFP fluorescence from a Prx3-GFP fusion construct, D) Superimposed image of B and C.

4.2.3 Discussion

This chapter reports the cDNA cloning and primary structure characterization of two new class III peroxidases from *C. roseus*. So far two other peroxidases have been reported from *C. roseus* were *CrPrx* (Kumar et al., 2007 a part of present dissertation) and *CrPrx1* (Costa et al., 2008). The cDNA clones of the peroxidase genes (*Prx3* and *Prx4*) were generated from RNA extracted from leaf tissue of plant.

In the present work, degenerate primers designed from conserved regions of class III peroxidases were used to amplify partial peroxidase clones. Several workers

had previously reported to clone different peroxidase genes using this technique (Marjamma et al., 2006 and Kumar et al., 2007). The peroxibase (peroxidase database) were utilized to prepare phylogentic tree based on classification as described in the database. Phylogenetic relationships were utilized to show cellular localization, tissue specific expression and stress regulation for the two peroxidases *Prx3* and *Prx4*.

Class III plant peroxidases (EC 1.11.1.7), often referred to as the classical plant peroxidases are targeted either to the vacuole or the extracellular space. These monomeric, usually N-glycosylated proteins of approximately 300 amino acids, are structurally very similar and contain four conserved disulfide bridges. The active site consists of a heme group that is coordinated to an invariant proximal histidine, whereas a conserved distal histidine is the essential catalytic residue for binding and heterolytic cleavage of H₂O₂ (Welinder, 1992). All these characteristics are found in the deduced amino acid sequence of *Prx3* and *Prx4*. Both *Prx3* and *Prx4* contains conserved Ca²⁺ ion binding sites, and recognizable eukaryotic N-terminal signal peptides Nielsen (1997) for possible ER-targeting and further processing. The four conserved disulfide bridges holds the α -helixes in compact globular structure, correspondingly as in the 3-D crystal structures of HRPC and other structurally described peroxidases (Schuller et al., 1996; Gajhede et al., 1997; Østergaard et al., 2000)

The theoretical molecular weight and isoelectric point of the mature *Prx3* and *Prx4* was found to be around 32 kDa and *pI* 9.2 respectively for both peroxidases. The *Prx3* and *Prx4* showed 71% similarity between each other at the level of amino acid sequence (Table 4.2.2).

Plant peroxidases are encoded by large multigene families. In *Arabidopsis* genome, 73 genes have been identified, most of them are expressed in roots. They account for 2.2% of root ESTs, but only a few show strict organ specificity (Tognolli et al., 2002; Welinder et al., 2002). In rice, 138 genes are distributed over all chromosomes (Passardi et al., 2004a). Peroxibase is a collection of heme and non-heme peroxidase sequences originated from annotated or not correctly annotated sequences deposited in the main repositories such as GenBank or UniProt knowledge base. Peroxidase database is freely accessible on internet (<http://peroxibase.isb-sib.ch>) (Passardi et al., 2007). The entries in peroxibase when classified based on tissue

specificity, showed maximum peroxidase were present in root followed by leaves (Fig. 4.2.11).

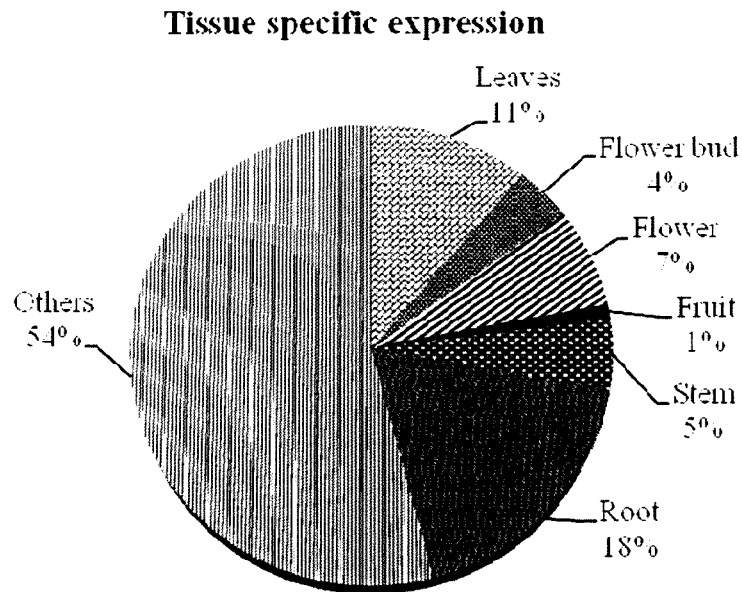


Fig. 4.2.11: Tissue specific expression of peroxidase sequence entries in peroxidase database. A total of 5142 sequences were classified in peroxidase database under tissue types, these sequence numbers were selected and presented in the chart as percentage form.

There are several ways of presenting the evolutionary relationship among the peroxidases. McInnis et al. (2005) selected peroxidase sequences based on the intron number and tissue specific expression for phylogenetic tree preparation. Result of tissue specific expression of *Prx3* and *Prx4* shows that these two were expressed maximum in stem tissue which was in accordance with their phylogenetic groupings (Fig. 4.2.8 and 4.2.9). It had also been noticed that other than stem *Prx3* was expressed maximum in flower tissue, correlating with phylogram result of a *Populus* peroxidase PtPrx41 expressed in flowers (Fig. 4.2.8, 4.2.9 and Table 4.2.5). Many plant peroxidases like *TOBPOXAN* are reported to be expressed throughout the floral organs after anthesis including the sepals and petals (Klotz et al., 1998). Flower specific peroxidase may play a role in pollen- stigma interaction, for instance in loosening stigma cell wall components to allow pollen tubes, to penetrate the stigma and to facilitate their growth between stigma cells towards stylar transmitting tissue. Flower specific *PRX* peroxidase from *Mercurialis annua* expression is correlated with the development of male flowers. *PRX* levels are found to be repressed in female

flowers and in genetically male flowers undergoing feminization by treatment with cytokinins (Biossay et al., 1996). Involvement of cationic peroxidases in the biosynthesis of lignin has been reported in many plant species (El Mansouri et al., 1990; Quiroga et al., 2000; Talas-Oğras et al., 2001; Blee et al., 2003; Koutaniemi et al., 2005; Gabaldón et al., 2005).

Spatio-temporal localization is an important factor in determining the function of different peroxidases, since they form a large family of oxidoreductases with similar substrate specificities (Welinder, 1992). Localization study carried out only for *Prx3*, predicted it to be cell wall localized. Based on phylogenetic relationship with other peroxidases as well its gene structure *Prx4* was predicted to be localized to cell wall. The possible function based on targeting studies relates *Prx3* and *Prx4* with cell wall synthesis. The cell wall peroxidases polymerize macromolecules, which are then deposited on the extracellular surface. The accumulation of these macromolecules strengthens the cell wall, thereby restricting cell expansion and pathogen invasion, and confers structural strength to the plant body. Wall modification by a cell wall bound tomato peroxidase (TPX2) also seems to be associated with resistance to hyperosmotic stress (Amaya et al., 1999). Real time PCR analysis indicated that *Prx3*, *Prx4* transcripts were maximum expressed in stem tissue. The expression data when coupled with localization and phylogenetic data indicates the function of *Prx3* and *Prx4* in secondary wall formation. Many cationic peroxidases were assigned the function of lignin polymerization on basis of their localization. Sasaki et al. (2006) reported the involvement of a cationic cell wall peroxidase in lignifications on the basis of its expression and localization. Similarly based on localization a cationic peroxidase from French bean had been reported to be involved in lignifications (Smith et al., 1994). Negligible expressions were visible for *Prx3* and *Prx4* in leaf tissue which limits the stress related expression studies of two peroxidases. The two peroxidases were found as single copy number in *Catharanthus* genome similar to the flower specific peroxidase reported in *Senecio squalidus* (McInnis et al., 2005).

Peroxidases generally react to compounds containing a hydroxyl group(s) attached to an aromatic ring. Guaiacol (*o*-methoxy phenol) is commonly used as a substrate for the measurement of peroxidase activity. As seen in the phylogram (Fig. 4.2.7) *Prx3* and *Prx4* are grouped in cluster with *AoPrx01* which is induced during

lignification as classified in peroxibase database. The overall scenario presents the possible function of Prx3 and Prx4 as lignifications but there may be different reasons for floral expression of *Prx3*. The versatility of certain enzymes is one of main driving forces in the evolution of land plants, and that there is a general consensus that such enzymes confer high metabolic plasticity to the lignin biosynthetic pathway (Boerjan et al., 2003).

4.2.4 Conclusion

Two novel peroxidase genes namely *Prx3* and *Prx4* have been cloned for the first time from *Catharanthus roseus* by PCR based strategy using degenerate primers from leaf tissue. Both *Prx3* and *Prx4* genes are present in single copy in *C. roseus* genome and showed maximum accumulation of transcripts in stem followed by flower and flower bud. The localization study using GFP-Prx3 fusion protein indicated that Prx3 follows a secretory path outside the cell. Similarly the Prx4 was shown to be an apoplastic in nature by an *in-silico* analysis. Phylogenetic analysis using sequences from peroxibase database predicts that both the genes are induced upon pathogen infection and during lignifications. The overall results suggest the possible involvement of *Prx3* and *Prx4* in the defense mechanism against pathogen, cell wall fortification and in the process of lignification.

*4.3: Ectopic expression of two differentially localized
Catharanthus roseus peroxidases CrPrx and CrPrx1
genes in Nicotiana tabacum*

4.3.1 Introduction

Peroxidase (EC 1.11.1.7; Hydrogen donor; H₂O₂ oxidoreductase) are heme containing enzymes that catalyze the single electron oxidation of several substrates at the expense of H₂O₂. The plant peroxidase super family is divided into three classes based on the differences in primary structure (Welinder, 1992). Class I plant peroxidases include the intracellular enzymes in plants, bacteria and yeast (*Saccharomyces cerevisiae*), such as microbial cytochrome c peroxidase (EC 1.11.1.5), bacterial catalase-peroxidase (EC 1.11.1.6), and ascorbate peroxidase (EC 1.11.1.11). Class II plant peroxidases are extracellular peroxidases from fungi including lignin peroxidase (EC 1.11.1.14) and Mn²⁺ independent peroxidase (EC 1.11.1.13). Class III plant peroxidases (EC 1.11.1.7) are characterized by having a multifunctional nature, with the capacity of recognizing a broad range of substrates, and by showing a remarkable polymorphism with overlapping substrate spectra (Ros Barceló and Munóz, 2000). The diversity among peroxidase is also found at gene level, since the sequencing of *Arabidopsis* genome enabled the identification of 73 Class III peroxidase genes in this plant (Tognolli et al., 2003; Welinder et al., 2002; Duroux and Welinder, 2003). The observed redundancy of peroxidase genes and proteins with similar reactivity properties may reflect the importance of this group of enzymes to plant fitness and survival, but also makes it very difficult to determine conclusively the function of individual isoenzymes. Several physiological functions such as lignin and suberin biosynthesis, cross linking of extensin and feruloyl-pectins, and cross linking of structural proteins such as hydroxyproline-rich glycoproteins, which determine the final architecture of cell wall had been attributed to the class III peroxidases based on their *in vitro* catalytic properties and subcellular localization. Plant peroxidases have also been implicated in auxin catabolism (Hinman and Lang, 1965) and in hydrogen peroxide scavenging as well as production (Sottomayor et al., 2004). Although several studies were performed on cell wall peroxidases, very little is known about vacuolar peroxidases (Welinder et al., 2002). *In vitro* studies had shown the capacity of plant peroxidases to accept a number of vacuolar metabolites as substrates such as phenols, flavonoids and alkaloids. However, a comprehensive study is still lacking in order to accumulate a consistent amount of evidence supporting a role *in planta*.

To date two peroxidase genes *CrPrx* (accession number AY924306 a part of present dissertation) and *CrPrx1* (accession number AM236087) have been cloned

and characterized from *Catharanthus roseus* (Kumar et al., 2007 and Costa et al., 2008). The *CrPrx* gene consists of four exons and three introns, while *CrPrx1* belongs to two intron class peroxidase. The amino acid residues deduced from nucleotide sequences also varies as 330 and 363 for *CrPrx* and *CrPrx1* respectively and sharing low identity (32%) with each other (Kumar et al., 2007 and Costa et al., 2008). These peroxidases, *CrPrx* and *CrPrx1* had shown to be diverse in function based on their subcellular localization. *CrPrx* being secretory in nature predicted to have function in cell wall synthesis (Kumar et al., 2007). *CrPrx1* was found to be vacuolar in nature and predicted to play a role in biosynthesis of vinblastine by dimerization of catharanthine and vindoline in Monoterpenoid Indole Alkaloid (MIA) pathway in *C. roseus*. The tissue specific transcript accumulation was diverse between two peroxidases as *CrPrx* is present in all the tissue with maxima in stem tissue, while *CrPrx1* was expressed highest in floral tissue.

An attempt to functionally characterize these peroxidase genes had been carried out by comparing the overexpression characteristics. The coding sequences of *CrPrx* and *CrPrx1* under the control of cauliflower mosaic virus (CaMV) 35S promoter was introduced into the tobacco to generate plants with modified peroxidase activity. The resulting transgenic tobacco showed enhanced peroxidase activity as well as oxidative stress tolerance. Evaluation of T1 generation transgenic showed clear difference between vacuolar and cell wall specific peroxidase as the later was unable to grow on stressed media. Both kinds of T1 transgenics were found to be well adaptive in cold condition. The objective of present work was to generate sense expression of *CrPrx* and *CrPrx1* in *Nicotiana tabacum* cloned under 35S CaMV promoter and analysis of the transgenic under abiotic stress.

4.3.2 Results

4.3.2.1 Construction of binary vector for overexpression of *CrPrx* and *CrPrx1* in tobacco

The overexpression construct was prepared in pBI121 binary vector under the control of 35S CaMV promoter. For preparation of *pBI-CrPrx* vector, PCR amplification was performed using PBIPF-1 and PBIPR-1 on plasmid DNA (pGEM-T-*CrPrx*) as template. The resulting construct was subsequently subcloned in pBI121 vector using

multiple cloning sites *Xba* I and *Sma* I (Fig. 4.3.1A). Similarly *pBI-CrPrx1* vector was prepared using PCR amplification with CPNRF-CPNRR primer pair on plasmid DNA of pGEM-T-*CrPrx1*, which later on was subcloned in *Xba* I and *Bam*H I multiple cloning sites of binary vector pBI121 (Fig. 4.3.1B). The resulting construct contains a NOS promoter regulating expression of *NPT* II gene required for kanamycin resistant plants followed by NOS terminator. The desirable insert (*CrPrx* and *CrPrx1*) was under the control of constitutive 35S CaMV promoter along with GUS gene (β -glucuronidase) but no fusion construct followed by NOS-terminator (Fig. 4.3.1A-B).

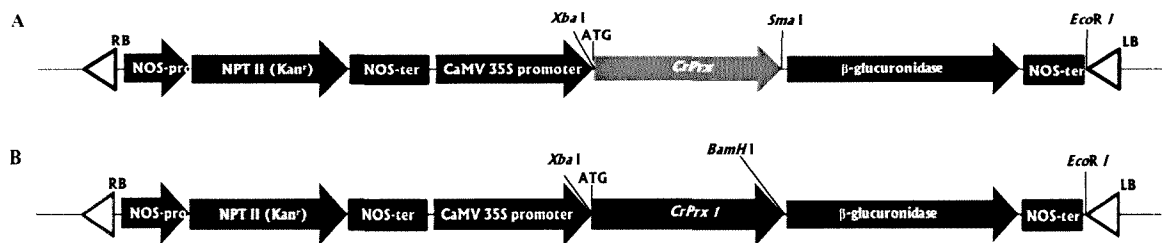


Fig. 4.3.1: Structure of Chimeric genes. A) The 1.1 kb *Catharanthus roseus* peroxidase *CrPrx* and B) 1.2 kb *CrPrx1* were cloned in pBI121 plasmid under the control of a cauliflower mosaic virus (CaMV) 35S promoter.

4.3.2.2 Preparation of transgenic tobacco plants

The recombinant binary vector was transformed into *Agrobacterium tumefaciens* strain LBA4404 using freeze thaw method (Chen et al., 1994). The leaf explants of *Nicotiana tabacum* were infected using recombinant *Agrobacterium* as described (Rogers et al., 1986). Disks were cut from *in vitro* grown sterile leaves with a paper punch (6 mm in diameter) and submerged in a culture of *A. tumefaciens* grown overnight in luria broth at 28⁰C. After gentle shaking to ensure that all edges were infected, the disk were blotted dry and incubated upside-down on tobacco shoot induction medium (TSM) (Fig. 4.3.2A). The age and titer of the bacterial inoculum had little influence on the effectiveness of the transformation, however it was important to avoid excessive soaking of the internal tissues of the leaf disk by the bacterial culture. After 2 to 3 days, the disks were transferred to TSM containing 100 mg/l kanamycin and cefotaxime 250 mg/l (Fig. 4.3.2B). After 2 to 4 weeks (Fig. 4.3.2C-D), shoots that developed were excised from calli and transplanted to a root-inducing medium (TRM) containing cefotoxime (250 mg /l) and kanamycin (100 mg/l) (Fig 4.3.2E). After 8 weeks, rooted plantlets (Fig. 4.3.2F) were transplanted to soil and shifted to greenhouse maintained at 25⁰C.

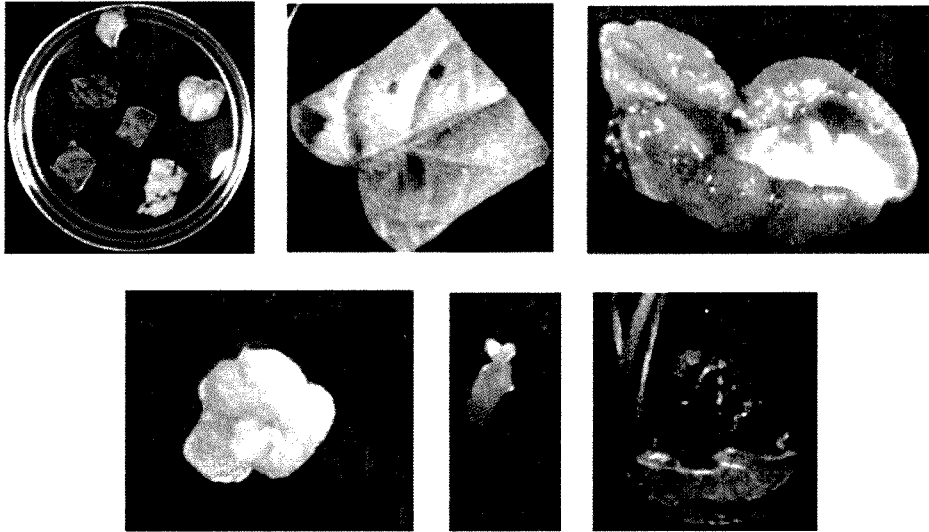


Fig. 4.3.2: Leaf disk transformation and selection of antibiotic-resistant cells. A-B) Leaf disks were cut from *in vitro* grown sterile leaf of *Nicotiana tabacum*, inoculated with *Agrobacterium tumefaciens* strains, cultured on TSM plates, C) leaf curling started after 7-days of transfer to shooting media, D) callus formation after 14 days on TSM, E) shoot initiation takes place after 4 weeks, F) plantlets with root appeared after 8 weeks on rooting media (TRM).

4.3.2.3 Southern blot analysis of selected transgenic lines

Genomic DNAs were extracted from leaves of fastest growing kanamycin-resistant tobacco plants and digested with *EcoR* I. The copy numbers of genes introduced in to transgenic plants were investigated from the Southern blot analysis using the specific probe of DNA fragment containing *CrPrx* and *CrPrx1* cDNA (Fig. 4.3.3A-B). As shown in figure 4.3.2, the transgenic tobacco had multiple copies of the chimeric genes ranging from 3 to 10. The transgene was integrated in different positions of the tobacco genome which gave rise to different sizes in Southern hybridization (Fig. 4.3.3A-B). The untransformed tobacco leaves showed no signal with either *CrPrx* or *CrPrx1* (Fig. 4.3.3A-B). Transgenic tobacco lines obtained from *CrPrx1* are labeled as 'A' followed by numbers while those from *CrPrx* are labeled as 'CRP' followed by numbers.

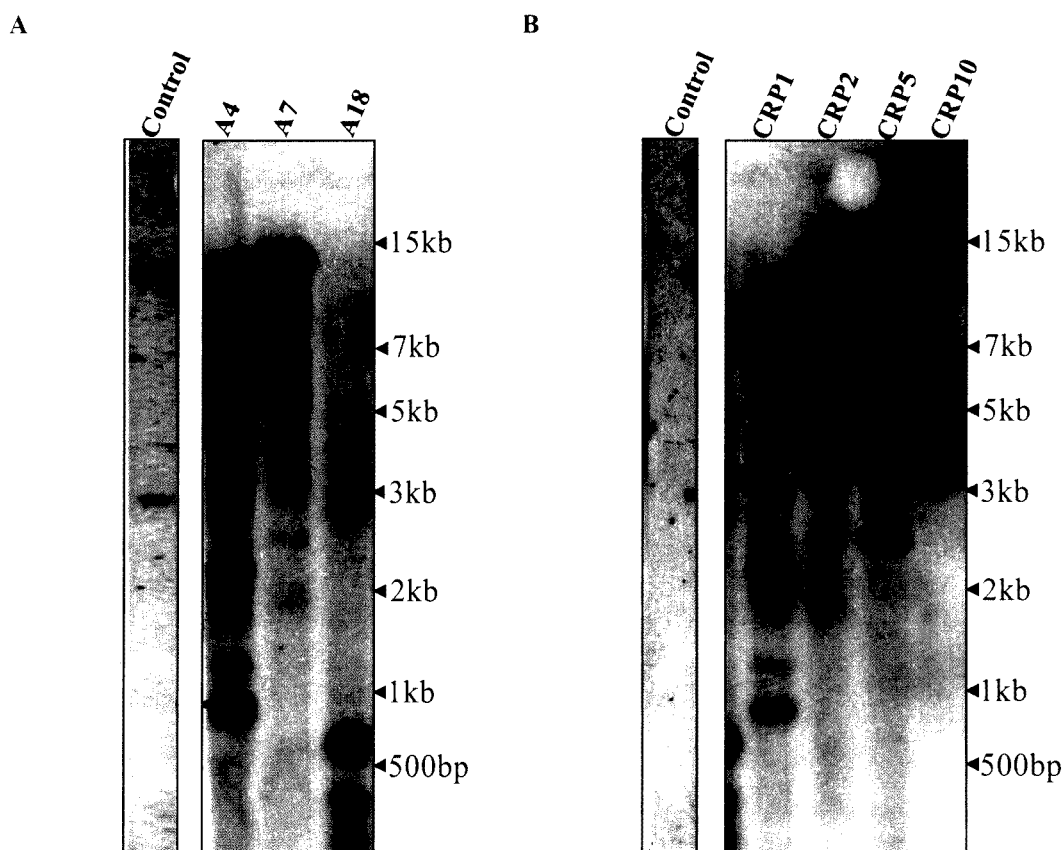


Fig. 4.3.3: Southern blot analysis of tobacco transgenics. Genomic DNA was extracted from leaves of kanamycin-resistant tobacco plants and was digested with *EcoR* I. A) transgenic lines generated from overexpression of *CrPrx1* cDNA named as A4, A7, A18 while from B) *CrPrx* cDNA were named as CRP1, CRP2, CRP5 and CRP10. Control lines without signal of transgene were shown in left.

4.3.2.4 Growth rate of the selected transgenic tobacco lines grown in green house under controlled condition

Growth rate of selected T0 transgenic tobacco were measured, the transgenics which were showing high growth rate were selected and length of the plant was measured weekly. The growth rate of transformed tobacco varied between two transgenic lines as well as among the same transgene transgenic lines (Fig. 4.3.4). The growth rate was found to be maximum in the CRP-5 line, a *CrPrx* transgenic line. The A7 lines inspite of presence of transgene doesn't show increase in growth rate. All the transgenic lines analyzed except A7 showed higher growth than vector control and wild tobacco plants on VIII week. Overall, on earlier weeks there was no significant change in the growth rate of transgenic lines compared to controls.

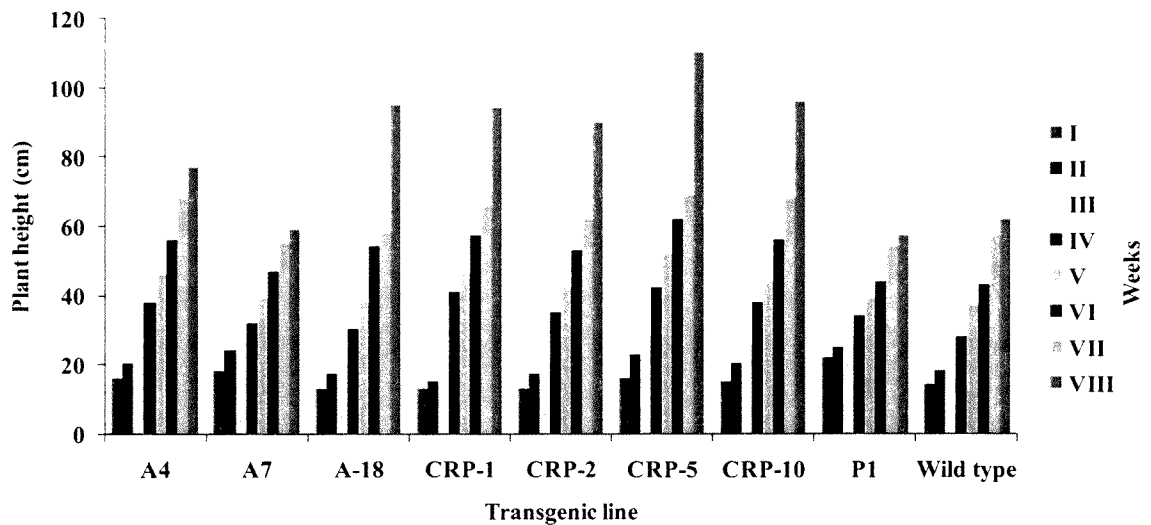


Fig. 4.3.4: Growth rate of transgenic tobacco plants. A4, A7 and A18 represent the transgenic plants transformed with 35S-*CrPrx1* gene, CRP1, CRP2 and CRP10 represents the transgenic plant transformed with 35S-*CrPrx* gene. Wild type tobacco and empty vector P1 was used as control plant.

4.3.2.5 Expression analysis of *CrPrx* and *CrPrx1* in transgenic tobacco

Northern blot analysis was carried out in order to investigate the expression of introduced chimeric genes in transgenic tobacco. Total RNA was extracted from young leaves of III week of kanamycin-resistant plants. The hybridization probe used was full-length *CrPrx* and *CrPrx1* cDNA. As shown in figure 4.3.5A-B, the expression varied among the transgenic lines. Strong expression observed in the leaves of CRP2 and A7 transgenic tobacco transformed with *CrPrx* and *CrPrx1* respectively, whereas no detectable transcript was observed in wild type and empty vector control (P1) transgenic tobacco (Fig. 4.3.5A-B).

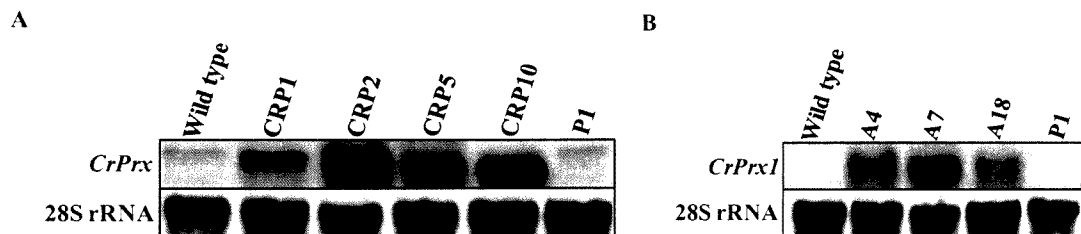


Fig. 4.3.5: Expression levels of the transgenes (*CrPrx* and *CrPrx1*) in the transformed plants. Total RNA extracted from leaves in the *in vitro* cultured transformed (CRP1, CRP2, CRP5, CRP10, P1, A4, A7 and A18) and wild type plants were fractionated by agarose gel. Hybridization was performed using a 1.1 kb *CrPrx* cDNA for CRP lines and 1.2 kb *CrPrx1* cDNA full-length for A-lines as a probe. Coomassie blue stained 28S ribosomal RNA is used as loading control.

4.3.2.6 Estimation of oxidative stress tolerance of the transformed plants overexpressing peroxidase

Elevated peroxidase activity level in plants is highly correlated with increased resistance to abiotic stresses, including oxidative stress (Hiraga et al., 2001). We therefore analyzed peroxidase-over-producing plants for their response towards oxidative stress. Oxidative stress was generated by exposing plant leaf tissues to H_2O_2 , which produces O^{2-} , reactive oxygen radicals (ROS). Oxidative damage was evaluated as percentage retention of chlorophyll after H_2O_2 treatments under strong light and dark growth conditions. No significant differences in damage were visible between wild type and transgenic plants using H_2O_2 up to 1.0 M (Fig. 4.3.6).

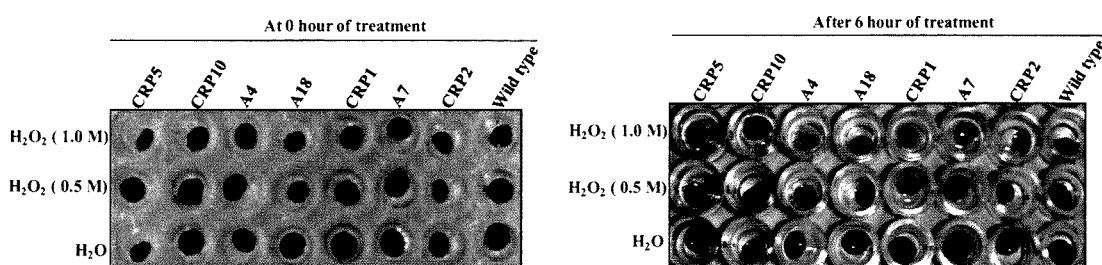


Fig. 4.3.6: Visualization of oxidative stress tolerance of the transformed plants overproducing peroxidase, grown under greenhouse conditions.

In spite of non-significant differences observed apparently between transgenic and control plants, the percentage chlorophyll retention was measured to check the possible bleaching by peroxide treatments. It was observed that leaf segments transgenic lines CRP5, CRP10, A7 kept in strong light of $2000 \mu \text{mole m}^{-2}\text{s}^{-1}$ could retain up to 60% of chlorophyll as compared to the wild type plants with 1.0 M of H_2O_2 after 6 h of treatment. In control plants 1.0 M H_2O_2 treatment resulted into less than 20% chlorophyll retention (Fig. 4.3.7A-B). The A7 line which showed maximum expression had highest retention of chlorophyll (Fig. 4.3.7B).

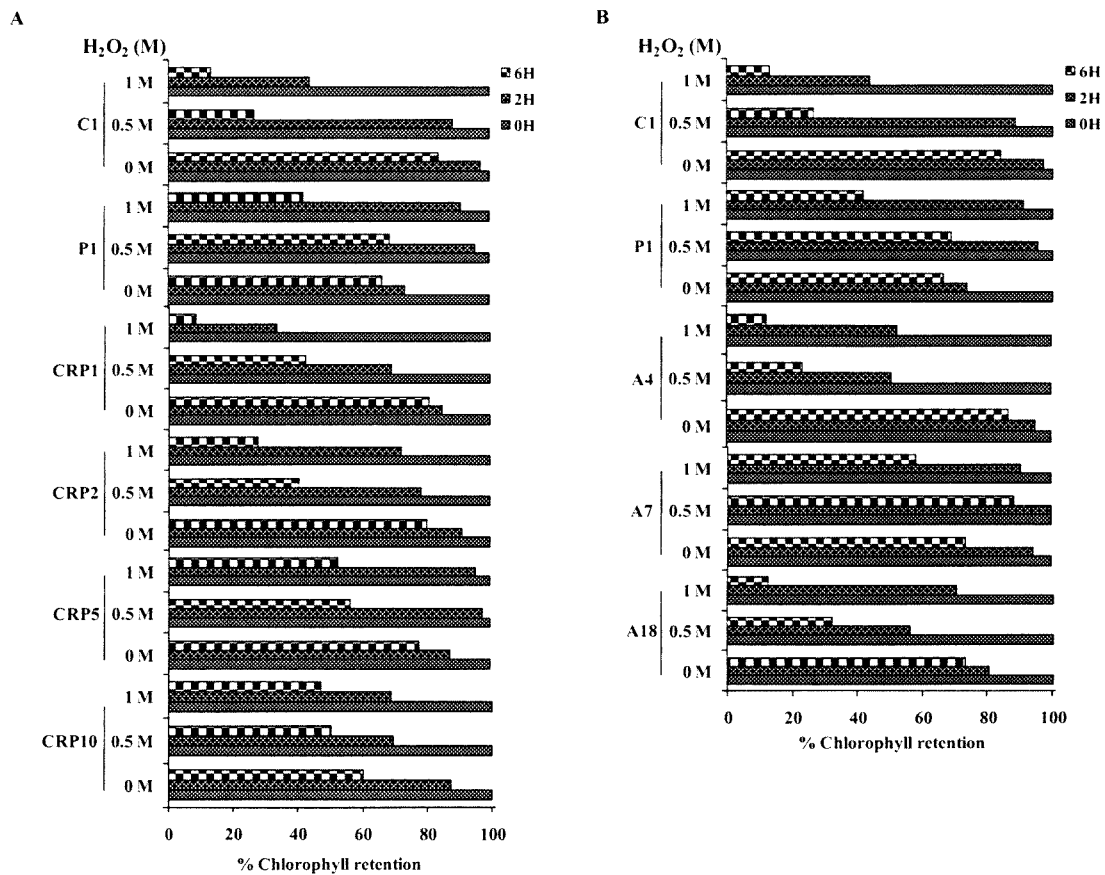


Fig. 4.3.7: Percent chlorophyll retention in the leaf disk in strong light of 2000 $\mu\text{mol m}^{-2} \text{s}^{-1}$. Leaf disk assay was performed to estimate the level of oxidative stress tolerance of T0 transgenic plants by floating the leaf segments from wild type and transgenic plants on 0.0 (Control), 0.5 and 1.0 M H₂O₂ solution. The leaf disks were kept under strong light of 2000 $\mu\text{mol m}^{-2} \text{s}^{-1}$ for 0, 2 and 6 h. A) C1, P1 and CRPs are wild type, transgenic lines with empty vector control and *CrPrx* resectively. B) C1, P1 and As are wild type, transgenic lines with empty vector control and *CrPrx1* resectively (n=3, SD<5%).

4.3.2.7 Assay of peroxidase activity in transgenic tobacco

Leaf tissue from three weeks old kanamycin-resistant plants were assayed for total peroxidase activity. A total peroxidase activity was measured by measuring guaiacol peroxidase activities of the soluble fractions extracted from leaves. As shown in figure 4.3.8, the peroxidase activities from both transgenic (A and CRP) plants were 2 to 5-fold higher than that seen in wild-type plants or empty vector control plants. These lines were further used to check the oxidative stress tolerance. As the growth habit and peroxidase activity between wild type and empty vector control remains same further experiments were conducted considering wild type as control.

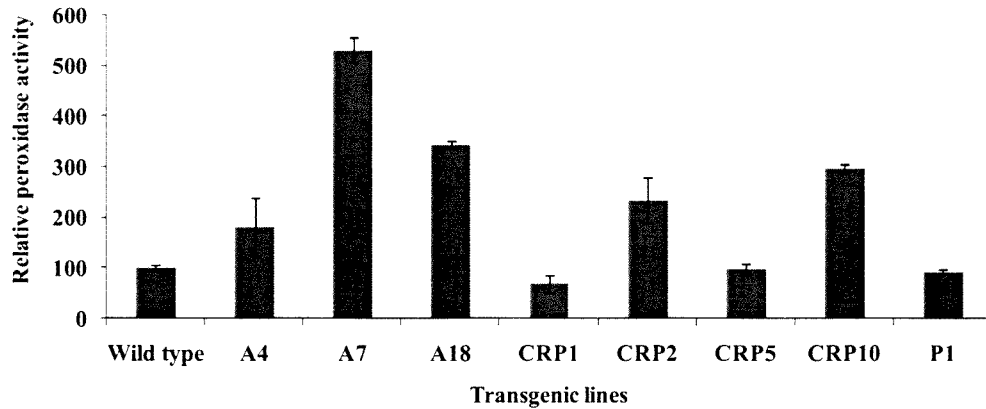


Fig. 4.3.8: Relative peroxidase activities in the *in vitro* cultured transgenic plants. The guaiacol peroxidase activities of the soluble fractions extracted from leaves in plants were measured. The enzyme activities were relative to the specific activity in the wild-type plant (=100%, 0.006 Units) (n=3).

4.3.2.8 Effect of peroxidase overexpression on photosynthesis of tobacco plants

4.3.2.8.1 Measurement of quantum efficiency (Fv/Fm) of photosystem II

To ascertain the effect of peroxidase overexpression in the physiology of transgenic tobacco plants, photosynthesis measurement was performed by measuring chlorophyll fluorescence using portable imaging-PAM chlorophyll fluorometer. The Fv/Fm value, which reflects the maximum quantum efficiency of PSII was found to be almost equal to healthy plant value of 0.8. The Fv/Fm value of the 3rd, 5th and 7th leaves for transgenic as well control plants remained almost same (Fig. 4.3.9).

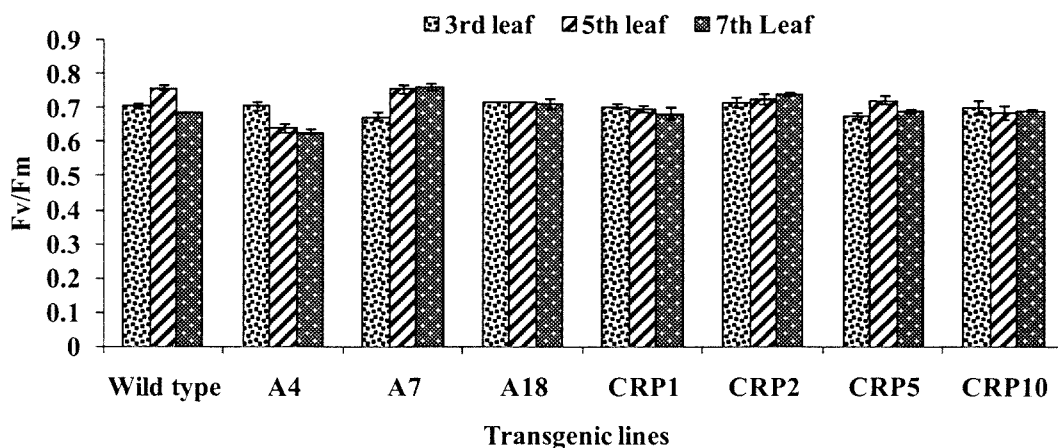


Fig. 4.3.9: Fluorescence measurements for the transgenic tobacco plants. Minimal fluorescence F_0 , Maximum fluorescence F_m and Maximum quantum efficiency F_v/F_m in transgenic Plants A) using 3rd leaves, B) using 5th leaves C) using 7th leaves of transgenic as well as control tobacco plants (n=3).

4.3.2.8.2 Measurement of effective quantum yield (YII) of photosystem II

Overall photosynthetic performance of plant can be measured by measuring the effective quantum yield Y(II) of photochemical energy conversion in light adapted state. In younger leaves (3rd and 5th) effective quantum yield was higher in transgenic lines (CRP2 and A7) than wild type plants (Fig. 4.3.10). In older leaves (7th) a reduction in photosynthetic yield was observed with transgenic plants of both *CrPrx* and *CrPrx1* as well as wild type plants (Fig. 4.3.10).

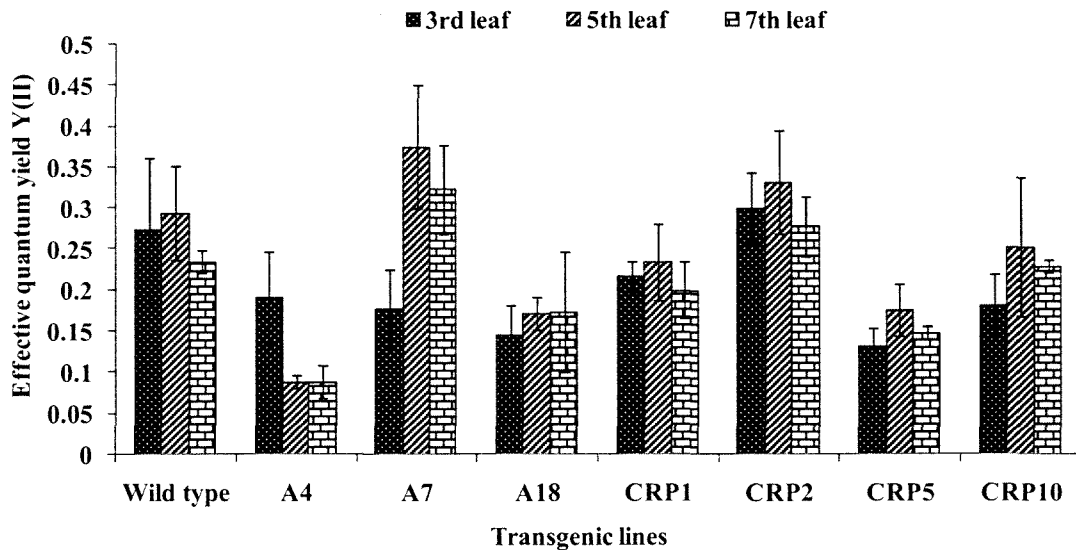


Fig. 4.3.10: PSII effective quantum yield Y(II) of transgenic lines *CrPrx* (designated as CRP) and *CrPrx1* (designated as A). The effective PSII photon yield measurements for 3rd, 5th and 7th leaves were measured (n=3)

4.3.2.9 Evaluation of T1 generation transgenic tobacco

The performance of transgenic tobacco lines harboring, *CrPrx* and *CrPrx1* were analyzed during salt, dehydration and cold stress. Three independent transgenic lines of *CrPrx1* (A4, A7 and A18) and four independent transgenic lines of *CrPrx1* (CRP1, CRP2, CRP5 and CRP10) were analyzed for stress tolerance.

4.3.2.9.1 Effect of Salt stress on germination

To investigate the effect of *CrPrx* and *CrPrx1* overexpression on germination under salt stress, seeds from transgenic lines of *CrPrx1* and selected transgenic lines of *CrPrx* along with a wild type, were germinated on MSH media containing NaCl at a concentration that severely impaired seed germination in wild type plants. At 250 mM NaCl, the germination of seeds from selected transgenic lines was significantly higher than that of control. The difference in germination was found in both transgenics viz vacuolar peroxidase *CrPrx1* and cell wall targeted peroxidase *CrPrx* (Fig. 4.3.11A-

B). However, in control experiment germination of the *CrPrx* and *CrPrx1* overexpressing seeds under non-stressed conditions was identical to wild-type plants (Fig. 4.3.11C). About 50% germination was observed (Fig. 4.3.11C) with the A7 transgenic lines which showed higher expression as well as activity of peroxidase. Interestingly when 250 mM of KCl was used as salt stress, the germination of both transgenic as well as wild type plants were severely hampered (Fig. 4.3.12A-B).

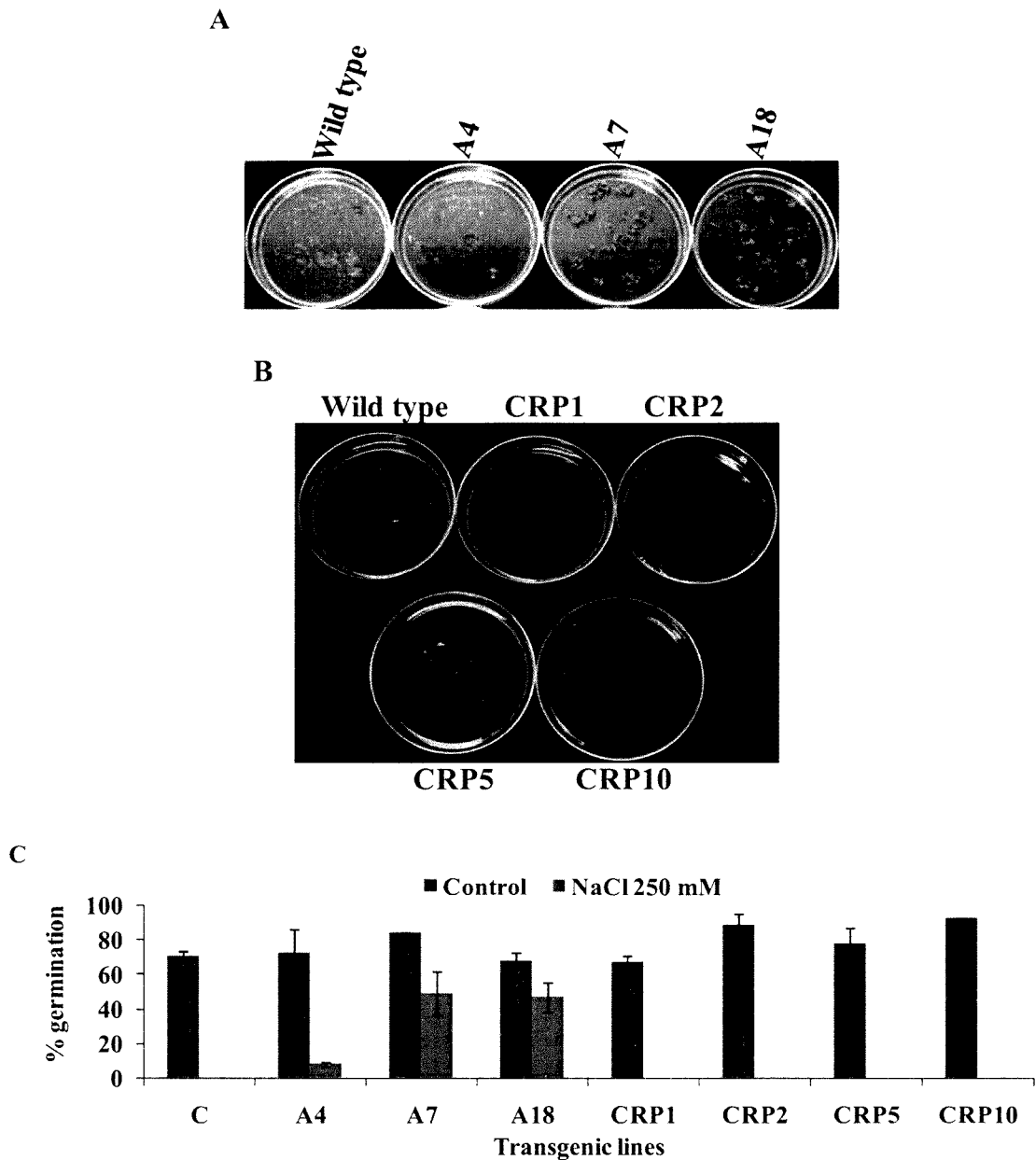


Fig. 4.3.11: Effect of NaCl salt stress on the survival and growth of wild type (and peroxidases overexpressing transgenic tobacco seedlings. T1 seeds were germinated on MSH media containing 250 mM NaCl. A) transgenic with vacuolar peroxidase *CrPrx1* B) transgenic with cell wall peroxidase *CrPrx*. C) percent germination of transgenic seeds.

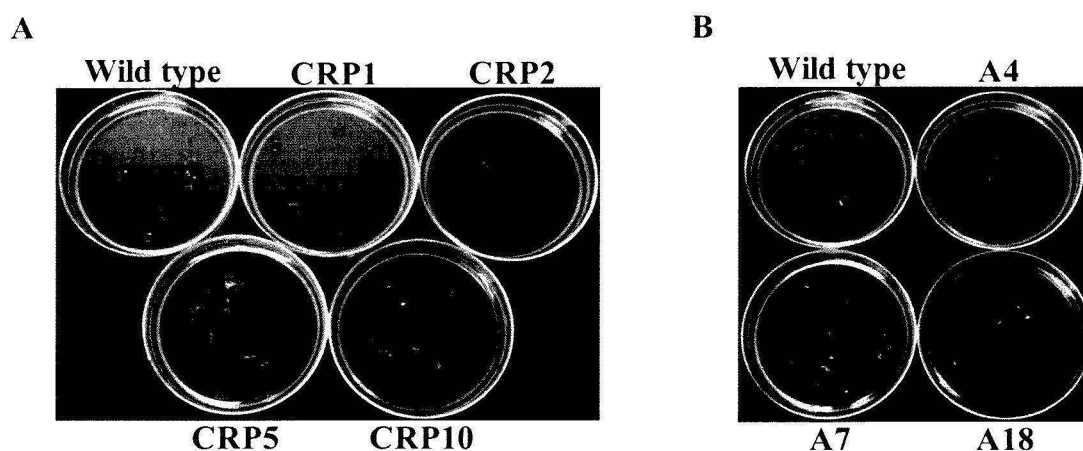


Fig. 4.3.12: Effect of KCl (250 mM) salt stress on transgenic seed germination. A) Seeds of *CrPrx* transgenic, B) seeds of *CrPrx1* transgenic lines. Wild type seeds were used as control.

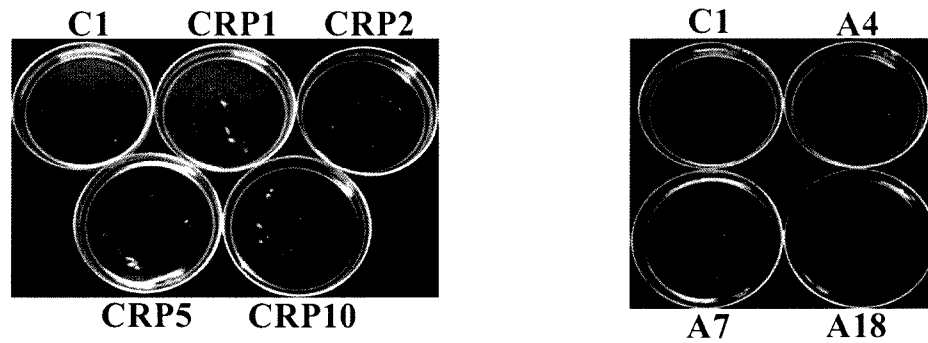
4.3.2.9.2 Effect of dehydration stress on seedling germination

Evaluation of *CrPrx* and *CrPrx1* overexpressing lines for dehydration stress tolerance revealed that the percentage germination of WT was almost nil in 0.3 M as well as 0.4 M mannitol in the MSH media (Fig. 4.3.12A-B). Interestingly it was also observed that the transgenics with cell wall specific peroxidase were unable to germinate on mannitol containing media. The percentage of germination was found to be maximum in A-18 lines in 0.3 M mannitol (Fig. 4.3.13C). However increase in mannitol concentration to 0.4 M reduced the germination of seeds severely. The transgenic line A7 which showed higher expression of peroxidase and its activity also had higher germination percentage under osmotic stress (Fig. 4.3.13A-B).

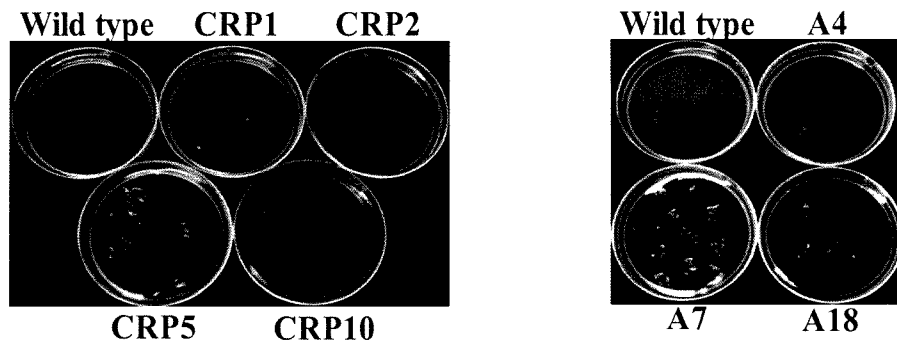
4.3.2.9.3 Cold stress and its effect on transgenic seedlings

Transgenic lines were analyzed for cold tolerance in the T1 generation. For cold stress the seeds were grown in medium containing half-strength Murashige and Skoog medium without sucrose and organic ingredients (MSH) for 21 days in a culture room maintained at $25 \pm 2^{\circ}\text{C}$ under a 16 h light/8 h dark cycle and each rack was illuminated with light ($50\text{-}100 \mu\text{mol.m}^{-2}$ per s) provided by four white fluorescent tubes Phillips Champion 40W/54). The 21-day-old seedlings were transferred to a cold chamber maintained at $8 \pm 1^{\circ}\text{C}$ for 15 days. The plates then were transferred back to culture-room conditions for recovery of seedlings. Observations were recorded after 15 days of recovery. The measurement of fresh weight of seedling after 15-day recovery

A



B



C

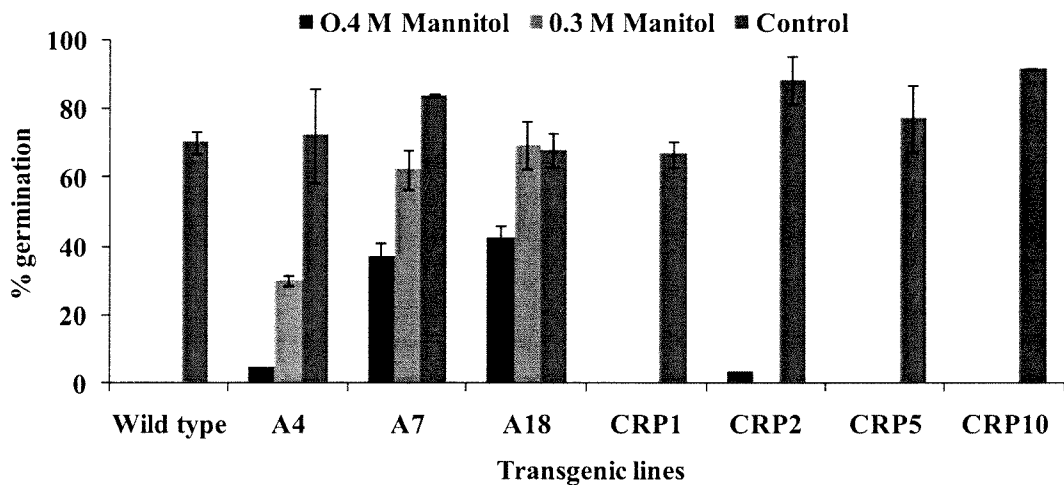


Fig. 4.3.13: Effect of dehydration stress on tobacco seedlings from WT, *CrPrx1* and *CrPrx*-overexpressing transgenic lines. Seeds were germinated on A) 0.3 M and B) 0.4 M mannitol. C) Graphical representation of germination in transgenic seeds.

period revealed that the stressed transgenic seedlings gained 80-100% fresh weight, where as untransformed (wild type) gained 60% fresh weight as compared to the unstressed seedlings (Fig. 4.3.14A). Additionally, the fresh weight of transgenic

seedlings was better than wild type seedlings at low temperature. Phenotypically, there was not much difference between transgenic and wild type seedlings (Fig. 4.3.14B).

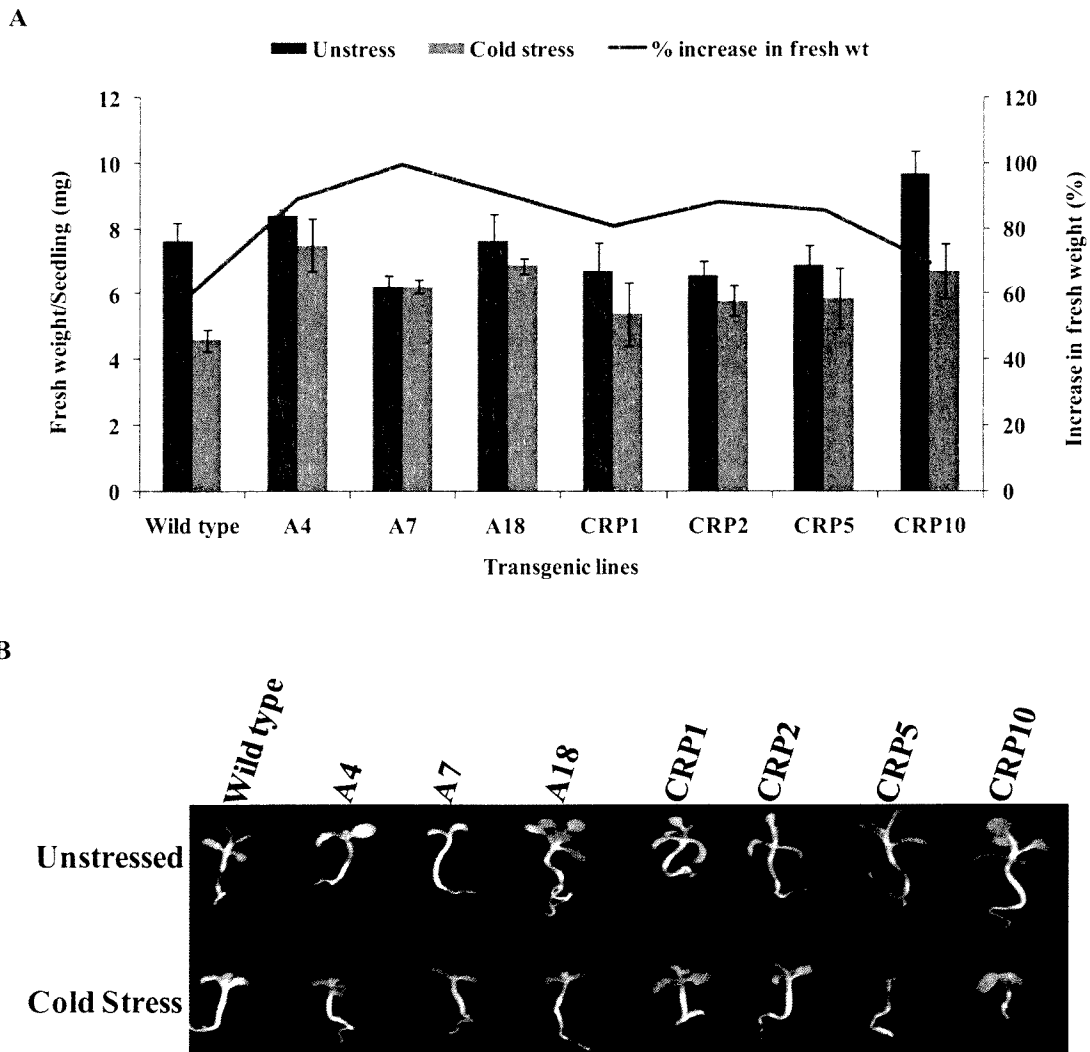


Fig. 4.3.14: Effect of cold stress on tobacco seedlings from wild type, *CrPrx1* and *CrPrx* overexpressing transgenic lines. A) Twenty-one-day-old seedlings were grown at $8\pm 1^{\circ}\text{C}$ for 15 days and transferred back to culture room conditions. A fresh weight was recorded for cold-stressed seedling after 15 days of cold stress recovery. Fresh weights of unstressed seedlings of the same age also were recorded and designated as control. Absolute variation of three replicates of two independent experiments is shown at the top of each bar B) Twenty-one-day-old seedlings of untransformed; *CrPrx1* and *CrPrx* overexpressing lines were cold stressed at $8\pm 1^{\circ}\text{C}$ for 15 days and then transferred back to MSH for recovery. Photograph of representative seedlings of wild type and five transgenic lines were taken after 15 days of recovery.

4.3.3 Discussion

This report is first attempt to study the functional characterization of a vacuolar targeted peroxidase and cell wall targeted peroxidase of *C. roseus in planta* in *Nicotiana tabacum*. Class III peroxidase is involved in many different processes in plant cell metabolism and it is mostly localized in the vacuole and in cell wall due to presence of secretory N-terminal signal. This class of enzymes is characterized by having a multifunctional nature, with the capacity of recognizing a broad range of substrates, and by showing a remarkable polymorphism (Ros Barcelo and Munoz, 2000). Two differentially targeted peroxidases from *C. roseus*, *CrPrx* and *CrPrx1* were ectopically expressed in *Nicotiana tabacum*. T1 generation of these transgenics were utilized for their behavior on stress media. The two peroxidase gene *CrPrx* and *CrPrx1* were introduced in tobacco under the control of the CaMV 35S promoter independently. Leaf disk method was used for transformation of *Nicotiana tabacum*. For many species, leaves provide a source of genetically uniform cells that have the capacity to regenerate whole plants when simple manipulation of the tissue culture is performed. The wounded edge of a leaf disk is susceptible to infection with *Agrobacterium* and on an appropriate culture medium, is also a site of rapid cell division and induction of shoot regeneration. This results in effective targeting of transformation and regeneration to the same set of cells at the edge of the disk. The phenotype with kanamycin resistance provides an effective means to select regeneration of transformed shoots or growth of transformed calli. By means of the leaf disk transformation system, transformed shoots could be obtained in 2 to 4 weeks and rooted plants in 4 to 7 weeks after leaf inoculation.

Transgenic from both type of peroxidase genes were expressed in higher amount (Fig. 4.3.5A-B). Although the total peroxidase activity in transgenic plant is the sum of activities between endogenous peroxidases and the product of the transgene, it seems that transgenic had higher peroxidase activity than wild type plants but it was difficult to correlate the total peroxidase with the inserted transgene copy number. The possible explanation could be position effect of insertion of the transgene at different sites in genome. Although there was no significant increase in growth of the transgenic tobacco harboring *CrPrx* and *CrPrx1* observed but a few transgenic lines showed higher growth rate than control plants. The reasons for cell elongation could be oxidation of Indole-3-acetic acid resulting in degradation of auxin (Hinnman et al., 1965). Lagrimini, (1993), reported that a purified tobacco anionic

peroxidase (TAP) catalyzes the oxidative decarboxylation of indoleacetic acid (IAA) *in vitro*, and transgenic tobacco overexpressing TAP showed less root growth compared to control plants (Lagrimini, 1993). Though from present study it is not clear whether the product of *CrPrx* and *CrPrx1* are involved in auxin catabolism. A possible mechanism for growth stimulation by over production of *CrPrx*, may be due to biosynthesis of lignin in cell wall, or decrease in stress due to over production of hydrogen peroxide. Another vacuolar peroxidase for which overexpression had shown to increase the growth rate and oxidative stress resistance in hybrid aspen was *prxC1a* from horseradish (*Armoracia rusticana*) (Kawaoka et al., 2003). It was shown that lignin content in stem was unaffected by overexpression of *prxC1a* gene (Kawaoka et al., 2003). Similarly enhanced growth rate of *CrPrx1* overexpressed lines was proposed to be related with phenomena other than lignin deposition. Although overexpression of both peroxidases did not had any effect towards activity of ascorbate but the protection of chloroplast from oxidative bleaching observed. The cytosolic ascorbate peroxidase activity of spinach (*Spinacia oleracea*) increases dramatically in response to oxidative stress (Yoshimura et al., 2000). Class I ascorbate peroxidase is ubiquitous in higher plants, and its major physiological function is the scavenging of H₂O₂ in chloroplast (Welinder, 1992). It has been pointed that water-water cycle, scavenges active oxygen ions in chloroplast (Asada, 2000). The possible mechanism of protection of chlorophyll from damage might be other than the change in ratio of ascorbate to dehydroascorbate in the apoplast.

In vivo chlorophyll fluorescence induction provides rapid, non-invasive methods for following changes in the photosynthetic apparatus before any visible symptoms can be observed (Janda et al., 1994; Pinhero et al., 1999; Bonfig et al., 2006; Berger et al., 2007). A decrease in Fv/Fm ratio indicates the lower photochemical efficiency of PSII, the part of the photosynthetic electron transport chain. Almost no significant difference was observed in the quantum efficiency of the peroxidase overexpressed lines. The effective quantum yields of the transgenic lines were almost similar to wild type (WT). Chlorosis is one of the most obvious symptoms of the senescent leaves which results in damaging of photosynthesis machinery and decrease in effective quantum yield. The overexpression of two peroxidases did not show any apparent effect on the photosynthetic efficiency of the transgenic plants.

Even though there were no clear cut differences observed with the overexpression of two differentially localized peroxidases in growth pattern of transgenic tobacco, vacuolar peroxidase overexpression greatly enhanced germination capacity under high osmotic conditions. Therefore, despite the ability of peroxidases to oxidize a variety of substrates *in vitro*, overexpression in plants lead to changes that are specific to one compartment. Salt tolerance in plants is a complex trait involving multiple physiological and biochemical mechanisms and numerous genes. Excess salts in the soil solution interfere with mineral nutrition and water uptake, and lead to undue accumulation of toxic ions. Plant growth under salt stress depends, among other concomitant processes, on the establishment of proper cellular ion homeostasis. Low cytosolic Na⁺ content is preserved by the concerted interplay of regulated ion uptake, vacuolar compartmentation and active extrusion to the extracellular milieu (Blumwald et al., 2000). Movements of ions in to the vacuole might occur directly from the apoplast into the vacuole through membrane vesiculation or a cytological process that juxtaposes the plasma membrane to the tonoplast. Then compartmentalization could be achieved with minimal or no exposure of the cytosol to toxic ions (Hasegawa et al., 2000).

During salt stress in plant cells there is a decrease in K⁺ uptake and increase in Na⁺ influx. As Na⁺ is toxic and K⁺ is the major solute contributing to osmotic pressure and ion strength there must be regulation at the tonoplast and plasma membrane to maintain homeostasis (Serrano and Rodriguez-Navarro, 2001). In plants, three mechanisms function cooperatively to prevent the accumulation of Na⁺ in the cytoplasm: restriction of Na⁺ influx; compartmentalization of Na⁺ into vacuoles; and an active Na⁺ efflux (Niu et al., 1995). Recent progress in molecular genetic studies of *Arabidopsis* revealed key Na⁺ transporting proteins that contribute to salt tolerance of plants. Several reports of higher peroxidase activity are reported with NaCl stress and mannitol stress in plants. Radić et al. (2006) had found that there is increased in soluble peroxidase activity of *Centaurea ragusina* when treated with different concentration of NaCl and mannitol stress. The overall mechanism by which overexpression of vacuolar peroxidase helps the seedlings to germinate in NaCl and mannitol stress is still not clear. It could be proposed here that the vacuolar peroxidase doesn't have any effect on modification of cell wall rather it helps in sequestration of the salts in vacuole which might help the germination of transgenic seeds. The transgenic approach had opened new path of research in salt and dehydration stress

where vacuolar peroxidase play important roles. However further investigation is needed to elucidate the role of interaction between vacuolar peroxidase and transporters.

4.3.4 Conclusion

CrPrx and *CrPrx1* functions with respect to stress tolerance *in planta* were addressed in transgenic tobacco plants that overexpressed the genes under CaMV 35S promoter. Total three transgenics lines (A4, A7 and A18) for *CrPrx1* and four for *CrPrx* (CRP1, CRP 2, CRP 5 and CRP 10) were obtained. All the lines were found to have multiple copies of the transgene and showed enhanced accumulation of transcripts. No significant difference was observed in the growth rate of T0 transgenic lines up to 7th week, however, except A7 all the lines showed higher growth rate than that of control on 8th week. Among all, the A7 line showed the highest peroxidase activity, chlorophyll retention with oxidative stress and photosynthetic quantum yield than that of CRP and control lines. Transgenic lines of T1 generation when evaluated for stress tolerance including salt, dehydration and cold stresses. A7 and A18 lines were found to be more tolerant in all the above stress conditions than that of CRP and control lines. Overall the transgenic lines with vacuolar peroxidase (*CrPrx1*) were more stress tolerant than that of the transgenic lines with cell wall peroxidase, (*CrPrx*). The result thus suggested the possible involvement of vacuolar peroxidase (*CrPrx1*) in conferring tolerance against stress conditions.

4.4: Over expression and down regulation of two differentially localized peroxidase CrPrx and CrPrx1 genes in Catharanthus roseus leaf induced calli lines

4.4.1 Introduction

Over 40 years ago, White and Brown (1942) and Gautheret (1946) initiated plant cell culture as a method of experimental morphology. The early objective of plant cell culture was to demonstrate theoretically indefinite longevity of meristems. Since then, the cell culture method has permitted substantial advances in understanding growth and differentiation of plants. Apart from basic studies, the cell culture technique has also been utilized for the production of various metabolites through callus culture in different plants.

It is well established that cultured plant cells behave differently from microorganisms (Yeoman and Yeoman, 1996). Since plants are multicellular, highly-differentiated structures, it might be expected that isolated plant cells might not produce the secondary metabolites normally associated with the differentiated structures in plant. Although for a number of compounds low or no production was observed in cell cultures, extensive screening programs of some plants resulted in high producing cell cultures as reported by Tabata et al. (1974) in *Lithospermum erythrorhizon* for the naphthoquinone production and by Sato and Yamada (1984) in *Coptis japonica* for antibacterial alkaloid berberine.

Recent progress in plant molecular biology has promised for the enhanced production of pharmaceutically valuable alkaloids through metabolic engineering of plant cell and tissue cultures. Metabolic engineering seeks to modify the amounts or chemical structures of specific metabolites, for example changes in the activities of biosynthetic enzymes or regulatory protein responsible for the co-ordinate expression of pathway genes, or induction of novel enzyme activities. Kutchan (1995) reviewed the cloning of alkaloid pathway genes and their expression by sense and antisense techniques. However, rational genetic manipulation of an alkaloid-producing pathway requires determination of points in the pathway at which flux is most severely restricted. Understanding of pathway biochemistry and its regulation is necessary in order to identify the tightly regulated points. Cell cultures of *C. roseus* have long been considered to be an alternative source of medicinally important indole alkaloids (Verpoorte et al., 1993). The early availability of clones for STR and TDC led to a few metabolic engineering studies. Constitutive expression of STR in cell cultures showed a surprising positive correlation to alkaloid levels (Canel et al., 1998), but

TDC expression resulted in elevated tryptamine levels only in transgenic cell culture (Canel et al., 1998) and crown gall calluses (Goddijn et al., 1995). Although elevated levels of TDC did not result in improved MIA accumulation, an antisense clone showed that MIAs were absent when TDC activity was ablated (Goddijn et al., 1995). The success of antisense expression demonstrates a tool to eliminate competing pathways. TDC has, however, proved useful in other systems like canola as a means of diverting flux to metabolic sink to reduce undesired products (Chavadej et al., 1994). It has been used to manipulate the alkaloid contents of *Cinchona officinalis* (Geerlings et al., 1999) and *Peganum harmala* (Berlin et al., 1993).

In *C. roseus*, methyl jasmonate is known to be a strong elicitor of MIA production, and a jasmonate responsive regulator ORCA3 was cloned (van der Fits and Memelink, 2000). Constitutive expression of the isolated regulator, ORCA3 resulted in induction of a number of genes including DXS, AS, TDC, STR and D4H. Unfortunately, a few genes including G10H, which is necessary for secologanin synthesis, showed no induction. Although the cell line studied did not synthesize MIAs due to the terpenoid deficiency, loganin feeding resulted in a threefold improvement in MIAs over control cultures. Since there are multiple controlled steps and engineering of more than a few steps in long pathways is currently beyond the capabilities, transcriptional activators may provide one of the most powerful tools to modulate long and complicated pathways. On contrary, activators could elicit the expression of other pathways that are detrimental to cell growth and therefore to overall alkaloid yields.

It is well known fact that terminal step is one of the most crucial part in secondary metabolic pathway (Verpoorte and Memelink, 2002). Peroxidases are known to be involved in the execution of terminal step of the Monoterpenoid Indole Alkaloid pathway (MIA) (Fig. 4.4.1). AVLB synthase, reported to be involved in dimerization of vindoline and catharanthine to form vincristine and vinblastine was later on characterized as peroxidase (Costa et al., 2008). A root specific vacuolar peroxidase was speculated to be involved in the oxidation of ajmalicine to serpentine (Misra et al., 2006).

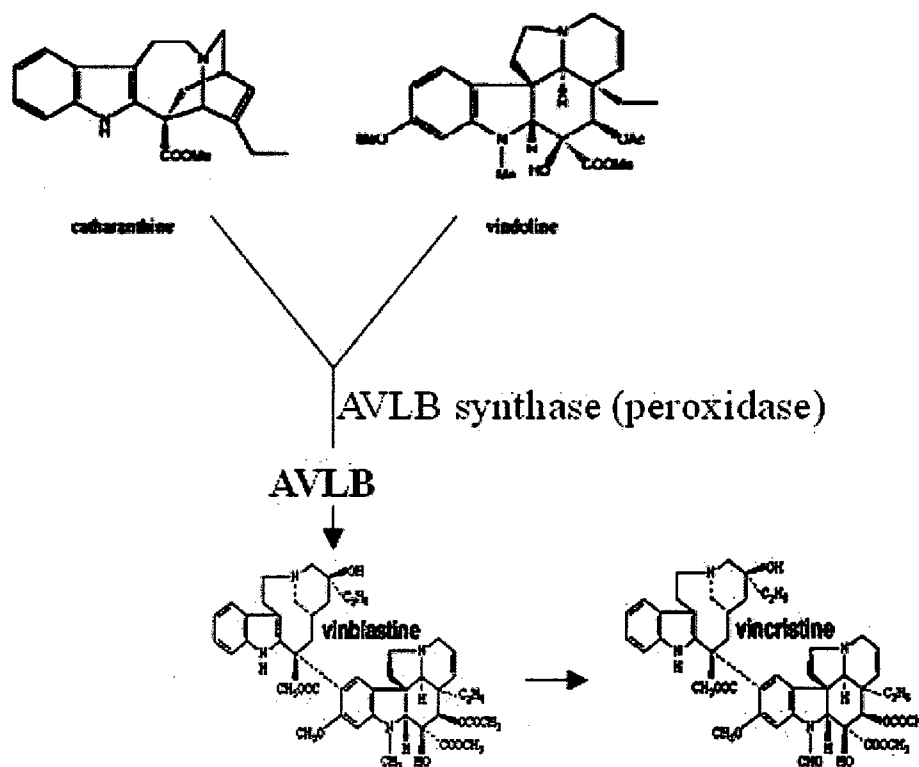


Fig. 4.4.1: Final steps of MIA biosynthetic pathway for the synthesis of dimeric alkaloids viz, VLB and VCR, the catalysis was performed by AVLB synthase, a peroxidase enzyme.

Two peroxidase genes had been characterized to date from *C. roseus*, *CrPrx* (accession number AY924306) and *CrPrx1* (accession number AM236087), the previous one is destined to be apoplastic in nature while later targeted to vacuole. Cloning and characterization of *CrPrx* is a part of the present dissertation (Kumar et al., 2007) while *CrPrx1* was recently reported by Costa et al. (2008). *CrPrx1* characterized to acts as anhydrovinblastine synthase and performed function on dimerization of catharanthine and vindoline to α -3', 4' anhydrovinblastine. The temporal expression studies show that *CrPrx1* does not express in root while expression of *CrPrx* was ubiquitous with exception of young leaves. Methyl jasmonate (MJ) was found to induce *CrPrx*, which correlates it with other MIA pathway genes (Kumar et al., 2007). However no conclusive evidence was made for involvement of *CrPrx* in MIA pathway.

We report in this chapter an attempt to study the effect of sense and antisense expression of apoplastic, *CrPrx* as well as vacuolar targeted *CrPrx1* peroxidase on the important MIA alkaloid content in *C. roseus* callus culture. The leaf explants were

infected with recombinant *Agrobacterium* to produce button shaped compact callus. These transgenic calli lines were further utilized for biochemical and molecular characterization.

4.4.2 Results

4.4.2.1 Overexpression and Suppression of *CrPrx* and *CrPrx1*

4.4.2.1.1 Construction of Chimeric *CrPrx* and *CrPrx1* sense gene in pBI121 vector

The full length of *C. roseus* peroxidase *CrPrx* was amplified using PBIPF-1 -PBIPR-1 primer pair from cDNA template and cloned in pGEMT-Easy vector which later on digested with *Sma*I and *Xba*I. The digested product was purified and subcloned between CaMV 35S promoter and nos terminator in the pre-linearized pBI121 vector to have pBI121-*CrPrx* construct (Fig. 4.4.2.iA).

Similarly, *CrPrx1* was PCR amplified using cDNA as template with CPNRF and CPNRR primer pair having *Sma*I and *Xba*I overhangs. The *Sma*I and *Xba*I digested fragment was ligated to the prelinearized pBI121 vector between CaMV 35S promoter and NOS terminator to have pBI121-*CrPrx1* construct (Fig. 4.4.2.iB).

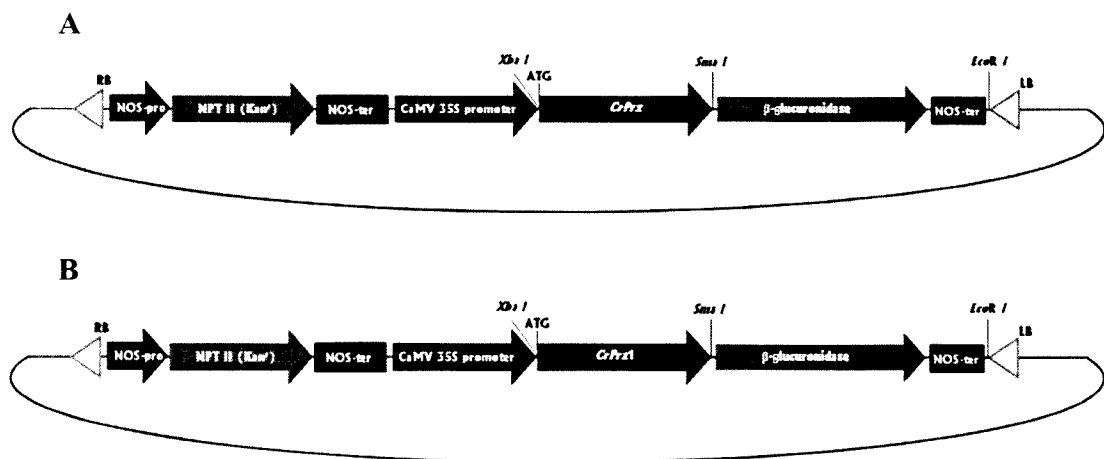


Fig. 4.4.2.i: Structure of chimeric genes. Sense gene construction under 35S CaMV promoter A) 1.2 kb *CrPrx*, B) 1.185 kb *CrPrx1*.

4.4.2.1.2 Antisense T-DNA construction

A 647 bp from 5' end of *CrPrx* gene was isolated after digesting with *Sma*I and *Bam*H I (*Sma*I site was introduced using overhang primer (CRPBIASF1) and was

inserted between the Cauliflower mosaic virus 35S promoter and NOS terminator. Its orientation was inverted with respect to the promoter to direct the synthesis of antisense RNA (Fig. 4.4.2.iiA). This chimeric antisense peroxidase gene was introduced into the binary vector pBI121. Similarly the antisense of *CrPrx1* was constructed in the pBI121 using the antisense primers as CPNAF and CPNAR. The amplified fragment which was 1185 bp long was inserted in pBI121 under 35S CaMV promoter in reverse orientation to have the antisense of the peroxidase gene (Fig. 4.4.2.iiB).

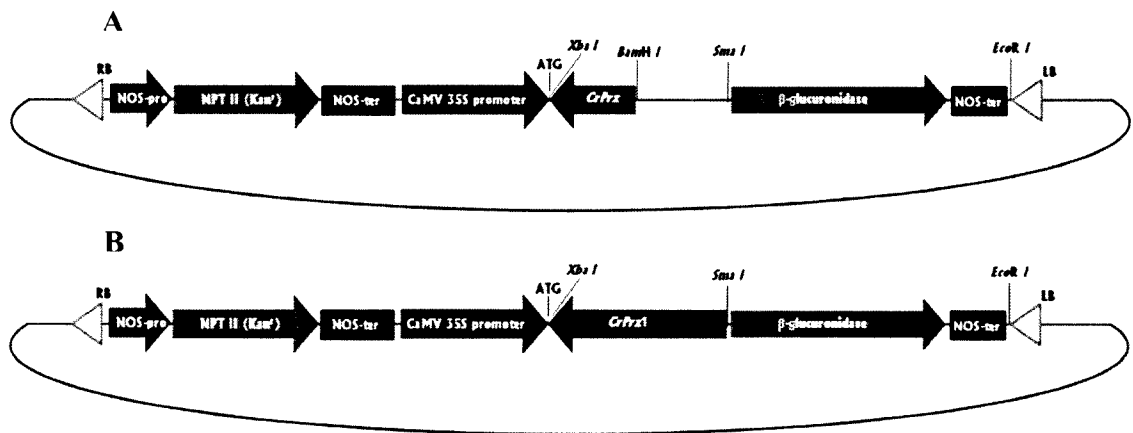


Fig. 4.4.2.ii: Structure of chimeric antisense genes. Antisense vector construction, A) 647 bp fragment of *CrPrx* gene and B) 1.185 kb of *CrPrx1* gene was inserted in reverse orientation under control of CaMV 35S promoter. See text for details.

The resulting chimeric genes of both sense and antisense was introduced into the *Agrobacterium tumefaciens* LBA4404 using modified freeze thaw method of DNA transformation to competent cells (Chen et al., 1994). Colony PCR was used to detect the presence of plasmid. PCR amplification performed with kanamycin gene specific primer KanF-KanR showed the expected size of 800 bp (Fig. 4.4.3 lane 1 to 5). In order to know whether the vectors after transformation contain the desired inserts, colony PCR was performed with vector specific primer (PBI121SF-PBI121SR). As seen in figure 4.4.4 lane 7, 9 and 10 the expected and observed size for sense of *CrPrx* and sense-antisense of *CrPrx1* was more than 1 kb while antisense of *CrPrx* in lane 8 was less than 1 kb.

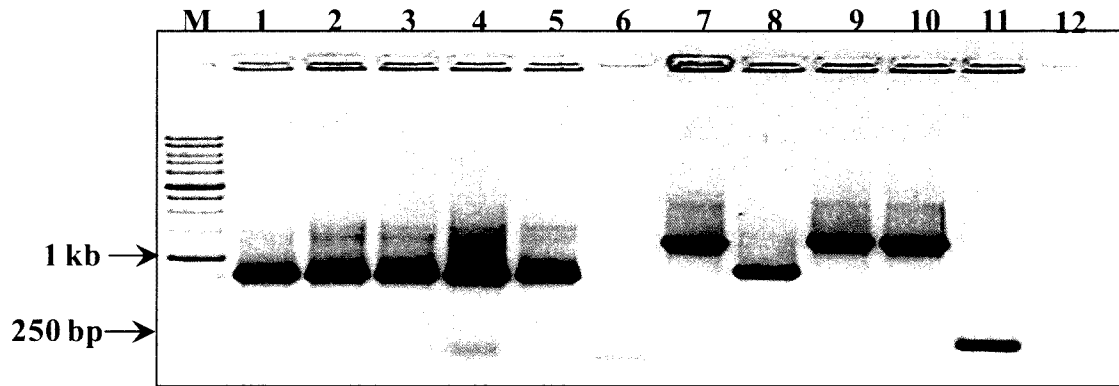


Fig. 4.4.3: Colony PCR of LBA4404 transformed with the recombinant pBI121 plasmid DNA. M 250 bp ladder, lane 1-6 PCR amplification was performed using KanF-KanR primer pair while lane 7-12 PCR amplification was performed using vector specific pBI121SF-pBI121SR primer pair. 1 and 7 sense of pBI121-*CrPrx*; 2 and 8 antisense of pBI121-*CrPrx*; 3 and 9 sense of pBI121-*CrPrx1*, 4 and 10 antisense of pBI121-*CrPrx1*; 5 and 10 pBI121 empty vector; 6 and 12 negative control as water.

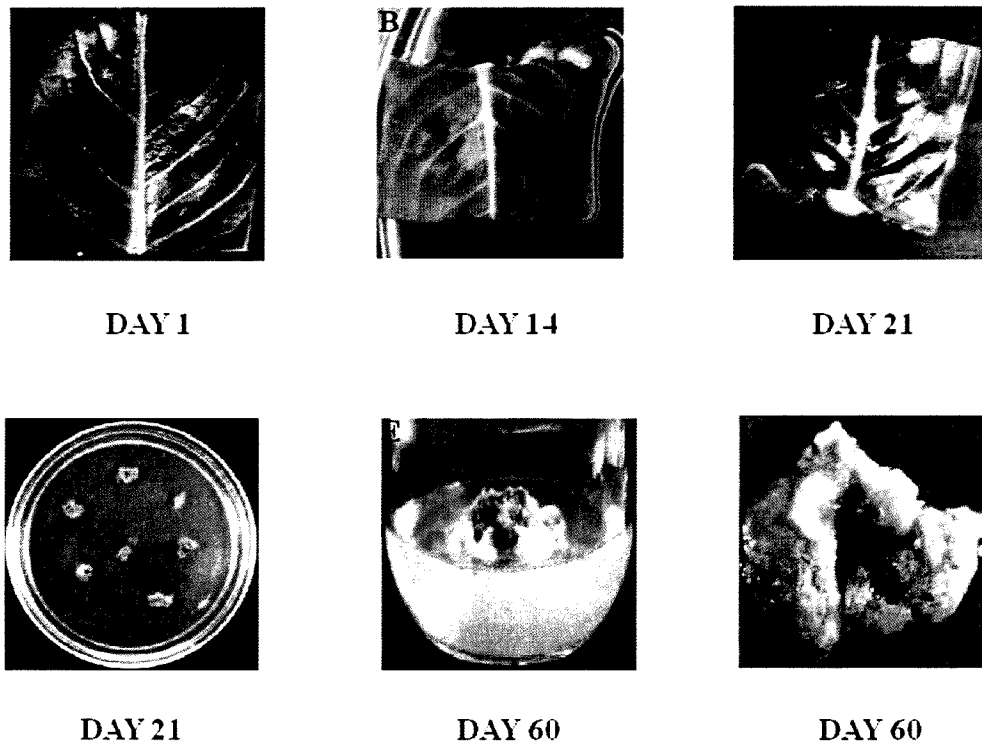


Fig. 4.4.4: Stages of transgenic calli at different time intervals and development of button shaped calli from *C. roseus* leaf explants. Leaf explant kept on callusing medium after A) One day, B) 14 days, C) 21 days, D) and E) leaf callus separated and transferred to new callusing medium. F) Callus as seen under 4X stereosome microscope.

4.4.2.2 Transformation of *C. roseus* leaf disk and generation of leaf calli

Leaves from two months old *in vitro* grown seedlings were used for the infection with recombinant *Agrobacterium* containing different constructs (Fig. 4.4.2A-B and Fig. 4.4.2.iiA-B). Mature leaves were cut into 0.5-1cm square and put on callus inducing medium (Fig. 4.4.4A). After 14 days, the button shaped calli were visible which became prominent after 21 days (Fig. 4.4.4B-C). These prominent calli were excised from parent explants and were separately cultivated in callusing media (TSM) containing kanamycin (300 mg/l) (Fig. 4.4.4D-E). The calli lines were later on sub cultured after every 21 days on TSM media containing kanamycin for transgenics and without antibiotics for untransformed plants (Fig. 4.4.4F).

4.4.2.3 Screening of transgenic *C. roseus* leaf calli

PCR based strategy was used to screen the presence of transgene among kanamycin resistant *C. roseus* leaf calli. The transgene status of calli was checked using both kanamycin gene specific primers KanF and KanR as well as pBI121 vector backbone specific primers (PBI121SF and PBI121SR). Kanamycin gene specific primer leads to amplicon size of 800 bp while vector bone specific primers gave rise to varied size of insert depending on sense or antisense construct. The transgenic lines transformed with sense construct of *CrPrx*, *CrPrx1* and antisense construct of *CrPrx1* leads to amplicon size of more than 1 kb with PBI121SF and PBI121SR. Calli lines transformed with antisense construct of *CrPrx* leads to amplicon size of less than 1.0 kb. The control calli were unable to give any amplified product with above primers (Fig. 4.4.5A-D).

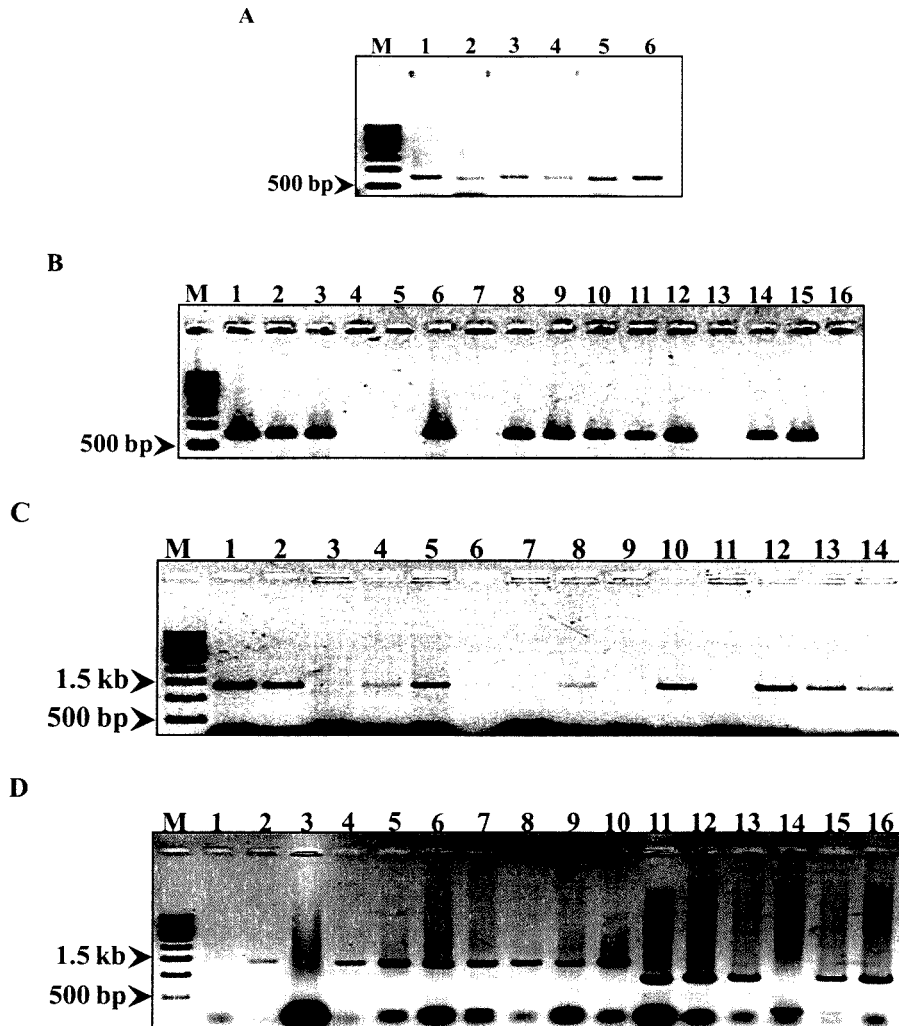


Fig. 4.4.5: Screening of kanamycin resistant calli for the presence of transgene through PCR analysis. The calli were grown as button shaped from the infected portion of leaf explants using *A. tumefaciens* containing pBI121-sCrPrx, pBI121-aCrPrx, pBI121-sCrPrx1 and pBI121-aCrPrx1 ; A and B, PCR with KanF-KanR primers on genomic DNA as template; C and D, PCR with vector specific primers pBI121SF-pBI121SR using genomic DNA as template. A) 1 positive control template as pBI12 plasmid DNA, 2-6 calli lines transformed with pBI121-sCrPrx. B) 1 positive control as pBI121 plasmid DNA, 2-6 leaf calli transformed pBI121-aCrPrx, 7-11 leaf calli transformed with pBI121-sCrPrx1 and 12-16 leaf calli transformed with pBI121-aCrPrx1. C) 1 positive control using pBI121-sCrPrx plasmid DNA, 2-7 leaf calli transformed with pBI121-aCrPrx, 8 positive control with pBI121-aCrPrx1 plasmid DNA, 9 negative control pBI121 plasmid DNA only 10-14 leaf calli transformed with pBI121-aCrPrx1. D) 1 negative control pBI121 plasmid DNA, 2-10 transgenic leaf calli harboring pBI121-sCrPrx construct, 11 positive control with pBI121-aCrPrx, 12-16 transgenic leaf explant calli harboring pBI121-aCrPrx construct.

Transgenic calli which were transformed with sense of *CrPrx* and *CrPrx1* were symbolized as sCrPrx and sCrPrx1 respectively. While antisense of *CrPrx* and *CrPrx1* were symbolized as aCrPrx and aCrPrx1 respectively. The numbers of transgenic calli lines varied depending upon initial explants utilized. sCrPrx a sense

line of *CrPrx* showed the highest numbers of transgenic calli (21) for which (109) leaf explants were utilized (Table 4.4.1). Several button shaped calli emerged from a single leaf explant and was treated as separate event (Fig. 4.4.4C). Each calli was picked and transferred to a new plate for further analysis.

Table 4.4.1: Construct and number of transgenic calli lines.

Construct	Number of transgenic calli
sCrPrx1	6
aCrPrx	14
aCrPrx1	10
sCrPrx	21

Among all the calli, the percentage of transgenic calli formation was highest with sCrPrx construct of ~9%, while other construct have similar transformation efficiency of ~5% (Fig. 4.4.6). It has also been noted here that not all the kanamycin resistant calli carried the transgenes. As the number of transgenic calli varied in different construct, only a few transgenic calli lines were selected on the basis of their alkaloid content for further studies.

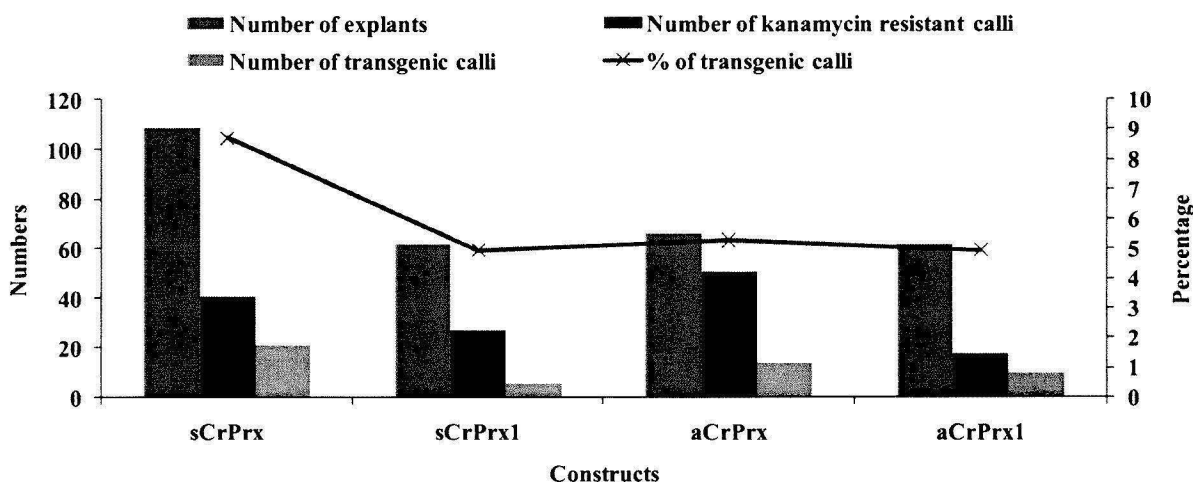


Fig. 4.4.6: Transformation efficiency of different transgenics Calli lines. The leaf explants were transfected with recombinant *Agrobacterium* LBA4404 harboring different plasmid construct.

4.4.2.4 Morphological features of the transgenic lines

The transgenic calli lines, irrespective of the construct show both brown as well as green callus (Fig. 4.4.7). Most of the calli lines were compact in nature with a few

exception of friable callus. Transgenic lines which showed higher amount of specific alkaloid were mostly brown in color.

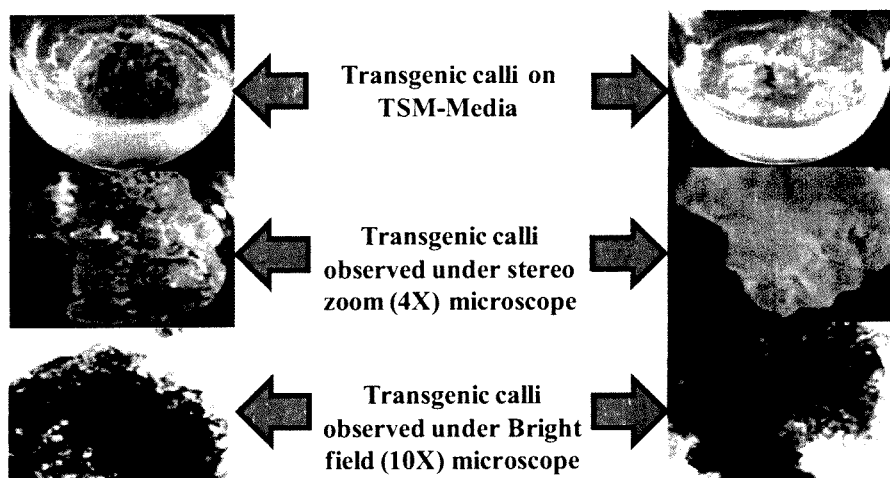


Fig. 4.4.7: Morphological features of the transgenic calli lines. The callus was observed after 60 days of leaf disk transformation.

The percentages of brown and green calli were almost equal irrespective of the type of transgene present (Fig. 4.4.8). Though there was slight variation observed in sCrPrx1 and aCrPrx1 calli lines. The antisense calli lines aCrPrx1 showed higher number of brown calli than green calli, whereas higher number of green calli were observed in case of sense line of *CrPrx*.

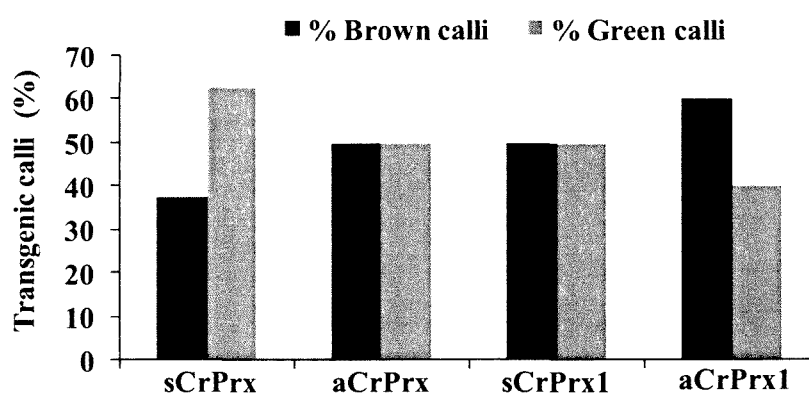


Fig. 4.4.8: Morphological features of transgenic calli lines. sCrPrx is sense *CrPrx*+pBI121; aCrPrx, antisense of *CrPrx*+pBI121; sCrPrx1, sense of *CrPrx1*+pBI121; aCrPrx1, antisense of *CrPrx1*+pBI121.

Further studies were performed using green calli lines.

4.4.2.5 Expression and down regulation of *CrPrx* and *CrPrx1* in *C. roseus* calli lines

Out of 35 transgenic calli lines (Table 4.4.1) with peroxidase genes (*CrPrx*) two sense and two antisense lines were selected on the basis of their growth habit for further analysis. Relative quantification using quantitative real time PCR was performed to check the expression level of *CrPrx* transcripts in transgenic calli lines. Four times accumulation of transcript was present in overexpressed calli lines (sCrPrx2 and sCrPrx5) compared to control line. The *CrPrx* transcript level was found to be completely abolished in antisense lines of *CrPrx* (aCrPrx36 and aCrPrx69) (Fig. 4.4.9).

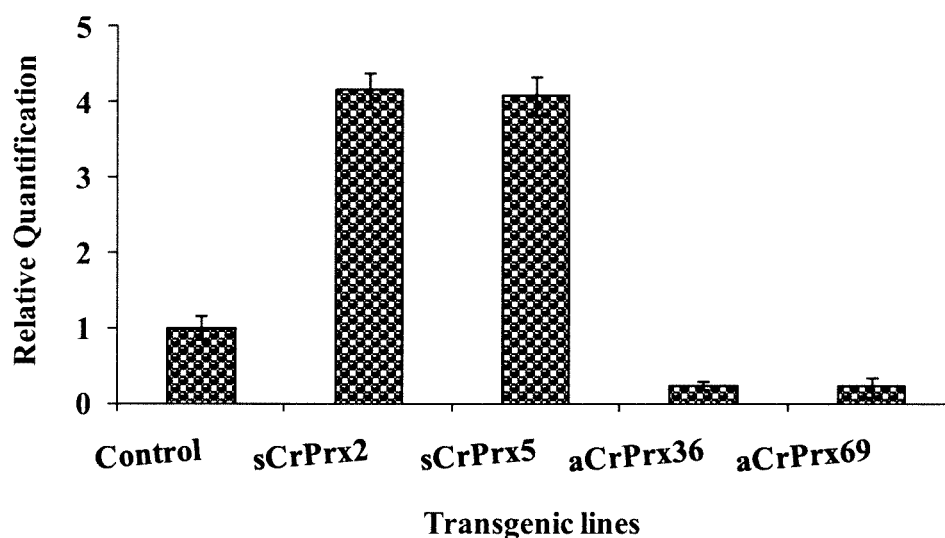


Fig. 4.4.9: Quantitative real time PCR analysis of *CrPrx* expression in transgenic calli lines. Five microgram of total RNA from each tissue sample was reverse-transcribed and subject to real-time PCR analysis. The relative expression value of each gene was normalized to an endogenous control *RPS9* and calculated using $\Delta\Delta CT$ method (Applied Biosystems). Values are the results of triplicate analysis of two biological replicates where standard deviation is less than 5%.

In case of transgenic lines with *CrPrx1* five potential lines of overexpressing sense and antisense of *CrPrx1* transcript were selected. The overexpressed calli lines (sCrPrx1-5 and sCrPrx1-14) showed 2.5 to 3.5 fold higher expression than the control lines. Among *CrPrx1* abolished lines (aCrPrx1-5, aCrPrx1-9 and aCrPrx1-8) the expression of *CrPrx1* was severely reduced (Fig. 4.4.10).

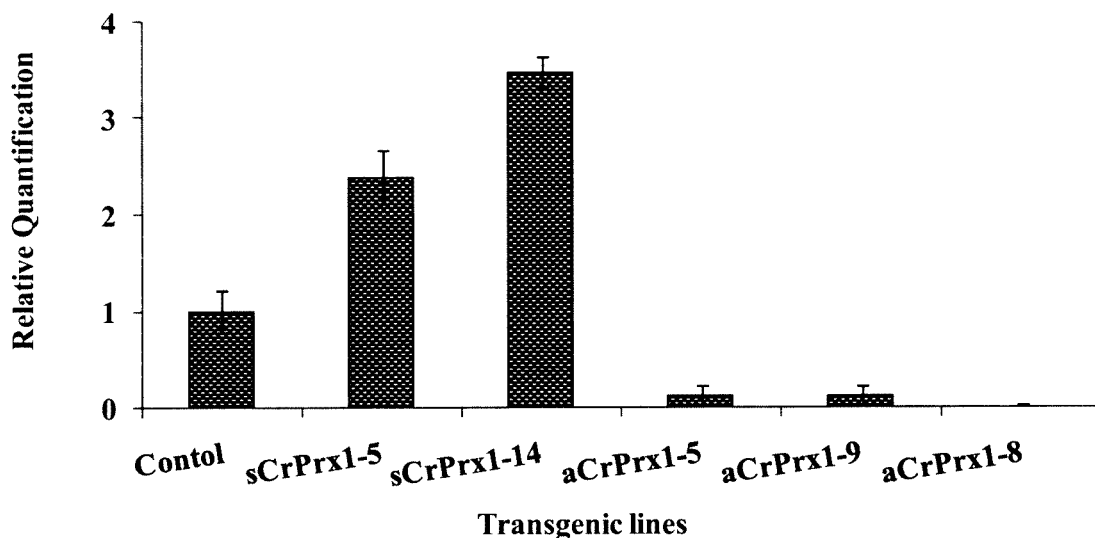


Fig. 4.4.10: Expression analysis of *CrPrx1* expression in transgenic calli lines. Quantitative Real time PCR was performed on cDNA prepared from five microgram of total RNA isolated from tissue sample of each transgenic calli lines. The relative expression value of each gene was normalized to an endogenous control *RPS9* and calculated using $\Delta\Delta CT$ method (Applied Biosystems). Values are the results of triplicate analysis of two biological replicates where standard deviation is less than 5%.

4.4.2.6 Study of growth index in selected transgenic calli lines

The transgenics which were showing altered expression of transgene were selected for growth index studies. The sense and antisense transgenic lines of *CrPrx* showed differential growth rate. Calli lines transformed with sense construct showed higher growth rate while antisense lines were slow in growth rate (Fig. 4.4.11A). The transgenic lines transformed with *CrPrx1* exhibited similar growth pattern for sense as well antisense calli lines (Fig. 4.4.11B). Untransformed calli lines were showing higher growth index than the sense and antisense transgenic calli lines with *CrPrx1*.

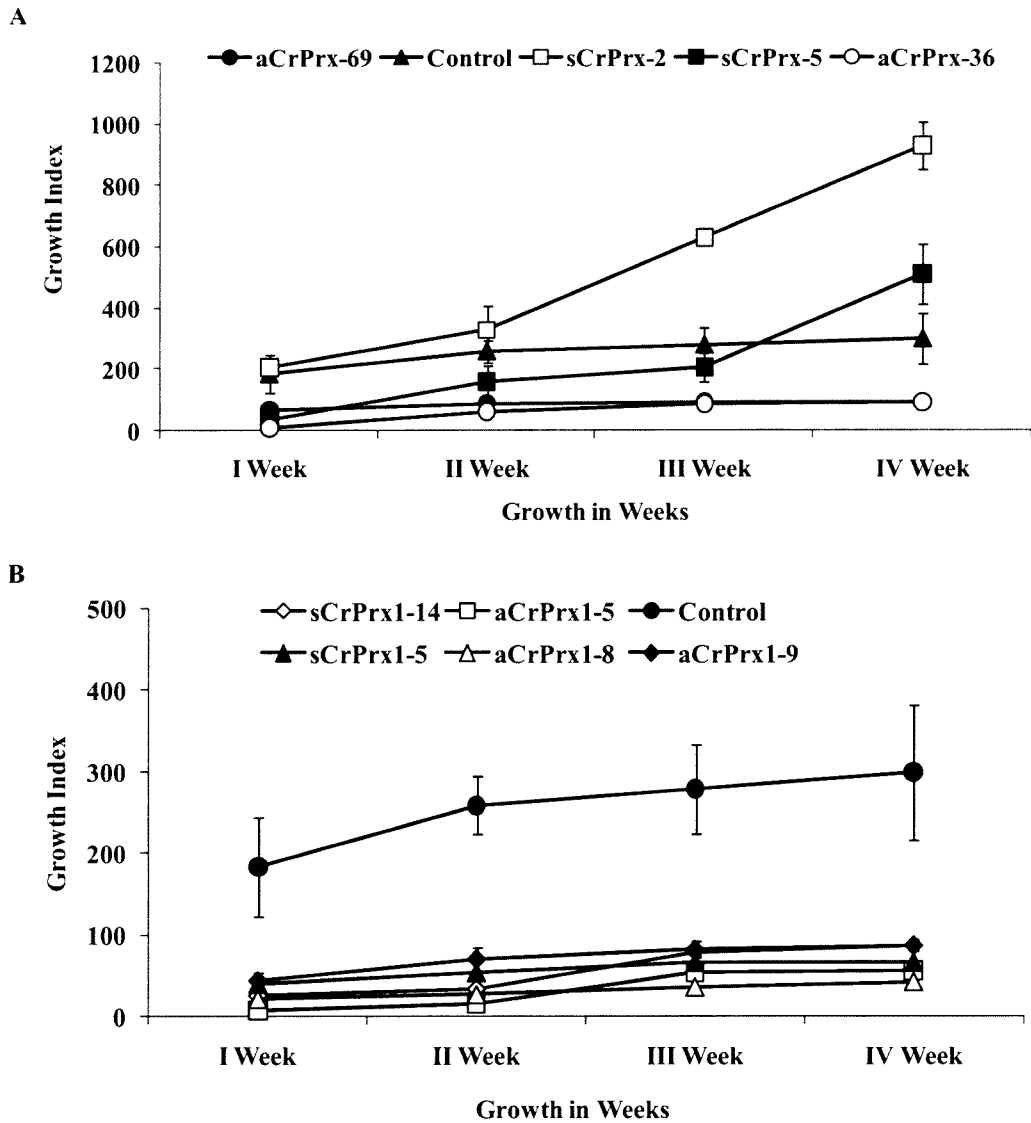


Fig. 4.4.11: Growth patterns of different transgenic calli lines. A) Transgenic calli lines with *CrPrx* gene sense lines are sCrPrx calli lines, aCrPrx are antisense calli lines. B) *CrPrx1* transgenic calli lines, sCrPrx1 as sense lines, aCrPrx1 as antisense lines.

4.4.2.7 Guaiacol peroxidase activity assays with transgenic calli

Transgenic calli lines after 9th subculture were used for estimation of total peroxidase activity. Relative peroxidase activity was measured using guaiacol as oxidizing substrate. The *CrPrx* overexpressed line (sCrPrx-5) showed 3 fold higher peroxidase activity than control and other overexpressed (sCrPrx-2) calli lines (Fig. 4.4.12). There was relatively lesser peroxidase activity present in both antisense lines (aCrPrx-36 and aCrPrx-69) but not completely abolished.

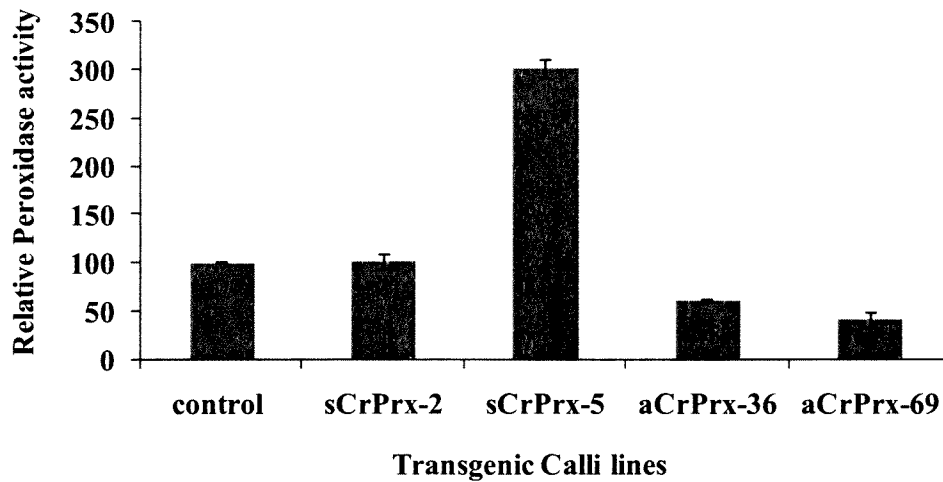


Fig. 4.4.12: Relative peroxidase activities of *CrPrx* transgenic calli lines. The guaiacol peroxidase activities of the soluble fractions extracted from sense and antisense expressed transgenic *CrPrx* calli lines were measured. The enzyme activities were relative to untransformed callus as Control (=100%, 0.244 Units). Each data point represents the average of three replicates.

Transgenic calli lines transformed with *CrPrx1* were also analyzed for the total peroxidase activity. Transgenic lines sCrPrx1-5 and sCrPrx1-14 with overexpressed *CrPrx1* showed 3 fold higher peroxidase activities than non-transgenic calli lines. Among antisense lines no change in total peroxidase activities was visible in aCrPrx1-5 and aCrPrx1-9 lines. A steep decrease in total peroxidase activity was found in aCrPrx1-8 antisense line (Fig. 4.4.13).

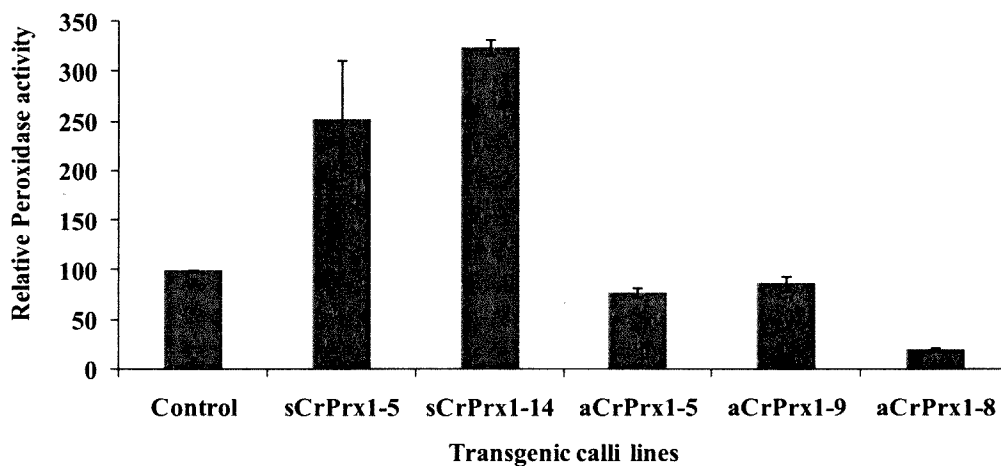


Fig. 4.4.13: Guaiacol peroxidase activity with transgenic calli lines transformed with sense and antisense of *CrPrx1* gene. The enzyme activities were relative to untransformed callus as control (=100%, 0.312 Units). Each data point presents average of three replicates.

4.4.2.8 Estimation of total alkaloid and targeted MIAs in transgenic calli

Leaf induced calli lines overexpressing sense and antisense of *CrPrx* and *CrPrx1* gene were further evaluated for accumulation of MIAs (Fig. 4.4.14A-D). Total alkaloid was extracted and quantitative analysis of specific alkaloid was carried out with HPLC. Three different alkaloids vincristine, ajmalicine and serpentine were found to be accumulated in these transgenic calli lines. Increase in the amount of total alkaloids as well as specific alkaloids were observed in case of both *CrPrx* and *CrPrx1* transgenic lines, with a wide range of variations.

4.4.2.9 Alkaloid profiles in transgenic calli lines with *CrPrx* sense and antisense construct

Among transgenic calli lines overexpressing sense and antisense of *CrPrx* gene, it was found that antisense lines (aCrPrx-36 and aCrPrx-69) showed higher amount of total alkaloids (Fig. 4.4.14A) than the rest of lines. Among all the transgenic lines selected for analysis of both serpentine and vincristine the highest amount was found in sCrPrx-5 (a sense overexpressed) lines than control lines (Fig. 4.4.14B-C). The ajmalicine content of the sCrPrx-5 and aCrPrx-69 lines were lower than untransformed lines (Fig. 4.4.14D). Among antisense lines aCrPrx-69 shows equal or lesser amount of vincristine and serpentine than the control calli lines. It was found that the amount of vincristine and serpentine in high yielding, calli line (sCrPrx-5) was 0.369 mg/g and 0.063mg/g of dry weight respectively.

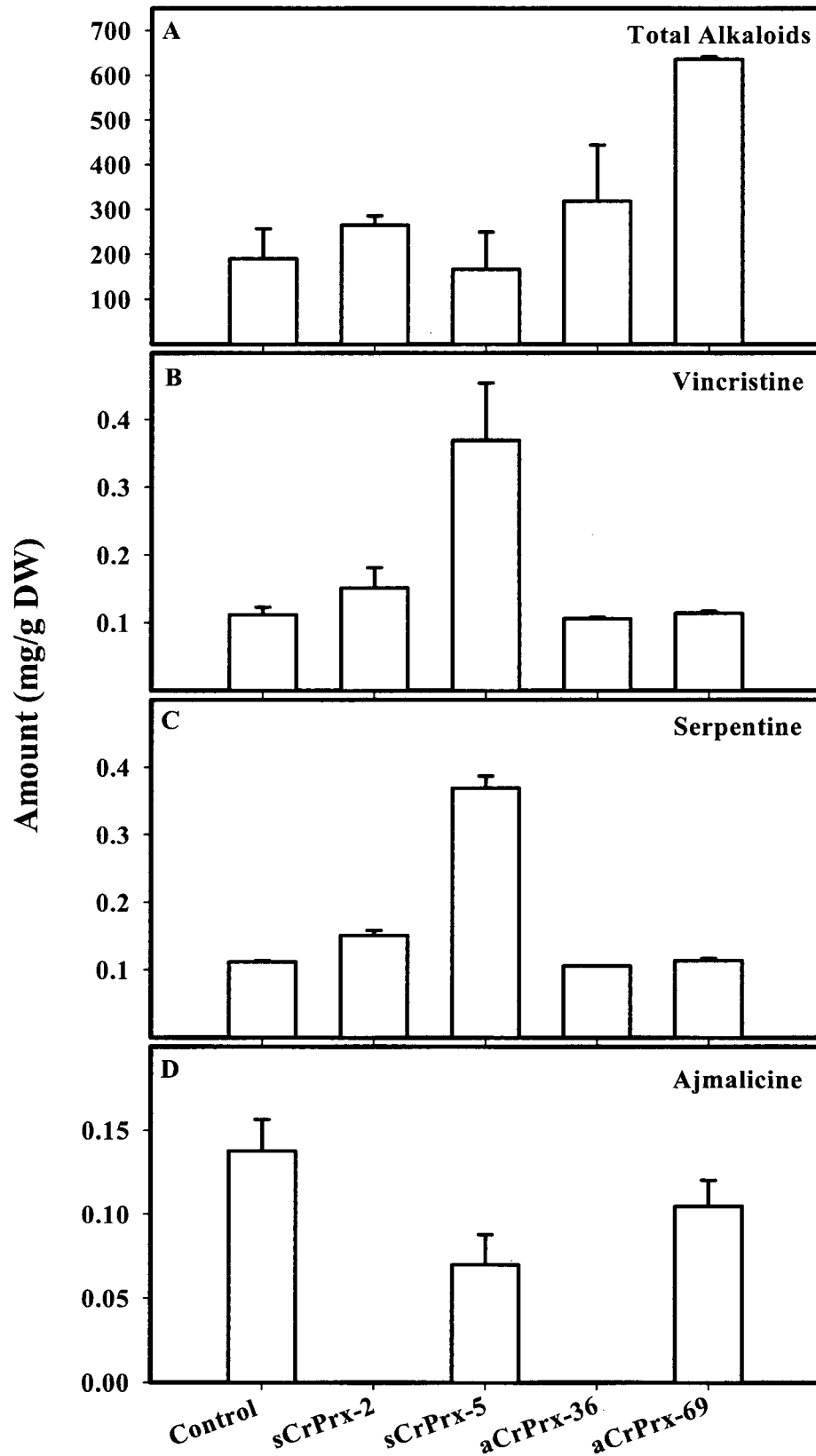


Fig. 4.4.14: Accumulation of MIAs in overexpressing sense (sCrPrx) and antisense (aCrPrx) *CrPrx* gene. A) Accumulation of total alkaloid, B) Vincristine C) Serpentine and D) Ajmalicine accumulation.

4.4.2.10 Alkaloid profiles in transgenic calli lines with *CrPrx1* sense and antisense construct

The transgenic calli lines which were transformed with sense and antisense construct of *CrPrx1* gene showed that the total alkaloid profile was higher among the sense transgenic calli lines (sCrPrx1). The antisense lines (aCrPrx1) showed lower amount of total alkaloid content, except aCrPrx1-5 where total alkaloid content was higher than the control lines. Total alkaloid content in sCrPrx1-14 lines was four times higher than the untransformed lines (Fig. 4.4.15A). In case of specific alkaloids the amount of vincristine varies among sense lines of *CrPrx1* and it was highest in the sCrPrx1-14 transgenic lines. Among antisense lines, amount of vincristine was either absent or present in trace amount, which was not detectable with HPLC (Fig. 4.4.15B). The amount of serpentine is much higher in sCrPrx1-14 than the rest of sense as well as control lines. Antisense lines of *CrPrx1* as aCrPrx1-5, aCrPrx1-9 and aCrPrx1-8 show lesser accumulation of serpentine amount (Fig. 4.4.15D). Oxidation of ajmalicine by vacuolar peroxidase leads to more production of serpentine, so higher the vacuolar peroxidase activity more is the amount of serpentine. Ironically the ajmalicine was found in higher amount in overexpressed sense *CrPrx1* (sCrPrx1-14), where the maximum oxidation takes place (Fig. 4.4.15C). The ajmalicine content in different calli lines were found to be more or less equal.

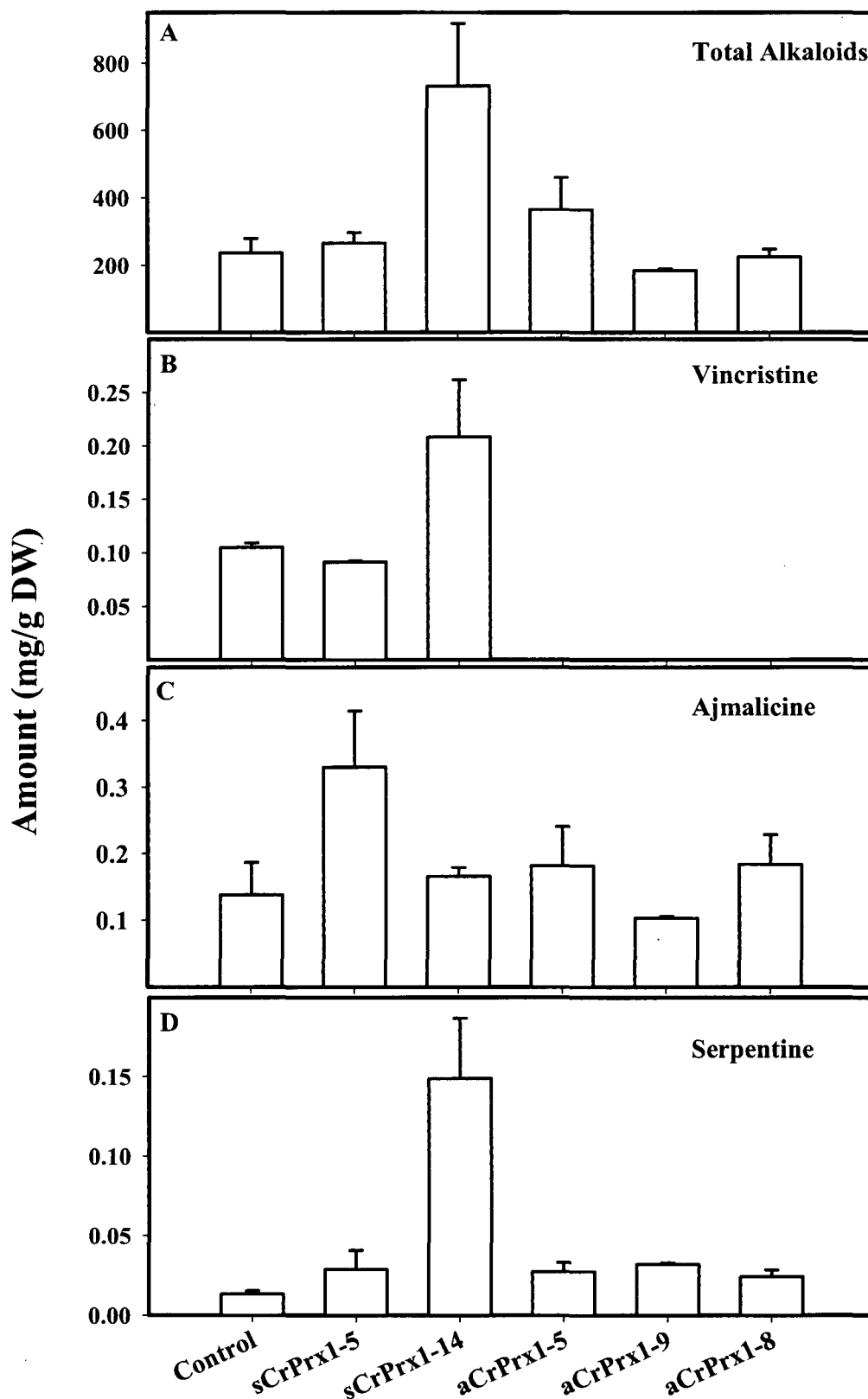


Fig. 4.4.15: Accumulation of MIAs in selected transgenic leaf calli overexpressing sense and antisense of *CrPrx1* gene. A) Total alkaloid profile, B) Amount of Vincristine C) Ajmalicine D) Serpentine content in the transgenics. The controls used were untransformed transgenic lines grown in same media.

4.4.2.11 Expression profile of MIA biosynthetic pathway genes in selected transgenics calli

To know the status of seven MIA pathway genes as well as the transgene expression in the manipulated sense and antisense calli lines of *CrPrx* and *CrPrx1*, relative quantification using real time PCR was performed. A multivariate analysis was performed with the $2^{-\Delta\Delta CT}$ value from real time PCR. Ribosomal protein subunit 9 RPS9 had been used as internal control to evaluate all the calli lines. The important pathway genes which were utilized for the quantitative study were as follows.

1. *TDC* gene produces tryptophan decarboxylase which converts primary metabolic products of pathway to secondary metabolic product.
2. *SGD* gene codes for, strictosidine β -glucosidase, an important MIA pathway gene
3. *G10H* (CYP76B6) codes for geraniol 10-hydroxylase. A possible bottle neck in the production of terpenoid moiety of MIA pathway because it was found as rate limiting step.
4. *STR* codes for strictosidine synthase enzyme which converse different metabolic pathway indole and secologanin and leads to formation of strictosidine.
5. *ORCA3* codes for a transcription factor ORCA3 which is an activator in MIA pathway and known to be a master regulator of many genes viz. *Tdc*, *Str*, *Sgd*, *Cpr*, and *D4h* (van der Fits and Memelink 2000). The expressions of these genes were found to be increased in ORCA3-tagged lines.
6. *ZCT1* codes for zinc finger like protein which is a transcription factor and act as a repressor in MIA pathway. The repressors are known to counter balance the effect of activator.
7. *GBF1* codes for a G-box binding factor which acts as repressor.

Based on $2^{-\Delta\Delta CT}$ value (Real time PCR data); a transcription matrix (genes versus transgenic calli lines) was constructed by hierarchical cluster analysis method for transgenic line *CrPrx1* (Fig. 4.4.16), which resulted in two clusters (A and B) with distinct pattern of expression of different genes. The cluster A is again subdivided in two subclusters A1 and A2. The subcluster A1 showed the grouping of two

independent overexpressed calli lines in which the expression of *CrPrx1* gene is more while *ORCA3* expression is less or slightly more than control lines. In another subcluster A2 which represents the antisense lines (aCrPrx1-8 and aCrPrx1-9) showed higher expression of *ORCA3*. Overall gene expression patterns of transgenics showed that GBF1 and SGD were down regulated in sCrPrx1-14 where as *ZCT1* and *ORCA3* were up regulated.

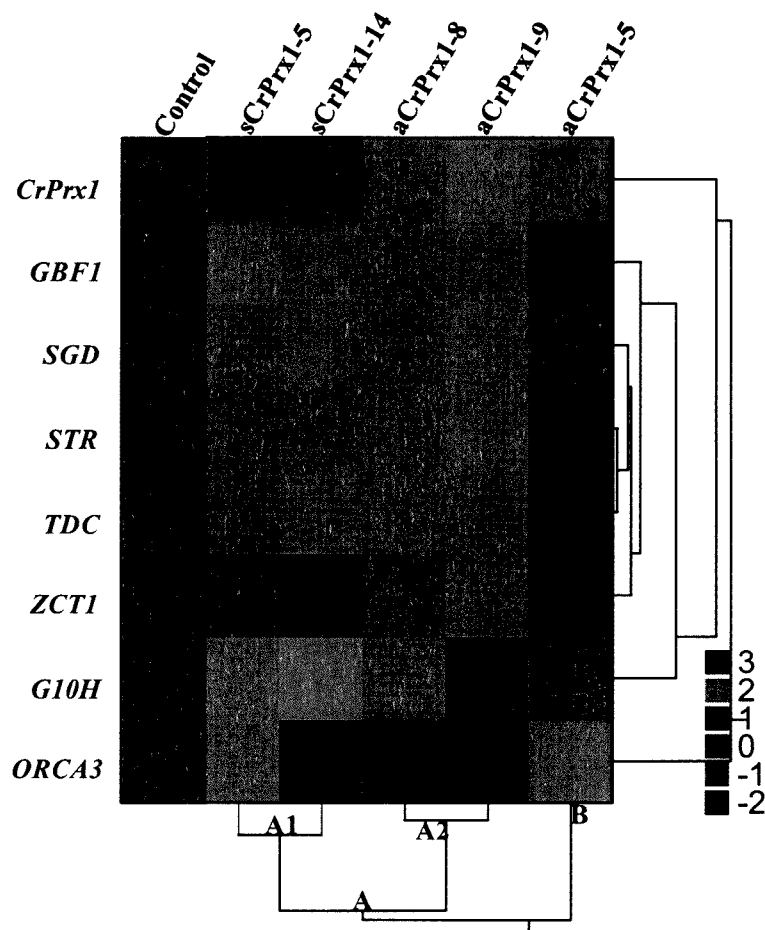


Fig. 4.4.16: Cluster diagram of important MIA biosynthetic pathway genes in *CrPrx1* transgenic calli lines. Grouping was performed using Hierarchical clustering, which are represented in four different colors. The intensities of the color increases with increasing differences in the expression profile of a particular gene as indicated on the side of each figure. Up regulated gene cluster are indicated in red or orange blocks. Down regulated gene clusters are indicated by blue blocks. The data was collected from relative expression value of each gene which was normalized to an endogenous control *RPS9* and calculated using $\Delta\Delta CT$ method (Applied Biosystems). Values are the results of triplicate analysis of two biological replicates with standard deviation less than 5%.

The expression profiles of seven genes that encode enzymes for MIA were monitored in *CrPrx1* transgenic calli by quantitative real time PCR analysis and compared with untransformed calli lines. Compared to control higher expression of

many genes were found in sense line of sCrPrx1-14 (Fig. 4.4.17). In antisense lines aCrPrx1-9 and aCrPrx1-8, expression of ORCA3 was highest compared to other MIA pathway genes (Fig. 4.4.17).

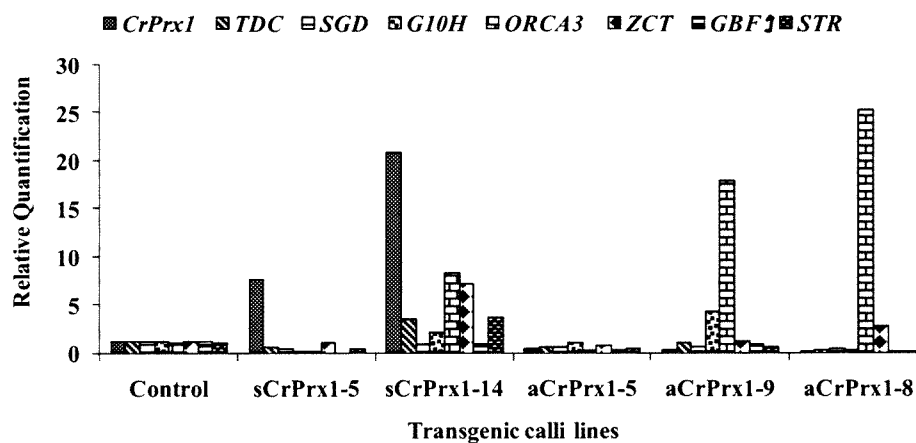


Fig. 4.4.17: Relative quantification of important MIA pathway genes in *CrPrx1* transgenic calli lines. cDNA was prepared from transgenic calli total RNA for interrogation by quantitative real time PCR. Unamplified cDNA was prepared directly from 5 µg of total RNA. The relative expression value of each gene was normalized to an endogenous control *RPS9* and calculated using $\Delta\Delta CT$ method (Applied Biosystems). Values are the results of triplicate analysis of two biological replicates where standard deviation is less than 5%.

Among the *CrPrx* transformed calli lines method a differential expression pattern of all MIA pathway genes were observed. Using hierarchical cluster analysis method it was found that most of the genes were down regulated in sCrPrx-2 (Fig. 4.4.18). *ORCA3* is a master regulator and transcriptional activator while *GBF1* is repressor of MIA pathway, both these genes were found to be down regulated in antisense line aCrPrx-36 as well as sense line sCrPrx-5 (Fig. 4.4.18). The overexpression of sense or antisense gene leads to down regulation of *G10H* expression which is considered to be the bottle neck of the pathway. sCrPrx-5, a sense overexpressed line of *CrPrx* which showed highest expression of transgene also shows the down regulation of all the repressors as well as activators (Fig. 4.4.18). Ironically in CrPrx-5 lines the bottle neck of the pathway (*G10H*) was up regulated. *STR* which converts indole and shikimate pathway in to a single pathway was found to be up regulated in antisense lines but down regulated in sense lines.

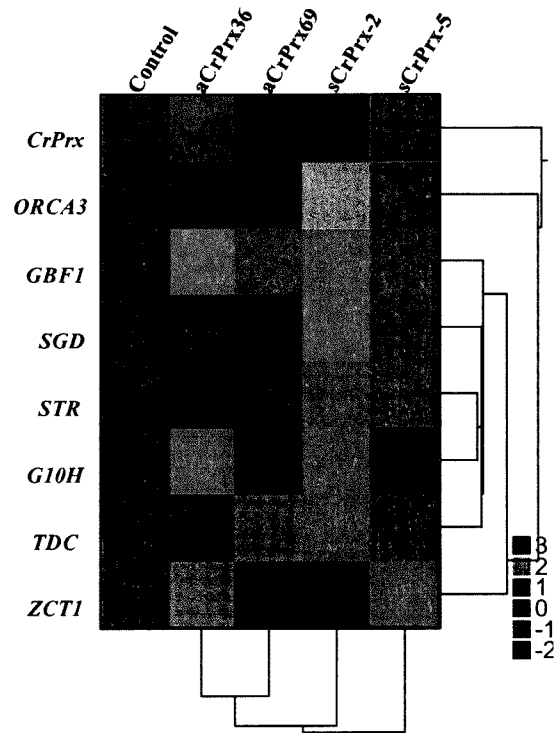


Fig. 4.4.18: Cluster diagram of important MIA biosynthetic pathway genes in *CrPrx* transgenic calli lines. Grouping was performed using Hierarchical clustering, which are represented in four different colors. The intensities of the color increases with increasing differences in the expression profile of a particular gene as indicated on the side of each figure. Up regulated gene cluster are indicated in red or orange blocks. Down regulated gene clusters are indicated by blue blocks. The data was collected from relative expression value of each gene which was normalized to an endogenous control *RPS9* and calculated using $\Delta\Delta CT$ method (Applied Biosystems). Values are the results of triplicate analysis of two biological replicates with standard deviation less than 5%.

The graphical representation of sense and antisense lines of *CrPrx1* showed the highest expression of *ORCA3* a master regulator and *ZCT1* a repressor of MIA pathway in sCrPrx-2 lines when measured by quantitative real time PCR (Fig. 4.4.19). In one of the antisense line aCrPrx-36 *ORCA3* expression was not observed. The expression of MIA pathway genes remains unchanged in aCrPrx-69 calli lines.

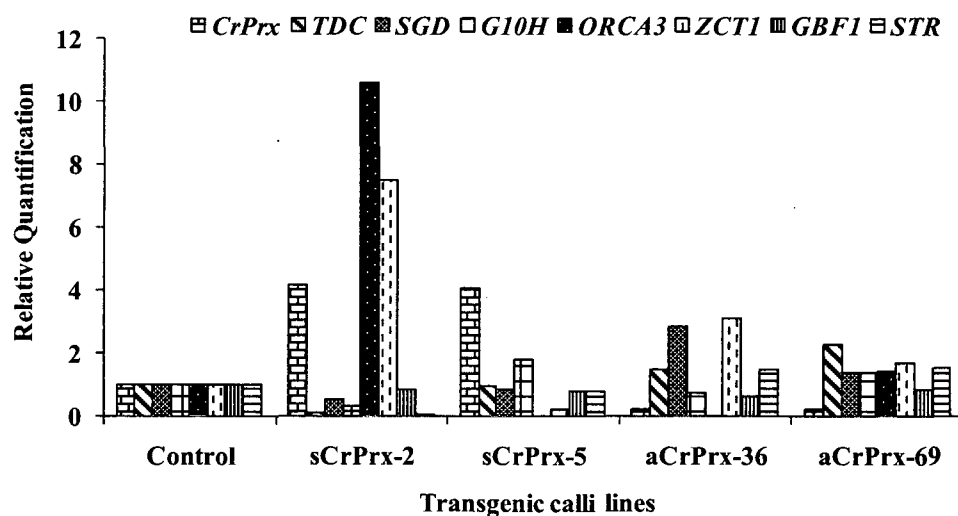


Fig. 4.4.19: Relative expression of important MIA pathway genes in the CrPrx transgenic calli. Quantitative real time PCR was performed with cDNA prepared using total RNA isolated from different leaf induced calli lines. The relative expression value of each gene was normalized to an endogenous control *RPS9* and calculated using $\Delta\Delta CT$ method (Applied Biosystems). Values are the results of triplicate analysis of two biological replicates where standard deviation is less than 5%.

4.4.3 Discussion

Metabolic engineering has proven to be a valuable tool for the production of many compounds in microorganisms, and it is hoped that it will provide similar progress in the engineering of plants for alkaloid production. For metabolic engineering it is a prerequisite to have functional protocols for gene transfer, including efficient tissue culture methods for regeneration. In *C. roseus* the regeneration of (transgenic) cells to plantlets has only been performed with low efficiency, due to this reason, only a few transgenic *C. roseus* plants have been produced. For *C. roseus* generally two transformation methods have been used: 1) initiation of cell cultures from leaf seedling transfected with agrobacterium (Canel et al., 1998) and 2) transformation of suspension cell culture by ternary transformation system (van der Fits et al., 2000).

In present chapter we reported the generation of *C. roseus* transgenic calli with overexpressed of sense and antisense construct of two different peroxidases namely *CrPrx* and *CrPrx1*. *CrPrx* is a novel peroxidase, cloned for the first time and is a part of present dissertation. *CrPrx* is found to be localized to cell wall (Kumar et al., 2007). *CrPrx1* is a vacuolar targeted peroxidase from *C. roseus* reported to function as AVL B synthase in the dimerization of catharanthine and vindoline to α -3', 4'-anhydrovinblastine (Costa et al., 2008). The calli lines which emerged from the leaf were single transgenic independent event and are used as separate lines. The growth

index of calli lines transformed with cell wall peroxidase was found to be higher than the control lines while transgenic with vacuolar peroxidase remained the same. Three possible explanations concerning with physiological roles of peroxidase can be speculated with higher growth index of transgenic calli lines transformed with sense *CrPrx*. First is auxin catabolism: peroxidase oxidizes IAA, resulting in the degradation of auxin (Hinnman and Lang, 1965). The ratio of auxin to cytokinin is thought to be important for plant growth and development (Romano et al., 2000). Cytokinin was observed to activate cell division through induction of CycD3 at the G1-S cell cycle phase transition (Riou-Khamlichi et al., 1999). Secondly, peroxidase is associated with the process of lignification during the last step of monolignol deposition (Whetten et al., 1998). To date, many studies have investigated the modification of lignin content or composition in transformed plants. Modified expression of the genes involved in lignin biosynthesis, such as Phe ammonia-lyase, coumaroyl CoA reductase, and caffeoyl-CoA O-methyl transferase, has been reported that severely reduced lignin content, resulting in abnormal phenotypes (Elkind et al., 1990; Piquemal et al., 1998; Zhong et al., 1998). Although the lignin content was not measured in calli lines but it may be the reason for higher growth rate of calli lines.

Plant cell growth imposes a unique set of constraints on cell division and elongation (Jacobs, 1997): Cell elongation occurs after cell division stops, several genes are known to control cell division (e.g. cyclin; Jacobs, 1997) and cell elongation (i.e. expansin; Cosgrove, 1996). It has been proposed that the expression of ascorbate oxidase and the production of dehydroascorbate are under the control of the cell cycle and that ascorbate oxidase might function in apoplast as an ascorbate oxidizer in the process of cell elongation (Kato and Esaka, 1999). The possibility of overexpressed peroxidase towards ascorbate oxidation has been ruled out as the ascorbate oxidation was not observed in the calli lines. We therefore speculate that the observed increase in growth may be due to auxin catabolism in the transgenic calli which expresses higher amount of cell wall peroxidase. The total guaiacol peroxidase activity was reduced in case of some *CrPrx* sense line due to existence of self controlling mechanism which regulate deleterious effect of gene.

In case of aCrPrx1 lines, vincristine as well as the precursors catharanthine and vindoline were not found. The data suggests towards a feedback phenomena leading to divergence of precursors to production of compounds like alstonine (Fig.

4.4.20). These antisense calli lines could prove to be an excellent material to study the feedback phenomena in MIA pathway.

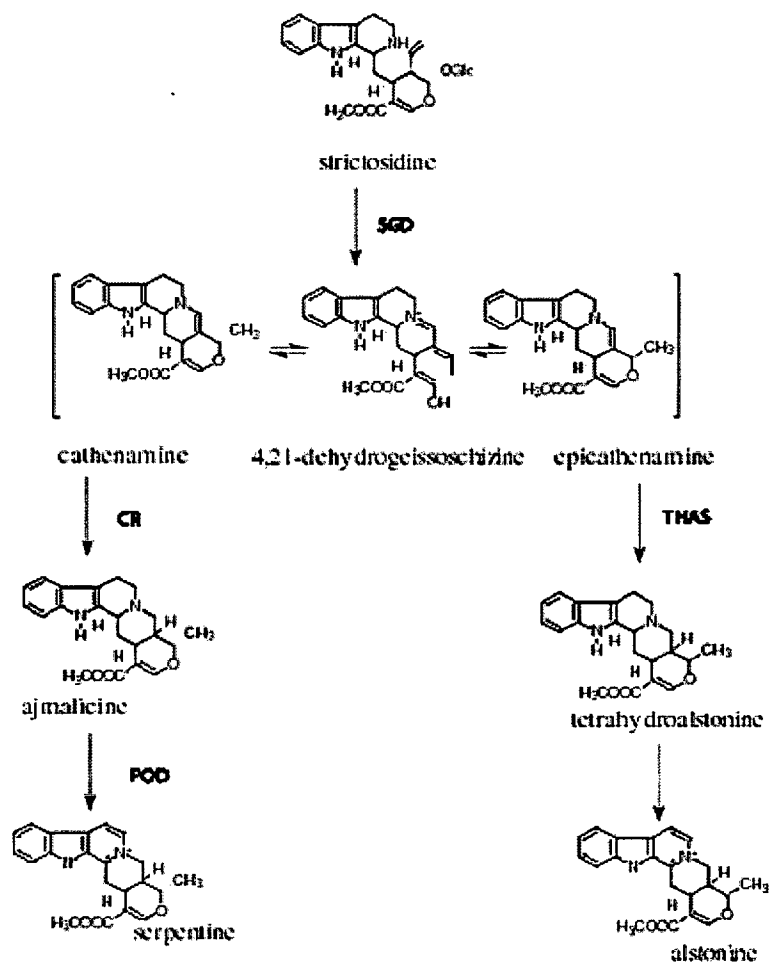


Fig. 4.4.20: Biosynthesis of ajmalicine, serpentine and tetrahydroalstonine in *C. roseus*. SGD strictosidine glucosidase, CR cathenamine reductase, POD peroxidase, THAS tetrahydroalstonine synthase.

Genes catalyzing secondary metabolite pathway in different plants are reported to be induced in response to environmental stimuli and stress mostly due to ROS generation (Gantet and Memelink, 2002). *C. roseus* cell line showing higher expression of two differentially localized peroxidases can be used as important model system to study the effect of ROS on MIAs. Overexpression of the vacuolar targeted peroxidase resulted in decomposition of several vacuolar metabolites and also reduction in reactive oxygen species. These events are sensed by regulators through unknown mechanism and reduction in the expression of *ORCA3* was also observed. Similarly in antisense lines the down regulation of *CrPrx1* is counter balanced by increase in *ORCA3* expression (Fig. 4.4.16). The only antisense line where ROS

activity had been increased in vacuole also showed higher expression of G10H, a protein present in vacuole (Fig. 4.4.16). It can be inferred that expressing antisense of a gene whose product is involved in terminal step feedbacks to increase in expression of MIA pathway genes. The sense overexpression of *CrPrx1* leads to reduction in expression of other MIA pathway genes probably to protect cells from damaging by over accumulation of vincristine. This hypothesis is substantiated as more number of dead cells on the edge of calli lines overexpressing *CrPrx1* was observed. More number of green calli were also observed in case of *CrPrx1* antisense lines which further validated the hypothesis.

The transgenic calli harbouring *CrPrx* which codes for peroxidase enzyme targeted to cell wall are probably involved in generation of ROS. The expression of different MIA pathway genes was varied in sense and antisense *CrPrx* transgenic lines. In case of sense transgenic lines most of the pathway genes were downregulated while in case of antisense transgenic lines the pathway genes were upregulated (Fig. 4.4.17). The reason for these two different phenomena can be either due to the ROS generation or ROS inhibition. There are several reports of peroxidases involved in cross linking of cell wall proteins or generation of ROS (Hilaire et al., 2001; De Biasi et al., 2003; Bindschedler et al., 2006). Apel and Hirt (2004) suggested that there are three principle modes of action that indicate how ROS affects gene expression: 1) extracellular and intracellular ROS could be sensed by ROS sensors such as membrane localized histidine kinases. A series of signaling cascades would be induced by the activation of ROS sensors ultimately affecting gene expression; 2) the components of signaling pathways could be directly oxidized by ROS. Intracellular ROS can influence mitogen-activated protein kinase (MAPK) signaling pathway through inhibition of MAPK phosphatases (PPases) or downstream transcription factors; and 3) ROS might change gene expression by targeting and modifying the activity of transcription factors. MAP kinases regulate gene expression by altering transcription factor activity through phosphorylation of serine and threonine residues, and ROS generation is regulated by oxidation of cysteine residues. ROS sensors could be activated to induce signaling cascades that ultimately impinge on gene expression. Alternatively, components of signaling pathways could be directly oxidized by ROS. Finally ROS might change gene expression by targeting and modifying the activity of transcription factors (Apel and Hirt, 2004). In tobacco leaves, ROS were reported to be involved in the induction of transcription of a gene encoding an enzyme of the

sesquiterpenoid biosynthetic pathway in response to glycoprotein elicitor (Costet et al., 2002). Pauw et al. (2001) had shown that the ROS generated by external stimuli were insufficient for the induction of MIA pathway genes and probably ROS generated from cell wall bound peroxidase were inducing MIA pathway genes. The data supports the hypothesis that ROS generated in overexpressed line through cell wall targeted peroxidase are involved in differential expression of MIA pathway genes. There are several stresses which are common to ROS generation, peroxidase activation and MIA pathway genes induction. One such mechanism was reported by Ramani and Jayabaskaran (2008) where they show UV induced ROS generation which leads the expression of MIA pathway genes through signaling cascades.

4.4.4 Conclusion

The role of *CrPrx* and *CrPrx1* in production of different MIAs was studied in transgenic callus culture of *C. roseus* that overexpressed the sense and antisense of *CrPrx* and *CrPrx1* under CaMV 35S promoter. Both cell wall (*CrPrx*) and vacuolar (*CrPrx1*) peroxidases were found to alter the expression of MIA pathway genes. In the antisense lines of *CrPrx1* (involved in the synthesis of AVL B) showed the expected inhibition of vincristine formation. However, there was no increase in accumulation of catharanthine and vindoline which are the precursors of vincristine. It was also inferred that although *CrPrx* is not directly involved in MIA pathway, the sCrPrx-5 which show higher peroxidase activity also found to have more amount of vincristine than that of control lines. The production or inhibition of ROS at relatively higher level by *CrPrx* in sCrPrx and aCrPrx lines could be attributed for differential expression of MIA biosynthetic genes.

CHAPTER 5



Summary and General Discussion

Peroxidases are ubiquitous class of enzymes which perform diverse functions by oxidation and reduction. Owing to their importance in survival of species by protection from ROS, they are multifunctional in nature and encoded by super family of genes. Peroxidases are classified in different classes based on their primary structure as Class I, Class II and Class III. Class I peroxidases are non-glycosylated, without signal peptide, calcium ions or disulfide bridges. Class II peroxidases are monomeric glycoproteins with four conserved disulfide bridges and two conserved calcium sites. Class III peroxidases are monomeric glycoproteins with four conserved disulfide bridges and two calcium ions but placement of disulfide bridges different than class II.

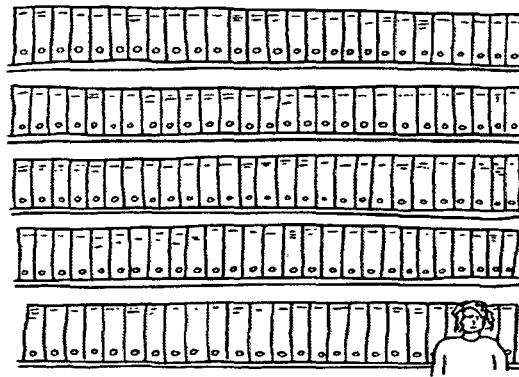
Class III peroxidase function by two different cycles viz. peroxidative and hydroxylic. The hydroxylic cycle can regulate H_2O_2 and release of ROS ('OH, HOO'). The peroxidative cycle can oxidize various substrates (XH) and release their oxidized form (X). Peroxidases play important roles in secondary metabolism both directly by participating in the pathway or indirectly by ROS generation. *CrPrx1* is a vacuolar peroxidase reported to be involved at terminal step of Monoterpenoid Indole Alkaloid (MIA) pathway (Costa et al., 2008). The importance of MIA pathway arises due to its end products i.e. formation of two important anticancerous compounds vincristine and vinblastine. Apart from involvement in MIA pathway several other functions have been attributed to peroxidases based on their expression and localization. The present work is an attempt to decipher the functions of various peroxidases present in *Catharanthus roseus*. The results obtained can be summarized as follows:

1. Six partial peroxidases were successfully cloned from *C. roseus* by utilizing degenerate primers, designed from conserved region of class III peroxidases.
2. Three different full-length peroxidase genes namely *CrPrx*, *Prx3* and *Prx4* were successfully cloned for the first time from *C. roseus* utilizing the method of cDNA library screening and rapid amplification cDNA ends (RACE).
3. The presence of N-terminal signal peptide and absence of C-terminal signal peptide leads all the three peroxidase genes to secretory pathway rather than to vacuole. Localization of *CrPrx* was found to be apoplasmic in nature.

4. Stress studies revealed that *CrPrx* gene is UV-rays and methyl jasmonate inducible.
5. Intron mapping revealed the presence of three intron in *CrPrx*. While with *Prx3* and *Prx4* the intron structures were unable to be deciphered probably due to large structure.
6. Phylogenetic analysis was successfully utilized for the first time to group *Prx3* and *Prx4* on the basis of their subcellular localization, stress specific regulation and temporal expression. The *Prx3* was localized to cell wall region, which later on was proved experimentally by gene targeting studies with *Prx3*-GFP fusion protein. The tissue specific expression of *Prx3* and *Prx4* indicated their maximum expression in stem and supported by phylogram study.
7. Functional characterization by ectopic expression of two differentially localized peroxidase genes *CrPrx1* and *CrPrx* (vacuoles and cell wall respectively) in *Nicotiana tabacum* revealed differential tolerance to salt and dehydration stresses. While *CrPrx1* transgenic *Nicotiana* seeds germinated well in MSH media containing NaCl, KCl and mannitol while *CrPrx* transgenic seeds were failed to germinate.
8. Over expression of *CrPrx* in *C. roseus* calli showed the higher accumulation of vincristine and serpentine while antisense of *CrPrx* doesn't lead to the corresponding increase in substrate viz. vindoline, catharanthine and ajmalicine. The results obtained from transgenic calli revealed that the manipulation of *CrPrx* gene had indirect effect on MIA pathway by scavenging or generation of ROS.
9. Increase in the expression of *CrPrx1* in *C. roseus* leaf calli by using overexpression cassettes resulted in increase in vincristine and serpentine amount but not in ajmalicine. The result supported the finding that *CrPrx1* is involved in conversion of vindoline and catharanthine to vincristine and vinblastine. On the other hand there were no increase in vindoline, catharanthine and ajmalicine in antisense leaf calli lines indicating that these substrates may be used by some different yet to be elucidated mechanism.

The dissertation characterized three new peroxidase genes from *C. roseus* for the first time. Two differentially localized peroxidase genes were utilized for metabolic engineering studies as well as preparation of stress tolerance transgenic seeds. Further this work leads to new insight in peroxidase gene studies where vacuolar peroxidases were supporting plants to cope with different stress. Metabolic engineering with two peroxidase genes expressed in leaf calli system can be utilized for large scale production of targeted MIAs in future.

CHAPTER 6



References

- Aerts RJ, Gisi D, De Carolis E, Luca V, Baumann TW. (1994) Methyl jasmonate vapor increases the developmentally controlled synthesis of alkaloids in *Catharanthus* and *Cinchona* seedlings. *Plant J.* 5: 635-643.
- Altschul SF, Madden TL, Schaffe AA, Zhang J, Zhang Z, Miller W, Lipman DJ. (1997) Gapped BLAST and PSI-BLAST: a new generation of protein database search programs. *Nucleic Acids Res* 25: 3389-3402.
- Amaya I, Botella MA, Calle M, Medina MI, Heredia A, Bressan RA, Hasegawa PM, Quesada MA, Valpuesta V. (1999) Improved germination under osmotic stress or tobacco plants overexpressing a cell wall peroxidase. *FEBS Lett.* 457: 80-84.
- Apel K, Hirt H. (2004) Reactive oxygen species: Metabolism, oxidative stress, and signal transduction. *Annual Rev. Plant Biol.* 55: 373-399.
- Asada K. (2000) The water-water cycle as alternative photon and electron sinks. *Philos. Trans. R. Soc. Lond. B.* 355: 1419-1431.
- Assigbetse K, Cuny G, Valette C, Delannoy E, Bresson E, Jalloul A, Daniel J-F, Geiger J-P, Nicole M. (1999) Cloning and characterization of a bacterial-induced peroxidase-encoding cDNA from cotton. *Plant Physiol.* 121: 312.
- Baga M, Chibbar RN, Kartha KK (1995). Molecular cloning and expression analysis of peroxidase genes from wheat. *Plant Mol. Biol.* 29: 647-662.
- Baier M, Dietz KJ. (1999) Alkyl hydroperoxide reductases: the way out of the oxidative breakdown of lipids in chloroplasts. *Trends in Plant Sci.* 4: 166-168.
- Baier M, Dietz KJ. (2005) Chloroplasts as source and target of cellular redox regulation: a discussion on chloroplast redox signals in the context of plant physiology. *J. Exp. Bot.* 56: 1449-1462.
- Balsevich J, Bishop G. (1989) Distribution of catharanthine, vindoline and 3,4-anhydrovinblastine in the aerial parts of some *Catharanthus roseus* plants and the significance there of in reaction to alkaloid production in cultured cells. In: Kurz WGW (ed) *Primary and Secondary metabolism of plant cell cultures.* Springer-Verlag, Germany, pp. 149-153.
- Barceló AR, Gómez Ros LV, Gabaldón C, López-Serrano M, Pomar F, Carrión JS, Pedreño MA. (2004) Basic peroxidases: The gateway for lignin evolution? *Phytochem. Rev.* 3: 61-78.
- Baxter RL, Dorschel CA, Lee SI, Scott AI. (1979) Biosynthesis of the antitumour *Catharanthus* alkaloids. Conversion of anhydrovinblastine in to vinblastine. *J. Chem. Soc. Chem. Commun.* 257-259.
- Baxter RL, Hasan M, Mackenzie NE, Scott AI. (1982) Biosynthesis of the antitumour *Catharanthus* alkaloids: The fate of the 21' a- hydrogen of anhydrovinblastine. *J. Chem. Soc. Chem. Commun.* 791-793.
- Bendtsen JD, Nielsen H, von Heijne G, Brunak S (2004) Improved prediction of signal peptides: SignalP 3.0. *J. Mol. Biol.* 340: 783-795.
- Berger S, Sinha AK, Roitsch T. (2007) Plant physiology meets phytopathology: plant primary metabolism and plant-pathogen interactions. *J. Exp. Bot.* 58: 4019-4026.
- Berlin J, Rugenhagen C, Dietze P, Fecker LF, Goddijn OJM, Hoge JHC. (1993) Increased production of serotonin by suspension and root cultures of *Peganum*

- harmala* transformed with a tryptophan decarboxylase cDNA clone from *Catharanthus roseus*. Transgenic Res. 2: 336-344.
- Bernards MA, Summerhurst DK, Razem FA. (2004) Oxidases, peroxidases and hydrogen peroxide: The suberin connection. Phytochem Rev. 3: 113-126.
- Bindschedler LV, Dewdney J, Blee KA, Stone JM, Asai T, Plotnikov J, Denoux C, Hayes T, Gerrish C, Davies DR. (2006) Peroxidase-dependent apoplastic oxidative burst in Arabidopsis required for pathogen resistance. Plant J. 47: 851-863.
- Birney E, Clamp M, Durbin R. (2004) GeneWise and Genomewise. Genome Res. 14, 988-995.
- Blee KA, Choi JW, Ó Connell AP, Schung W, Lewis NG, Bolwell GP. (2003) A lignin specific peroxidase in tobacco whose antisense suppression leads to vascular tissue modification. Phytochemistry 64: 163-176.
- Blom TJM, Sierra M, Van Vliet TB, Franke-van Dijk MEI, De Koning P, Van Iren F, Verpoorte R, Libbenga KR. (1991) Uptake and accumulation of ajmalicine in to isolated vacuoles of cultured cells of *Catharanthus roseus* (L.) G. Don and its conversion in to serpentine. Planta, 183: 170-177.
- Blumwald E, Aharon GS, Apse MP. (2000) Sodium transport in plant cells. Biochim. Biophys. Acta 1465: 140-151.
- Boerjan W, Ralph J, Boucher M. (2003) Lignin biosynthesis. Annu. Rev. Plant Biol. 54: 519-546.
- Bonfig KB, Schreiber U, Gabler A, Roitsch T, Berger S. (2006) Infection with virulent and avirulent *P. syringae* strains differentially affects photosynthesis and sink metabolism in *Arabidopsis* leaves. Planta 225:1-12.
- Bongaerts RJM. (1998) The chorismate branching point in *Catharanthus roseus*: Aspects of anthranilate synthase regulation in relation to indole alkaloid biosynthesis. PhD Thesis, Leiden University, The Netherlands.
- Botella MA, Quesada MA, Hasegawa PM, Valpuesta V. (1993) Nucleotide sequences of two peroxidase genes from tomato (*Lycopersicon esculentum*). Plant Physiol. 103: 665-666.
- Bowler C, Van Camp W, Van Montagu M, Inze D. (1994) Superoxide dismutase in plants. Crit. Rev. Plant Sci. 13: 199-218.
- Bradford MM. (1976) A rapid and sensitive for the quantitation of microgram quantities of protein utilizing the principle of protein-dye binding. Anal. Biochem. 72: 248-254.
- Breda CB, Buffard D, van Huystee RB, Esnault R. (1993) Differential expression of two peanut peroxidase cDNA clones in peanut plants and cells in suspension culture in response to stress. Plant Cell Rep. 12: 268-272.
- Brisson L, Charest PM, De Luca V, Ibrahim RK. (1992) Immuno cytochemical localization of vindoline in mesophyll protoplasts of *Catharanthus roseus*. Phytochemistry 31: 465-470.
- Buchwald W, Dedio I, Kozłowski J, Łata B. (2007) Hydroponic culture of *Catharanthus roseus* (L.) G. Don and studies on seed production Phytochem. Rev. 6: 413-417.

- Buffard D, Breda C, van Huyste RB, Asemota O, Pierre M, Daug Ha DB, Esnault R. (1990) Molecular cloning of complementaryDNAs encoding two cationic peroxidases from cultivated peanut cells. *Proc. Natl. Acad. Sci. USA* 87: 8874-8878.
- Burlat V, Oudin A, Courtois M, Rideau M, St-Pierre B. (2004) Co-expression of three MEP pathway genes and geraniol 10-hydroxylase in internal phloem parenchyma of *Catharanthus roseus* implicates multicellular translocation of intermediates during the biosynthesis of monoterpene indole alkaloids and isoprenoid-derived primary metabolites. *Plant J.* 38: 131-141.
- Canel C, Lopes-Cordoso MI, Whitmer S, van der Fits L, Pasquali G, van der Heijden R, Hoge JHC, Verpoorte R. (1998) Effects of over-expression of strictosidine synthase and tryptophan decarboxylase on alkaloid production by cell cultures of *Catharanthus roseus*. *Planta* 205: 414-419.
- Capelli N, Tognolli M, Flach J, Overney S, Penel C, Greppin H, Simon P. (1996) Eleven cDNA clones from *Arabidopsis thaliana* encoding isoperoxidases (accession nos. X98313, X98314, X98315, X98316, X98317, X98318, X98319, X98320, X98321, X98322 and X98323). *Plant Physiol.* 112: 446.
- Carpin S, Crevecoeur M, de Meyer M, Simon P, Greppin H, Penel C. (2001) Identification of a Ca²⁺-pectate binding site on an apoplastic peroxidase. *Plant Cell* 13: 511-520.
- Casacuberta JM, Santiago N. (2003) Plant LTR-retrotransposons and MITEs: control of transposition and impact on the evolution of plant genes and genomes. *Gene* 311: 1-11.
- Cosgrove DJ. (1996) Plant cell enlargement and the action of expansins. *BioEssays* 18: 533-540.
- Chahed K, Oudin A, Guivarçh N, Hamdi S, Chénieux JC, Rideau M, Clastre M. (2000) 1-Deoxy-D-xylulose 5-phosphate synthase from periwinkle: cDNA identification and induced gene expression in terpenoid indole alkaloid-producing cells. *Plant Physiol. Biochem.* 38: 559-566.
- Chaloupkova K, Smart CC. (1994) The abscisic acid induction of a novel peroxidase is antagonized by cytokinin in *Spirodela polyrrhiza* L. *Plant Physiol.* 105: 497-507.
- Charvet-Candela V, Hitchin S, Reddy MS, Cournoyer B, Marmeisse R, Gay G. (2002) Characterization of a *Pinus pinaster* cDNA encoding an auxin up-regulated putative peroxidase in roots. *Tree Physiol.* 22: 231-238.
- Chavadej S, Brisson N, McNeil JN, De Luca V. (1994) Redirection of tryptophan leads to production of low indole glucosinolate canola. *Proc. Natl. Acad. Sci. USA* 91: 2166-2170.
- Chen H, Nelson RS, Sherwood JL. (1994) Enhanced recovery of transformants of *Agrobacterium tumefaciens* after freeze-thaw transformation and drug selection. *Biotechniques* 16: 664-668.
- Cheong YH, Chang HS, Gupta R, Wang X, Zhu T, Luan S. (2002) Transcriptional profiling reveals novel interactions between wounding, pathogen, abiotic stress, and hormonal responses in *Arabidopsis*. *Plant Physiol.* 129: 661-677.

- Chittoor JM, Leach JE, White EF. (1999) Induction of peroxidase during defence against pathogens. In: Datta SK, Muthukrishnan SK (eds). Pathogenesis-related proteins in plants, CRC Press, New York, pp. 171-193.
- Chittoor JM, Leach JE, White FF. (1997) Differential induction of a peroxidase gene family during infection of rice by *Xanthomonas oryzae* pv. *oryzae*. Mol. Plant Microbe Interact. 10: 861-871.
- Christensen JH, Overney S, Rohde A, Diaz WA, Bauw G, Simon P, Van Montagu M, Boerjan W. (2001) The syringaldazineoxidizing peroxidase PXP 3-4 from poplar xylem: DNA isolation, characterization and expression. Plant Mol. Biol. 47: 581-593.
- Churin Y, Schilling S, Börner T. (1999) A gene family encoding glutathione peroxidase homologues in *Hordeum vulgare* (barley). FEBS Lett. 459: 33-38.
- Coelho AC. (2003) Identification of molecular markers in *Quercus suber* linked to resistance to *Phytophthora cinnamomi*. Thesis, Universidade do Algravo, Faro, Portugal.
- Collinge M, Boller T. (2001) Differential induction of two potato genes, Stprx2 and StNAC, in response to infection by *Phytophthora infestans* and to wounding. Plant Mol. Biol. 46: 521-529.
- Collu G, Unver N, Peltenburg-Looman AMG, van der Heijden R, Verpoorte R, Memelink J. (2001) Geraniol 10-hydroxylase, a cytochrome P450 enzyme involved in terpenoid indole alkaloid biosynthesis. FEBS Lett. 508: 215-220.
- Contin A, van der Heijden R, Lefeber AW, Verpoorte R. (1998) The iridoid glucoside secologanin is derived from the novel triose phosphate/pyruvate pathway in a *Catharanthus roseus* cell culture. FEBS Lett. 434: 413-416.
- Contin A, van der Heijden R, Verpoorte R. (1999) Accumulation of loganin and secologanin in vacuoles from suspension cultured *Catharanthus roseus* cells. Plant Sci. 147: 177-183.
- Costa MMR, Hilliou F, Duarte P, Pereira LG, Almeida I, Leech M, Memelink J, Barcelo AR, Sottomayor M. (2008) Molecular cloning and characterization of a vacuolar class III peroxidase involved in the metabolism of anticancer alkaloids in *Catharanthus roseus*. Plant Physiol. 146: 403-417.
- Costet L, Dorey S, Fritig B, Kaumann S. (2002) A pharmacological approach to test the diffusible signal activity of reactive oxygen intermediates in elicitor-treated tobacco leaves. Plant Cell Physiol. 43: 91-98.
- Creasey WA. (1994) Pharmacology, biochemistry and clinical applications of the monoterpenoid alkaloids. In: Saxton JE (ed) The monoterpenoid Indole Alkaloids, John Wiley & Sons, Chichester, New York, Brisbane, Toronto, Singapore, pp. 715-753.
- Croteau R, Kutchan M, Lewis NG. (2000) Natural products (secondary metabolites). In: Buchanan BB, Gruissem W, Jones RL (eds) Biochemistry and Molecular Biology of Plants. American Society of Plant Physiologists, Rockville, USA, pp 1250-1318.
- Courdavault V, Burlat V, St-Pierre B, Giglioli-Guivarc'h N. (2005) Characterization of CaaX-prenyltransferases in *Catharanthus roseus*: relationships with the

- expression of genes involved in the early stages of monoterpene biosynthetic pathway. *Plant Sci.* 168: 1097-1107.
- Curtis MD, Rae AL, Rusu AG, Harrison SJ, Manners JM. (1997) A peroxidase gene promoter induced by phytopathogens and methyl jasmonate in transgenic plants. *Mol. Plant Microbe Interact.* 10: 326-338.
- De Biasi MG, Astolfi S, Acampora A, Zuchi S, Fonzo V, Santangelo E, Caccia R, Badiani M, Soressi GP. (2003) A H₂O₂-forming peroxidase rather than a NAD(P)H-dependent O²⁻ synthase may be the major player in cell death responses controlled by the *Pto-Fen* complex following fenthion treatment. *Funct. Plant Biol.* 30: 409-417.
- De Luca V, Cutler AJ. (1987) Subcellular localization of enzymes involved in indole alkaloid biosynthesis in *Catharanthus roseus*. *Plant Physiol.* 85: 1099-1102.
- De Luca V, Marineau C, Brisson N. (1989) Molecular cloning and analysis of cDNA encoding a plant tryptophan decarboxylase: Comparison with animal dopa decarboxylases. *Proc. Natl. Acad. Sci. USA* 86: 2582-2586.
- De Luca V, St Pierre B, Vazquez Flota F, Laflamme P. (1998) The uses of molecular approaches to produce phytomedicines in the *Catharanthus roseus* model system. In: Ageton H, Aimi N, Ebizuka Y, Fujita T, Honda G (eds) *Towards natural medicine research in the 21st century*. Elsevier Science BV, The Netherlands, pp. 363-370.
- De Luca, V. (1993) Indole alkaloid biosynthesis. In: Lea P (ed) *Methods in Plant Biochemistry. Enzymes of Secondary Metabolism*, Vol. 9. Academic Press, London, pp 345-368.
- Den Herder J, Lievens S, Rombauts S, Holsters M, Goormachtig S. (2007) A symbiotic plant peroxidase involved in bacterial invasion of the tropical legume *Sesbania rostrata*. *Plant Physiol.* 144: 717-727.
- Dethier M, De Luca V. (1993) Partial purification of an N-methyltransferase involved in vindoline biosynthesis in *Catharanthus roseus*. *Phytochemistry* 32: 673-678.
- Dewick PM. (2002) *Medicinal Natural products: A Biosynthetic Approach*, 2nd edn, John Wiley and Sons, USA, 507 pp.
- Di Fiore S, Li Q, Leech MJ, Schuster F, Emans N, Fischer R, Schillberg S. (2002) Targeting tryptophan decarboxylase to selected subcellular compartments of tobacco plants affects enzyme stability and in vivo function and leads to a lesion-mimic phenotype. *Plant Physiol.* 129: 1160-1169.
- Dietz KJ. (2003) Plant peroxiredoxins. *Annu. Rev. Plant Biol.* 54: 93-107.
- Do HM, Hong JK, Jung HW, Kim SH, Ham JH, Hwang BK. (2003) Expression of peroxidase-like genes, H₂O₂ production, and peroxidase activity during the hypersensitive response to *Xanthomonas campestris* pv. *vesicatoria* in *Capsicum annuum*. *Mol. Plant Microbe Interact.* 16: 196-205.
- Duroux L, Welinder KG. (2003) The peroxidase gene family in plants: a physiological overview. *J Mol. Evol.* 57: 397-407.
- Dutta A. (2006) Molecular and abiotic stress signal transduction studies on TIA biosynthetic pathway genes in periwinkle. PhD Thesis, Delhi University, India.

- Eck RV, Dayhoff MO. (1966) Atlas of Protein Sequence and Structure. National Biomedical Research Foundation, Silver Spring, USA.
- Edwards K, Johnstone C, Thompson C. (1991) A simple and rapid method for the preparation of plant genomic DNA for PCR analysis. Nucl. Acid Res. 19: 1349.
- Elkind Y, Edwards R, Mavandad M, Hedrick SA, Ribak O, Dixon RA, Lamb CJ. (1990) Abnormal plant development and down-regulation of phenylpropanoid biosynthesis in transgenic tobacco containing a heterologous phenylalanine ammonia-lyase gene. Proc. Natl. Acad. Sci. USA 87: 9057-9061.
- El Mansouri I, Mercado JA, Santiago-Dómenech N, Pliego-Alfaro F, Valpuestra V, Quesada MA. (1999) Biochemical and phenotypical characterization of transgenic tomato plants overexpressing a basic peroxidase. Physiol. Plant. 106: 355-362.
- El-Sayed M, Verpoorte R. (2005) Methyljasmonate accelerates catabolism of monoterpenoid indole alkaloids in *Catharanthus roseus* during leaf processing. Fitoterapia 76: 83-90.
- el-Turk J, Asemota O, Leymarie J, Sallaud C, Mesnage S, Breda C, Buffard D, Kondorosi A, Esnault R. (1996) Nucleotide sequences of four pathogen-induced alfalfa peroxidase-encoding cDNAs. Gene 170: 213-216.
- Endo T, Goodbody A, Vukovic J, Misawa M. (1988) Enzymes from *Catharanthus roseus* cell suspension cultures that couple vindoline and catharanthine to form 3, 4-anhydrovinblastine. Phytochemistry 27: 2147-2149.
- Eulgem T, Rushton PJ, Robatzek S, Somssich IE. (2000) The WRKY superfamily of plant transcription factors. Trends Plant Sci. 5: 199-206.
- Facchini PJ. (2001) Alkaloid biosynthesis in plant: Biochemistry, cell biology, molecular regulation and metabolic engineering applications. Annu. Rev. Plant Physiol. Plant Mol. Biol. 52: 29-66.
- Felsenstein J. (1985) Confidence limits on phylogenies: An approach using the bootstrap. Evolution 39: 783-791.
- Flota-Vázquez F, Valenzuela-Moreno O, Miranda-Ham ML, Coello-Coello J, Loyola-Vargas VM. (1994) Catharanthine and ajmalicine synthesis in *Catharanthus roseus* hairy root cultures. Plant tissue and Organ. culture 38: 273-279.
- Fossdal CG, Sharma P, Lonneborg A. (2001) Isolation of the first putative peroxidase cDNA from a conifer and the local and systemic accumulation of related proteins upon pathogen infection. Plant Mol. Biol. 47: 423-435.
- Froehlich JE, Itoh A, Howe GA. (2001) Tomato allene oxide synthase and fatty acid hydroperoxide lyase, two cytochrome P450s involved in oxylipin metabolism, are targeted to different membranes of chloroplast envelope. Plant Physiol. 125: 306-317.
- Fry SC. (2004) Oxidative coupling of tyrosine and ferulic acid residues: Intra- and extra-protoplasmic occurrence, predominance of trimers and larger products, and possible role in inter-polymeric cross-linking. Phytochem Rev. 3: 97-111.
- Fujiyama K, Takemura H, Shibayama S, Kobayashi K, Choi JK, Shinmyo A, Takano M, Okada H. (1988) Structure of the horseradish peroxidase isozyme C genes. Eur. J. Biochem. 173: 681-687.

- Fujiyama K, Takemura H, Shinmyo A, Okada H, Takano M. (1990) Genomic DNA structure of two new horseradish-peroxidase encoding genes. *Gene* 89: 163-169.
- Gabaldón C, López-Serrano M, Pedreño M, Ros Barceló A. (2005) Cloning and molecular characterization of the basic peroxidase isoenzyme from *Zinnia elegans*, an enzyme involved in lignin biosynthesis. *Plant Physiol.* 139: 1138-1154.
- Gajhede M, Schuller DJ, Henriksen A, Smith AT, Poulos TL. (1997) Crystal structure of horseradish peroxidase C at 2.15 Å resolution. *Nat. Struct. Biol.* 4: 1032-1038.
- Gamborg OL, Miller RA, Ojima K. (1968) Nutrient requirements of suspension cultures of soybean root cells. *Exp. Cell Res.* 50: 151-158.
- Gantet P, Memelink J. (2002) Transcription factors: tools to engineer the production of pharmacologically active plant metabolites. *Trends Pharmacol. Sci.* 23: 563-569.
- Gautheret RJ. (1946) Comparaison entre l'actions de l'acide indoleacetique et celle du *Phytomonas tumefaciens* sur la croissance des tissus végétaux. *C. R. Soc. Biol. (Paris)* 140: 169-171.
- Geerlings A, Hallard D, Caballero AM, Cardoso, IL, van der Heijden R, Verpoorte R. (1999) Alkaloid production by a *Cinchona officinalis* "Ledgeriana" hairy root culture containing constitutive expression constructs of tryptophan decarboxylase and strictosidine synthase cDNAs from *Catharanthus roseus*. *Plant Cell Rep.* 19: 191-196.
- Geerlings A, Ibanez MM, Memelink J, van der Heijden R, Verpoorte R. (2000) Molecular cloning and analysis of strictosidine beta-D-glucosidase, an enzyme in terpenoid indole alkaloid biosynthesis in *Catharanthus roseus*. *J. Biol. Chem.* 275: 3051-3056.
- Goddijn OJM, Pennings EJM, van der Helm P, Schilperoort RA, Verpoorte R, Hoge JHC. (1995) Overexpression of a tryptophan decarboxylase cDNA in *Catharanthus roseus* crown gall calluses results in increases tryptamine levels but not in increased terpenoid indole alkaloid production. *Transgenic Res.* 4: 315-323.
- Goodbody AE, Endo T, Vukovic J, Kutney JP, Choi LS, Misawa M. (1988) Enzymic coupling of catharanthine and vindoline to form 3, 4-anhydrovinblastine by horseradish peroxidase. *Planta Med.* 54: 136-140.
- Gröger D. (1985) Alkaloids derived from tryptophan. In: Mothes K, Schütte HR, Luckner M (eds) *Biochemistry of alkaloids*, VEB Deutscher Verlag der Wissenschaften, Germany, pp. 272-313.
- Gupta R. (1977) Periwinkle produces anticancer drug. *Indian Farming* 7: 11-13.
- Haas BJ, Volfovsky N, Town CD, Troukhan M, Alexandrov N, Feldmann KA, Flavell RB, White O, Salzberg SL. (2002) Full-length messenger RNA sequences greatly improve genome annotation. *Genome Biol.* 3: R29.1-R29.12.
- Herder JD, Lievens S, Rombauts S, Marcelle H, Goormachtig S. (2007) A symbiotic plant peroxidase involved in bacterial invasion of the tropical legume *Sesbania rostrata*. *Plant Physiol.* 144: 717-727.
- Hasegawa PM, Bressan RA, Zhu JK, Bohnert HJ. (2000) Plant cellular and molecular responses to high salinity. *Annu. Rev. Plant Physiol. Plant Mol. Biol.* 51: 463-499.

- Hemscheidt T, Zenk MH. (1985) Partial purification and characterization of a NADPH dependent tetrahydroalstonine synthase from *Catharanthus roseus* cell suspension cultures. *Plant Cell Rep.* 4: 216-219.
- Henriksen A, Mirza O, Indiani C, Teilum K, Smulevich G, Welinder KG, Gajhede M. (2001) Structure of soybean seed coat peroxidase: a plant peroxidase with unusual stability and haem-apoprotein interactions. *Protein Sci.* 10: 108-115
- Hilaire E, Young SA, Willard LH, McGee JD, Sweat T, Chittoor JM, Guikema JA, Leach JE. (2001) Vascular defense responses in rice: peroxidase accumulation in xylem parenchyma cells and xylem wall thickening. *Mol. Plant Microbe Interact.* 14: 1411-1419.
- Hinman RL, Lang J. (1965) Peroxidase-catalyzed oxidation of indole-3-acetic acid. *Biochemistry.* 4: 144-158.
- Hiraga S, Ito H, Matsui H, Honma M, Ohashi Y. (1999) cDNA sequences for two novel tobacco peroxidase isoenzymes (accession nos. AB027752 and AB027753) (PGR99-09). *Plant Physiol.* 120: 1205.
- Hiraga S, Sasaki K, Ito H, Ohashi Y, Matsui H. (2001) A large family of class III plant peroxidases. *Plant Cell Physiol.* 42: 462-468.
- Hiraga S, Sasaki K, Yamakawa H, Mitsuhara I, Toshima H, Matsui H, Honma M, Ohashi Y. (2000) Wound-induced expression of a tobacco peroxidase is not enhanced by ethephon and suppressed by methyl jasmonate and coronatine. *Plant Cell Physiol.* 41:165-170.
- Holm KB, Andreassen PH, Eckloff RM, Kristensen BK, Rasmussen SK. (2003) Three differentially expressed basic peroxidases from wound-lignifying *Asparagus officinalis*. *J. Exp. Bot.* 54: 2275-2284.
- Huangpu J, Graham MC, Graham JS. (1996) Cloning of a soybean cDNA (accession no. U41657) encoding the abundant anionic seed coat peroxidase (PGR95-136). *Plant Physiol.* 110:714.
- Huh GH, Lee SJ, Bae YS, Liu JR, Kwak SS. (1997) Molecular cloning and characterization of cDNAs for anionic and neutral peroxidases from suspension-cultured-cells of sweet potato and their differential expression in response to stress. *Mol. Gen. Genet.* 255:382-391.
- Hushpulian DM, Poloznikov AA, Savitski PA, Rozhkova AM, Chubar TA, Fechina VA, Orlova MA, Tishkov VI, Gazaryan IG, Lagrimini LM. (2007) Glutamic acid-141: a heme 'bodyguard' in anionic tobacco peroxidase. *Biol Chem.* 388: 373-380.
- Inoue H, Nojima H, Okayama H. (1990) High efficiency transformation of *Escherichia coli* with plasmids. *Gene* 96: 23-28.
- Intapruk C, Takano M, Shinmyo A. (1994) Nucleotide sequence of a new cDNA for peroxidase from *Arabidopsis thaliana*. *Plant Physiol.* 104: 285-286.
- Irmiler S, Schröder G, St-Pierre B, Crouch NP, Hotze M, Schmidt J, Strack D, Matern U, Schröder J. (2000) Indole alkaloid biosynthesis in *Catharanthus roseus*: new enzyme activities and identification of cytochrome P450 CYP72A1 as secologanin synthase. *Plant J.* 24: 797-804.
- Ishige F, Mori H, Yamazaki K, Imaseki H. (1993) Identification of a basic glycoprotein induced by ethylene *Plant Physiol.* 101: 193-199.

- Ito H, Kimizuka F, Ohbayashi A, Matsui H, Honma M, Shinmyo A, Ohashi Y, Rodrigues RL. (1994) Molecular cloning and characterization of two complementary cDNAs encoding putative peroxidase from rice (*Oryza sativa* L.). *Plant Cell Rep.* 13: 361-366.
- Ito H, Tsugawa H, Matsui H, Honma M, Otsuki Y, Murakami T, Ohashi Y. (2000) Xylem-specific expression of wound-inducible rice peroxidase genes in transgenic plants. *Plant Sci.* 155: 85-100.
- Ivan AR. (2003) *Medicinal Plants of the World: Chemical Constituents, Traditional and Modern Medicinal Uses* 2nd edn. Humana Press, USA, pp 175-185.
- Janda T, Szalai G, Kissimon J, Páldi E, Marton C, Szigeti Z. (1994) Role of irradiance in the chilling injury of young maize plants studied by chlorophyll fluorescence induction measurements. *Photosynthetica* 30:293-299.
- Jacobs T. (1997) Why do plant cells divide? *Plant cell* 9: 1021-1029.
- Johansson A, Rasmussen SK, Harthill JE, Welinder KG. (1992) cDNA, amino acid and carbohydrate sequence of barley seed-specific peroxidase BP 1. *Plant Mol. Biol.* 18: 1151-1161.
- Kanneganti V, Gupta AK. (2008) Overexpression of OsiSAP8, a member of stress associated protein (SAP) gene family of rice confers tolerance to salt, drought and cold stress in transgenic tobacco and rice. *Plant Mol. Biol.* 66: 445-462.
- Kaothien P, Kawaoka A, Ebinuma H, Yoshida K, Shinmyo A. (2002) Ntlm1, a PAL-box binding factor, controls the promoter activity of horseradish wound-induced peroxidase gene. *Plant Mol. Biol.* 49: 591-599.
- Kaothien P, Shimokawatoko Y, Kawaoka A, Yoshida K, Shinmyo A. (2000) A cis element containing a PAL-box functions in the expression of the wound-inducible peroxidase gene of horseradish. *Plant Cell Rep.* 19: 558-562.
- Kasahara H, Hanada A, Kuzuyama T, Takagi M, Kamiya Y, Yamaguchi S. (2002) Contribution of the mevalonate and methylerythritol phosphate pathways to the biosynthesis of gibberellins in *Arabidopsis*. *J. Biol. Chem.* 277: 45188-45194.
- Katoh K, Kuma K, Toh H, Miyata T. (2005) MAFFT version 5: improvement in accuracy of multiple sequence alignment. *Nucleic Acids Res.* 33: 511-518.
- Kato N, Esaka M. (1999) Changes in ascorbate oxidase gene expression and ascorbate levels in cell division and cell elongation in tobacco cells. *Physiol. Plant.* 105: 321-329.
- Kawaoka A, Kawamoto T, Ohta H, Sekine M, Takano M, Shinmyo A. (1994) Wound-induced expression of horseradish peroxidase. *Plant Cell Rep.* 13: 149-154.
- Kawaoka A, Matsunaga E, Endo S, Kondo S, Yoshida K, Shinmyo A, Ebinuma H. (2003) Ectopic expression of a horseradish peroxidase enhances growth rate and increases oxidative stress resistance in hybrid Aspen. *Plant Physiol.* 132: 1177-1185.
- Kim KY, Huh GH, Lee HS, Kwon SY, Hur Y, Kwak SS. (1999) Molecular characterization of cDNAs for two anionic peroxidases from suspension cultures of sweet potato. *Mol. Gen. Genet.* 261: 941-947.

- Kjaersgard IV, Jespersen HM, Rasmussen SK, Welinder KG. (1997) Sequence and RT-PCR expression analysis of two peroxidases from *Arabidopsis thaliana* belonging to a novel evolutionary branch of plant peroxidases. *Plant Mol. Biol.* 33: 699-708.
- Klotz KL, Liu TTY, Liu L, Lagrimini LM. (1998) Expression of the tobacco anionic peroxidase gene is tissue-specific and developmentally regulated. *Plant Mol. Biol.* 36: 509-520.
- Kohlmüzer S. (1968) Alkaloidy *Catharanthus roseus* G. Donnowa grupa związkó wbiologicznie czynnych (Alkaloids of *Catharanthus roseus* (L.) G. Don a new group of biologically active compounds). *Post Biochem.* 14: 209-232.
- Koutaniemi S, Toikka MM, Kärkönen A, Mustonen M, Lundell T, Simola LK, Kilpeläinen IA, Teeri TH. (2005) Characterization of basic p-coumaryl and coniferyl alcohol oxidizing peroxidases from lignin forming *Picea abies* suspension culture. *Plant Mol. Biol.* 58: 141-157.
- Kumar S, Dutta A, Sinha AK, Sen J. (2007) Cloning, characterization and localization of a novel basic peroxidase gene from *Catharanthus roseus*. *FEBS J.* 274: 1290-1303.
- Kumar S, Tamura K, Jakobsen IB, Nei M. (2001) MEGA2: molecular evolutionary genetics analysis software. *Bioinformatics* 17: 1244-1245.
- Kutchan TM. (1993) Strictosidine: from alkaloid to enzyme to gene. *Phytochemistry* 32:493-506.
- Kutchan TM. (1995) Alkaloid biosynthesis-The basis for metabolic engineering of medicinal plants. *Plant Cell* 7: 1059-1070.
- Laflamme P, St-Pierre B, De Luca V. (2001) Molecular and biochemical analysis of a Madagascar periwinkle rootspecific minovincinine-19-hydroxy-O-acetyltransferase. *Plant Physiol.* 125: 189-198.
- Lagrimini LM, Bradford S, Rothstein S. (1990) Peroxidase-induced wilting in transgenic tobacco plants. *Plant Cell* 2: 7-18.
- Lagrimini LM, Joly RJ, Dunlap JR, Liu TY. (1997) The consequence of peroxidase overexpression in transgenic plants on root growth and development. *Plant Mol. Biol.* 33: 887-895.
- Lagrimini LM, Rothstein S. (1987) Tissue specificity of tobacco peroxidase isozymes and their induction by wounding and tobacco mosaic virus infection. *Plant Physiol.* 84: 438-442.
- Langlois N, Gueritte F, Langlois Y, Potier P. (1976) Application of a modification of the Polonovski reaction to the synthesis of vinblastine-type alkaloids. *J. Am. Chem. Soc.* 98: 7017-7024.
- Levac D, Murata J, Kim WS, De Luca V. (2008) Application of carborundum abrasion for investigating leaf epidermis: Molecular cloning of *Catharanthus roseus* 16-hydroxytabersonine-16-O-methyltransferase. *Plant J.* 53: 225-236.
- Lichtenthaler HK, Schwender J, Disch A, Rohmer M. (1997) Biosynthesis of isoprenoids in higher plant chloroplasts proceeds via a mevalonate-independent pathway. *FEBS Lett.* 400: 271-274.

- Lichtenthaler HK. (1999) The 1-deoxy-D-xylulose 5-phosphate pathway of isoprenoid biosynthesis in plants. *Annu. Rev. Plant Physiol. Plant Mol. Biol.* 50: 47-65.
- Liu G, Sheng X, Greenshields DL, Ogieglo A, Kaminskyj S, Selvaraj G, Wei Y. (2005) Profiling of wheat class III peroxidase genes derived from powdery mildew-attacked epidermis reveals distinct sequence-associated expression patterns. *Mol. Plant Microbe Interact.* 18: 730-741.
- Llorente F, Lopez-Cobollo RM, Catala R, Martinez- Zapater JM, Salinas J. (2002) A novel cold-inducible gene from *Arabidopsis*, RCI3, encodes a peroxidase that constitutes a component for stress tolerance. *Plant J.* 32: 13-24.
- Lois R, Dietrich A, Hahlbrock K, Schulz W. (1989) A phenylalanine ammonia-lyase gene from parsley: structure, regulation, and identification of elicitor and light responsive cis-acting elements. *EMBO J.* 8: 1641-1648.
- Mahroug S, Courdavault V, Thiersault M, St-Pierre B, Burlat V. (2006) Epidermis is a pivotal site of at least four secondary metabolic pathways in *Catharanthus roseus* aerial organs. *Planta* 223: 1191-1200.
- Marjamaa K, Hildén K, Kukkola E, Lehtonen M, Holkeri H, Haapaniemi P, Koutaniemi S, Teeri TH, Fagerstedt K, Lundell T. (2006) Cloning, characterization and localization of three novel class III peroxidases in lignifying xylem of Norway spruce (*Picea abies*). *Plant Mol. Biol.* 61: 719-732.
- Mao L, Begum D, Chuang H-W, Budiman MA, Szymkoiak EJ, Irish EE, Wing RA (2000) JOINTLESS is a MADS-box gene controlling tomato flower abscission zone development, *Nature* 406: 910-913.
- McInnis SM, Costa LM, Gutierrez-Marcos JF, Henderson CA, Hiscock SJ. (2005) Isolation and characterization of a polymorphic stigma-specific class III peroxidase gene from *Senecio squalidus* L. (Asteraceae). *Plant Mol. Biol.* 57: 659-677.
- McKnight TD, Bergey DR, Burnett RJ, Nessler CL. (1991) Expression of enzymatically active and correctly targeted strictosidine synthase in transgenic tobacco plants. *Planta* 185: 148-152.
- McKnight TD, Roessner CA, Devagupta R, Scott AI, Nessler CL. (1990) Nucleotide sequence of a cDNA encoding the vacuolar protein strictosidine synthase from *Catharanthus roseus*. *Nucleic Acids Res.* 18:4939.
- Meijer AH, Verpoorte R, Hoge JHC. (1993a) Regulation of enzymes and genes involved in terpenoid indole alkaloid biosynthesis in *Catharanthus roseus* J. *Plant Res.* 3: 145-165.
- Meijer AH, Lopes Cardoso MI, Voskuilen JT, de Waal A, Verpoorte R, Hoge JH. (1993b) Isolation and characterization of a cDNA clone from *Catharanthus roseus* encoding NADPH:cytochrome P-450 reductase, an enzyme essential for reactions catalysed by cytochrome P-450 mono-oxygenases in plants. *Plant J.* 4: 47-60.
- Memelink J, Verpoorte R, Kijne JW. (2001) ORCAnization of jasmonate-responsive gene expression in alkaloid metabolism. *Trends Plant Sci.* 6: 212-219.

- Misawa M, Endo T, Goodbody A, Vukovic J, Chapple C, Choi L, Kutney JP. (1988) Synthesis of dimeric indole alkaloids by cell free extracts from cell suspension cultures of *Catharanthus roseus*. *Phytochemistry* 27: 1355-1359.
- Mishra P, Uniyal GC, Sharma S, Kumar S. (2001) Pattern of diversity for morphological and alkaloid yield related traits among the periwinkle *Catharanthus roseus* accessions collected from in and around Indian subcontinent. *Genet. Resour. Crop Evalu.* 48: 273-286.
- Misra N, Luthra R, Kumar S. (2006) Bioconversion of ajmalicine to serpentine in *Catharanthus roseus* roots. *J. of Plant Sci.* 1: 340-347.
- Mohan R, Bajar AM, Kolattukudy PE. (1993a) Induction of a tomato anionic peroxidase gene (*tap1*) by wounding in transgenic tobacco and activation of *tap1*/GUS and *tap2*/GUS chimeric gene fusions in transgenic tobacco by wounding and pathogen attack. *Plant Mol. Biol.* 21: 341-354.
- Mohan R, Vijayan P, Kolattukudy PE. (1993b) Developmental and tissue-specific expression of a tomato anionic peroxidase (*tap1*) gene by a minimal promoter, with wound and pathogen induction by an additional 5'-flanking region. *Plant Mol. Biol.* 22: 475-490.
- Moreno PRH, van der Heijden R, Verpoorte R. (1995) Cell and tissue cultures of *Catharanthus roseus* (L.) G. Don: a literature survey II. Updating from 1988 to 1993. *Plant Cell Tissue Org. Cult.* 42: 1-25.
- Morgens PH, Callahan AM, Dunn LJ, Abeles FB. (1990) Isolation and sequencing of cDNA clones encoding ethylene-induced putative peroxidases from cucumber cotyledons. *Plant Mol. Biol.* 14: 715-725.
- Münzenberger B, Otter T, Wüstrich D, Polle A. (1997) Peroxidase and laccase activities in mycorrhizal and non-mycorrhizal fine roots of Norway spruce (*Picea abies*) and larch (*Larix decidua*). *Can. J. Bot.* 78: 932-938.
- Mura A, Medda R, Longu S, Floris G, Rinaldi AC, Padiglia A. (2005) A Ca²⁺ / calmodulin-binding peroxidase from Euphorbia latex: novel aspects of calcium hydrogen peroxide cross-talk in the regulation of plant defenses. *Biochemistry* 44: 14120-14130.
- Naaranlahti T, Auriola S, Lapinjoki SP. (1991) Growth related dimerization of vindoline and catharanthine in *Catharanthus roseus* effect of wounding on the process. *Phytochemistry* 30: 1451-1453.
- Nei M, Kumar S (2000) *Molecular Evolution and Phylogenetics*. Oxford University Press, New York.
- Nielsen H, Engelbrecht J, Brunak S, von Heijne G. (1997) Identification of prokaryotic and eukaryotic signal peptides and prediction of their cleavage sites. *Prot. Eng.* 10: 1-6.
- Niu X, Bressan RA, Hasegawa PM, Pardo JM. (1995) Ion homeostasis in NaCl stress environments. *Plant Physiol.* 109: 735-742.
- Okuda KI. (1994) Liver mitochondrial P450 involved in cholesterol catabolism and vitamin D activation. *J. Lipid Res.* 35: 361-372.

- Örvar BL, Ellis BE. (1997) Transgenic tobacco plants expressing antisense RNA for cytosolic ascorbate peroxidase show increased susceptibility to ozone injury. *Plant J.* 11: 1297-1305.
- Østergaard L, Teilum K, Mirza O, Mattsson O, Petersen M, Welinder KG, Mundy J, Gajhede M, Henriksen A. (2000) Arabidopsis ATP A2 peroxidase. Expression and high-resolution structure of a plant peroxidase with implications for lignification. *Plant Mol. Biol.* 44: 231-243.
- Oudin A, Courtois M, Rideau M, Clastre M. (2007a) The iridoid pathway in *Catharanthus roseus* alkaloid biosynthesis. *Phytochem. Rev.* 6: 259-276.
- Oudin A, Mahroug S, Courdavault V, Hervouet N, Zelwer C, Rodriguez-Concepcion M, St-Pierre B, Burlat V. (2007b) Spatial distribution and hormonal regulation of gene products from methyl erythritol phosphate and monoterpene-secoiridoid pathways in *Catharanthus roseus*. *Plant Mol. Biol.* 65: 13-30.
- Park SY, Ryu SH, Kwon SY, Lee HS, Kim JG, Kwak SS. (2003) Differential expression of six novel peroxidase cDNAs from cell cultures of sweetpotato in response to stress. *Mol. Genet. Genomics* 269, 542-552.
- Parrek SK, Singh S, Srivastava VK, Mandal S, Maheswari ML, Gupta R. (1981) Advances in periwinkle cultivation. *Indian Farming* 31: 18-21.
- Passardi F, Cosio C, Penel C, Dunand C. (2005) Peroxidases have more functions than a Swiss army knife. *Plant cell Rep.* 24: 255-265.
- Passardi F, Longet D, Penel C, Dunand C. (2004) The class III peroxidase multigene family in rice and its evolution in land plants. *Phytochemistry* 65: 1879-1893.
- Passardi F, Longet D, Penel C, Dunand C. (2004a) The class III peroxidase multigenic family in rice and its evolution in land plants. *Phytochemistry* 65: 1879-1893.
- Passardi F, Penel C, Dunand C. (2004b) Performing the paradoxical: how plant peroxidases modify the cell wall. *Trends Plant Sci.* 9: 534-540.
- Passardi F, Theiler G, Zamocky M, Cosio C, Rouhier N, Teixeira F, Margis-Pinheiro M, Ioannidis V, Penel C, Falquet L, Dunand C. (2007) PeroxiBase: the peroxidase database. *Phytochemistry* 68: 1605-1611.
- Pasquali G, Goddijn OJM, De Waal A, Verpoorte R, Schilperoort RA, Hoge JHC, Memelink J. (1992) Coordinated regulation of two indole alkaloid biosynthetic genes from *Catharanthus roseus* by auxin and elicitors. *Plant Mol. Biol.* 18: 1121-1131.
- Pauw B, van Duijn B, Kijne JW. (2001) Activation of the oxidative burst by yeast elicitor in *Catharanthus roseus* cells occurs independently of the activation of genes involved in alkaloid biosynthesis. *Plant Mol. Biol.* 55: 797-805.
- Penel C. (2000) The peroxidase system in higher plants. In: Greppin H, Penel C, Broughton WJ, Strasser R, (eds) *Integrated Plant Systems*, University of Geneva, Switzerland, pp. 359-367.
- Pezzuto JM. (1997) Plant-derived anti-cancer agents. *Biochem. Pharmacol.* 53: 121-133.

- Pinhero RG, Paliyath G, Yada RY, Mur DP. (1999) Chloroplast membrane organization in chilling-tolerant and chilling sensitive maize seedlings. *J. Plant Physiol.* 155: 691-698.
- Piquemal J, Lapiere C, Myton K, O'Connell A, Schuch W, Grima-Pettenati J, Boudet AM. (1998) Down regulation of cinnamoyl-CoA reductase induces significant changes of lignin profiles in transgenic tobacco plants. *Plant J.* 13: 71-83.
- Potier P, Langlois N, Langlois Y, Gueritte F. (1975) Partial synthesis of vinblastine-type alkaloids. *J. Chem. Soc. Chem. Commun.* 670-671.
- Quiroga M, Guerrero C, Botella MA, Barceló A, Amaya I, Medina MI, Alonso FJ, Milrad de Forchetti S, Tigier H, Valpuesta V. (2000) A tomato peroxidase involved in the synthesis of lignin and suberin. *Plant Physiol.* 122: 1119-1127.
- Radić S, Radić-Stojković M, Pevalek-Kozlina B. (2006) Influence of NaCl and mannitol on peroxidase activity and lipid peroxidation in *Centaurea ragusina* L. roots and shoots. *J Plant Physiol.* 163: 1284-1292.
- Ralph J, Lundquist K, Brunow G, Lu F, Kim H, Schatz PF, Marita JM, Hatfield RD, Ralph SA, Christensen JH, Boerjan W. (2004) Lignins: Natural polymers from oxidative coupling of 4-hydroxyphenyl-propanoids. *Phytochem. Rev.* 3: 29
- Ramani S, Jayabaskaran C. (2008) Enhanced catharanthine and vindoline production in suspension cultures of *Catharanthus roseus* by ultraviolet-B light. *J. Mol. Signal* 3: 9.
- Reymond P, Farmer EE. (1998) Jasmonate and salicylate as global signals for defense gene expression. *Curr. Opin. Plant Biol.* 1: 404-411.
- Rhee SG, Chae HZ, Kim K. (2005) Peroxiredoxins: a historical overview and speculative preview of novel mechanisms and emerging concepts in cell signalling. *Free Radic. Biol. Med.* 38: 1543-1552.
- Reichmann JL and Meyerowitz EM. (1998) The AP2/EREBP family of plant transcription factors. *Biol. Chem.* 379: 633-664.
- Riou-Khamlichi C, Huntley R, Jacqmard A, Murray JAH. (1999) Cytokinin activation of Arabidopsis cell division through a D-type cyclin. *Science* 283: 1541-1544.
- Rizhsky L, Hallak-Herr E, Van Breusegem F, Rachmilevitch S, Barr JE, Rodermel S, Inze D, Mittler R. (2002) Double antisense plants lacking ascorbate peroxidase and catalase are less sensitive to oxidative stress than single antisense plants lacking ascorbate peroxidase or catalase. *Plant J.* 32: 329-342.
- Roberts E, Kolattukudy PE. (1989) Molecular cloning, nucleotide sequence, and abscisic acid induction of a suberization associated highly anionic peroxidase. *Mol. Gen. Genet.* 217: 223-232.
- Rodríguez-Concepción M, Boronat A. (2002) Elucidation of the methylerythritol phosphate pathway for isoprenoids biosynthesis in bacteria and plastids. A metabolic milestone achieved through genomics. *Plant Physiol.* 130: 1079-1089.
- Rogers SG, Horsch RB, Fraley RT. (1986) Gene transfer in plants: production of transformed plants using Ti plasmid vectors. *Meth. Enzym.* 118: 627-640
- Romano M, Baralle FE, Patriarca P. (2000) Expression and characterization of recombinant human eosinophil peroxidase. Impact of the R286H substitution on the biosynthesis and activity of the enzyme. *Eur. J. Biochem.* 267: 3704-3711.

- Ros Barceló A, Muñoz R. (2000) Metabolic plasticity of plant peroxidases. In: Hemantaranjan A (ed) *Advances in Plant Physiology*, Scientific Publishers, India, pp. 71-92.
- Rouhier N, Jacquot JP. (2002) Plant peroxiredoxins: alternative hydroperoxide scavenging enzymes. *Photosynthesis Res.* 74: 93-107.
- Salzwedel JL, Dazzo FB. (1993) pSym nod gene influence on elicitation of peroxidase activity from white clover and pea roots by rhizobia and their cell-free supernatants. *Mol. Plant-Microbe Interact.* 6: 127-134.
- Sambrook J, Russell DW. (2001) Southern blotting: Capillary transfer of DNA to membranes. In: *Molecular Cloning-A laboratory manual (Vol I)* Sambrook J, Russell DW (eds) Cold Spring Harbor Laboratory Press. New York pp. 6.39-6.46.
- Sambrook F, Fritsch EF, Maniatis F. (1989) *Molecular cloning: A laboratory manual*, Cold Spring Harbour Laboratory, New York.
- Samira M, Vincent C, Maritime T, Benoit S, Vincent B. (2006) Epidermis is a pivotal site of at least four secondary metabolic pathways in *C. roseus* aerial organs. *Planta* 223: 1191-1200.
- Samuelsson G. (1999) *Drugs of natural origin. A textbook of pharmacognosy*, 4 edn. Swedish Pharmaceutical Press, Sweden, pp 484-487.
- Sanger F, Nicklen S, Coulson AR. (1977) DNA sequencing with chain terminating inhibitors. *Proc. Natl. Acad. Sci. USA* 74: 5463-5467.
- Sasaki S, Baba K, Nishida T, Tsutsumi Y, Kondo R. (2006) The cationic cell-wall-peroxidase having oxidation ability for polymeric substrate participates in the late stage of lignification of *Populus alba* L. *Plant Mol Biol.* 62: 797-807.
- Sato F, Yamada Y. (1984) High berberine producing cultures of *Coptis japonica* cells. *Phytochemistry* 23: 281-285.
- Sato Y, Demura T, Yamawaki K, Inoue Y, Sato S, Sugiyama M, Fukuda H. (2006) Isolation and characterization of a novel peroxidase gene ZPO-C whose expression and function are closely associated with lignification during tracheary element differentiation. *Plant Cell Physiol.* 47: 493-503.
- Schröder G, Unterbusch E, Kaltenbach M, Schmidt J, Strack D, De Luca V, Schröder J. (1999) Light-induced cytochrome P450-dependent enzyme in indole alkaloid biosynthesis: tabersonine 16-hydroxylase. *FEBS Lett.* 458: 97-102.
- Schuller DJ, Ban N, Huystee RB, McPherson A, Poulos TL. (1996) The crystal structure of peanut peroxidase. *Structure* 4: 311-321.
- Schütte HR. (1986) Secondary plant substances: monoterpenoid indole alkaloids. *Progr. Botany* 48: 151-166.
- Scott AI, Gueritte F, Lee SL. (1978) Role of anhydrovinblastine in the biosynthesis of the antitumour dimeric indole alkaloids. *J. Am. Chem. Soc.* 100: 6253-6255.
- Serrano R, Rodriguez-Navarro A. (2001) Ion homeostasis during salt stress in plants. *Curr. Opin. Cell Biol.* 13: 399-404.
- Sherf BA, Bajar AM, Kolattukudy PE. (1993) Abolition of an inducible highly anionic peroxidase activity in transgenic tomato. *Plant Physiol.* 101: 201-208.

- Siegel BZ. (1993) Plant Peroxidases- an organismic perspective. *Plant Growth Reg.* 12: 303-312.
- Simon P. (1993) Diversity and conservation of plant peroxidases. *Plant Peroxidase Newslett.* 1: 4-7.
- Singh DV, Maithy A, Verma RK, Gupta MM, Kumar S. (2000) Simultaneous determination of *Catharanthus* alkaloids using reversed phase high performance liquid chromatography. *J. Liq. Chromatogr.* 23: 601-607.
- Skrabanek L, Wolfe KH. (1998) Eukaryote genome duplication- Where's the evidence? *Curr. Opin. Genet. Dev.* 8: 694-700.
- Smith AT, Veitch NC. (1998) Substrate binding and catalysis in heme peroxidases. *Curr. Opin. Chem. Biol.* 2: 269-278.
- Smith CG, Rodgers MW, Zimmerlin A, Ferdinando D, Bolwell GP. (1994) Tissue and subcellular immunolocalisation of enzymes of lignin synthesis in differentiating and wounded hypocotyl tissue of French bean (*Phaseolus vulgaris* L.). *Planta* 192: 155-164.
- Smith JI, Amouzou E, Yamagushi A, McLean S, Di Cosmo F. (1988) Peroxidase from bioreactor-cultivated *Catharanthus roseus* cell culture mediates biosynthesis of α -3',4'-anhydrovinblastine. *Biotechnol. Appl. Bioeng.* 10: 568-575.
- Sottomayor M, Cardoso IL, Pereira LG, Ros Barceló A. (2004) Peroxidase and the biosynthesis of terpenoid indole alkaloids in the medicinal plant *Catharanthus roseus* (L.) G. Don. *Phytochem. Rev.* 3: 159-171.
- Sottomayor M, de Pinto MC, Salema R, DiCosmo F, Pedreño MA, Ros Barceló A. (1996) The vacuolar localization of a basic peroxidase isoenzyme responsible for the synthesis of α -3',4'-anhydrovinblastine in *Catharanthus roseus* (L.) G. Don leaves. *Plant Cell Environ.* 19: 761-767.
- Sottomayor M, López-Serrano M, DiCosmo F, Ros Barceló A. (1998) Purification and characterization of alpha-3',4'-anhydrovinblastine synthase (peroxidase-like) from *Catharanthus roseus* (L.) G. Don. *FEBS Lett.* 428: 299-303.
- Sottomayor M, Ros Barceló A. (2003) Peroxidase from *Catharanthus roseus* (L.) G. Don and the biosynthesis of α -3', 4'-anhydrovinblastine: A specific role for a multifunctional enzyme. *Protoplasma* 222: 97-105.
- Stevens LH, Blom TJM, Verpoorte R. (1993) subcellular localization of tryptophan decarboxylase, strictosidine synthase and strictosidine glucosidase in suspension cultured cells of *Catharanthus roseus* and *Tabernaemontana divaricata*. *Plant Cell Rep.* 12: 573-576.
- Stewart Jr CN, Laura EV. (1993) A rapid CTAB DNA isolation technique useful for RAPD finger printing and other PCR applications. *Biotechnique* 14: 748-753.
- St-Pierre B, De Luca V. (1995) A cytochrome P-450 monooxygenase catalyzes the first step in the conversion of tabersonine to vindoline in *Catharanthus roseus*. *Plant Physiol.* 109: 131-139.
- St-Pierre B, Laflamme P, Alarco AM, De Luca V. (1998) The terminal O-acetyltransferase involved in vindoline biosynthesis defines a new class of proteins responsible for coenzyme A-dependent acyl transfer. *Plant J.* 14: 703-713.

- St-Pierre B, Vazquez-Flota FA, De Luca V. (1999) Multicellular compartmentation of *Catharanthus roseus* alkaloid biosynthesis predicts intercellular translocation of a pathway intermediate. *Plant Cell* 11: 887-900.
- Stuart KL, Kutney JP, Honda T, Worth BR. (1978) Intermediacy of 3', 4'-dehydrovinblastine in the biosynthesis of vinblastine type alkaloids. *Heterocycles* 9: 1419-1426.
- Tabata M, Hiraoka N. (1976) Variation in alkaloid production in *Nicotiana rustica* callus cultures. *Physiol. Plant.* 38: 19-23.
- Takahama U, Oniki T. (1991) Participation of peroxidase in the metabolism of 3, 4-dihydroxyphenylalanine and hydrogen peroxide in Vacuoles of *Vicia faba* L. mesophyll cells *Plant Cell Physiol.* 32: 745-754.
- Takahama U. (1992) Hydrogen peroxide scavenging systems in vacuoles of mesophyll cells of *Vicia faba* L. *Phytochemistry* 32: 1127-1133.
- Talas-Oğras T, Kazan K, Gözkirmizi N. (2001) Decreased peroxidase activity in transgenic tobacco and its effects on lignification. *Biotech. Lett.* 23: 267-273.
- Tamura K, Dudley J, Nei M, Kumar S. (2007) MEGA4: Molecular Evolutionary Genetics Analysis (MEGA) Software Version 4.0. *Mol. Biol. Evol.* 24: 1596-1599.
- Tanaka S, Ikeda K, Ono M, Miyasaka H. (2002) Isolation of several anti-stress genes from mangrove plant *Avicennia marina*. *World J. Microbiol. Biotechnol.* 18: 801-804.
- Taurog A. (1999) Molecular evolution of thyroid peroxidase. *Biochimie.* 81: 557-562.
- Tognolli M, Penel C, Greppin H, Simon P. (2002) Analysis and expression of the class III peroxidase large gene family in *Arabidopsis thaliana*. *Gene* 288: 129-138.
- Tyler VE. (1988) Medicinal plant research: 1953-1987. *Planta Med.* 54: 95-100.
- Valério L, De Meyer M, Penel C, Dunand S. (2004) Expression analysis of the *Arabidopsis* peroxidase multigene family. *Phytochemistry* 65: 1331-1342.
- van der Fits L, Deakin EA, Hoge JHC, Memelink J. (2000) The ternary transformation system: constitutive virG on a compatible plasmid dramatically increases *Agrobacterium*-mediated plant transformation. *Plant Mol. Biol.* 43: 495-502.
- van der Fits L, Memelink J. (2000) ORCA3, a jasmonate- responsive transcriptional regulator of plant primary and secondary metabolism. *Science* 289: 295-297.
- van der Heijden R, Jabos DJ, Snoeijer W, Hallard D, Verpoorte R. (2004) The *Catharanthus* alkaloids: pharmacognosy and biotechnology. *Curr. Med. Chem.* 11: 607-628.
- Vazquez-Flota F, De Carolis E, Alarco AM, De Luca V. (1997) Molecular cloning and characterization of desacetoxyvindoline-4-hydroxylase, a 2-oxoglutarate dependent-dioxygenase involved in the biosynthesis of vindoline in *Catharanthus roseus* (L.) G. Don. *Plant Mol. Biol.* 34: 935-948.

- Veau B, Courtois M, Oudin A, Chénieux JC, Rideau M, Clastre M. (2000) Cloning and expression of cDNAs encoding two enzymes of the MEP pathway in *Catharanthus roseus*. *Biochim. Biophys. Acta.* 1517: 159-163.
- Veitch NC, Smith AT. (2001) Horseradish peroxidase. *Adv. Inorg. Chem.* 51: 107-161.
- Verpoorte R, Memelink J. (2002) Engineering secondary metabolite production in plants. *Curr. Opin. Biotechnol.* 13: 181-187.
- Verpoorte R, van der Heiden R, ten Hoopen HJG, Memelink J. (1999) Metabolic engineering of plant secondary metabolite pathways for the production of fine chemicals *Biotech. Lett.* 21: 467-479.
- Verpoorte R, van der Heijden R, Memelink J. (2000) Engineering the plant cell factory for secondary metabolite production. *Transgenic Res.* 9: 323-343.
- Verpoorte R, van der Heijden R, Moreno PRH. (1997) Biosynthesis of terpenoid indole alkaloids in *Catharanthus roseus* cells. In: Cordell GA (ed) *The alkaloids*, vol 49. Academic Press, San Diego, USA, pp. 221.
- Verpoorte R, van der Heijden R, Schripsema J, Hoge JHC, ten Hoopen HJG. (1993) Plant cell biotechnology for the production of alkaloids present status and prospects. *J. Nat. Prod.* 56: 186-207.
- Watson CJ, Froehlich JE, Josefsson CA, Chapple C, Durst F, Benveniste I, Coolbaugh RC. (2001) Localization of CYP86B1 in the outer envelope of chloroplasts. *Plant Cell Physiol.* 42: 873-878.
- Welinder KG. (1992) Superfamily of plant, fungal and bacterial peroxidases. *Curr. Opin. Struct. Biol.* 2: 388-393.
- Welinder KG, Justesen AF, Kjærsgård IVH, Jensen RB, Rasmussen SK, Jespersen HM, Duroux L. (2002) Structural diversity and transcription of class III peroxidases from *Arabidopsis thaliana*. *Eur. J. Biochem.* 269: 6063-6081.
- Welinder KG, Mauro JM, Nørskov-Lauritsen L. (1992) Structure of plant and fungal peroxidases. *Biochem. Soc. Trans.* 20: 337-340.
- Welinder KG. (1976) Covalent structure of the glycoprotein horseradish peroxidase EC 1.11.1.7. *FEBS Lett.* 72: 19-23.
- Welinder KG. (1985) Plant peroxidase: Their primary, secondary and tertiary structures, and relation to cytochrome c peroxidase, *Eur. J. Biochem.* 151: 497-504.
- Welinder KG. (1991) The plant peroxidase superfamily. In: Lobarzewski J, Greppin H, Penel C, Gaspar Th (eds) *Biochemical, Molecular and Physiological Aspects of Plant peroxidases*. University of Geneva, Switzerland, pp. 3-13.
- Welinder KG. (1992) Superfamily of plant, fungal and bacterial peroxidases. *Curr. Opin. Struct. Biol.* 2: 388-393.
- Welinder KG. (1992a) Plant peroxidases: structure-function relationships. In: C Penel, Gaspar Th, Greppin H (eds) *Plant Peroxidases* University of Geneva, Switzerland pp 1980-1990.
- Whetten RW, Mackay JJ, Sederoff RR. (1998) Recent advances in understanding lignin biosynthesis. *Annu. Rev. Plant Physiol. Plant Mol. Biol.* 49: 585-609.

- White PR, Braun AC. (1942) A cancerous neoplasm of plants. Autonomous bacteria-free crown-gall tissue. *Cancer Res.* 2: 597-617.
- Wink M. (2004) *Medicinal plants of the world: An illustrated scientific guide to important medicinal plants and their uses.* Timber press, USA, pp 480.
- Yeoman MM, Yeoman CL. (1996) Tansley review No 90 Manipulating secondary metabolism in cultured plant cells. *New Phytol.* 134: 553-569.
- Yi SY, Hwang BK. (1998) Molecular cloning and characterization of a new basic peroxidase cDNA from soybean hypocotyls infected with *Phytophthora sojae f.sp. glycines*. *Mol. Cells* 31: 556-564.
- Yoshida K, Kaothien P, Matsui T, Kawaoka A, Shinmyo A. (2003) Molecular biology and application of plant peroxidase genes. *Appl. Microbiol. Biotechnol.* 60: 665-670.
- Yoshimura K, Yabuta Y, Ishikawa T, Shigeoka S. (2000) Expression of spinach ascorbate peroxidase isoenzymes in response to oxidative stress. *Plant Physiol.* 123: 223-233.
- Yun BW, Huh GH, Lee HS, Kwon SY, Jo JK, Kim JS, Cho KY, Kwak SS. (2000) Differential resistance to methyl viologen in transgenic tobacco plants that express sweet potato peroxidases. *J. Plant Physiol.* 156: 504-509.
- Zhang J. (2003) "Evolution by gene duplication: an update", *Trends in Ecology and Evolution*, 18: 292-298.
- Zhong R, Herbert Morrison III W, Negrel J, Ye Z-H. (1998) Dual methylation pathways in lignin biosynthesis. *Plant Cell* 10: 2033-2046.

Cloning, characterization and localization of a novel basic peroxidase gene from *Catharanthus roseus*

Santosh Kumar, Ajaswata Dutta, Alok K. Sinha and Jayanti Sen

National Centre for Plant Genome Research, JNU Campus, Aruna Asaf Ali Marg, New Delhi, India

Keywords

Catharanthus roseus; organ specific; peroxidase; terpenoid indole alkaloid; subcellular localization

Correspondence

A. K. Sinha, National Centre for Plant Genome Research, JNU Campus, Aruna Asaf Ali Marg, New Delhi 110 067, India
Fax: +91 11 26716658
Tel: +91 11 26735188
E-mail: alokksinha@yahoo.com
Website: <http://www.ncpgr.nic.in>

Note

This paper is dedicated to the inspirational memory of Dr Jayanti Sen

(Received 1 December 2006, revised 2 January 2007, accepted 3 January 2007)

doi:10.1111/j.1742-4658.2007.05677.x

Catharanthus roseus (L.) G. Don produces a class of secondary metabolites, namely, terpenoid indole alkaloids (TIAs), with antitumor properties. Two of these leaf-specific dimeric alkaloids, vinblastine and vincristine, are used as valuable drugs in cancer chemotherapy. Owing to the medicinal importance of these alkaloids and their low levels in *C. roseus in vivo*, TIA biosynthesis has been intensively studied in this plant. The TIA biosynthetic pathway (supplementary Fig. S1) is highly complex, involves more than 20 enzymatic steps, and is reported to be stress-induced, mainly due to the increased transcription of biosynthetic genes [1,2]. How-

Catharanthus roseus (L.) G. Don produces a number of biologically active terpenoid indole alkaloids via a complex terpenoid indole alkaloid biosynthetic pathway. The final dimerization step of this pathway, leading to the synthesis of a dimeric alkaloid, vinblastine, was demonstrated to be catalyzed by a basic peroxidase. However, reports of the gene encoding this enzyme are scarce for *C. roseus*. We report here for the first time the cloning, characterization and localization of a novel basic peroxidase, CrPrx, from *C. roseus*. A 394 bp partial peroxidase cDNA (*CrInt1*) was initially amplified from the internodal stem tissue, using degenerate oligonucleotide primers, and cloned. The full-length coding region of *CrPrx* cDNA was isolated by screening a leaf-specific cDNA library with *CrInt1* as probe. The *CrPrx* nucleotide sequence encodes a deduced translation product of 330 amino acids with a 21 amino acid signal peptide, suggesting that CrPrx is secretory in nature. The molecular mass of this unprocessed and unmodified deduced protein is estimated to be 37.43 kDa, and the pI value is 8.68. *CrPrx* was found to belong to a 'three intron' category of gene that encodes a class III basic secretory peroxidase. CrPrx protein and mRNA were found to be present in specific organs and were regulated by different stress treatments. Using a β -glucuronidase-green fluorescent protein fusion of CrPrx protein, we demonstrated that the fused protein is localized in leaf epidermal and guard cell walls of transiently transformed tobacco. We propose that *CrPrx* is involved in cell wall synthesis, and also that the gene is induced under methyl jasmonate treatment. Its potential involvement in the terpenoid indole alkaloid biosynthetic pathway is discussed.

ever, the genes involved in the final dimerizing step of the coupling of monomeric precursors, catharanthine and vindoline, to yield leaf-specific α -3'-4'-anhydrovinblastine (AVLB), and the final step of conversion of root-specific ajmalicine to serpentine, have not yet been identified. Previous studies have led to the finding of a class III basic peroxidase in *C. roseus* that shows AVLB synthase activity and is localized in vacuoles [3–5].

Plant peroxidases are reported to be involved in various physiological processes [6–9]. Class III plant peroxidases, considered to be plant-specific oxidoreductases, have been found to participate in lignification

Abbreviations

AVLB, α -3'-4'-anhydrovinblastine; GFP, green fluorescent protein; GST, glutathione *S*-transferase; GUS, β -glucuronidase; HRP, horseradish peroxidase; MJ, methyl jasmonate; TIA, terpenoid indole alkaloid.

[10], wound healing [11], defense against pathogen attack, including crosslinking of cell wall protein [12], and aspects of plant growth regulator action [13]. Furthermore, the presence of a separate hydroxylic cycle, which leads to the formation of various radical species, opens a new range of possibilities for this class of enzymes [14]. Plant peroxidases are reported to have many different isoforms; 73 members have so far been identified in *Arabidopsis thaliana* [15]. The expressed proteins of these genes are reported to be localized either in the cell wall or in the vacuole. In this article, we report the cDNA cloning, characterization and sub-cellular localization of a novel stress-induced peroxidase (*CrPrx*) from *C. roseus* belonging to the class III basic peroxidase family. The observed expression patterns suggest its potential role during stress conditions and elicitor treatment in *C. roseus*. *CrPrx* tagged with β -glucuronidase (GUS)-green fluorescent protein (GFP) was expressed in *Nicotiana tabacum* and *C. roseus* leaf epidermal cells as well as in xylem cell wall thickening. The possibility of its involvement in the TIA biosynthetic pathway has also been discussed.

Results

CrPrx cDNA is 1197 bp long

Degenerate oligonucleotide primers, PF1 and PR1, were designed on the basis of the conserved amino acid sequences of proteins (RLHFHDC and VALLGAHSVG) encoded by the class III peroxidase gene family and used to amplify cDNA fragments from different tissues of *C. roseus* var. Pink. A 394 bp partial peroxidase cDNA (*CrInt1*; accession number AY769111) was amplified from the internodal stem tissue by RT-PCR; upon sequencing, this showed similarity with a truncated class III peroxidase ORF. Full-length *C. roseus* peroxidase cDNA (*CrPrx*) was isolated by screening a leaf-specific cDNA library with the 394 bp partial *CrInt1* as a probe. A single positive plaque that was identified after tertiary screening revealed a 1357 bp full-length cDNA with a 5'-UTR and a 3'-UTR upon sequencing (accession number AY924306) (Fig. 1). The complete coding region for *CrPrx* was then amplified using a primer pair complementary to the 5'-UTR and 3'-UTR regions of *CrPrx* that was 1197 bp in length, excluding part of the 3'-UTR and the polyA tail (accession number DQ415956).

CrPrx encodes a class III peroxidase

Computational analysis of the *CrPrx* nucleotide sequence showed that it encodes a 330 amino acid

polypeptide (Fig. 1). The molecular mass of this deduced protein is calculated to be 37.43 kDa, and it has a theoretical pI of 8.68. The analysis of *CrPrx* protein using SIGNAL P v3.0 software [16] identified a putative 21 amino acid signal peptide that was cleaved between Ala21 and Glu22. *CrPrx* protein showed an N-terminal extension of eight amino acids (Glu-Asn-Glu-Ala-Glu-Ala-Asp-Pro) before the start of the mature protein as an NX-propeptide (Fig. 1). BLAST searches [17] revealed significant sequence identity between *CrPrx* and a number of other class III plant peroxidases (EC 1.11.1.7), notably secretory peroxidases from *Avicennia marina* (accession number AB049589) and *Nicotiana tabacum* (accession number AF149252) (Fig. 2). The amino acid sequences of seven mature peroxidases, including *CrPrx*, were all close to 300 residues (Fig. 2). They showed 33–86% amino acid identity and share 67 conserved residues. When compared with horseradish peroxidase (HRP)-C [18], the translated polypeptide showed that it contains all the eight conserved cysteines for disulfide bonds, and all the indispensable amino acids required for heme binding, peroxidase function, and coordination of two Ca^{2+} ions (Fig. 2).

CrPrx contains three introns and four exons

To obtain an insight into the complete sequence of *CrPrx*, PCR was performed using primer pair PFLF1 and PFLR1, designed to anneal to conserved 5'-UTR and 3'-UTR regions (accession number DQ415956), with genomic DNA of *C. roseus* as template. The amplified product upon cloning and sequencing was found to be 1793 bp long (accession number DQ484051). *CrPrx* consists of four exons (268 bp, 189 bp, 172 bp, 405 bp, stop at UAG) and three introns (95 bp, 435 bp, 79 bp) (Fig. 3A,B). The first and third introns were more or less similar in size. The second intron in *CrPrx* was found to be the largest, and was even larger in size than the exons. This *CrPrx* structure supports the concept of origin of peroxidases from a common ancestral gene of peroxidases with three introns and four exons.

CrPrx is present in single copy in the *C. roseus* genome

Southern blot analysis was performed on genomic DNA of *C. roseus* plants (obtained by self-pollination), digested with *Bgl*II, *Eco*RV and *Hind*III (with 0, 1 and 0 cut site, respectively) and probed with full-length *CrPrx* cDNA at high stringency (Fig. 4). The auto-

```

1 ggcacgagctgaccttcactgtctacttcggacacgtaatcc
43 ATGGCTTCCAAACTCTCTTCTCCTTGTCATTCTCTCCTTCTCT
1
88 GCTCTCTCAACTTTTGCTGAAAATGAAGCCGAGGCAGACCCTGGT
16
133 CTTGTAATGAACATTACAAGGATTCATGTCCTCAAGCTGAAGAT
31 L V M N Y Y K D S C P Q A E D
178 ATCATCAGGGAACAAGTCAAACCTTTTACAAACATCACAAGAAC
46 I I R E Q V K L L Y K H H K N
223 ACCGCTTTCTCTTGGCTAAGGAACATTTTCCATGATTGCTTTGTC
61 T A F S W L R N I F H D C F V
268 GAATCTTGTGATGCTTCATTGTTGCTGGACTCAACTAAAAAGTC
76 E S C D A S L L L D S T K K V
313 CTGTCTGAGAAGGAAACAGATAGGAGTTTTGGAATGAGGAATTTT
91 L S E K E T D R S F G M R N F
358 AGATACCTTGAAGCATCAAAGAAGCCCTTGAAAGGGAGTGTCTCT
106 R Y L E D I K E A L E R E C P
403 GGAGTTGTTTCTTGTGCTGATATTCTTGTGTTTGTCTGCAAGAAAT
121 G V V S C A D I L V L S A R N
448 GGCATTGTTTCGTTAGGAGGGCCATTTATCCCTCTTAAAACCGGA
136 G I V S L G G P F I P L K T G
493 AGAAGAGATGGCAGGAGAAGCAGAGCAGAGATACTGGAGCAACAT
151 R R D G R R S R A E I L E Q H
538 CTCCCAGACCACAATGAGAGCCTCACTGTTGTTCTTGAGAGGTTT
166 L P D H N E S L T V V L E R F
583 GGATCTATTGGCATCAATACCCCTGGCTTGGTTGCCTTGCTAGGT
171 G S I G I N T P G L V A L L G
628 GCTCATAGTGTGGGAGAACCCTGTTGTAAGCTGGTTCATCGT
186 A H S V G R T H C V K L V H R
673 TTATATCCAGVGTGGATCCTGCATTTCCAGAGGCCATGTTTCAG
201 L Y P E V D P A F P E S H V Q
718 CACATGTTAAAGAAGTGCCCTGATCCAATTCCTGATCCAAAGGCA
216 H M L K K C P D P I P D P K A
763 GTACAATATGTAAGAAATGACAGAGGAACACCTATGAAATTAGAC
231 V Q Y V R N D R G T P M K L D
808 AACAAATTATTACAGAAACATCTTGGACAACAAGGGCTTGTGCTA
246 N N Y Y R N I L D N K G L L L
853 GTCGATACCAATTAGCCACAGACAAAAGAACAAAACCATTTGTC
261 V D H Q L A T D K R T K P F V
898 AAGAAATGGCAAAAAGCCAAGATTACTTCTTAAAGGAATTTGCA
276 K K M A K S Q D Y F F K E F A
943 AGAGCCATTACTATCTGTCTGAAAATAACCCTCTTACTGGTACT
293 R A I T I L S E N N P L T G T
988 AAAGGTGAGATTAGAAAGCAGTGAATGTAGCTAATAAGTTACAT
318 K G E I R K Q C N V A N K L H
1033 TAGaagattagattatgaaatcccccttctttctttcatgattgt
333 *
1077 aatcaattgtaatcatgaggaagaagaaccagaggggatggatggaataagttgt:ttttaa
1141 aaggcctgccaanaatagtgtagttgctttggcataggcaa:tgtaatggtggtgagcatttc
1207 tgtgttacttgcactatcattgtactagggtgcttctcatgttcccttcatgtttatggg
1278 ggggctgatggccatggatgcttgaatattggatgaatgcatctgtaatacaagttg
1345 tttt taaaaaaaaaaaaaaaaaaaaaa

```

Fig. 1. The complete *CrPrx* cDNA sequence and its translation product. The 5'-UTR and 3'-UTR are represented in lower case; the stop codon is indicated by *. The putative signal peptide is boxed in gray. A predicted NX-propeptide is boxed. A predicted N-glycosylation site (NESL) is underlined. Nucleotide sequences in red represent predicted polyA signal sequences.

radiograph, showing bands of different sizes, revealed that *CrPrx* occurs as single copy in the *Catharanthus* diploid genome of *C. roseus* plants.

Phylogenetic analysis

The relationship between *CrPrx* cDNA and other cDNAs encoding class III peroxidases was investigated using a parsimonious phylogenetic analysis. BLAST searches were used to identify other full-length peroxidase cDNA sequences showing close similarity to *CrPrx*. The varying degrees of expression patterns of peroxidase cDNAs in different tissues in different plant systems under stress was taken into considera-

tion during this study (Table 1). Phylogenetic analysis was performed on the aligned nucleotide sequences corresponding to the cDNA ORFs (Fig. 5). The tree was rooted with the *Spinacea prx14* sequence, which may be distantly related to the *CrPrx* sequence. Most of these cDNAs, with a few exceptions, are expressed in both vegetative and reproductive tissues, and are stress-induced. *CrPrx* expression was also noted in all the tissues tested and found to be stress-inducible. After its origin from *Spinacea prx14*, the tree showed a divergence from a liverwort peroxidase, indicating a distant relationship of ancestral *Marchantia* peroxidase with this angiosperm *CrPrx* sequence.

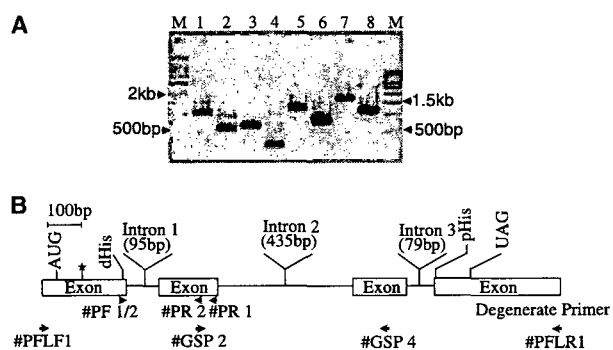


Fig. 3. Intron mapping of *CrPrx* gene. (A) Lanes M show size markers in base pairs. Lanes 2, 4, 6 and 8 show PCR reactions run on plasmid DNA harboring *CrPrx* cDNA, and lanes 1, 3, 5 and 7 show the same using genomic DNA of *C. roseus*. Primer pairs were: #GSP-4 and #PFLR1 (lanes 1 and 2); #GSP-2 and #GSP-4 (lanes 3 and 4); #GSP-2 and #PFLR-1 (lanes 5 and 6); and #PFLR-1 and #PFLR-1 (lanes 7 and 8). (B) Schematic organization of the *CrPrx* gene. The asterisk indicates the position of the codon encoding the first amino acid of the mature protein, and the regions of the distal and proximal histidines are indicated by dHis and pHis.

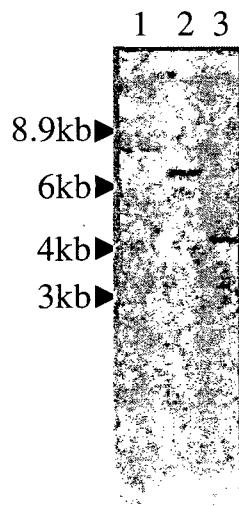


Fig. 4. DNA gel blot of *C. roseus* probed with full-length *CrPrx* cDNA. Lanes 1, 2 and 3 show the genomic DNA digested with *Bgl*II, *Eco*RV and *Hind*III restriction enzymes, respectively.

Internodal stem tissue shows maximum *CrPrx* expression

Northern blot analysis revealed expression of *CrPrx* in different organs of *C. roseus*, i.e. leaves (young, mature and old), flower buds, open flowers, fruits, roots, and internodal stem tissue (Fig. 6A). Among vegetative tissues, the transcript was maximal in internodal stem

Table 1. References used for sequence and expression data presented in Fig. 5. for phylogenetic analysis. NA, not available.

Label	Accession no.	MIPS	Reference
Glycine <i>Prx2b</i>	AF145348	NA	Unpublished
<i>Cicer</i> peroxidase	AJ271660	NA	Unpublished
<i>Avicennia</i> peroxidase	AJ271660	NA	[25]
<i>Nicotiana</i> peroxidase	AF149251	NA	[7]
<i>CrPrx</i>	AY924306	NA	Present study
<i>Arabidopsis ATP1a</i>	X98189	NA	[43]
<i>Arabidopsis prx5</i>	X98317	NA	[43]
<i>Arabidopsis prx</i>	AY087458	NA	[44]
<i>Marchantia MpPOD1</i>	AB086023	NA	Unpublished
<i>Oryza prx71</i>	BN000600	NA	[14]
<i>prx97</i>	BN000626	NA	[14]
<i>TPA inf</i>	BN000568	NA	[14]
<i>Triticum POX7</i>	AY857761	NA	[45]
<i>Hordeum BP1</i>	M73234	NA	[46]
<i>WSP1</i>	AF525425	NA	Unpublished
<i>Arabidopsis RC13A</i>	U97684	NA	[47]
<i>Arabidopsis BT024864</i>	BT024864	At5g40150	Unpublished
<i>Senecio SSP5</i>	AJ810536	NA	[48]
<i>Spinacia PC42</i>	Y10464	NA	[49]
<i>Spinacia PB11</i>	Y10462	NA	[49]
<i>Euphorbia prx</i>	AY586601	NA	[50]
<i>Vigna prx</i>	D11337	NA	[51]
<i>Catharanthus prx1</i>	AM236087	NA	Unpublished
<i>Medicago prx</i>	X90693	NA	[52]
<i>Zinnia ZPO-C</i>	AB023959	NA	[53]
<i>Glycine GMIPER1</i>	AF007211	NA	[54]
<i>Spinacia PC23</i>	Y10467	NA	[49]
<i>Quercus POX2</i>	AY443340	NA	[55]
<i>Ipomoea swpb3</i>	AY206414	NA	[56]
<i>AtPrx</i>	AY065270	At5g05340	Unpublished
<i>Asparagus prx3</i>	AJ544516	NA	[57]
<i>Picea SPI2</i>	AJ250121	NA	[58]
<i>Picea px17</i>	AM293547	NA	Unpublished
<i>Picea px16</i>	AM293546	NA	Unpublished
<i>Nicotiana PER4</i>	AY032675	NA	Unpublished
<i>Dimocarpus POD1</i>	DQ650638	NA	Unpublished
<i>Ipomoea swpb1</i>	AY206412	NA	[56]
<i>Ipomoea swpb2</i>	AY206413	NA	[56]
<i>Spinacia prx14</i>	AF244923	NA	Unpublished

tissues, followed by roots, young leaves, and mature leaves. Among reproductive tissues, the transcript was most abundant in fruits, followed by young buds. *CrPrx* expression was not detected in old leaves and flowers.

In order to purify *CrPrx* for preparation of antibody, a glutathione *S*-transferase (GST)-*CrPrx* fusion protein was constructed in pGEX 4T-2 vector with *CrPrx* ORF (PPGX) and expressed in a bacterial system. As the protein was repeatedly found in inclusion bodies, different concentrations of glutathione, sarcosyl and Triton X-100 were tested to achieve purification of the fusion protein (Fig. 6B). The purified protein was

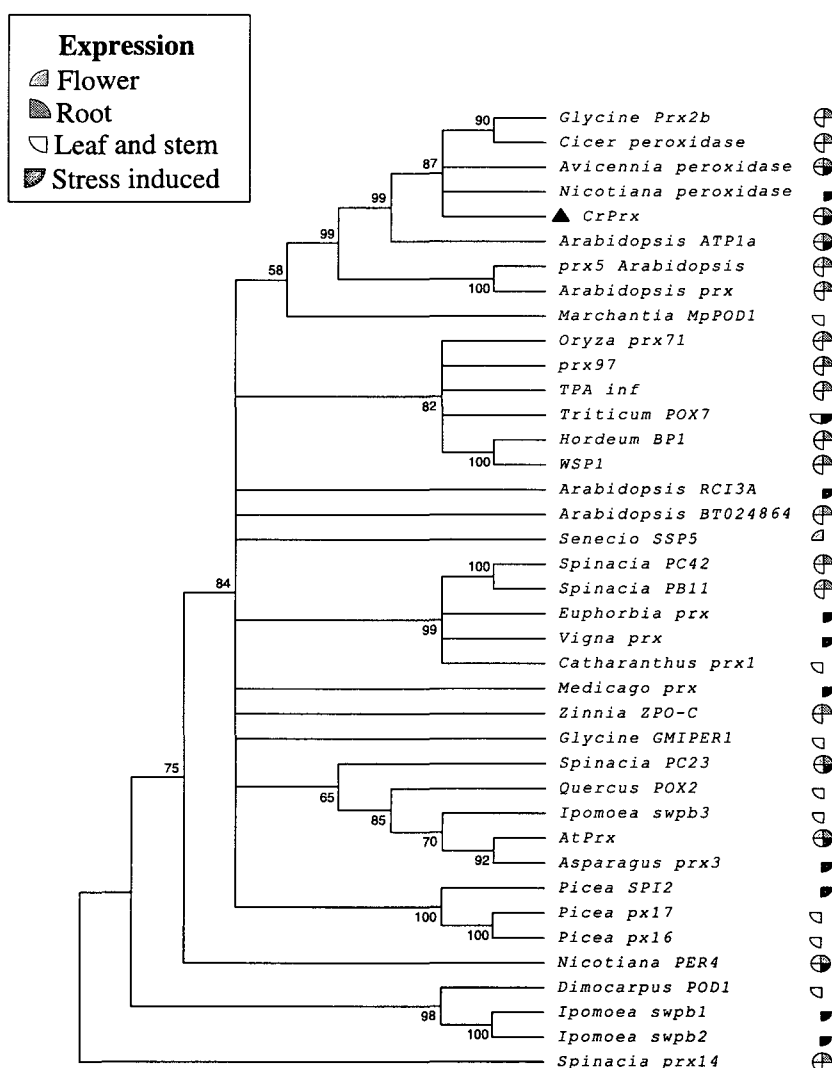


Fig. 5. Phylogenetic relationships between peroxidase cDNA, *CrPrx* and other related class III peroxidases. Alignment consists of the nucleotide sequences of coding regions. Bootstrap values mark the percentage frequency at which sequences group in 100 resampling replicates. The expression pattern is represented by semi-color circles indicating: floral, vegetative and stress-inducible (abiotic and biotic) expression. Information on expression is referenced in Table 1, gathered from published and unpublished sources and from NCBI databases.

used for preparation of polyclonal antibodies against *CrPrx* in rabbit. Immunoblot analysis performed using different organs of *C. roseus* revealed differential accumulation of *CrPrx* in different organs, with a maximum level of accumulation in the internodes (Fig. 6C). *CrPrx* was detected at 37 kDa, whereas heterologously expressed GST-*CrPrx* was detected at 63 kDa (Fig. 6C, first lane).

***CrPrx* transcript is induced by various abiotic stresses and methyl jasmonate**

Many plant peroxidase genes are reported to be induced in vegetative tissues by stress, particularly wounding [19,20]. To investigate whether *CrPrx* expression is stress-induced, leaves of *C. roseus* were subjected to different stress conditions as well as

methyl jasmonate (MJ) treatment, and analyzed for *CrPrx* transcript regulation over a time course of 24 h (Fig. 7A,B). An increase in the level of *CrPrx* expression was noted with increasing time when leaves were either wounded or exposed to UV and cold treatments. The expression level reached its peak after 6 h of wound treatment, following an initial decline during the first hour. In the case of UV and cold exposure, the maximum transcript level was observed at 12 and 24 h, respectively. On the other hand, a gradual steady-state increase in the expression level of *CrPrx* was noted with increasing time in response to application of 100 μ M MJ on leaves. This was later confirmed by immunoblot analysis, which revealed accumulation of *CrPrx* in *C. roseus* leaves after 6 h of wound stress and 6–12 h of treatment with 100 μ M MJ (Fig. 7C).

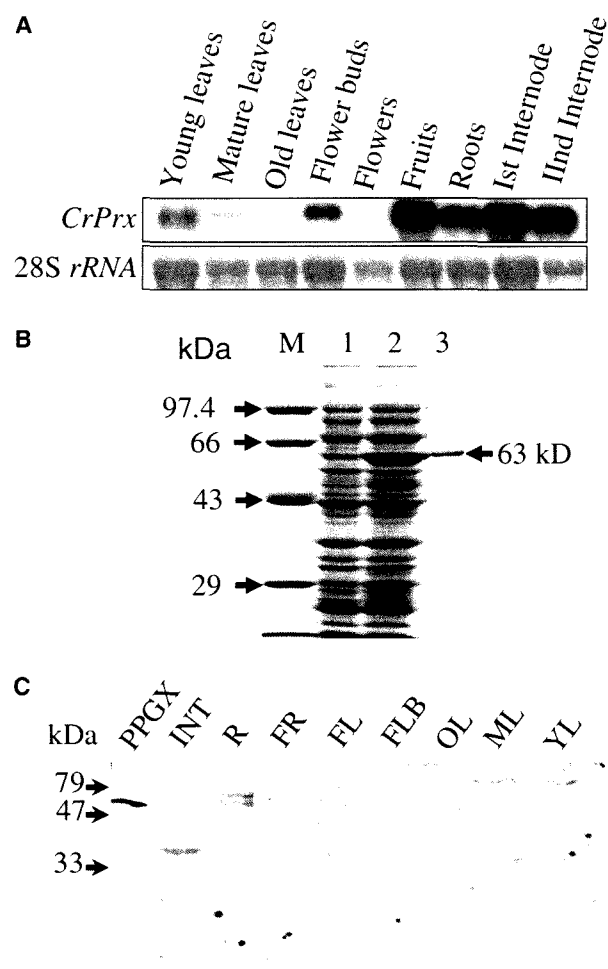


Fig. 6. (A) Northern blot analysis. Upper panel shows *CrPrx* expression, with each lane containing 20 μ g of total RNA. (B) Large-scale purification of GST fusion CrPrx protein; the mobility of the fusion protein matches its predicted molecular weight. Lanes M, 1, 2 and 3 show molecular weight markers, total protein from uninduced bacterial culture, induced bacterial lysate, and purified eluted CrPrx fusion protein, respectively. (C) Immunoblot analyses of *CrPrx* expression in various tissue types; denaturing SDS/PAGE of total proteins extracted from various organs, followed by immunoblotting using the antibodies to CrPrx. The blot was imaged on X-ray film using chemiluminescent substrate. PPGX is CrPrx cloned in PGEX 4T-2 fusion vector as a purified GST fusion protein.

Subcellular localization of GUS-GFP fused CrPrx

To examine the subcellular localization of CrPrx in *N. tabacum* and *C. roseus*, the *CrPrx* coding region was fused in-frame to the coding region for the N-terminal side of GUS and GFP under the control of the 35S promoter of cauliflower mosaic virus (*CaMV*) in pCambia 1303. When the construct *CrPrx-GUS-GFP* was expressed in transformed tobacco and in

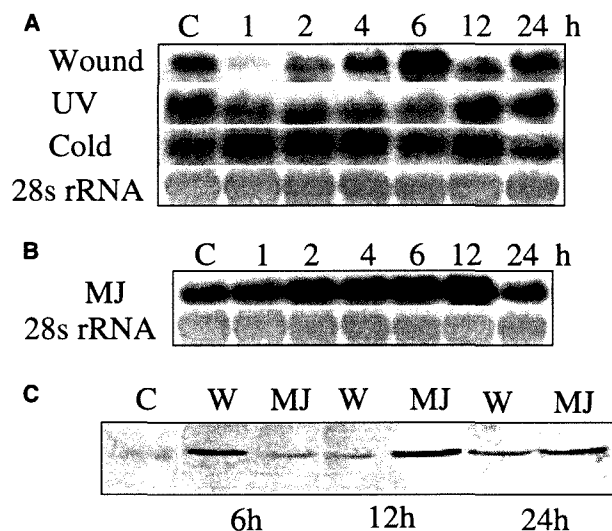


Fig. 7. Northern blot and immunoblot analysis of *CrPrx* transcript and protein, respectively. (A, B) Transcript regulation of *CrPrx* under different abiotic stress conditions and 100 μ M MJ; the lower panel shows methylene blue-stained 28S rRNA as loading control. (C) Immunoblot analysis of CrPrx after wounding and 100 μ M MJ treatment with antibodies to CrPrx. Blots were imaged on X-ray film using chemiluminescent substrate. C, untreated control; W, wounding.

C. roseus, GUS staining and green fluorescence were observed in the epidermal parenchymatous cells, stomatal guard cells, and vascular tissues (xylem tissue) (Figs 8A–F and 9A–E). However, in epidermal parenchymatous and stomatal guard cells, CrPrx-GUS-GFP was found to be accumulated mostly in the cell walls, outer cell membranes and associated structures (Figs 8A,B and 9A,B). On detailed examination, CrPrx-GFP fluorescent dots were visible in the part of the epidermal cell wall abutting a mature guard cell in tobacco leaf tissue (Fig. 8B). In xylem tissue, CrPrx-GFP fluorescence was observed specifically in the secondary wall thickenings both in tobacco and in *C. roseus* (Figs 8F and 9D,E).

Discussion

We report here the cloning, characterization and localization of a novel *C. roseus* peroxidase, CrPrx, for the first time. This particular full-length *CrPrx* cDNA (1359 bp) and its functional product were noted to be localized and expressed in different tissues of the plant tested. Computational analysis revealed that the translated polypeptide sequence of CrPrx contains eight conserved cysteine residues forming disulfide bridges, two Ca^{2+} -binding ligands, and distal and proximal heme-binding domains, in

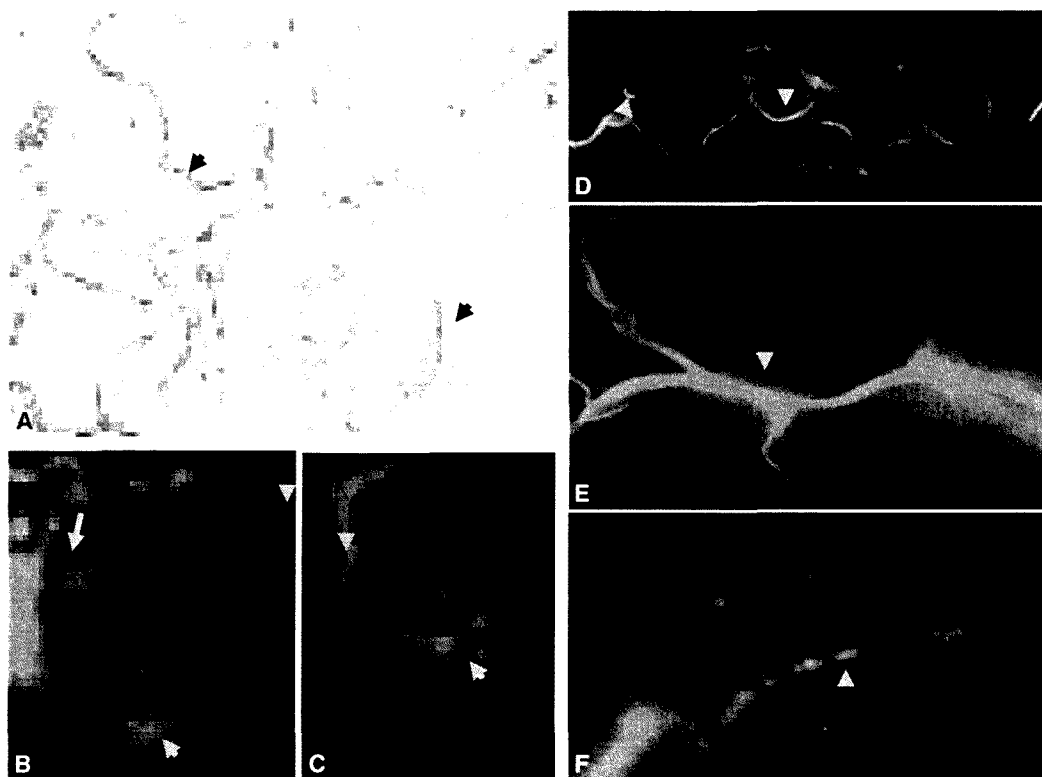


Fig. 8. GUS and GFP fluorescence patterns of *CrPrx* expression in *N. tabacum* leaf. (A) GUS staining and (B) GFP fluorescence patterns of the same. (C–E) GFP fluorescence patterns of stomatal guard cells, leaf epidermal cells and (F) xylem cells of transiently transformed *N. tabacum* with *CrPrx*–GUS–GFP. In epidermal and stomatal guard cells, *CrPrx*–GFP is restricted to the cell wall and associated structures, the membranes of the central vacuole, and the wall thickening of xylem cells (→).

common with other plant peroxidases [18,21,22]. The inclusion of Ser96 and Asp99 in a salt bridge motif at the beginning of helix D and its connection to the following long loop by a tight hydrogen bonding network with Gly121–Arg122 was also an important feature in *CrPrx* [15]. The presence of a signal peptide and the lack of a carboxyl extension identifies *CrPrx* as a secretory (class III) plant peroxidase, rather than a vacuolar plant peroxidase. Unlike other class III peroxidases, the mature *CrPrx* polypeptide starts with a glycine (G) residue and not with glutamine (Q) residue. This feature will possibly make the *CrPrx* polypeptide unable to generate a pyrrolidone carboxyl residue (Z) [23].

The full-length *CrPrx* gene, like most of the plant peroxidase genes, contains three introns, which differ in their sizes [24]. Phylogenetic analysis grouped *CrPrx* cDNA with the ancestral *Marchantia* peroxidase cDNA. The two peroxidase cDNAs that were found to be structurally most closely related to *CrPrx* are *Av. marina* [25] and *N. tabacum* [7] peroxidase cDNAs.

The *CrPrx* transcript and its translated product were found to be differentially expressed in different

vegetative as well as reproductive tissues of *C. roseus* under normal conditions and upon exposure to stress as well as MJ treatment, confirming that it is organ-specific, developmentally regulated, and stress-inducible as well as elicitor-inducible. The subcellular localization study using *CrPrx*–GUS–GFP is indicative of a correlation between the accumulation of *CrPrx* fusion protein and the parenchymatous as well as xylem cell wall thickening, both in tobacco and in *C. roseus*. The classical plant peroxidases (class III) are ascribed a variety of functional roles in plant systems, which include lignification, suberization, auxin catabolism, defense, stress, and developmentally related processes [6,15,26,27]. The stress-inducible nature of *CrPrx* cDNA and the localization of its functional product in cell walls in the present study suggest its apoplastic nature and its involvement in the stress-related as well as developmental processes in *C. roseus*.

Jasmonic acid and its volatile derivative, MJ, collectively called jasmonates, are plant stress hormones that act as regulators of defense responses [28]. The induction of secondary metabolite accumulation is an

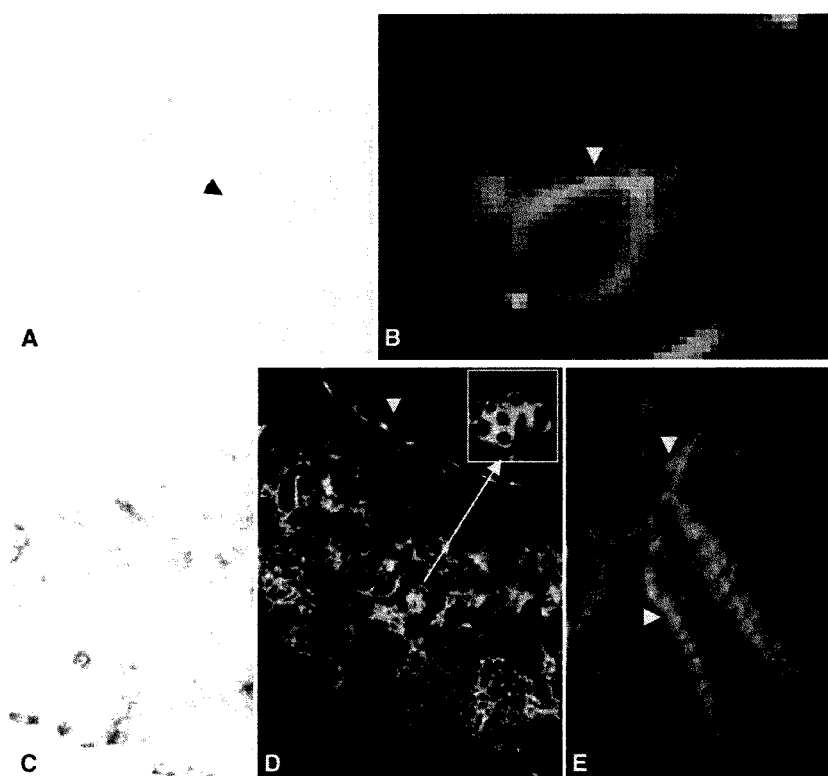


Fig. 9. GUS and GFP fluorescence patterns of *CrPrx* expression in *C. roseus* leaf. (A) GUS staining and (B) GFP fluorescence patterns of stomatal guard cells of *C. roseus*. (C) GUS staining and (D) GFP fluorescence patterns of leaf sections of *C. roseus*. (B, D, E) *CrPrx*-GFP is restricted to the leaf epidermal cells (B), guard cell walls (D) and the wall thickening of xylem tissues (E) of transiently transformed *C. roseus* with *CrPrx*-GFP.

important stress response that depends on jasmonate as a regulatory signal [2]. In the present study, *CrPrx* was found to be expressed upon elicitation by MJ. A number of TIA biosynthetic pathway genes have also been shown to be regulated by jasmonate-responsive AP2 domain transcription factor (ORCAs) [29–31]. These findings demonstrate that, like that of other TIA biosynthetic pathway genes, expression of *CrPrx* falls under an MJ-responsive control mechanism that operates in *C. roseus* under stress conditions. However, it is difficult to ascertain from the present investigation whether *CrPrx* has a similar function to that of AVLB synthase in *C. roseus*, because *CrPrx* was found to lack a vacuolar targeting signal and to be apoplastic in nature.

In conclusion, we report the cloning of a novel *CrPrx* gene from *C. roseus* that encodes a functional product and is localized in epidermal cells as well as vascular cell walls in leaves of tobacco and *C. roseus*. All the accumulated evidence suggests that it encodes a 'three intron' class III secretory peroxidase that shows organ-specific and stress-inducible as well as MJ-inducible expression. Accordingly, we assume its involvement during stress regulation and developmental processes in *C. roseus*. The possibility of using *CrPrx* for manipulation of the TIA pathway needs further experimental investigation.

Experimental procedures

Plant materials

Seeds of *C. roseus* var. Pink were obtained from Rajdhani nursery, New Delhi and grown in the experimental nursery of the National Centre for Plant Genome Research, New Delhi, India. Different parts of the plant, i.e. young (first to third from the shoot apex), mature (fourth to sixth from shoot apex) and old (eighth and ninth from shoot apex) leaves, internodal segments, flower buds, open flowers, pods and roots (branched side roots) from 6-month-old nursery-grown plants were used as plant materials. Leaves of 1-month-old aseptically grown plantlets of *N. tabacum* and *C. roseus* were used as explants for transformation experiments.

Stress treatments

Six-month-old potted mature plants of *C. roseus* var. Pink were subjected to different stress conditions in the following manner.

Wounding stress was performed by puncturing the young leaves attached to plants several times across the apical lamina with a surgical blade, which effectively wounded ~40% of the leaf area. For cold stress, whole plants were kept at 4 °C, and control plants were maintained in the greenhouse at 25 °C. MJ treatment was applied on leaves

detached from plants and kept on paper soaked in 1/10 Murashige Skoog (MS) basal medium by painting on the adaxial surface of the leaves, and the tray containing the leaves was sealed with saran wrap. In control experiments, similar leaves were painted with double-distilled water containing the same amount of ethanol required for dissolving MJ. For UV treatment, young leaves were detached from the plants and kept on 1/10 MS media. A short-term exposure (2 min) of leaves under a UV lamp (λ_{max} 312 nm; $28 \text{ J}\cdot\text{m}^{-2}\cdot\text{s}^{-1}$) was given, and this was followed by incubation on 1/10 MS medium for various time periods before harvesting. For each treatment, young leaves, the first to the third from the shoot apex, were used. The leaves were harvested at different time points by snap freezing in liquid nitrogen, and stored at -80°C for further analyses.

Cloning of *CrPrx* cDNA and gene

Total RNA was isolated from vegetative tissue (roots, stem, leaves) as well as reproductive tissues (flower buds, open flowers and pods) of *C. roseus* using the LiCl precipitation method [36]. First-strand cDNA synthesis was carried out with 5 μg of total RNA using oligo-dT₁₅ primer (Promega, Madison, WI, USA) and Powerscript reverse transcriptase (BD Biosciences, Palo Alto, CA, USA) following the manufacturer's instruction, and used as the template for PCRs.

PCR amplifications were performed with degenerate oligonucleotide primers PF-1 (5'-AGRCTTCAYTTYCAT GAYTGC), PF-2 (5'-AGRCTTCAYTTYCATGAYTGT'), PR-1 (5'-GTGNSCMCCDRRSARRGCDAC), and PR-2 (5'-CATYTCDGHYCAHGABAC), which were designed on the basis of highly conserved amino acid sequences of proteins encoded by the peroxidase gene family, namely, RLHFHDC, VALLGAHSV, and VSCSDI. PCR conditions used were initial denaturation at 94°C for 2 min, followed by 29 cycles of denaturation at 94°C for 45 s, annealing at 45°C for 30 s, and extension at 72°C for 1 min, with a final extension at 72°C for 10 min. Amplified products of the expected size were gel purified using the MinElute Gel Extraction Kit (Qiagen, Hilden, Germany), and cloned directly into the pGEM-T Easy cloning vector (Promega), following the manufacturer's instructions. Clones were sequenced using Big Dye terminator v3.1 cycle sequencing (Applied Biosystems, Foster City, CA, USA) chemistry on an ABI prism DNA sequencer (DNA sequencing facility, National Centre for Plant Genome Research, New Delhi, India).

In order to clone complete *CrPrx* cDNA, a λ -ZapII-oriented leaf-specific cDNA library was screened under high-stringency conditions with modified church buffer at 60°C [36]. The 394 bp (*CrInt1*) PCR product obtained using degenerate PCR primers was used as a probe (accession number AY769111). One positive plaque was obtained after a final wash of the membrane at high stringency

with $0.1 \times \text{NaCl/Cit}$ and 0.1% SDS at 65°C . The 1359 bp full-length clone was identified after *in vivo* excision in the phagemid vector pBSK⁺ (Clontech, Palo Alto, CA, USA).

The complete cDNA coding region was PCR amplified using forward primer PFLF1 (5'-CACGAGCTGACCTT-CACTGTC) and reverse primer PFLR1 (5'-GCTCACCAC-CATTACATTGC), designed to anneal with the 5'-UTR and 3'-UTR regions. PCR amplification consisted of 2 μL of cDNA template in a reaction volume of 50 μL , $1 \times$ ThermoPol buffer, 1.5 mM MgCl₂, 0.4 mM dNTPs, 0.2 μM each primer, and 1 U of Deep Vent_R DNA Polymerase (NEB, Beverly, MA, USA). Thermal cycling was carried out on an MJ Research Master Cycler (Global Medical Instrumentation, Ramsey, MN, USA) with the following conditions: initial denaturation at 94°C for 2 min, followed by 29 cycles of denaturation at 94°C for 45 s, annealing at 60°C for 30 s, extension at 72°C for 1 min, and a final extension at 72°C for 10 min. The corresponding genomic sequence for *CrPrx* was PCR-amplified using the same primer pair PFLF1 and PFLR1. The PCR product was cloned into the vector pGEM-T Easy (Promega), and sequenced as mentioned above. Gene-specific primers GSP2 (5'-CCCTTCAAAGGGAGTGTCTCTGGAGTTGG) and GSP4 (5'-GAGGCTCTCATTGTGGTCTG-GGATG) were designed from the 380 bp and 532 bp positions of the cDNA sequence, respectively, for subcloning the *CrPrx* gene.

Southern blot analysis

Catharanthus roseus genomic DNA was purified using the hexadecyltrimethyl ammonium bromide method [32]. Thirty micrograms of *Bgl*II-, *Eco*RV- and *Hind*III-digested genomic DNA was separated on 0.7% agarose $1 \times$ TAE gel at 40 V for 8 h. DNA was then transferred to a Hybond-N membrane, following the manufacturer's instructions. Pre-hybridization and hybridization of membranes were carried out at 60°C in modified church buffer (7% SDS, 0.5 M NaPO₄, 10 mM EDTA, pH 7.2) [33]. Blots were probed with [³²P]dCTP[α P] *CrPrx* cDNA. Blots were finally washed in $1 \times \text{NaCl/Cit}$ and 0.1% SDS at 60°C [33]. Membranes were wrapped in Klin Wrap (Flexo film wraps, Aurangabad, India) and exposed to XBT-5 CAT film (Kodak, Mumbai, India).

Northern blot analysis

Total RNA (20 μg) was separated on a 1.2% denaturing agarose gel at 60 V for 6 h and blotted onto Hybond-N membrane (Amersham-Pharmacia, Piscataway, NJ, USA) using standard procedures [34]. Following transfer, blots were rinsed briefly in diethylpyrocarbonate-treated water, and the RNA was immobilized on the membrane by UV-crosslinking using a Stratalinker (Model 1800; Stratagene,

La Jolla, CA, USA) at an energy of 12 000 $\mu\text{J}\cdot\text{cm}^{-2}$ for approximately 2 min, and then air-dried.

Blots were prehybridized and hybridized in modified church buffer at 60 °C [32,34]. Blots were probed as described for Southern blot analysis.

Purification of GST-fused CrPrx protein from *Escherichia coli* and production of antibodies to CrPrx

The 330 amino acid ORF of the CrPrx clone was amplified by PCR using Deep Vent_R DNA Polymerase (NEB) and primers GSTPF2 (5'-GGAATTCCTCCATGGCTTCCAAAAC) and GSTPRI (5'-GGTCGACCTCACCACCATTA CA), according to the manufacturer's instructions. The amplified fragment was restricted with *EcoRI* and *SalI* endonucleases, and inserted in the corresponding restriction sites of the pGEX4T-2 expression vector in the reading frame to obtain the N-terminal GST fusion product (Amersham). Clone PPGX (pGEX 4T-2 with CrPrx ORF) was transformed to BL21-CodonPlus-RP competent cells (Stratagene). The fusion protein was induced at 37 °C by adding 0.05 mM isopropyl thio- β -D-galactoside at a growth stage at D_{600} of 0.5. Purification of insoluble fusion protein was performed using the method as described in Frangioni & Neel [35], with slight modifications. Two hundred milliliters of induced culture of bacteria was pelleted at 3000 *g* at 4 °C for 15 min using a Sorvall RC 5C centrifuge (Global Medical Instrumentation) with GSA rotor, and washed twice with 1 \times NaCl/P_i (8.4 mM Na₂HPO₄, 1.9 mM NaH₂PO₄, pH 7.4, 150 mM NaCl). The pelleted bacteria were dissolved in STE buffer (10 mM Tris/HCl, pH 8.0, 1 mM EDTA, 150 mM NaCl) containing 1 mM phenylmethanesulfonyl fluoride as protease inhibitor; this was followed by lysozyme (1 mg·mL⁻¹) treatment and incubation on ice for 30 min. The lysate was sonicated using a sonicator (UP 200S Ultrasonic Processor; Hielscher Ultrasound Technology, Ringwood, NJ, USA) three times separately on ice for 30 s each (amplitude 1, 20% duty cycle). After sonication, the lysate was clarified by centrifugation for 20 min at 37 000 *g* at 4 °C using an Eppendorf 5415R centrifuge (Westbury, NY, USA) with standard 24 \times 1.5 mL/2.0 mL aerosol-tight rotor. The supernatant was transferred to another tube, and Triton X-100 (final concentration of 2%) was added from a 10% stock in STE and well mixed. In addition, 400 μL of washed 50% GST beads were also added and agitated on rocker for 1 h at 4 °C. The beads were washed 10–12 times with ice-cold 1 \times NaCl/P_i by repeated centrifugation at 500 *g* for 5 min at 4 °C (Eppendorf 5415R with standard 24 \times 1.5 mL/2.0 mL rotor), and resuspended in five volumes of elution buffer [10 mM reduced L-glutathione (G4251; Sigma Aldrich, St Louis, MO, USA) dissolved in 50 mM Tris/HCl, pH 8.0] in different fractions. Each fraction was checked on SDS/PAGE (10% resolving gel). The purified protein was dialyzed and

supplied to a company (Banglore Genie, Bangalore, India) for raising polyclonal antibodies in rabbit. The preimmune serum and sera after inoculation were collected and tested for binding to *C. roseus* proteins by immunoblotting analysis. The preimmune serum did not lead to the detection of any protein band specific to *C. roseus* by immunoblotting (data not shown).

Protein extraction and immunoblot analysis

Frozen tissues (2 g fresh weight) were ground to a fine powder in a chilled mortar and pestle in the presence of liquid nitrogen. Half of the sample was used for protein extraction, and the other half was used for RNA extraction. Crude protein extracts were prepared by adding protein extraction buffer (100 mM sodium phosphate, pH 7.5, 2 mM dithiothreitol, 5% w/v polyvinylpyrrolidone) at a 1 : 4 (w/v) ratio, as described previously [36]. The homogeneous mixture was centrifuged at 17 500 *g* for 30 min at 4 °C using an Eppendorf 5415R centrifuge with standard 24 \times 1.5 mL/2.0 mL aerosol-tight rotor to separate the protein fraction from cell debris. The supernatant containing the total soluble protein was analyzed by means of immunoblot analysis. Protein concentration was determined following the method described by Bradford [37], using BSA as standard. All steps of protein extraction were performed at 4 °C. Extracted protein was electrophoresed in 12% SDS/PAGE [38]. Samples (20 μg of each) were boiled for 10 min in an equal volume of 2 \times SDS/PAGE sample buffer with 0.2 M dithiothreitol. Insoluble materials were removed by centrifugation at 10 000 *g* using an Eppendorf 5415R centrifuge with standard 24 \times 1.5 mL/2.0 mL aerosol-tight rotor. Prestained protein molecular weight markers (MBI Fermentas, Hanover, MD, USA) were used in gels to visualize the size of protein and efficiency of transfer onto the nylon membrane (Hybond C-extra; Amersham). The proteins were electroblotted overnight at 90 mA in a Bio-Rad (Hercules, CA, USA) mini trans-blot system. The blotting buffer was 192 mM glycine and 25 mM Tris (pH 8.3), containing 10% (v/v) methanol. For immunodetection, blotted nylon membrane was blocked with blocking buffer, i.e. 5% decreamed milk in TBS (10 mM Tris pH 7.6 and 0.15 M NaCl) for 1 h. The blocked nylon membrane was incubated with CrPrx antibodies at 1 : 1000 dilution in buffer containing 1% decreamed milk in TTBS (10 mM Tris, pH 7.6, 150 mM NaCl, 0.05% w/v Tween-20) for 1 h. Unbound primary antibodies were removed by washing in TTBS buffer, and the membrane was then incubated for 1 h at room temperature in TBS buffer containing HRP-conjugated goat anti-(rabbit IgG) (diluted to 1 : 100 000). Following the removal of unbound secondary antibody, peroxidase activity of HRP was determined using Super-Signal West Pico Chemiluminescent Substrate (Pierce, Rockford, IL, USA).

Construction of GFP fusion protein for expression in tobacco and *C. roseus* leaf discs

The coding region of *CrPrx* was amplified by PCR with the oligonucleotide primers GSTPF2 (5'-GGAATTCATG GCTTCCAAAAC) and PGFPR1 (5'-GGACTAGTATG TAACTTATTAGCT-ACATAT) using Deep Vent_R DNA Polymerase (NEB). The amplified product contains *Nco*I and *Spe*I restriction enzyme cut sites, respectively. After digestion with *Nco*I and *Spe*I, the PCR product was directly integrated into pCAMBIA1303 (35S-GUS-mGFP5) vector to generate a CrPrx-GUS-GFP fusion protein transformation vector. The resulting plasmids were used to transform *Agrobacterium tumefaciens* strain GV3101. A standard leaf-disk transformation method [39] was used to generate transformants of tobacco and *C. roseus* expressing CrPrx-GUS-GFP and GUS-GFP via *Agrobacterium*-mediated transformation. Transformed tobacco and *C. roseus* leaf discs were grown on MS basal medium supplemented with 1-naphthaleneacetic acid 1 p.p.m. and 6-benzylaminopurine 0.1 p.p.m. for tobacco, and 2,4-dichlorophenoxyacetic acid 1.0 p.p.m. and 6-benzylaminopurine 0.1 p.p.m. for *C. roseus*. After 1 week of incubation at 25 °C ± 2 °C, leaf tissues were harvested for histochemical studies.

Histochemical GUS staining and fluorescence microscopy

Histochemical localization of GUS activity was analyzed after incubating the samples in X-Gluc buffer (50 mM sodium phosphate buffer, pH 7.0, 10 mM EDTA, 0.1% Triton X-100, 5 mM potassium ferrocyanide, 3.8 mM 5-bromo-4-chloro-3-indolyl glucuronide) at 37 °C for 12 h. For sectioning, leaf disks stained with GUS were mounted in Jung tissue freezing medium (Leica CM 1510S, Leica Microsystems GmbH, Wetzlar, Germany). Frozen sections of 30 µm were layered on glass slides with a cryomicrotome (CM 1510S; Leica Instruments) adjusted to -16 °C for microscopy. Sections (30 µm) were placed under a coverslip and viewed by Diascopic microscopy (Nikon Eclipse 80i, Tokyo, Japan) for histochemical GUS staining. GFP localization was determined by Epifluorescence microscopy (Nikon Eclipse 80i) using cubes of dichroic mirror with excitation filter and barrier filter combination sets for detection of fluorescein isothiocyanate. Images were captured with a digital camera (model DXM 1200C; Nikon) and saved using image-capturing software ACT-1C (Nikon), and further processed using IMAGE-PRO EXPRESS image-analysis software (Media Cybernetics, Silver Spring, MD, USA).

Bioinformatics analysis of CrPrx

The initial design of degenerate primers was done using WISE2 [40] and CLUSTALW 1.82 alignment software, freely

available at the bioinformatics server of the European Bioinformatics Institute (<http://ebi.ac.uk>). Similarity searches were performed using BLAST analysis methods [17]. Predictions based on translated amino acid sequences were generated by software programs available at the EXPASY proteomics server of the Swiss Institute of Bioinformatics (<http://www.expasy.org>). The nucleotide alignment of peroxidases for making the phylogenetic tree was done using the MAFFT version 5.667 program [41]. The phylogenetic tree was constructed following the maximum parsimony method using the MEGA2 program [42]. A parameter of close-neighbor interchanges (CNI) with a search level of 3 and 100 bootstrap replicates were considered for this purpose.

Acknowledgements

Senior Research Fellowships to SK and AD from the Council of Scientific and Industrial Research (CSIR) India are gratefully acknowledged. We thank the Department of Biotechnology (DBT), Government of India for its financial support. SK, AD and AKS pay their tribute to Jayanti Sen, who passed away while the manuscript was under consideration for publication.

References

- Hilliou F, van der Fits L & Memelink J (2001) Molecular regulation of monoterpenoid indole alkaloid biosynthesis. In *Regulation of Phytochemicals by Molecular Techniques* (Romeo JT, Sanders JA & Matthews BF, eds), pp. 275–295. *Recent Advances in Phytochemistry*, Vol. 35. Elsevier Science, Oxford.
- Memelink J, Verpoorte R & Kijne JW (2001) ORCAnization of jasmonate-responsive gene expression in alkaloid metabolism. *Trends Plant Sci* **6**, 212–219.
- Sottomayor M, de Pinto MC, Salema R, DiCosmo F, Pedreño MA & Ros Barceló A (1996) The vacuolar localization of a basic peroxidase isoenzyme responsible for the synthesis of α -3',4'-anhydrovinblastine in *Catharanthus roseus* (L) G. Don leaves. *Plant Cell Environ* **19**, 761–767.
- Sottomayor M, López-Serrano M, DiCosmo F & Ros Barceló A (1998) Purification and characterization of α -3',4'-anhydrovinblastine synthase (peroxidase-like) from *Catharanthus roseus* (L) G. Don. *FEBS Lett* **428**, 299–303.
- Sottomayor M & Ros Barceló A (2003) Peroxidase from *Catharanthus roseus* (L) G. Don and the biosynthesis of α -3',4'-anhydrovinblastine: a specific role for a multifunctional enzyme. *Protoplasma* **222**, 97–105.
- Hiraga S, Sasaki K, Ito H, Ohashi Y & Matsui H (2001) A large family of class III plant peroxidases. *Plant Cell Physiol* **42**, 462–468.

- 7 Blee KA, Choi JW, O'Connell AP, Schuch W, Lewis NG & Bolwell GP (2003) A lignin-specific peroxidase in tobacco whose antisense suppression leads to vascular tissue modification. *Phytochemistry* **64**, 163–176.
- 8 Passardi F, Cosio C, Penel C & Dunand C (2005) Peroxidases have more functions than a Swiss army knife. *Plant Cell Rep* **24**, 255–265.
- 9 Sottomayor M, Cardoso LI, Pereira LG & Ros Barceló A (2004) Peroxidase and the biosynthesis of terpenoid indole alkaloids in the medicinal plant *Catharanthus roseus* (L.) G Don. *Phytochem* **3**, 159–171.
- 10 Lewis NG (1999) A 20th century roller coaster ride: a short account of lignification. *Curr Opin Plant Biol* **2**, 153–162.
- 11 Bernards MA, Fleming WD, Llewellyn DB, Priefer R, Yang X, Sabatino A & Plourde GL (1999) Biochemical characterization of the suberization-associated anionic peroxidase of potato. *Plant Physiol* **121**, 135–146.
- 12 Wojtaszek P, Trethowan J & Bolwell GP (1997) Reconstitution *in vitro* of the components and conditions required for the oxidative cross-linking of extracellular proteins in French bean (*Phaseolus vulgaris* L.). *FEBS Lett* **405**, 95–98.
- 13 Gazarian IG, Lagrimini LM, Mellon FA, Naldrett MJ, Ashby GA & Thorneley RNF (1998) Identification of skatolyl hydroperoxide and its role in the peroxidase-catalysed oxidation of indol-3-yl acetic acid. *Biochem J* **333**, 223–232.
- 14 Passardi F, Longet D, Penel C & Dunand C (2004) The class III peroxidase multigenic family in rice and its evolution in land plants. *Phytochemistry* **65**, 1879–1893.
- 15 Welinder KG, Justesen AF, Kjærsgård IVH, Jensen RB, Rasmussen SK, Jespersen HM & Duroux L (2002) Structural diversity and transcription of class III peroxidases from *Arabidopsis thaliana*. *Eur J Biochem* **269**, 6063–6081.
- 16 Bendtsen JD, Nielsen H, von Heijne G & Brunak S (2004) Improved prediction of signal peptides: SignalP 3.0. *J Mol Biol* **340**, 783–795.
- 17 Altschul SF, Madden TL, Schaffer AA, Zhang J, Zhang Z, Miller W & Lipman DJ (1997) Gapped BLAST and PSI-BLAST: a new generation of protein database search programs. *Nucleic Acids Res* **25**, 3389–3402.
- 18 Welinder KG (1976) Covalent structure of the glycoprotein horseradish peroxidase EC 1.11.1.7. *FEBS Lett* **72**, 19–23.
- 19 Mohan R, Bajar AM & Kolattukudy PE (1993) Induction of a tomato anionic peroxidase gene (*tap1*) by wounding in transgenic tobacco and activation of *tap1*/GUS and *tap2*/GUS chimeric gene fusions in transgenic tobacco by wounding and pathogen attack. *Plant Mol Biol* **21**, 341–354.
- 20 Mohan R, Vijayan P & Kolattukudy PE (1993) Developmental and tissue-specific expression of a tomato anionic peroxidase (*tap1*) gene by a minimal promoter, with wound and pathogen induction by an additional 5'-flanking region. *Plant Mol Biol* **22**, 475–490.
- 21 Welinder KG, Mauro JM & Nørskov-Lauritsen L (1992) Structure of plant and fungal peroxidases. *Biochem Soc Trans* **20**, 337–340.
- 22 Smith AT & Veitch NC (1998) Substrate binding and catalysis in heme peroxidases. *Curr Opin Chem Biol* **2**, 269–278.
- 23 Gabaldon C, Lopez-Serrano M, Pedreno MA & Barcelo AR (2005) Cloning and molecular characterization of the basic peroxidase isoenzyme from *Zinnia elegans*, an enzyme involved in lignin biosynthesis. *Plant Physiol* **139**, 1138–1154.
- 24 Tognolli M, Penel C, Greppin H & Simon P (2002) Analysis and expression of the class III peroxidase large gene family in *Arabidopsis thaliana*. *Gene* **288**, 129–138.
- 25 Tanaka S, Ikeda K, Ono M & Miyasaka H (2002) Isolation of several anti-stress genes from mangrove plant *Avicennia marina*. *World J Microbiol Biotechnol* **18**, 801–804.
- 26 Veitch NC & Smith AT (2001) Horseradish peroxidase. *Adv Inorg Chem* **51**, 107–161.
- 27 Do HM, Hong JK, Jung HW, Kim SH, Ham JH & Hwang BK (2003) Expression of peroxidase-like genes, H₂O₂ production, and peroxidase activity during the hypersensitive response to *Xanthomonas campestris* pv. *vesicatoria* in *Capsicum annum*. *Mol Plant Microbe Interact* **16**, 196–205.
- 28 Reymond P & Farmer EE (1998) Jasmonate and salicylate as global signals for defense gene expression. *Curr Opin Plant Biol* **1**, 404–411.
- 29 van der Fits L & Memelink J (2000) ORCA3, a jasmonate-responsive transcriptional regulator of plant primary and secondary metabolism. *Science* **289**, 295–297.
- 30 Aerts RJ, Gisi D, De Carolis E, Luca V & Baumann TW (1994) Methyl jasmonate vapor increases the developmentally controlled synthesis of alkaloids in *Catharanthus* and *Cinchona* seedlings. *Plant J* **5**, 635–643.
- 31 El-Sayed M & Verpoorte R (2005) Methyljasmonate accelerates catabolism of monoterpenoid indole alkaloids in *Catharanthus roseus* during leaf processing. *Fitoterapia* **76**, 83–90.
- 32 Batra J, Dutta A, Singh D, Kumar S & Sen J (2004) Growth and terpenoid indole alkaloid production in *Catharanthus roseus* hairy root clones in relation to left- and right-termini-linked Ri T-DNA gene integration. *Plant Cell Rep* **23**, 148–154.
- 33 Sambrook J & Russell DW (2001) *Molecular Cloning. A Laboratory Manual*, 3rd edn. Cold Spring Harbor Laboratory Press, Cold Spring Harbor, NY.
- 34 Dutta A, Batra J, Pandey-Rai S, Singh D, Kumar S & Sen J (2005) Expression of terpenoid indole alkaloid biosynthetic pathway genes corresponds to accumulation of related alkaloids in *Catharanthus roseus* (L.) G. Don. *Planta* **220**, 376–383.

- 35 Frangioni JV & Neel BG (1993) Solubilization and purification of enzymatically active glutathione S-transferase (pGEX) fusion proteins. *Anal Biochem* **210**, 179–187.
- 36 Di Fiore S, Li Q, Leech MJ, Schuster F, Emans N, Fischer R & Schillberg S (2002) Targeting tryptophan decarboxylase to selected subcellular compartments of tobacco plants affects enzyme stability and in vivo function and leads to a lesion-mimic phenotype. *Plant Physiol* **129**, 1160–1169.
- 37 Bradford MM (1976) A rapid and sensitive method for the quantitation of microgram quantities of protein utilizing the principle of protein-dye binding. *Anal Biochem* **72**, 248–254.
- 38 Laemmli UK (1970) Cleavage of structural proteins during the assembly of the head of bacteriophage T4. *Nature* **227**, 680–685.
- 39 Horsch RB, Fry J, Hoffmann NL, Wallroth M, Eichholtz D, Rogers SG & Fraley RT (1985) A simple and general method for transferring genes in to plants. *Science* **227**, 1229–1231.
- 40 Birney E, Clamp M & Durbin R (2004) GeneWise and Genomewise. *Genome Res* **14**, 988–995.
- 41 Katoh K, Kuma K, Toh H & Miyata T (2005) MAFFT, version 5: improvement in accuracy of multiple sequence alignment. *Nucleic Acids Res* **33**, 511–518.
- 42 Kumar S, Tamura K, Jakobsen IB & Nei M (2001) MEGA2: molecular evolutionary genetics analysis software. *Bioinformatics* **17**, 1244–1245.
- 43 Kjærsgård IVH, Jespersen HM, Rasmussen SK & Welinder KG (1997) Sequence and RT-PCR expression analysis of two peroxidases from *Arabidopsis thaliana* belonging to a novel evolutionary branch of plant peroxidases. *Plant Mol Biol* **33**, 699–708.
- 44 Haas BJ, Volfovsky N, Town CD, Troukhan M, Alexandrov N, Feldmann KA, Flavell RB, White O & Salzberg SL (2002) Full-length messenger RNA sequences greatly improve genome annotation. *Genome Biol* **3**, R29.1–R29.12.
- 45 Liu G, Sheng X, Greenshields DL, Ogieglo A, Kaminskyj S, Selvaraj G & Wei Y (2005) Profiling of wheat class III peroxidase genes derived from powdery mildew-attacked epidermis reveals distinct sequence-associated expression patterns. *Mol Plant Microbe Interact* **18**, 730–741.
- 46 Johansson A, Rasmussen SK, Harthill JE & Welinder KG (1992) cDNA, amino acid and carbohydrate sequence of barley seed-specific peroxidase BP 1. *Plant Mol Biol* **18**, 1151–1161.
- 47 Llorente F, Lopez-Cobollo RM, Catala R, Martinez-Zapater JM & Salinas J (2002) A novel cold-inducible gene from *Arabidopsis*, RCI3, encodes a peroxidase that constitutes a component for stress tolerance. *Plant J* **32**, 13–24.
- 48 McInnis SM, Costa LM, Gutierrez-Marcos JF, Henderson CA & Hiscock SJ (2005) Isolation and characterization of a polymorphic stigma-specific class III peroxidase gene from *Senecio squalidus* L. (Asteraceae). *Plant Mol Biol* **57**, 659–677.
- 49 Simon P (1993) Diversity and conservation of plant peroxidases. *Plant Peroxidase Newslett.* **1**, 4–7.
- 50 Mura A, Medda R, Longu S, Floris G, Rinaldi AC & Padiglia A (2005) A Ca²⁺/calmodulin-binding peroxidase from *Euphorbia latex*: novel aspects of calcium-hydrogen peroxide cross-talk in the regulation of plant defenses. *Biochemistry* **44**, 14120–14130.
- 51 Ishige F, Mori H, Yamazaki K & Imaseki H (1993) Identification of a basic glycoprotein induced by ethylene in primary leaves of azuki bean as a cationic peroxidase. *Plant Physiol* **101**, 193–199.
- 52 el-Turk J, Asemota O, Leymarie J, Sallaud C, Mesnage S, Breda C, Buffard D, Kondorosi A & Esnault R (1996) Nucleotide sequences of four pathogen-induced alfalfa peroxidase-encoding cDNAs. *Gene* **170**, 213–216.
- 53 Sato Y, Demura T, Yamawaki K, Inoue Y, Sato S, Sugiyama M & Fukuda H (2006) Isolation and characterization of a novel peroxidase gene ZPO-C whose expression and function are closely associated with lignification during tracheary element differentiation. *Plant Cell Physiol* **47**, 493–503.
- 54 Yi SY & Hwang BK (1998) Molecular cloning and characterization of a new basic peroxidase cDNA from soybean hypocotyls infected with *Phytophthora sojae* f.sp. *glycines*. *Mol Cells* **31**, 556–564.
- 55 Coelho AC (2003) *Identification of molecular markers in Quercus suber linked to resistance to Phytophthora cinnamomi*. Thesis, Universidade do Algravo, Faro, Portugal.
- 56 Park SY, Ryu SH, Kwon SY, Lee HS, Kim JG & Kwak SS (2003) Differential expression of six novel peroxidase cDNAs from cell cultures of sweetpotato in response to stress. *Mol Genet Genomics* **269**, 542–552.
- 57 Holm KB, Andreasen PH, Eckloff RM, Kristensen BK & Rasmussen SK (2003) Three differentially expressed basic peroxidases from wound-lignifying *Asparagus officinalis*. *J Exp Bot* **54**, 2275–2284.
- 58 Fossdal CG, Sharma P & Lonneborg A (2001) Isolation of the first putative peroxidase cDNA from a conifer and the local and systemic accumulation of related proteins upon pathogen infection. *Plant Mol Biol* **47**, 423–435.

Supplementary material

The following supplementary material is available online: **Fig. S1**. Schematic representation of TIA pathway. This material is available as part of the online article from <http://www.blackwell-synergy.com> Please note: Blackwell Publishing is not responsible for the content or functionality of any supplementary materials supplied by the authors. Any queries (other than missing material) should be directed to the corresponding author for the article.